DOCTORAL THESIS AT THE MEDICAL UNIVERSITY OF VIENNA FOR OBTAINING THE "DOCTOR OF PHILOSOPHY" DEGREE

ENDOGENOUS MODULATORS OF INFLAMMATION AND ITS IMPACT ON INFECTIOUS DISEASES

AUTHOR: DR. MED. UNIV. ULRICH MATT

SUPERVISOR: PROF. DR. SYLVIA KNAPP, PHD

Research Center for Molecular Medicine (CeMM) of the Austrian Academy of Sciences, and Department of Medicine I, Div. of Infectious Diseases and Tropical Medicine Medical University Vienna, Austria

VIENNA, 8TH OF APRIL 2010

to my family
in memory to my brother Flori

TABLE OF CONTENTS

1. ABSTRACT _ ENGLISH

A tightly balanced pro-inflammatory and anti-inflammatory program enables the successful elimination of bacteria, while simultaneously minimizing organ damage. If this balance is lost, as in sepsis, the resulting damage can be detrimental to the host.

The potential risk of overwhelming inflammation depends on the causative pathogen as well as the site of infection. Gram-negative bacterial infections, such as *E. coli* peritonitis, are classically associated with systemic inflammation and sepsis. Likewise, acute lung injury, which is a potential complication of aspiration and/or lung infection, is characterized by uncontrolled pulmonary inflammation and increased risk of secondary infection. Bacterial pneumonias as such are the most frequent cause of sepsis. In severe infections resolution of inflammation is detrimental for the host´s survival. In this context accumulating evidence suggests an important role for endogenous modulators of inflammation.

In the presented work the biological function of three different endogenous modulators during infection was studied *in vivo* and *in vitro* by focusing on innate immune responses and resolution of inflammation: (1) the role of oxidized phospholipids in *E. coli* peritonitis, (2) the role of the fibrin derived peptide $B\beta_{15-42}$ in models of acute lung injury, and (3) the role of the PI3kinase antagonist PTEN during bacterial pneumonia.

Oxidized lipids inhibit phagocytosis, and thereby exert detrimental effects during bacterial peritonitis. The fibrin derived peptide $B\beta_{15-42}$ exhibits anti-inflammatory properties in the lung, whereas PTEN's function is very pleiotropic, as it mediates both pro-inflammatory and anti-bactericidal properties.

2. ABSTRACT _ DEUTSCH

Ein genau abgestimmter pro- und antiinflammatorischer Prozess ermöglicht einerseits die erfolgreiche Eliminierung von Bakterien, und andererseits die Minimierung eines Organschadens.

Das mögliche Risiko einer überwältigenden Entzündungsreaktion hängt sowohl vom Erreger als auch vom Infektionsort ab. Gram-negative bakterielle Infektionen wie zum Beispiel *E. coli*-Peritonitis, gehen klassischerweise mit einer systemischen Inflammation und Sepsis einher. Ebenso, „acute lung injury" (akuter Lungenschaden), welcher eine mögliche Komplikation einer gastralen Aspiration oder einer Lungeninfektion darstellt, zeichnet sich durch unkontrollierte Lungenentzündung und erhöhtes Risiko für sekundäre Infektionen aus. Bakterielle Pneumonien selbst sind die häufigste Ursache für Sepsis. In schwerwiegenden Infektionen ist die Auflösung der Entzündung massgeblich für das Überleben des Wirtes. In diesem Zusammenhang deuten immer mehr Daten auf eine wichtige Rolle von endogenen Entzündungsmodulatoren.

In dieser Arbeit wurden die biologischen Eigenschaften von drei verschiedenen endogenen Entzündungsmodulatoren im Rahmen von Infektionen *in vivo* und *in vitro* studiert, wobei der Schwerpunkt auf das angeborene Immunsystem und die Auflösung der Entzündung gelegt wurde: (1) die Rolle von oxidierten Phospholipiden bei *E. coli*-Peritonitis, (2) die Eigenschaften des Fibrinspaltproduktes $B\beta_{15-42}$ bei akutem Lungenschaden, und (3) die Funktion des PI3K-Antagonisten PTEN bei bakterieller Lungenentzündung.

Oxidierte Phospholipide inhibierten die Phagozytose, und übten dadurch einen verheerenden Effekt bei bakterieller Peritonitis aus. Das Fibrinspaltprodukt $B\beta_{15-42}$ zeigt antiinflammatorische Wirkungen in der Lunge, während PTEN äusserst pleiotrope Eigenschaften aufweist, und sowohl pro-inflammatorische als auch bakterizide Wirkungen aufweist.

3. INTRODUCTION & BACKGROUND

3.1. GENERAL INTRODUCTION

This work comprises three chapters on different endogenous modulators of inflammation and their impact on infectious diseases: 1) oxidized phospholipids in the context of E. coli peritonitis, 2) the fibrin-derived peptide $B\beta_{15-42}$ during acute lung injury, and 3) phosphatase and tensin homolog deleted on chromosome 10 (PTEN) in bacterial pneumonia.

In the beginning I give a very brief general overview over the immune system with emphasis on the role of macrophages, which is the primary cell type studied throughout this work. This is followed by a concise description of the pathophysiology and importance of the two main disease models used: acute lung injury and peritonitis.

The research results of this thesis are then presented in form of publications (accepted or submitted at the time of thesis submission). Each chapter starts with an introduction to the sub-topic (oxidized phospholipids, $B\beta_{15-42}$, or PTEN, respectively), followed by the aim of the study, and the respective publications resulting from our research.

3.2. THE IMMUNE SYSTEM

The immune system is divided in two branches: the innate and the adaptive immune system. For a long time it was thought that innate immunity is solely the immediate response until the adaptive system takes over. With the discovery of germ-line encoded receptors, the so-called Toll-like receptors (TLRs)[1], the innate immune system is more and more recognized as an active modulator of adaptive immunity[2], and research in the field has substantially increased

in the last decade. Its main effector mechanisms are epithelial barriers, the complement system, macrophages, dendritic cells and neutrophils.

The cellular composition of the adaptive immune system consists of lymphocytes. Their receptors are generated randomly during development, and can therefore recognize a huge variety of antigens (10^{14}-10^{18}). Every B- or T-cell receptor recognizes different epitopes, and upon binding to its antigen clonal expansion takes place. The generation of sufficient numbers of a specific lymphocyte takes three to five days. Besides, memory cells, which are B- or T-cells that persist after clonal expansion, ensure long-lived immunity. Thus, the adaptive immune system is specific, needs time to respond, and disposes of immunological memory.

The innate immune system

The first line of defense against invading pathogens is comprised by epithelial barriers. The skin and the mucous membranes cover enormous inner and outer surfaces, and provide efficient physical and chemical protection (Fig. 1). Injuries within these epithelial barriers can be the entry point of infectious agents. Next to the epithelium innate effectors like antimicrobial peptides or the complement system serve as an immediate first line of defense (Fig. 1).

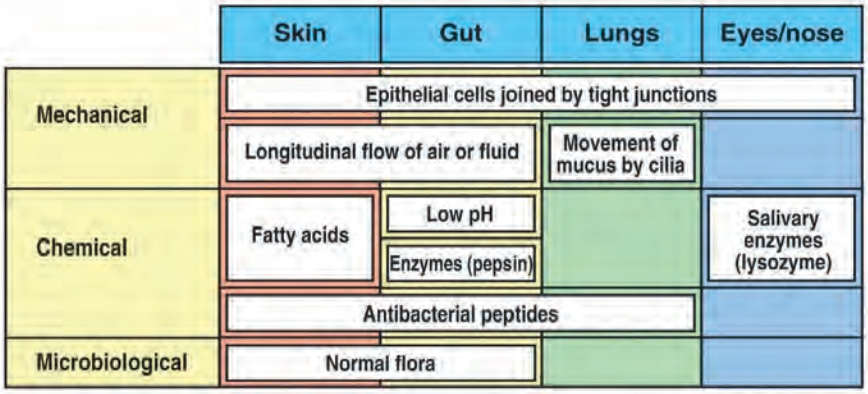

Figure 1. Overview of barriers protecting against invasion of pathogens (from "Immunobiology"; Janeway; Garland Science Publishing; 6th edition; 2005)

Even if an infection gets established, it remains localized most of the time, as effector cells of the innate immune system immediately fend off or limit the invasion of pathogens. These effector cells include epithelial cells, macrophages, dendritic cells and neutrophils. They express pattern-recognition receptors (PRRs), capable of sensing pathogen associated molecular patterns (PAMPs). PRRs are germ-line encoded receptors and recognize broadly expressed pathogenic molecules of viruses, bacteria, fungi and parasites. Toll-like receptors are the most prominent and probably most important group of PRRs, as they are broadly expressed on sentinel cells of the immune system. Overall 12 TLRs were so far identified. TLR1, TLR2, TLR4, TLR5, TLR6 and TLR11 (which is only expressed in mice) are expressed on the cell surface. TLR3, TLR7, TLR8 and TLR9 are expressed in intracellular compartments such as the endosome and the endoplasmatic reticulum and sense viral and/or bacterial nucleic acids[3]. To state some other important examples: TLR4 recognizes lipopolysaccharide, which is expressed by all gram-negative bacteria, or mannan from Candida. TLR2 senses peptidoglycan from gram-positive bacteria, lipoarabinomannan (LAM) from mycobacteria, or together with TLR6 lipoteichoic acid from gram-positive bacteria[4].

It is important to note however that TLRs are only one arm of the sophisticated mechanism whereby cells of the innate immune response sense and eliminate microbes. Intracellular sensors possessing a conserved CARD (caspase recruitment) domain, (analogous to the TIR (toll/interleukin-1) domain of TLRs), also recognize PAMPS. Briefly, NOD1 and NOD2 constitute such CARD domain containing proteins, and recognize bacterial peptidoglycan[5]. Other CARD containing proteins include IPAF (ICE protease activating factor), ASC (apoptosis associated speck like protein), RIG-I (retinoic acid inducible gene I) and Mda5 (melanoma differentiation associated gene 5)[5]. IPAF and ASC plays a role in inflammasome activation (which is involved in the production

of the mature form of the cytokine IL-1β) in response to various stimuli such as salmonella infection and RIG-I and Mda5 recognize double stranded RNA from viruses and are hence important for anti-viral defense.

Binding of PAMPs to respective PRRs leads to signaling events that activate effector functions and results in the secretion of cytokines and chemokines. This response then leads to the attraction of neutrophils and activation of the adaptive immune system (Fig. 2 and Fig. 3). Furthermore these receptors can facilitate phagocytosis of microbes.

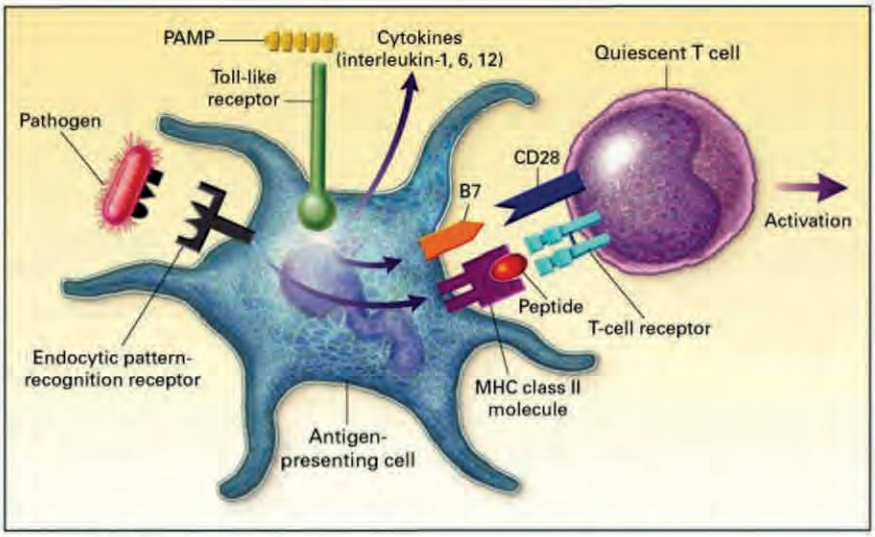

Figure 2. Macrophages are key initiators and modulators of immune responses to invading pathogens. Common structures of microbes (pathogen associated molecular patterns, PAMPs) are recognized by pattern-recognition receptors, such as the toll-like receptors. This alert of the macrophage results in: production of cytokines, activation of the adaptive immune system by costimulation, phagocytosis of the microbe (adapted from[6]).

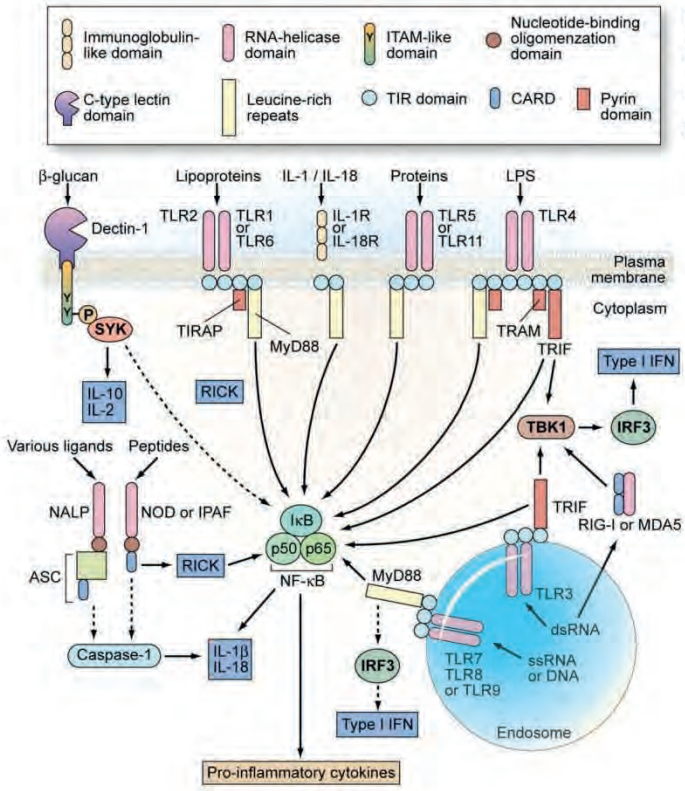

Figure 3. Overview of different pattern-recognition receptors and the main intracellular signaling pathways they elicit (adapted from[7]).

Macrophages

As sentinel cells macrophages are present in all kinds of tissues and organs. They originate from blood monocytes, which migrate into these tissues, and differentiate into resident macrophages. Brain and alveolar macrophages were also shown to be capable of local proliferation[8,9], but it is not entirely clear if all tissue macrophage populations have the ability of local self-replenishment[10]. Monocytes themselves originate from myeloid progenitor cells in the bone marrow. This myeloid stem cell is also the precursor of neutrophils, eosinophils, basophils and mast cells. Every organ harbors different macrophage subtypes, examples are: osteoclasts (bone), Kupffer cells (liver), histiocytes (connective tissue), microglial cells (central nervous system), alveolar macrophages, peritoneal macrophages, and different kinds of spleen macrophages. Depending on their environment, resident macrophages show distinct features and functions. Alveolar macrophages for example have a high

expression of pattern-recognition receptors and scavenger receptors, which enables them to clear viruses, microbes and particles[10]. Macrophages of the gut were shown to have potent phagocytic and bactericidal properties, but secret comparatively low amounts of pro-inflammatory cytokines[11]. Although such differences make sense, and might be expected, these distinct properties of tissue macrophages are only recognized recently.

Macrophages regulate tissue homeostasis by clearing apoptotic cells, debris and senescent erythrocytes (in the spleen), furthermore they support wound-healing and repair of tissue after inflammation[12] As an illustration: macrophages sequester 2 x 10^{11} erythrocytes per day, which equals almost 3 kg of iron and hemoglobin per year[13]. Macrophages are the first cells to get in contact with pathogens, and are therefore key inducers and effectors of an immediate immune response.

Depending on the context and the stage of an inflammation, macrophages can change their phenotype tremendously. Classically activated macrophages ("M1 macrophages") are induced by the pro-inflammatory cytokine IFNγ produced by other immune cells (Fig. 4). This triggers a robust release of pro-inflammatory cytokines, enhanced antigen presentation and an increased capacity to kill pathogens[14]. The more heterogenous group of alternatively activated macrophages ("M2 macrophages") arise in response to IL-4 and/or IL-13, they are important for anti-parasitic immune responses and contribute to tissue repair, while production of pro-inflammatory cytokines and antimicrobial capacity is decreased[14]. This classification is currently debated[13], and can only be an approximation, as many more subtle differences within and between the groups might exist. Furthermore, the phenotypical characterization of macrophages remains difficult in vivo.

Altogether macrophages play a key role in controlling tissue homeostasis and their plasticity ensures an appropriate immune response during different stages and different types of infection.

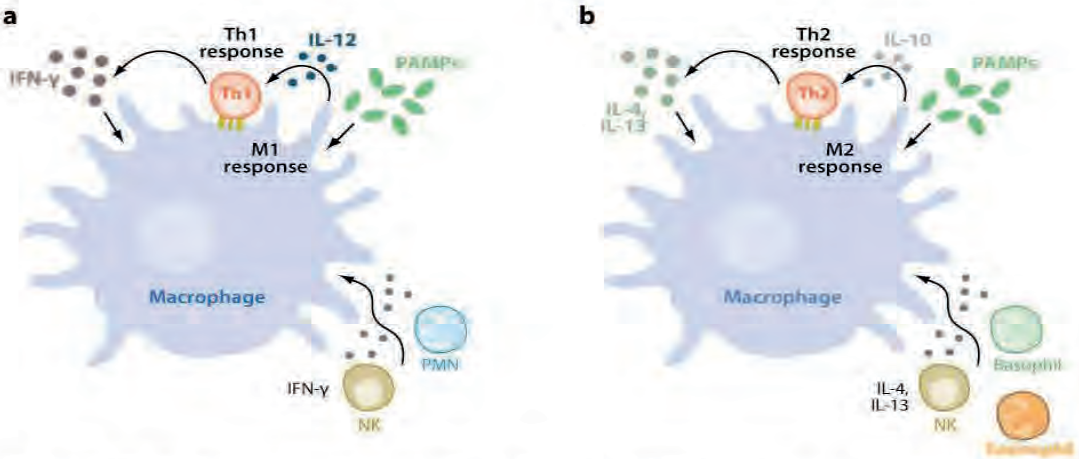

Figure 4. Distinct macrophage activation, which requires two signals: recognition of PAMPs by PRRs and stimulation with IFN-γ or IL-4. (a) Classically activated macrophages are induced by IFN-γ, which is produced by naïve T-cells and natural killer (NK) cells. This results in a Th1 response, supporting intracellular killing of microbes. (b) Alternatively activation of macrophages is induced by IL-4 and IL-13 (via unknown PRRs), which is produced by eosinophils, basophils and naïve T-lymphocytes. This leads to a Th2 response, essential for an extra-cellular immune response against parasites, and as an unwanted effect supporting allergies. Secretion of IL-10 suppresses Th1-responses (adapted from[14]).

The immune system has evolved to sense pathogens. Microbes themselves have evolved strategies to circumvent their own recognition. While much attention has been paid to activators of an immune response: how microbial products bind to receptors and thereby induce a cascade of pro-inflammatory events, little is known how the inflammatory response is balanced or switched off[15]. Microbial products themselves might only exert anti-inflammatory properties to trick the host's immune system (i.e. inhibition of phagosomal maturation by *Mycobacterium tuberculosis*[16]). So, who controls resolution and down-regulation of inflammation? Endogenous modulators of inflammation are more and more recognized as important mediators herein[17,18] (Table 1).

Resolution of inflammation, especially in the context of infectious diseases is a neglected field of research. In this thesis we delineated the roles of three endogenous mediators in clinically relevant infections, putting emphasis on successful resolution of inflammation: oxidized phospholipids during *E. coli* peritonitis, the fibrin-derived peptide $B\beta_{15-42}$ in acute lung injury followed by secondary Pseudomonas aeruginosa pneumonia, and PTEN during bacterial pneumonia.

Table 1: Mediators recently found to be involved in pro-resolution

• Cyclopentenone prostaglandins
• Lipoxins/resolvins
• NF- B (p50/p50)
• Mediators of apoptosis (caspases, CD44, etc.)
• Annexin-1

3.3. BACTERIAL PERITONITIS

The peritoneum is a serous membrane, consisting of a mesothelial cell layer. It covers the visceral organs, and thereby confines the peritoneal cavity. The peritoneal cavity contains a small volume of fluid, which harbors resident and migratory cells. The predominant cell type found in the peritoneal cavity is the peritoneal macrophage. Other cells are lymphocytes, NK-cells, dendritic cells and mast cells[19]. The peritoneum is sterile under normal conditions. The macrophages are considered the first cells of defense upon bacterial infection[20]. Bacterial peritonitis can be spontaneous (=primary peritonitis), due to perforation of organs of the gastrointestinal tract (=secondary peritonitis), or might persist or recur after secondary peritonitis leading to tertiary peritonitis. Treatment includes antibiotics, surgical intervention, and supportive care. Due to diverse etiologies like perforation of a diverticulitis or appendicitis, liver abscess, mesenteric ischemia with bowel infarction, or pancreatitis diagnosis and clinical management are difficult[21]. Despite antibiotic therapy and intensive care, tertiary peritonitis has a mortality rate ranging from 30-64%[22]. The peritoneum's central location, and its vicinity to an enormous amount of blood vessels favors the quick spread of bacteria, resulting in sepsis and multiple organ-failure, which are associated with high mortality[23]. Thus containment of the infectious process is crucial. After bacterial pneumonias, peritonitis is the most frequent cause for sepsis[24], and *E. coli* is the most frequently isolated pathogen in peritonitis (Table 1).

Table 1. Microbiology of peritonitis

Primary Peritonitis	Secondary Peritonitis		Tertiary Peritonitis
Gram-negative bacteria	Gram-negative bacteria		Gram-negative bacteria
Eschecheri coli	*E. coli*	32–61%	*Pseudomonas*
Klebsiella	*Enterobacter*	8–26%	*Enterobacter*
	Klebsiella	6–26%	*Acinetobacter*
	Proteus	4–23%	
Gram-positive bacteria	Gram-positive bacteria		Gram-positive bacteria
S. aureus	*Enterococci*	18–24%	*Enterococci*
Enterococci	*Streptococci*	6–55%	Coagulase-negative
	Staphylococci	6–16%	*Staphylococci*
	Anerobic bacteria		
	Bacteroides	25–80%	
	Clostridium	5–18%	
	Fungi	2–15%	Fungi
			Candida

Figure 1: The peritoneum covers the visceral organs. **Table 1:** Microbiology of peritonitis (adapted from[25]).

Antibiotic therapy and surgical intervention are most important. However, dysregulated inflammation like impaired bacterial clearance can impede successful resolution of inflammation. Immune-modulation might be a promising approach to treat bacterial peritonitis. Moreover, the anatomically defined and easily accessible peritoneum facilitate experimental studies, thus complex analysis of cell composition, activation status of cells and mediator release are feasible. We performed our studies on the influence of endogenously generated oxidized phospholipids in a model of *E. coli* peritonitis, focusing on the role of resident peritoneal macrophages.

3.4. ACUTE LUNG INJURY

Acute lung injury (ALI) is a dreaded clinical complication among intensive care unit (ICU) patients. With a reported in-hospital mortality of 38.5 percent, ALI accounts for 75.000 deaths per year in the United States[26]. ALI is defined by acute hypoxemic respiratory failure, rapid-onset bilateral pulmonary infiltrates consistent with edema, and normal cardiac filling pressures[27]. Severe lung injury, defined by a higher degree of hypoxemia is called acute respiratory distress syndrome (ARDS). The syndrome can be caused by direct or indirect lung injury. Common causes are bacterial pneumonia, aspiration of gastric contents, sepsis or trauma[28]. Treatment strategies are limited to supportive care. Both ALI and ARDS share characteristic features such as edema formation, neutrophil influx, and secretion of cytokines and chemokines[29-30] (Fig. 2).

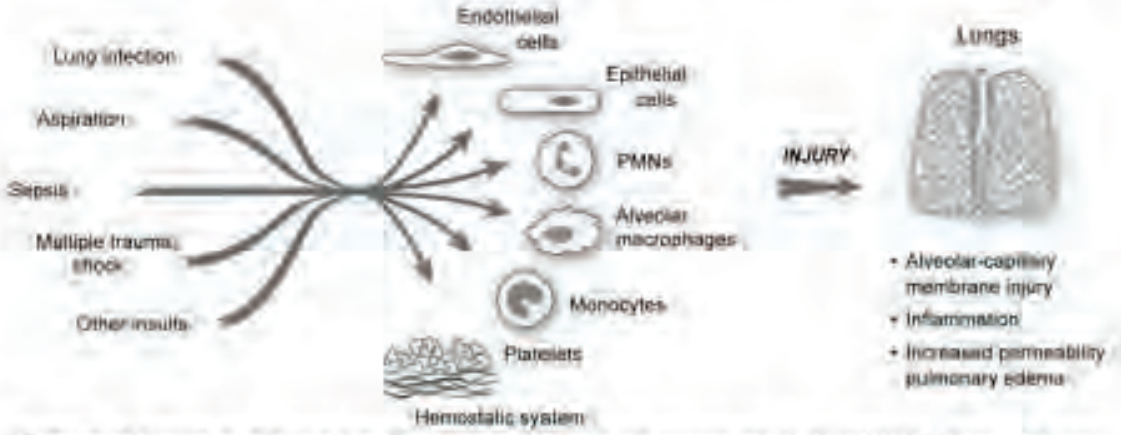

Figure 2: Direct or indirect lung injuries lead to the development of ALI/ARDS. Although having heterogenous etiologies, edema formation, PMN recruitment, and cytokine secretion are common features (adapted from[31]).

The inflammatory process importantly contributes to damages of the lung parenchyma: activated neutrophils release oxidants and proteases, cytokines and chemokines secreted further entertain the inflammation[31]. As a consequence of edema formation, cell debris accumulation, fibroproliferation, and deposition of extracellular matrix, proper lung function is impaired[31].

In order to restore gas exchange and to prevent secondary bacterial infections,

it is essential that the inflammatory process resolves (Fig. 3). Mechanisms involved in lung repair are incompletely understood[31]. Furthermore, the different etiologies of ALI impede mechanistic studies and clinical trials alike[32,33].

Animal models allow studies which focus on a specific protein or process by using gene deficient mice or pharmacological inhibitors. At the same time in vivo models mimic the complexity of biological systems. These advantages make their use indispensable. Preclinical acute lung injury models are used and attempt to mimic the clinical situation. As such models of pneumonia, acid aspiration, sepsis or hyperoxia are applied. Other models mimic the pathological process that is characteristic of ALI and are achieved by local LPS administration, the instillation of oleic acid or bleomycin[34]. Existing animal models reflect hallmarks of ALI such as edema formation and neutrophil accumulation[34], but have to be interpreted within their limitations.

The fibrin-derived peptide $B\beta_{15-42}$ was shown to exert beneficial anti-inflammatory properties in myocardial reperfusion injury in rats and humans[35,36]. As acid aspiration predisposes for secondary pulmonary infections, we aimed to test its immune-modulatory properties in acute lung injury using LPS inhalation and acid aspiration with and without secondary *Pseudomonas aeruginosa* pneumonia (Chapter 2).

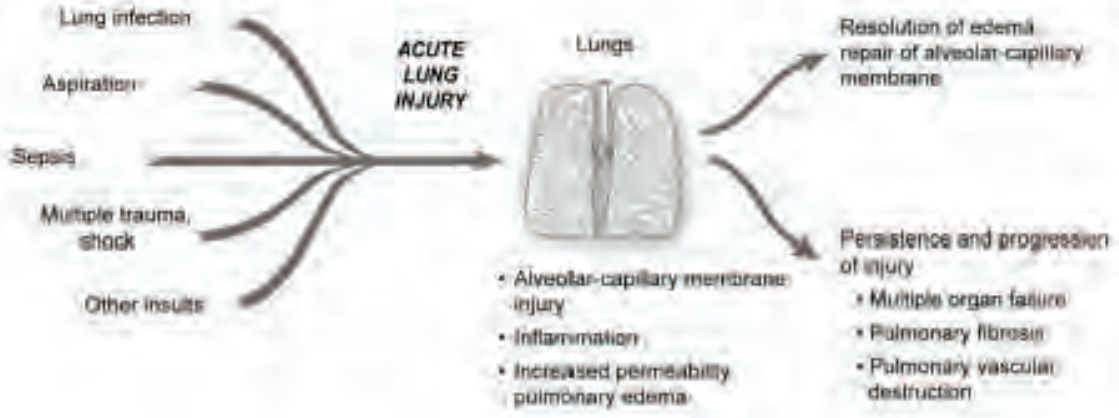

Figure 3: To restore lung function alveolar function has to be restored. Persisting ALI/ARDS potentially leads to multiple organ failure, irreversible lung damage, or death (adapted from[31]).

Bacterial pneumonia

Bacterial lung infections are the leading cause for sepsis[24]. The overall global disease burden caused by lung infections exceeds the burden caused by cancer, heart attacks, strokes, HIV/AIDS, malaria or tuberculosis[37]. Increasing bacterial resistance to antibiotics furthermore highlights the importance of research in the field[38,39]. The most frequent cause of community acquired pneumonia is Streptococcus pneumoniae (others are *Hemophilus influenzae*, *Staphylococcus aureus*, *Legionella*, *Mycoplasma pneumoniae or Chlamydia pneumoniae*)[40]. Nosocomial pneumonia is often caused by *Pseudomonas aeruginosa*, *Staphylococcus aureus* or *Acinetobacter baumannii* (others are *Klebsiella pneumoniae* or *Escherichia coli*)[41].

To gain further insight in the pathophysiology of pneumonia we studied pneumococcal pneumonia, and *Acinetobacter baumannii* pneumonia in genetically modified mice, which lack myeloid PTEN. PTEN is known as a tumor suppressor, which antagonizes PI3-kinase function. PI3-kinase exerts diverse effects on immune functions. Studies using PTEN-deficient mice in the context of infectious diseases and particularly pneumonia are so far missing (Chapter 3).

4. SPECIFIC TOPICS

4.1. IMMUNMODULATORY EFFECTS OF OXIDIZED PHOSPHOLIPIDS DURING BACTERIAL INFECTIONS

Phospholipids: structure, function, oxidation

Phospholipids are part of cell membranes and lipoproteins, and therefore abundantly found throughout the body. Glycerophospholipids, which comprise of a glycerol backbone with three carbon residues, are the main components of phospholipids. The first two residues are connected to fatty acid chains, which form the hydrophobic tails and the third residue with a negatively charged phosphate group, forming phosphatidic acid. Choline, serine, ethanolamine, or inositol can additionally bind to the polar head group. The most abundant phospholipid is phosphatidylcholine (PC), which is located mainly in the extracytosolic leaflet of the plasma membrane, whereas phosphatidylserine, phosphatidylethanolamine, phosphatidylinositol or phosphatidic acid are found in the cytosolic leaflet[42] . Polyunsaturated fatty acids, which are often found at the sn-2 position are highly prone to oxidation. Oxidation occurs either enzymatically e.g. by lipoxygenases or non-enzymatically by oxygen radicals produced by macrophages and neutrophils during the oxidative burst[43,44]. In this respect oxidized phospholipids (OxPL) differ from other mediators generated by oxidation of polyunsaturated fatty acids such as prostaglandins and leukotrienes, which are exclusively formed by enzymatic reactions[45]. The diversity of glycerophospholipids and the different chemical and enzymatic reactions involved, gives rise to a plethora of oxidized phospholipids. Macrophages and activated neutrophils that are recruited to the site of infection produce a plethora of cytokines and oxygen radicals that assist in the killing of microbes. At the same time, these oxygen radicals can also affect the host by peroxidation

of endogenous lipids[43]. In their native, unoxidized form these lipids are biologically inert but upon oxidation they actively modulate the inflammatory process. The presence of oxidized lipids was so far detected in different organs and diseases, such as atherosclerosis[46-49], plasma of patients with coronary artery disease[50], inflamed lung[51-53], diabetic renal glomerulopathy[54], in hemochromatosis[55], in apoptotic cells[49,56,57], in cells stimulated with inflammatory agonists[58], and in CNS lesions in multiple sclerosis[59] and Alzheimer disease[60], but also in healthy mice[49]. Since in vivo concentrations are locally regulated and most likely transient, they might be significantly higher than those that are actually detected. Therefore, the measurement of oxidized phospholipids is rather difficult.

In our in vivo and in vitro studies we used polyunsaturated fatty acids as can be found in 1-palmitoyl-2-arachidonoyl-sn-phosphatidylcholine (PAPC), which is a prototypic mixture of phospholipids that are especially prone to oxidation, resulting in the generation of OxPAPC. This mixture is widely used, and contains different lipids with the same phosphocholine (PC) head group (Fig. 1).

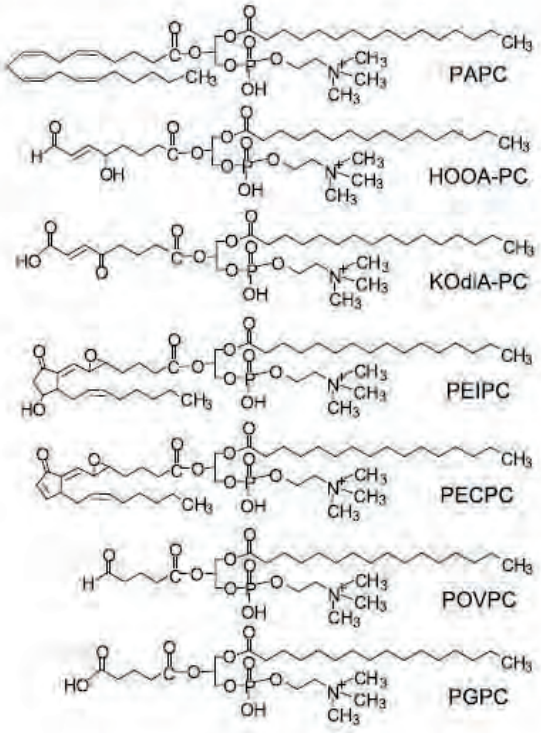

Figure 1: Chemical structures of biologically active oxidized phospholipids. The abbreviations used are: PAPC – 1-palmitoyl-2-arachidonoyl-sn-glycero-3-phosphocholine; HOOA-PC – 5-hydroxy-8-oxo-6-octenoyl-phosphocholine; KOdiA-PC – 5-keto-6-octendioic acid ester of 2-lyso-phosphocholine; PEIPC – 1-palmitoyl-2-(5,6-epoxyprostane E2)-sn-glycero-3-phosphocholine; PECP – 1-palmitoyl-2-(5,6-epoxy-cyclopentenone)-sn-glycero-3-phosphocholine; POVPC – 1-palmitoyl-2-(5-oxovaleroyl)-sn-glycero-3-phosphocholine; PGPC – 1-palmitoyl-2-glutaroyl-sn-glycero-3--phosphocholine[45].

Oxidized phospholipids in atherosclerosis

First evidence for the immunomodulatory role of OxPLs arose from studies in atherosclerosis, where accumulation and oxidation of low density lipoprotein (LDL) is a characteristic feature[61]. An increasing body of evidence showed that these modified lipoproteins are able to mimic and foster the chronic inflammation observed in the course of atherosclerosis[62,63]. Most importantly, oxidized LDL (oxLDL) enhance the recruitment of monocytes, exert procoagulant properties, and increase the uptake of LDL by macrophages, thus leading to the formation of foam cells and thereby entertaining a vicious circle towards progression of atherosclerosis[64,65]. Hence, they became increasingly recognized as culprits of cardiovascular diseases[66] (Fig. 2), which led to the classical view of OxPL as pro-inflammatory mediators, and atherosclerosis as an inflammatory disease.

Oxidation specific epitopes on OxLDL are recognized by scavenger receptors (SRs), such as SRA-1 and-2, CD36, SR-B1, and/or LOX-1[67]. The biological role of these scavenger receptors has been demonstrated in studies using CD36 and SR-A deficient mice, which are protected from atherosclerosis[68-70]. CD36 has been repeatedly shown to be important for the recognition of PC on oxidized phospholipids[71]. Although CD36 was found to structurally bind to OxPAPC[72], induction of cytokine secretion in endothelial cells was shown to be independent of CD36[73]. Thus, different receptors might be responsible for effects of OxPAPC.

Binder et al. intriguingly demonstrated a molecular mimicry between PC of oxLDL and the PC of Streptococcus pneumoniae[74]. Plasma of mice immunized against pneumococci blocked the binding of oxLDL to macrophages[74], and consequently reduced lesion size in atherosclerotic mice[74,75].

Strikingly, antibodies recognizing the PC-head group of oxidized phospholipids are not only found in atherosclerotic mice, but also in naïve germ-free mice and human umbilical vein blood[49]. Thus, the ubiquitous oxygenation of lipids found e.g. in apoptotic cell walls leads to the generation of self-reactive antibodies, which might play a crucial role in homeostasis.

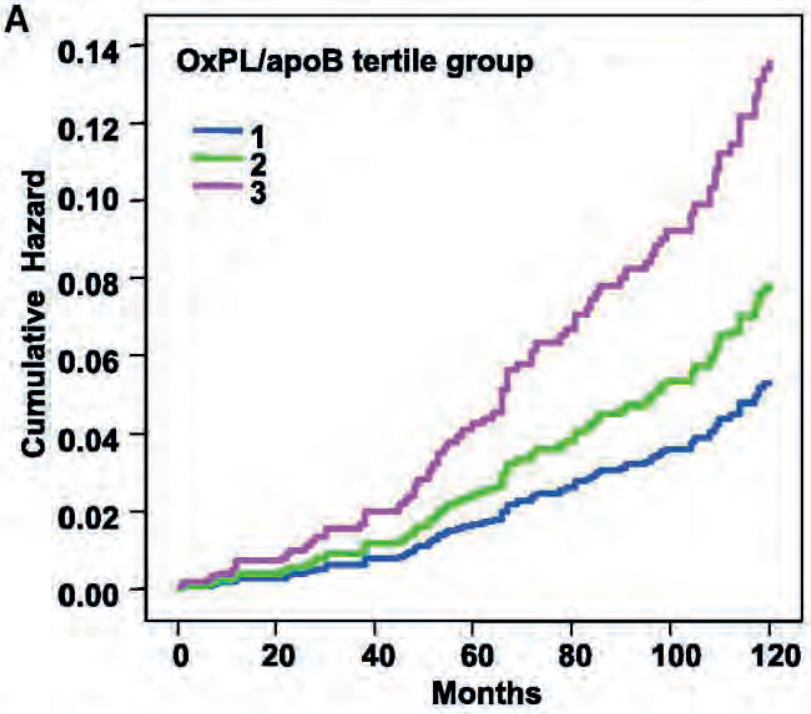

Figure 2. The Bruneck Study: OxPL/apoB levels predict 10-year CVD event rates independently of traditional risk factors. Oxidized phospholipids (OxPL) circulate on apolipoprotein B-100 particles (OxPL/apoB). The figure shows cumulative hazard curves of cardiovascular disease incidents from 1995 to 2005 for tertiles of OxPL/apoB (adapted from[66]).

Oxidized Phospholipids in inflammation and infection

Among other reports, the discovery that OxPAPC inhibits the interaction of LPS with the TLR4 complex, more precisely CD14 and the LPS binding protein, resulting in improved survival in a murine LPS shock model, suggested that these lipids also exert anti-inflammatory properties (Fig. 3)[76].

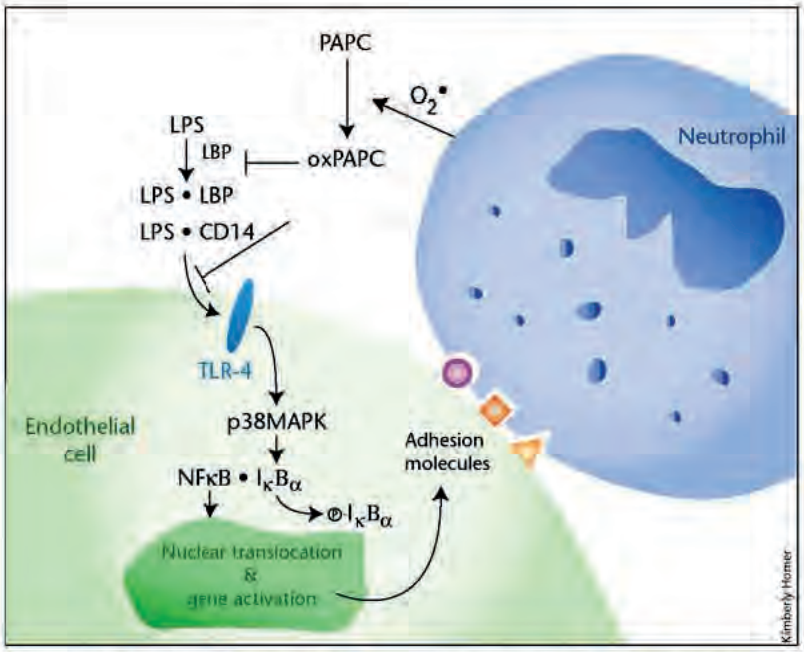

Figure 3. OxPAPC inhibits the binding of LPS to LBP and CD14. Reactive oxygen species like $O_2^{\bullet}$ from activated neutrophils oxidize PAPC. OxPAPC blunts the innate immune response to LPS via TLR-4, resulting in decreased activation of kinase p38MAPK, phosphorylation of I-κBα and activation of the transcription factor NF-κB. This impairs to decreased neutrophil attachment and activation, which might represent a negative feedback mechanism on neutrophil recruitment and activation (adapted from[77]).

These findings were extended to different OxPLs, demonstrating that the TLR4 antagonism is not dependent on the PC-head group[78]. Furthermore it was shown, that OxPLs themselves are no agonist for TLR4 in terms of acute inflammatory gene activation in several cell types (endothelial cells, whole blood, monocytes and fibroblasts)[78]. Recently another group found that OxPAPC is not only interfering with the recognition of LPS via TLR4, but also blocks TLR2-signalling in macrophages, and epithelial cells, whereas signaling via TLRs 3, 7, 8, and 9 remained intact[79]. In dendritic cells OxPAPC blocked LPS (a TLR4 ligand), and poly(I:C) (TLR3 ligand) driven maturation, while Pam3CSK4 or PGN (TLR2 ligands) induced maturation was only slightly inhibited[80]. In PMNs unoxidized phospholipids were shown to induce the production of ROS, whereas in their oxidized form they suppressed the respiratory burst, while MAPkinase activation upon stimulation with PMA or

fMLP remained unchanged[81]. This is in contrast to another report, showing that OxPL increase the generation of reactive oxygen species in bovine aortic endothelial cells[82]. Another important finding is the induction of the potent anti-inflammatory mediator heme oxygenase-1 in a cAMP dependent manner in endothelial cells[83]. Thus, OxPL apparently cause different effects depending on the cell type and the context.

In line with the TLR4 antagonistic properties of OxPAPC, Nonas *et al.* showed that the intravenous administration of OxPAPC attenuated important features of ALI such as neutrophil migration and edema formation with concomitantly decreased pro-inflammatory cytokines like IL-6 and IL-1β after intratracheal LPS instillation in rats[84]. Interestingly, the same group demonstrated endothelial barrier protective effects of OxPAPC in human pulmonary endothelial cells upon challenge with thrombin[85]. In severe forms of ALI, oxidized phospholipids are generated locally within the lungs, and were shown to actively trigger lung inflammation in a TLR4-TRIF-TRAF-6 dependent manner[53] (Fig. 4). Furthermore chemical injury with acid and inactivated H5N1 virus can directly trigger the generation of ROS in monocytes and alveolar macrophages, thereby entertaining a vicious circle. In a serious of in vivo studies the authors demonstrated, that TLR4, TRIF and TRAF-6 knockout mice are resistant to acid induced lung injury, and that myeloid cells, particularly alveolar macrophages are the relevant cells, responding to OxPAPC with ROS production and secretion of pro-inflammatory cytokines. In line with these findings TLR4 was shown to mediate IL-8 secretion by OxPAPC in aortic endothelial cells[73], and minimally modified LDL (mmLDL) triggered production of pro-inflammatory cytokines in macrophages[86].

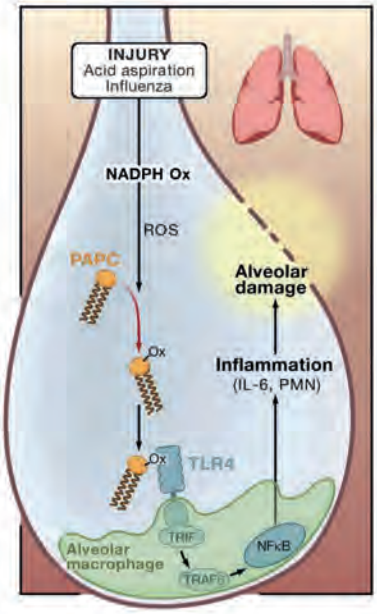

Figure 4. OxPAPC induces lung damage via TLR4. Imai et al. show, that injury to the lungs through acid aspiration or viral infection leads to activation of NADPH oxidase (NADPH Ox) and production of reactive oxygen species (ROS), which oxidize 1-palmitoyl-2-arachidonoyl-phosphatidylcholine (PAPC, OxPAPC). OxPAPC activates TLR4 expressed by myeloid cells (an alveolar macrophage is shown), and the intracellular signal is transduced by the adaptor proteins TRIF and TRAF6, leading to interleukin 6 (IL-6) production, inflammation, and alveolar damage. PMN, polymorphonuclear leukocyte (adapted from[87]).

Taken together OxPL can no longer be seen as exclusively pro-inflammatory agents. The inhibition of TLR-signaling in various cell types, the inhibition of respiratory burst in neutrophils and the induction of heme-oxygenase 1 clearly shows potent anti-inflammatory properties, pointing towards a role in the resolution of inflammatory programs. On the other hand, a detrimental role for OxPLs has been recently demonstrated in ALI[53], which draws an even more complex picture on their role during inflammation.

Aim of the project

Since data on the role of OxPL in the course of infectious diseases are lacking, and most studies use LPS instead of living bacteria, we became interested in testing the contribution of OxPL during "real" infectious diseases *in vivo*. Particularly Bochkov's observation that LPS-induced inflammation was dampened by OxPAPC, led us to investigate the role of OxPAPC in an *E. coli* peritonitis model. We hypothesized that administration of OxPAPC in *E. coli* peritonitis would diminish the initial inflammatory response by impairing the recognition of LPS via TLR4.

4.1.1. OXIDIZED PHOSPHOLIPIDS INHIBIT PHAGOCYTOSIS AND IMPAIR OUTCOME IN GRAM-NEGATIVE SEPSIS *IN VIVO*

Sylvia Knapp *†‡, Ulrich Matt †‡, Norbert Leitinger § and Tom van der Poll *¶

*Center for Experimental and Molecular Medicine and ¶Center for Infection and Immunity Amsterdam (CINIMA), Academic Medical Center, University of Amsterdam, 1105 AZ Amsterdam, The Netherlands; †Center of Molecular Medicine (CeMM) of the Austrian Academy of Sciences, Vienna, Austria; ‡Department of Internal Medicine 1, Medical University of Vienna, 1090 Vienna, Austria; §Cardiovascular Research Center and Department of Pharmacology, University of Virginia, Charlottesville, VA 22908.

Running Title: oxidized phospholipids in *E. coli* peritonitis

Keywords: Inflammation, Bacterial, Knockout, Macrophages, Phagocytosis

Corresponding Author:

Sylvia Knapp, M.D., Ph.D.

Center for Molecular Medicine of teh Austrian Academy of Sciences; Department of Medicine 1, Div. Of Infectious Diseases and Tropical Medicine, Medical University Vienna

Waehringer Guertel 18-20; 1090 Vienna, Austria

Phone: 0043-1-40400-4954 or 4492 FAX: 0043-1-40400-4498

E-mail: sylvia.knapp@meduniwien.ac.at

Abstract:

Oxidized phospholipids that are generated during inflammation exert anti-inflammatory properties and prevent death during murine endotoxemia. Oxidized 1-palmitoyl-2-arachidonoyl-*sn*-glycero-3-phosphorylcholine (OxPAPC) inhibits the interaction of lipopolysaccharide (LPS) with LPS-binding protein (LBP) and CD14. We here determined the functional properties of OxPAPC and potential interference with CD14 during abdominal sepsis caused by *Escherichia (E.) coli*. Administration of OxPAPC rendered mice highly susceptible to *E.coli* peritonitis, as indicated by an accelerated mortality and enhanced bacterial outgrowth and dissemination. $CD14^{-/-}$ mice also displayed increased mortality and bacterial outgrowth and OxPAPC did not further impair host defense in these animals. The mechanisms by which OxPAPC and CD14 deficiency impaired the immune response differed: whereas $CD14^{-/-}$ mice demonstrated a strongly reduced recruitment of phagocytes to the site of the infection, OxPAPC did not influence the influx of inflammatory cells but strongly diminished the phagocytosing capacity of neutrophils and macrophages by a CD14 independent mechanism. Furthermore, OxPAPC potently inhibited uptake of fluorospheres as well as receptor-mediated endocytosis and fluid-phase pinocytosis. These data suggest that oxidized phospholipids such as produced during inflammatory reactions may contribute to mortality during Gram-negative sepsis *in vivo* via impairment of the phagocytic properties of professional phagocytes.

Introduction:

Acute bacterial peritonitis is a life-threatening infection characterized by the presence of bacteria in the normally germ-free peritoneal cavity. Almost invariably caused by perforation of intestines, the most frequently encountered pathogens are enteric Gram-negative bacteria such as *Escherichia coli (E. coli)*, which can be found in up to 60% of the cases (1). Mortality rates of peritonitis range between 30 and 50% despite advances in surgery and antimicrobial therapy. A serious complication originating from peritonitis is systemic inflammation and sepsis with mortality rates of up to 80% (2).

The prompt initiation of host defense mechanisms is essential for the host to survive. The innate immune system, that is responsible for mounting an immediate response to invading pathogens, is considered the central element of host defense in peritonitis. Lipopolysaccharide (LPS) is a major constituent of the outer cell wall of Gram-negative bacteria, such as *E. coli*, and the principal inducer of inflammatory responses to these pathogens. CD14, Toll-like Receptor (TLR) 4 and MD-2 make up the LPS receptor complex involved in the cellular recognition of and signaling by LPS (3-8). LPS-binding protein (LBP) greatly augments the transfer of LPS to the CD14/TLR4 complex. Recently, we demonstrated the pivotal role of LBP during murine *E. coli* peritonitis: the rapid recruitment of polymorphonuclear cells (PMNs) to the site of infection critically depended on the presence of LBP and mice lacking LBP displayed a greatly increased bacterial outgrowth and dissemination that led to early death (9).

PMNs are key phagocytes required for the immediate elimination of bacteria. One of the most powerful weapons generated by activated PMNs are reactive oxygen species that are utilized for antibacterial defense. However, in parallel with the killing of bacteria, free radicals may damage host molecules, and

in particular induce lipid peroxidation. Oxidized phospholipids (OxPL) are generated in vivo at sites of acute and chronic inflammation (10-12). Accumulating evidence suggests that OxPL are not merely by-products of the inflammatory response, but can actively regulate inflammation (13). Most previous studies focused on the pro-inflammatory effects of OxPL, which are thought to play a role in initiating and maintaining chronic inflammation such as atherosclerosis (13-15). However, it is increasingly recognized that OxPL at the same time possess potent anti-inflammatory properties, which include the direct antagonism of LPS recognition by cells of the innate immune system. Indeed, OxPL effectively inhibit the interaction of LPS with LBP, CD14 and TLR4 (16). The biological significance of this finding was further underlined by the observation that the exogenous administration of OxPL could prevent mortality of mice exposed to high doses of LPS; in this respect OxPL reproduced the LPS resistant phenotype of mice lacking LBP, CD14 or TLR4 (16-20).

The biological role of OxPL during Gram-negative infection with viable bacteria has not been studied so far. We therefore decided to investigate the effects of OxPL during *E. coli* induced abdominal sepsis *in vivo* and the role of CD14 herein.

Materials and Methods:

Mice:

Pathogen-free 9-11 week old male C57BL/6 wild type mice were purchased from Harlan Sprague-Dawley (Horst, The Netherlands). CD14 gene deficient ($CD14^{-/-}$) mice were obtained from Jackson laboratories (Bar Harbor, ME) (21) and backcrossed to C57BL/6 background 6 times. Age and sex matched mice were used in all experiments. The Animal Care and Use Committee of the University of Amsterdam (Amsterdam, The Netherlands) approved all experiments.

Phospholipids:

1-palmitoyl-2-arachidonoyl-sn-glycero-3-phosphorylcholine (PAPC) and dimyristoylphosphatodylcholine (DMPC) were purchased from Sigma Aldrich (Vienna, Austria). DMPC was used as negative control due to the fact that DMPC lacks unsaturated fatty acids and thus cannot be oxidized. Oxidized PAPC (OxPAPC) was generated by air oxidation as described recently and stored in chloroform at -70C (16). The extent of PAPC oxidation was routinely confirmed by ESI-MS (22), and only preparations showing a reproducible pattern of lipid oxidation products were used in the study. These preparations were routinely tested in *in vitro* assays for biological activity as well as LPS content using the Limulus assay. Directly before use, OxPAPC were dried in glass tubes under the stream of N_2 and resuspended in NaCl by vortexing.

Induction of peritonitis:

Peritonitis was induced as described previously (9, 23, 24). In brief, *E.coli* O18:K1 was cultured in Luria Bertani medium (LB, Difco, Detroit, MI) at 37°C, harvested at mid-log phase and washed twice before inoculation. Mice were injected i.p. with 1-2 x 10^4 colony forming units (CFU) *E. coli* in 200µl sterile saline. The inoculum was plated on blood agar plates to determine viable counts. OxPAPC (12.5mg/kg) or control lipids (DMPC) (12.5mg/kg in 200µl NaCl) or the same volume of carrier were injected *i.p.* immediately before bacterial inoculation.

Monitoring of mortality and enumeration of bacteria:

In survival studies, 8-12 mice per treatment group were inoculated with *E.coli*. Since mortality occurs primarily between 24 and 48 hours after infection in this model, mortality was assessed every 2 hours in this period; thereafter mortality was monitored every 6 hours. In separate studies, mice were sacrificed 4h or 20h after infection; at these time-points, mice were anesthetized by inhalation of isoflurane and peritoneal lavage was performed with 5ml of sterile isotonic saline using an 18-gauge needle. Lavage fluid was collected in sterile tubes and put on ice. After collection of peritoneal fluid, deeper anesthesia was induced by *i.p.* injection of 0.07ml/g FFM mixture (Fentanyl 0.315mg/ml, Fluanisone 10mg/ml (both Janssen, Beersen, Belgium), and Midazolam 5mg/ml (Roche, Mijdrecht, The Netherlands). After opening of the abdomen blood was drawn from the lower caval vein and collected in sterile tubes containing heparin and immediately placed on ice. Liver lobes were harvested and homogenized at 4°C in 4 volumes of sterile saline using a tissue homogenizer (Biospec Products, Bartlesville, OK). CFUs were determined from serial dilutions of peritoneal lavage, liver homogenates and blood, plated on blood agar plates and incubated at 37°C for 16 h before colonies were counted.

Cell counts and differentials:

Cell counts, determined on each peritoneal lavage sample stained with Türck's solution (Merck, Darmstadt, Germany), were counted in a hemocytometer (Türck counting chamber). The cells were then diluted to a final concentration of 10^5 cells/ml and differential cell counts were performed on cytospin preparations stained with Giemsa.

Cytokine/chemokine assays:

Cytokines and chemokines (tumor necrosis factor (TNF)-α, interleukin (IL)-6, IL-10, monocyte chemoattractant peptide (MCP)-1) were measured using the cytometric bead array (CBA) multiplex assay (Becton Dickinson, San Diego, CA) according to the manufacturer's instructions. The detection limits were 5 pg/ml. Keratinocyte-derived chemokine (KC), macrophage-inflammatory protein (MIP)-2 and IL-1β concentrations were determined using commercially available ELISAs (R&D Systems, Minneapolis, MN).

Bacterial killing assay:

Bacterial killing was determined according to a protocol published recently (25). In brief, RAW 264.7 cells (ATCC, Manassas, VA) were mobilized using 5mg/ml lidocaine in PBS, washed and plated in 24-well plates at a density of $2x10^5$ cells/well. Cells were allowed to adhere for 2h at 37C and washed thoroughly with serum-free (SF) RPMI. *E. coli* O18:K1 were added at a multiplicity of infection (MOI) of 100 and spun onto cells at 2000rpm for 5min, after which plates were placed at 37C for 10min. Each well was then washed 5 times with ice-cold PBS to remove extracellular bacteria. To determine bacterial uptake after 10min, triplicate of wells were lysed with sterile H_2O and designated

as t=0. Pre-warmed SF-RPMI with or without 50µg/ml OxPAPC was added to remaining wells and plates were placed at 37C for 5, 10, 30, 60 or 90min after which cells were again washed 5 times with ice-cold PBS and lysed as described above. Cell-lysates were plated in serial-fold dilutions on blood agar plates and bacterial counts were enumerated after 16h. Bacterial killing was expressed as the percentage of killed bacteria in relation to t=0 (percent killing = 100 – {(# CFU at time x / # CFU at time 0) x 100}).

Phagocytosis assays:

Phagocytosis was evaluated in essence as described before (26, 27). Peritoneal lavage was performed in wild type and $CD14^{-/-}$ mice (n=8 per strain) using 5ml of sterile saline. Lavage fluid was collected in sterile tubes and put on ice. Peritoneal macrophages were washed, counted and resuspended in RPMI 1640 at a final concentration of $1x10^6$ cells/ml. Cells were then allowed to adhere in 12-well microtiter plates (Greiner, Alphen a/d Rijn, The Netherlands) over night. Adherent monolayer cells were washed thoroughly with Hanks' balanced salt solution (HBSS) and incubated with FITC-labeled heat-killed *E. coli* (O18:K1, $1x10^8$ CFU/ml) in the presence or absence of 50µg/ml OxPAPC at 37C or 4C for 30min. Immediately thereafter cells were put on ice, washed in PBS, suspended in "Quenching" solution (Orpegen, Heidelberg, Germany) and analyzed using a FACSCalibur (Becton Dickinson). To obtain primary PMNs, wild type mice (n=8) were injected i.p. with 4% proteose peptone (Difco, Detroit, MI). The next day mice were anesthetized by inhalation of isoflurane (Abbott Laboratories, Kent, U.K.) and peritoneal lavage was performed with 5ml of sterile saline using an 18-gauge needle. Lavage fluid was collected in sterile tubes, washed twice and cells were seeded in tissue culture plates to get rid of adherent macrophages. Non-adherent cells were counted after 2 hours and consisted of >95% PMNs. Phagocytosis-assay was performed

as described above. The phagocytosis index of each sample was calculated: (mean fluorescence x % positive cells at 37C) minus (mean fluorescence x % positive cells at 4C). The same procedure was followed when using RAW 264.7 cells with the exception of different incubation times (up to 240min) and an additional proteinase K (Promega, Leiden, the Netherlands) step (250µg/ml at RT for 30min) to remove extracellular bacteria before FACS analysis. In some experiments LPS (100ng/ml; from E.coli O55:B5, Sigma) was added during overnight adherence. When indicated anti-SR-A antibody (clone 2F8, Serotec, Kidlington, UK) or isotype control (Serotec) were added at 10µg/ml. Phagocytosis of fluorescent polystyrene microspheres (FluoroSpheres® 1µm, Molecular Probes, Eugene, OR) was performed with RAW 264.7 cells that were co-incubated with increasing doses of OxPAPC (10-50-100µg/ml), DMPC (50µg/ml) or carrier at 37C. Uptake was analyzed by FACS after 120min and related to 4C controls as described above.

Endocytosis/Pinocytosis assays:

Cellular uptake of horseradish peroxidase (HRP; Sigma), FITC-dextran (Molecular Probes), Lucifer Yellow (LY; Molecular Probes) or mannosylated BSA-FITC (Sigma) was determined as reported earlier (28). RAW 264.7 cells were cultured in 12-well plates at a concentration of $0.5x10^6$ cells/well and allowed to adhere over night in RPMI supplemented with 10%FCS. The next day, cells were washed thoroughly in serum-free RPMI and FITC-dextran (1mg/ml), LY (1mg/ml) or mannosylated BSA-FITC (10µg/ml) were added and cells were incubated at 37C for indicated times. In some experiments excess mannan (from Saccharomyces cervisiae, Sigma) was added at a concentration of 3mg/ml. At indicated time-points, cells were put on ice, washed thoroughly with cold PBS and analysed by FACS analysis. Cells pulsed at 4C were used to determine background uptake. The uptake index

of each sample was calculated: (MF * % positive cells at 37C) minus (MF * % positive cells at 4C). To determine uptake of HRP, cells were cultured as described above, HRP was added at indicated concentrations and incubated for 3h at 37C. Next, cells were washed 4 times, lysed with 0.05% Triton X-100 in 10mM Tris buffer, pH 7.4 for 30min. The enzyme activity of the lysate was measured using o-phenzlendiamine and H_2O_2 as substrate.

Statistical analysis:

Differences between groups were calculated by Mann-Whitney U test or one-way ANOVA. For survival analysis, Kaplan-Meier analysis followed by log rank test was performed. Values are expressed as mean±SEM. A p-value <0.05 was considered statistically significant.

Results:

OxPL impair survival during E.coli peritonitis in vivo

OxPL have been shown to improve survival during murine endotoxemia due to their capacity to reduce the bioavailability of LPS, thereby attenuating overwhelming systemic inflammation (16). We consequently were interested in studying the effect of OxPL such as oxidized 1-palmitoyl-2-arachidonoyl-sn-glycero-3-phosphorylcholin (OxPAPC) on the course of septic peritonitis induced by viable Gram-negative bacteria, i.e. microorganisms that express LPS. Mice were inoculated intraperitoneally (i.p.) with *E. coli* together with OxPAPC or vehicle and observed for 5 days. As depicted in Fig. 1A, OxPAPC treated mice started to succumb as early as 20h after infection while all control mice remained alive till t=38h. In total 92% (11/12) of OxPAPC treated mice died versus only 42% (5/12) of the control animals (p=0.004). Hence, the administration of OxPAPC rendered mice more susceptible to *E. coli* peritonitis.

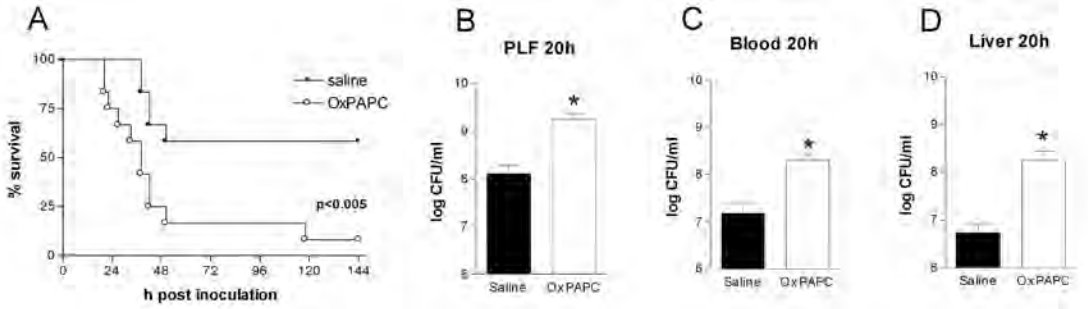

Fig. 1. OxPAPC increases mortality and facilitates bacterial outgrowth and dissemination.

Mice received either OxPAPC (12.5 mg/kg i.p.; open symbols) or carrier (saline; closed symbols) and were *i.p.* infected with 1.2×10^4 CFUs *E.coli*. (A) Survival data are representative of two independent experiments of n=12 per group; p value indicates the difference between survivals by log rank test. (B) In separate experiments, mice were treated as above and PLF, blood and liver CFUs were determined 20 hours after infection. Data are mean±SEM of n=8 mice per group. Results are representative of 2 independent experiments. * indicates $p<0.05$ versus control mice.

OxPL facilitate bacterial growth and dissemination

To obtain insight in the mechanism underlying the accelerated and higher mortality of mice that received OxPAPC, we repeated this experiment and sacrificed mice 4 or 20h after infection to enumerate bacterial counts in peritoneal lavage fluid (PLF, the primary site of infection), blood and liver (to evaluate to which extent the infection became systemic). Already 4h after induction of peritonitis bacterial counts in OxPAPC-treated mice were up to one log higher than in controls, but the differences between groups did not reach statistical significance (control versus OxPAPC (x 10^3 CFU/mL): PLF: 2.0±0.6 vs. 10.2±3.6; blood: 1.8±0.8 vs. 20.9±9.6; liver: 8.8±6.0 vs. 27.8±12.5). Thereafter, *E. coli* grew exponentially in all body compartments but much faster in OxPAPC treated animals and significantly increased CFU counts were recovered from PLF, blood and liver from these mice 20h after infection (Fig. 1B to D). Therefore, the i.p. administration of OxPAPC is associated with an increased bacterial outgrowth and dissemination during *E. coli* peritonitis.

OxPL transform wild type mice into a CD14-deficient phenotype

Because earlier findings pointed towards the fact that OxPL inhibit the interaction of LPS with LBP and CD14 (16) and since LPS is a major immunogenic component of *E. coli* (29), we next aimed to clarify whether the effects of OxPAPC described above could be explained by a functional CD14-blockade in the presence of these phospholipids. For this purpose $CD14^{-/-}$ and wild-type mice were treated with OxPAPC or control lipids (dimyristoylphosphatodylcholine, DMPC) and infected i.p. with *E. coli*. Survival studies disclosed that $CD14^{-/-}$ mice were highly susceptible to *E. coli* peritonitis and succumbed quickly

(Fig. 2A). The administration of OxPAPC transformed wild-type mice into a $CD14^{-/-}$ phenotype whereas no additional effect on lethality was observed in $CD14^{-/-}$ animals treated with OxPAPC (Fig. 2B). Of note, to exclude potential non-specific effects of lipids, we used control lipids (DMPC) instead of carrier (NaCl) in this set of experiments. As expected, DMPC treated mice behaved exactly like mice that received carrier in earlier experiments, i.e. they showed an improved survival when compared to OxPAPC treated animals. Mortality rates were slightly higher in this experiment (compared to Fig. 1A), due to the – in retrospect – higher number of bacteria mice were infected with. We then repeated this experiment and enumerated bacterial counts 20h after infection. $CD14^{-/-}$ mice treated with control lipids (DMPC) displayed significantly increased bacterial counts in PLF, liver and blood when compared with DMPC treated wild type mice (Figure 2C-E). OxPAPC treatment enhanced bacterial outgrowth in wild type mice, confirming the experiments shown in Figure 1 (again illustrating the fact that DMPC treatment results in identical results as carrier treatment). Importantly, OxPAPC did not further increase bacterial loads in $CD14^{-/-}$ mice (Fig. 2C, D, E). In addition, although the numbers of *E.coli* CFU tended to be higher in blood and livers of OxPAPC treated $CD14^{-/-}$ mice than in OxPAPC treated wild type mice (Figure 2D and E), the differences between groups did not reach statistical significance. Together, these findings underline the importance of CD14 during Gram-negative peritonitis and lay emphasis on CD14 as a potential target molecule that might explain the detrimental effects induced by OxPL *in vivo*.

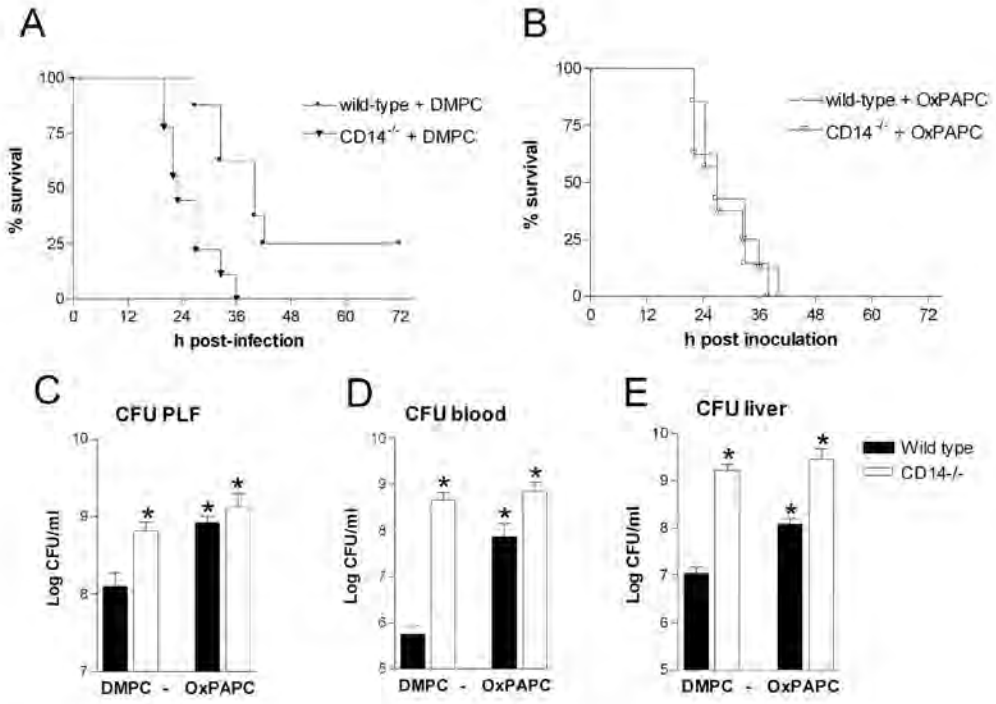

Fig. 2. OxPAPC does not further increase the enhanced mortality of CD14$^{-/-}$ mice.

Wild type and CD14$^{-/-}$ mice were *i.p.* infected with 2x10^4 CFUs *E. coli* in addition to administration of 12.5mg/kg control lipids (DMPC; A) or OxPAPC (B). All four groups of mice were infected simultaneously and survival curves were separated for reasons of clarity (all CD14$^{-/-}$ and/or OxPAPC treated mice succumbed at the same pace with $p<0.05$ versus wild-type mice that received DMPC). Survival was monitored over 1 week, n=8 per group; P value indicates the difference between survivals by log rank test. Experiments were repeated and mice were infected *i.p.* with 1.2x10^4 CFUs E. coli 20h before bacterial counts were enumerated in PLF (C), blood (D) and liver (E). * $p<0.05$ versus wild type DMPC mice.

OxPL do not influence early cytokine/chemokine responses

Having shown that OxPL impaired outcome, we then asked which factors might be involved in the outgrowth and spread of *E. coli*. Responses accountable for an appropriate innate immune response during peritonitis include the local production of proinflammatory cytokines and chemokines at the site of the infection (27, 30, 31). Since OxPL can inhibit LPS bioavailability (16), we considered it possible that OxPAPC would impair the early cytokine/ chemokine response to *E. coli* thereby enhancing susceptibility to abdominal sepsis. To address this issue we measured IL-6, TNF-α, IL-1β, MCP-1, KC, MIP-2 and IL-10 in PLF and plasma. As shown in Table 1, OxPL did not impair

the early induction of pro-inflammatory cytokines after *i.p.* infection with *E. coli.* Peritoneal IL-6, TNF-α, MCP-1 and KC concentrations even were higher in OxPL treated mice at t=4h, which indicates that a suppressed early immune response cannot explain differences in outcome and bacterial elimination (Table 1).

Table 1

OxPAPC does not impair the early cytokine/chemokine response

	PLF		Plasma	
(pg/ml)	Co	OxPAPC	Co	OxPAPC
IL-6	28.4±6.7	256.6±77.7 [A]	1,535±423	2,559±791
TNF-α	8.8±0.5	14.3±2.0 [A]	436±173	639±201
IL-1β	136±51	358±38 [A]	ND	ND
MCP-1	152.6±29.1	548.9±137.8 [A]	6,230±1,431	6,732±1,386
KC	25.5±0.5	273.5±104 [A]	24,183±5,897	6,963±3,198 [A]
MIP-2	125.6±0.6	149.9±19.9	845±173	763±228
IL-10	89.4±5.2	98.1±4.1	4.9±1.3	19.6±3.1 [A]

Wild type mice (n=8 per group and time-point) were inoculated *i.p.* with $1.2x10^4$ CFU *E. coli* and 12.5mg/kg OxPAPC or carrier (NaCl, control mice). PLF and plasma was obtained after 4h and cytokines/chemokine concentrations were assayed as described in M&M. Data are mean±SEM, [A] indicates $p<0.05$ versus NaCl treated control mice; ND indicates: not detectable.

Since PMN influx to the peritoneal cavity is a critical component of the innate immune response during peritonitis, we next determined leukocyte counts in PLF. However, 4h after induction of peritonitis we did not find any indication for an impaired leukocyte influx (Table 2).

Table 2

OxPAPC does not attenuate early cell recruitment

	4h (cells$x10^4$/ml)		
	Total	PMN	PM
NaCl	37.2 ± 11.4	23.0 ± 6.6	14.2 ± 5.2
OxPAPC	108.0 ± 37.9	57.0 ± 22.8	51.0 ± 15.7 [A]

Wild type mice (n=8) were infected i.p. with $1.2x10^4$ CFU E. coli and 12.5mg/kg OxPAPC or carrier (NaCl) and PLF was obtained after 4h and 20h. Total cell counts were determined and differentials done on cytospin preparations stained with Giemsa. Data are mean ± SEM, [A] indicates $p<0.05$ versus NaCl treated mice.

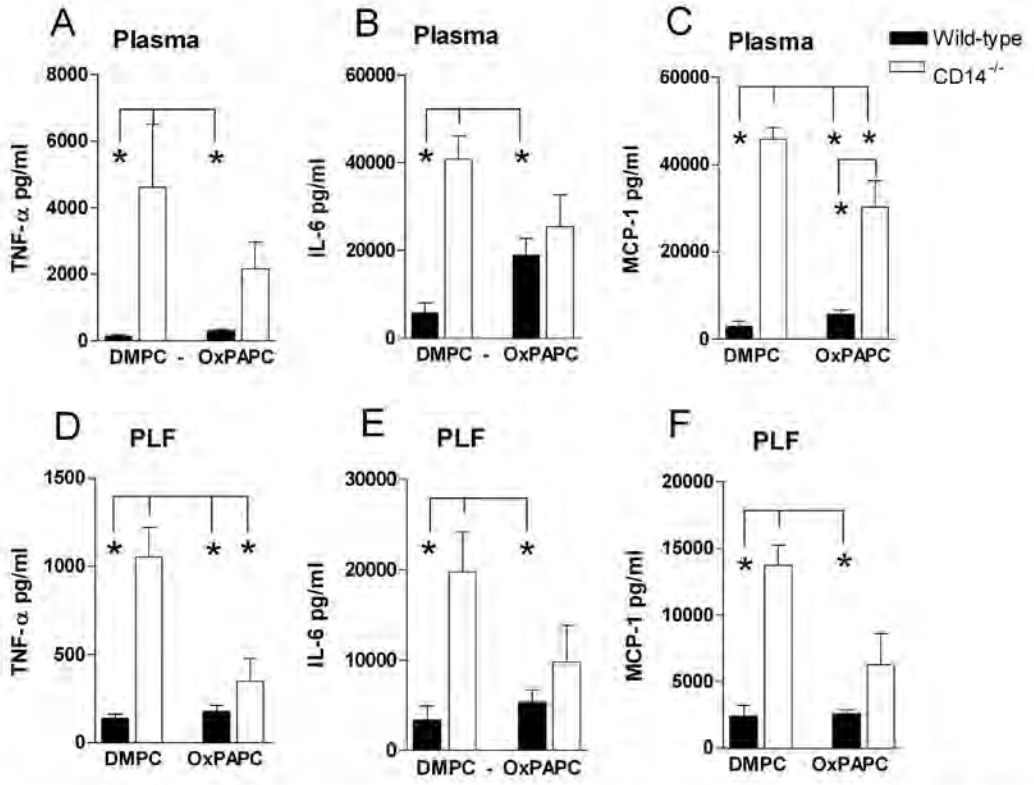

Fig. 3. Cytokine/Chemokine response in wild-type and CD14$^{-/-}$ mice treated with OxPL.

Wild type (filled bars) and CD14$^{-/-}$ (open bars) mice were treated with 12.5mg/kg control lipids (DMPC) or OxPAPC and infected with 1.2x10^4 CFUs *E. coli i.p.*. PLF and plasma TNF-α, IL-6 and MCP-1 concentrations were measured after 20h. Mean±SEM; * $p<0.05$ versus indicated group.

On the contrary, OxPAPC treated mice had the tendency to attract more leukocytes than control mice, likely as a result of the higher bacterial load in these mice. Thus, the number of PMN at the site of infection does not explain differences in bacterial clearance and outcome. When examining the local peritoneal and systemic cytokine/chemokine response in wild-type and CD14$^{-/-}$ mice at t=20h, we identified an enormously increased release of IL-6, TNF-α and MCP-1 in PLF and plasma of CD14$^{-/-}$ animals after 20h (Fig. 3), whereas MIP-2 and KC levels were similar in all groups (data not shown). These values by far exceeded the levels measured in wild-type mice treated with OxPAPC. Of interest, CD14$^{-/-}$ control mice (i.e. DMPC treated) had highest cytokine/chemokine concentrations, whereas CD14$^{-/-}$ animals

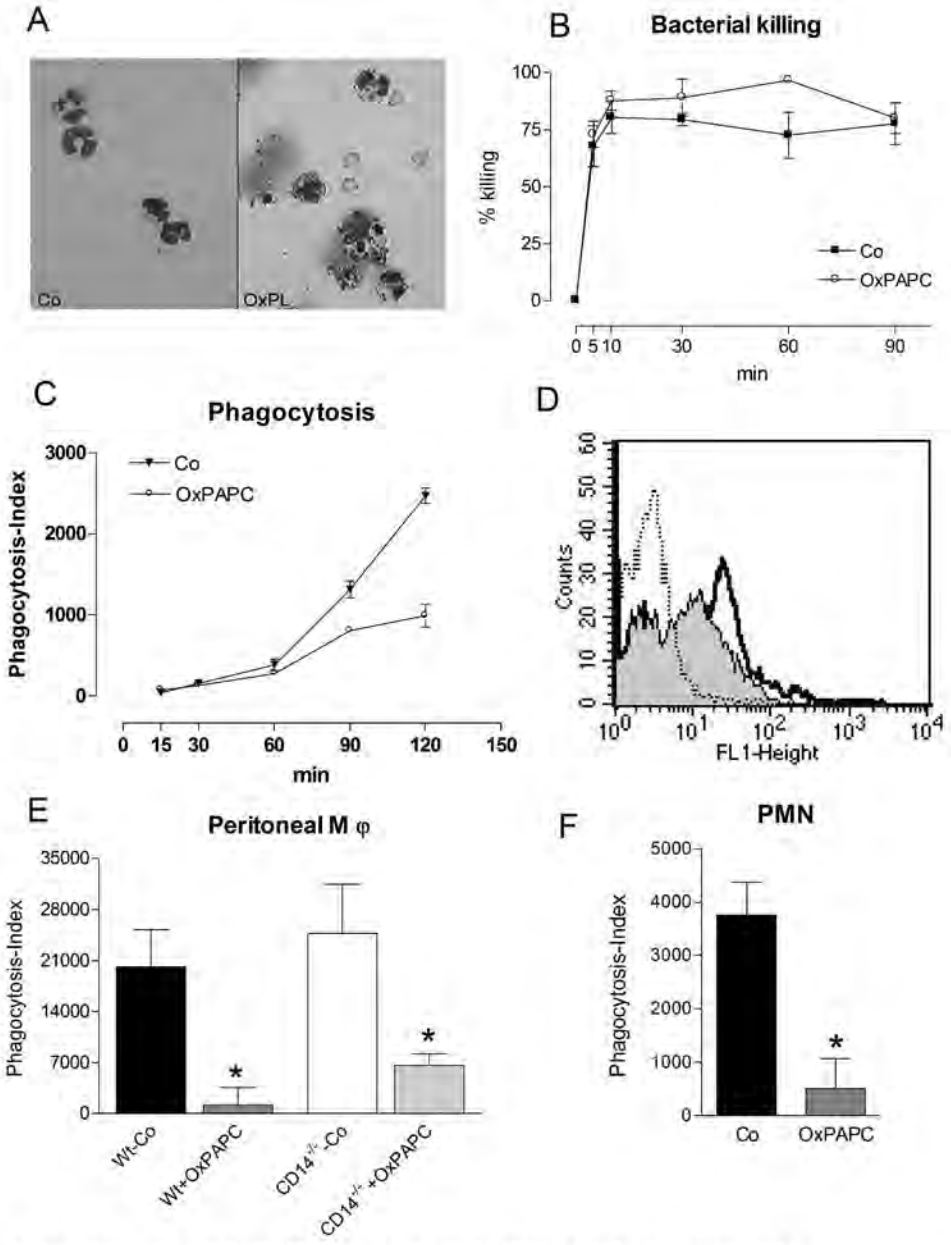

Fig. 4. Impact of OxPAPC on bacterial killing and phagocytosis.

(A) Representative cytospin preparations of peritoneal lavage cells stained with Giemsa 20h after infection with $1.2x10^4$ CFU *E. coli.* (left: control mice, right: OxPAPC-treated animals). (B) RAW 264.7 cells were incubated with viable *E. coli* (MOI 100) and bacterial killing was assessed in the presence of carrier (Co) or OxPAPC (50µg/ml) over time. (C and D) RAW 264.7 cells ($1x10^6$/ml) were incubated at 37C with $1x10^8$ CFU/ml FITC-labeled E. coli and time-dependent phagocytosis was quantified in the presence or absence of OxPAPC (50µg/ml) by FACS analysis. (D) Representative histogram at t=120min: hatched line: 4C control; black line: 37C control group; filled grey: 37C OxPAPC group. Depicted are results from at least 2 independent experiments performed in triplicate. Primary peritoneal macrophages (E) or primary PMNs (F) of wild-type and $CD14^{-/-}$ mice (both $1x10^6$/ml) were incubated with $1x10^8$ CFU/ml FITC-labeled *E. coli* for 30min. Phagocytosis was quantified in the presence or absence of OxPAPC (50µg/ml) by FACS analysis. Data are mean±SEM of n=4 (E) or n=8 (F) per group; * indicates $p<0.05$ versus controls.

that received OxPAPC showed less pronounced elevations (Fig. 3). Hence, OxPAPC modestly reduced the cytokine response in $CD14^{-/-}$ but not in wild type mice *in vivo*. On the other hand, $CD14^{-/-}$ animals displayed a severely impaired ability to attract PMNs and macrophages to the peritoneal cavity, irrespective of OxPAPC treatment (Table 3).

Table 3

Differential effects of CD14 deficiency and OxPAPC on cell recruitment

Group	20h (cells x 10^6/ml)		
	Total	PMN	PM
Wt DMPC	23.3±1.6	18.9±1.3	7.1±1.2
$CD14^{-/-}$ DMPC	2.9±0.4 [A]	2.6±0.3 [A]	0.3±0.1 [A]
Wt OxPAPC	16.2±2.7	13.6±2.1	2.6±0.7
$CD14^{-/-}$ OxPAPC	2.7±0.7 [A]	2.4±0.6 [A]	0.3±0.1 [A]

Wild type (Wt) and $CD14^{-/-}$ mice (n=8 per strain and treatment) were inoculated i.p. with $1.2x10^4$ CFU *E. coli* and 12.5mg/kg OxPAPC or DMPC, respectively, and PLF was obtained after 20h. Total cell counts were determined in a Tuerck chamber and differentials done on cytospin preparations stained with Giemsa. Data are mean ± SEM, [A] indicates $p<0.05$ versus wild type mice that received the same lipid preparation.

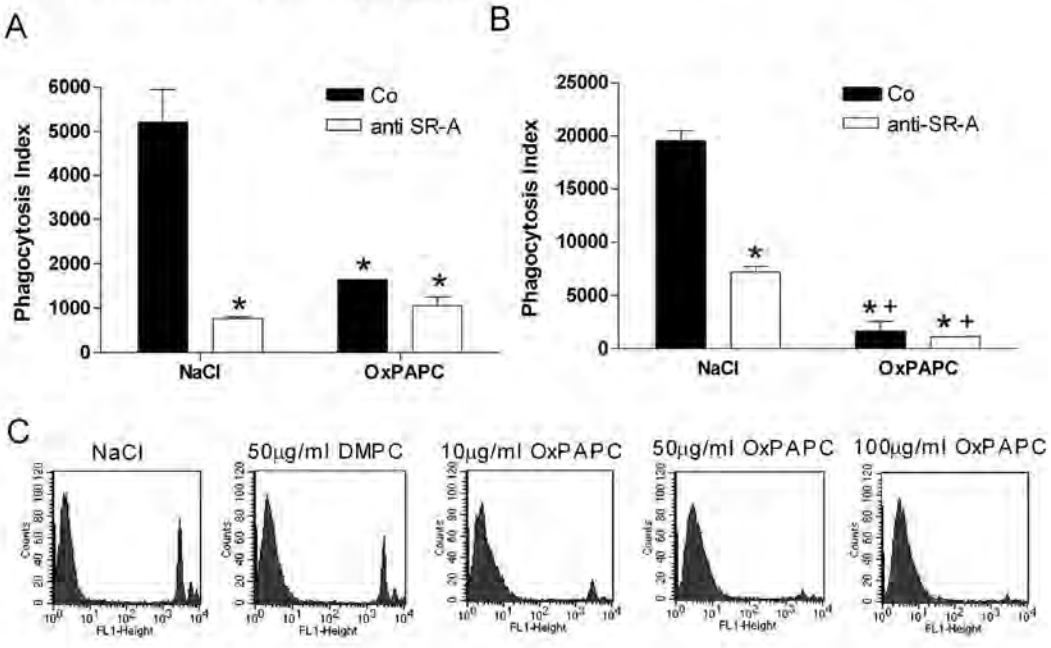

Fig. 5. OxPAPC impair phagocytosis of *E.coli* and Fluorospheres.

Unstimulated (A) or LPS-stimulated (B) RAW 264.7 cells were incubated with $1x10^8$ CFU/ml FITC-labeled *E. coli* in the presence of carrier or OxPAPC (50µg/ml) and/or anti-SR-A (10µg/ml) or isotype control (Co) and uptake was assessed by FACS. Data are mean±SEM; * indicates $p<0.05$ versus carrier+isotype control, + indicates $p<0.05$ versus carrier+anti-SR-A. (C) RAW 264.7 cells were incubated with Fluorospheres in the presence of carrier, DMPC or indicated amounts of OxPAPC and uptake at t=120min was measured by FACS.

Even 20h after the induction of peritonitis when vast amounts of bacteria were encountered in all mice, the number of PMNs and macrophages was significantly reduced in the absence of CD14. Hence, while OxPAPC did not impair the attraction of inflammatory cells to the site of infection, CD14 crucially contributes to this important host defense mechanism.

OxPAPC impairs the phagocytic capacity of peritoneal macrophages and PMN

Having shown that OxPAPC affects CD14-independent pathways of the innate immune response, we next aimed to investigate the functional and cellular alterations induced by OxPAPC. Microscopic evaluation of infiltrating leukocytes in PLF of OxPAPC-treated mice revealed a high proportion of cells covered by enormous amounts of bacteria (Fig. 4A). Although bacteria were also visible in samples from control mice, the number and close association with leukocytes was much less impressive. This led us to examine whether OxPAPC influences functional properties of leukocytes, such as killing or phagocytosis of bacteria. Using primary peritoneal macrophages and PMNs from C57/BL6 mice or RAW 264.7 peritoneal macrophages, we studied both phagocytosis and bacterial killing in the presence of absence of OxPAPC. As depicted in Fig. 4B, the addition of OxPAPC following uptake of bacteria did not affect the killing properties of macrophages. However, OxPAPC impaired the ability of phagocytes to internalize E. coli in a time-dependent manner (Fig. 4C and D). In addition, both primary peritoneal macrophages and PMNs showed an impaired phagocytosis of FITC-labeled E.coli in the presence of OxPAPC (Fig. 4E and F). Of importance, CD14 did not interfere with the phagocytic properties of macrophages or PMNs, as indicated by unaltered phagocytosis rates of primary cells from $CD14^{-/-}$ mice (Fig. 4E). Together,

these data showed that OxPAPC inhibits phagocytosis of E.coli but does not influence bacterial killing.

OxPAPC impairs endocytosis by macrophages

In order to further understand the impact of OxPL on phagocytosis, we then asked whether our finding of impaired phagocytosis in the presence of OxPAPC is specific for pathogens such as *E. coli,* or reflects a more general phenomenon. Since we performed all phagocytosis assays (Fig. 4) under serum-free conditions using non-opsonized bacteria, the possibility that OxPAPC interferes with Fc-receptor or complement-mediated phagocytosis is unlikely. However, scavenger receptors (SR-)A have been identified as important receptors that specifically contribute to Fc-receptor independent phagocytosis of *E.coli* (32). We therefore investigated the potential contribution of SR-A and found, in accordance with earlier reports (32), that blocking SR-A with anti-SR-A antibodies significantly reduced uptake of *E. coli* by macrophages (Fig. 5A). Addition of OxPAPC alone showed exactly the same inhibitory effect as anti-SR-A alone and no additive effect was observed when the combination of both reagents was tested (Fig. 5A). We then tried to more closely imitate the *in vivo* situation seen during peritonitis, when peritoneal macrophages encounter LPS or bacteria that activate them before they phagocytose whole bacteria, and pre-incubated macrophages with LPS prior to the addition of *E. coli*. As expected, phagocytosis of *E.coli* was tremendously increased when macrophages were pre-activated by LPS (Fig. 5B; compare Y-axes of panels A and B). In addition, when anti-SR-A or OxPAPC were added to these activated macrophages, the inhibitory action of OxPAPC clearly exceeded that of anti-SR-A (Fig. 5B).

Together these findings indicate that OxPAPC either interferes with phagocytosis receptors other than SR-A, or that OxPAPC utilizes additional

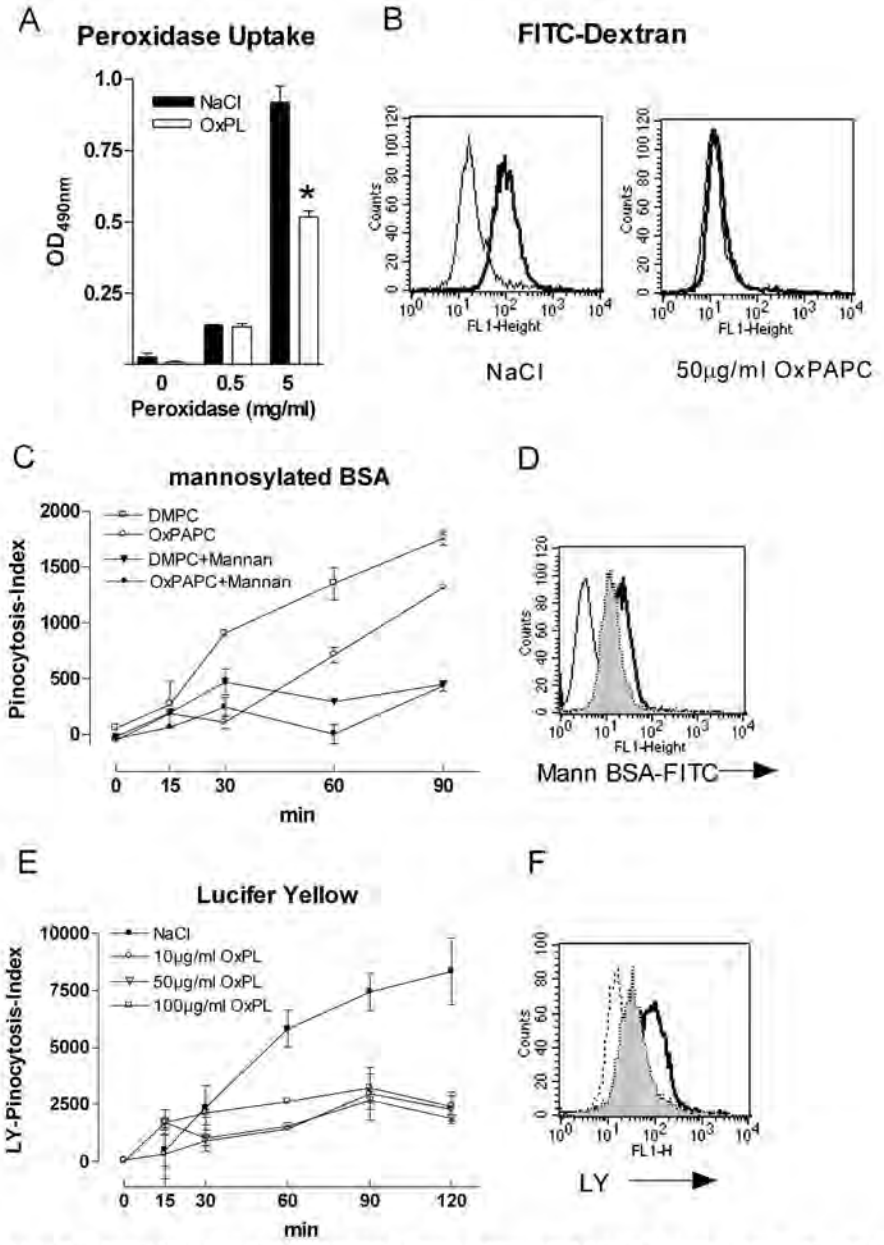

Fig. 6. OxPAPC inhibit receptor-mediated and fluid-phase endocytosis.

(A) RAW 264.7 cells were incubated with indicated amounts of HRP in the presence of OxPAPC (50µg/ml) or carrier. HRP uptake was measured photometrically (490nm) in cell lysates after addition of OPD. RAW 264.7 cells were incubated with FITC-Dextran (B), mannoslyated BSA-FITC (C and D) or LY (E and F) for indicated times in the presence of carrier or OxPAPC and uptake was measured by FACS. (B) Depicts a representative histogram after 60min incubation with FITC-Dextran. (C) Time-dependent reduction of mann-BSA uptake in the presence of OxPAPC (50µg/ml, open circles) as compared to DMPC (open squares). Excess mannan (3mg/ml) inhibits uptake of mann-BSA-FITC irrespective of OxPAPC (C, filled symbols). (D) Representative histogram after incubation with mann-BSA-FITC at t=30min (thin line: 4C control, thick line: 37C carrier, filled grey: 37C OxPAPC). (E) Fluid phase pinocytosis of LY is inhibited in the presence of OxPAPC (10, 50 or 100 µg/ml, open symbols) as compared to carrier (closed symbola). A representative histogram at t=120min is depicted in F (thin line: 4C control; thick line: 37C carrier; filled grey: 37C 10µg/ml OxPAPC). Mean±SEM; * indicates $p<0.05$ versus carrier.

(possibly activation-dependent) pathways. To assess SR-A-independent phagocytosis and the role of OxPAPC herein, we next investigated the uptake of polystyrene microspheres and identified that OxPAPC dose-dependently inhibited the uptake of these microspheres (Fig. 5C). Importantly, control lipids (DMPC) did not show this effect.

Considering the fact that macrophages are quite unique in their capacity to not only phagocytose but also ingest particles via fluid phase pinocytosis and macropinocytosis, the latter also involving actin remodeling (33), we next examined whether these properties were also influenced by OxPAPC. For this purpose we first analyzed the uptake of peroxidase (HRP) by macrophages and found reduced internalization when OxPAPC was added (Fig. 6A). To study effects on a single cell level, we then chose to test the uptake of FITC-dextran, which is internalized via macropinocytosis, representing an uptake mechanism that is quite uniquely found in macrophages, DCs and epithelial cells (33). For this purpose, macrophages were incubated with FITC-Dextran and OxPAPC clearly diminished the macropinocytotic uptake of FITC-dextran (Fig. 6B). Because HRP and dextran uptake has been shown to partly depend on mannose-receptor (MR) (28), we then investigated the uptake of a well-defined, pure MR ligand, namely mannosylated BSA-FITC (28). The addition of OxPAPC reduced receptor-mediated endocytosis of mannosylated BSA when compared to DMPC (Fig. 6C) or carrier (Fig. 6D). Moreover, addition of excess mannan abolished the uptake of mannosylated BSA thus confirming the specificity of this mechanism (Fig. 6C). We finally studied whether OxPAPC also interferes with receptor-independent, fluid-phase endocytosis. Lucifer yellow (LY) has been described as a receptor-independent ligand that is taken up by cells via pinocytosis (28, 34). We found that even small amounts of OxPAPC diminished the uptake of LY (Fig. 6E and F). Together, OxPAPC inhibits phagocytosis as well as receptor-mediated and receptor-independent pathways of endocytosis/pinocytosis by macrophages.

Discussion:

Gram-negative peritonitis is a life threatening condition frequently associated with systemic dissemination of bacteria and septic shock. Host defense in peritonitis is an established domain of the innate immune system as the rapid response to invading pathogens is essential for the host to survive. OxPL are endogenous mediators of inflammation and products of oxidative stress that have been shown to also exert anti-inflammatory effects (11, 16, 35). Inhibition of LPS-LBP and LPS-CD14 interactions by OxPAPC protected mice from overwhelming inflammation during endotoxemia (16). In the present study we examined the functional *in vivo* role of OxPAPC and its potential interaction with CD14 during murine *E. coli* peritonitis. Our key finding was that OxPAPC, in sharp contrast to its protective effect during LPS-induced shock, rendered mice highly susceptible to abdominal sepsis induced by viable *E. coli* by a mechanism that is CD14 independent. Although both administration of OxPAPC and CD14 deficiency resulted in increased mortality and bacterial growth after *i.p.* infection with *E. coli*, the mechanisms accounting for these findings differed: whereas OxPAPC interfered with crucial functional properties of recruited phagocytes reducing their phagocytic capacity, CD14 deficiency resulted in an attenuated recruitment of phagocytes to the site of the infection. The present data reveal for the first time that OxPL may impair host defense against Gram-negative infection.

Host defense in peritonitis is a delicate balance between pro-inflammatory pathways aimed at the rapid elimination of bacteria and anti-inflammatory pathways intended to prevent systemic inflammation (36). Any imbalance in pro- or anti-inflammatory mediators might prove harmful. We initially considered it conceivable that OxPAPC, due to their anti-inflammatory properties described in models of acute inflammation (16), might represent an

endogenous mediator that assists preventing overwhelming inflammation and therefore would reduce mortality in mice suffering from severe peritonitis. Our findings, however, could not confirm this hypothesis but rather disclosed an important, though detrimental, role for OxPAPC in host defense against *E. coli in vivo.* In the presence of OxPAPC a higher proportion of mice succumbed and this was accompanied by an increased bacterial load in all organs tested. The important attraction of phagocytes to the peritoneal cavity was not compromised by OxPAPC. It has been reported earlier, that OxPL themselves induce the production of chemokines such as IL-8, KC and MCP-1 *in vitro* as well as *in vivo* (11, 14, 37). In our hands, the addition of OxPAPC during *E. coli* peritonitis *in vivo* was accompanied by increased peritoneal MCP-1 and KC concentrations, which may have contributed to the elevated number of PMNs and monocytes/macrophages in peritoneal fluid early (t=4h) after induction of peritonitis.

OxPAPC can inhibit the interaction of LPS with CD14 (16). Since CD14 is a major component of the LPS-signaling complex on innate immune cells and an important player in host defense against Gram-negative bacterial infections (3, 38-42), we were interested to study whether our observations of increased bacterial outgrowth and mortality in OxPAPC-treated mice were linked to an inhibitory action of OxPL on the interaction of LPS with CD14. Using CD14 gene-deficient mice, we first were able to demonstrate an important role of CD14 in the innate immune response during *E. coli* peritonitis *in vivo.* Analogous to our earlier studies, where we investigated the role of LBP in this infection model and in line with earlier reports in Salmonella peritonitis, an inadequate onset of inflammation in $CD14^{-/-}$ mice led to early systemic dissemination and increased bacterial outgrowth (9, 43). Although bacterial dissemination and survival rates were identical in $CD14^{-/-}$ and OxPAPC-treated mice, the underlying mechanisms differed. OxPAPC administration had no influence

on the number of PMN attracted to the peritoneal cavity but recruited PMNs imposed covered by bacteria. This inspired us to investigate the functional properties of PMNs and macrophages and led us to discover an impaired phagocytosis by professional phagocytes in the presence of OxPAPC. Indeed, RAW cells as well as primary PMNs and peritoneal macrophages were less capable of effectively phagocytosing *E. coli* in the presence of OxPAPC. Although CD14 was attributed to phagocytosis of Gram negative bacteria by an earlier report (44), we could not disclose a role for this receptor. In line, our laboratory previously found no effect of a blocking anti-CD14 antibody intravenously administered to human subjects on phagocytosis by blood monocytes and PMNs (42). However, CD14 is known to participate in the elimination of apoptotic cells and OxPAPC – due to its capacity to interfere with CD14 - is certainly a candidate molecule that might interact with this process (45). In fact, one report showed an impaired phagocytosis of apoptotic cells in the presence of minimally modified LDL that bind to CD14 and concurrently enhance the uptake of OxLDL (46). Nevertheless, the potential impact of OxPL on phagocytosis of bacteria has not been investigated thus far and we hereby report for the first time that OxPAPC interfere with the elimination of bacteria in vivo and that this mechanism does not depend on CD14.

Another receptor that crucially contributes to opsonin-independent phagocytosis of *E.coli* is SR-A (32). SR-A recognizes a wide range of polyanions including LPS from Gram-negative bacteria. Although not known so far, the possibility exists that OxPAPC interferes with the binding of polyanions to SR-A, thereby preventing the phagocytosis of Gram-negative bacteria. However, our data from activated macrophages clearly demonstrate that OxPAPC inhibits phagocytosis to a greater degree than blocking Ab against SR-A. Addition of OxPAPC to anti-SR-A further reduced the uptake of *E.coli*, thus indicating different inhibitory pathways. Of note, although the class B scavenger receptor

CD36 has been shown to bind OxPAPC (47), CD36 is not involved in the phagocytosis of *E. coli* (48), which precluded us from investigating CD36 as a target receptor that might explain the effects of OxPAPC observed in this study.

Our data indicate that the inhibitory action of OxPAPC is not restricted to phagocytosis of *E. coli.* Considering the multitude of endocytotic pathways elicited by macrophages, we found OxPAPC to not only impair phagocytosis of bacteria but also polystyrene particles as well as receptor-mediated and fluid-phase endocytosis. These findings definitely underline the broad, and potentially harmful, impact of oxidation products generated during bacterial infections or chronic inflammation *in vivo.* Although the pathophysiological impact of these findings remains to be established, we propose a detrimental role for OxPL during bacterial infections. Beside infections, OxPL are found predominantly during chronic inflammation such as atherosclerosis. The here described observations of impaired endocytosis in the presence of OxPL could explain the very recent finding of diverse bacterial products within a single plaque specimen from patients with coronary heart disease (49). The possibility exists that OxPL, present in atherosclerotic plaques, prevent the effective elimination of bacteria that are encountered during asymptomatic phases of bacteremia (such as after dental procedures or translocation from the intestines) thus leading to the accumulation of intracellular bacterial products that in turn might contribute to ongoing inflammation.

It should be noted that although OxPAPC and CD14 deficiency negatively influenced the outcome of *E. coli* peritonitis by different mechanisms, OxPAPC did not further impair host defense in $CD14^{-/-}$ mice. Importantly, however, OxPAPC and CD14 deficiency both impacted on PMNs and macrophages, and although OxPAPC profoundly diminished the capacity of $CD14^{-/-}$ PMNs

and macrophages to phagocytose *E.coli in vitro*, apparently this immune suppressing effect did not further impact on the outcome of $CD14^{-/-}$ mice *in vivo* due to the fact that these animals had very few PMNs and macrophages in their peritoneal cavity and as a consequence already had a severely hampered cellular immune response.

In conclusion, we here demonstrate that OxPAPC reduce host defense against abdominal sepsis caused by *E. coli* most likely by inhibiting the phagocytosing capacity of cells involved in innate immunity by a CD14 independent mechanism. While OxPL might be able to prevent overwhelming inflammation in settings of sterile inflammatory disorders, our results suggest that OxPL generated at sites of inflammation impair the innate immune response to bacterial infections.

Acknowledgements:

We thank I. Kop and J. Daalhuisen for expert technical assistance.

Nonstandard abbreviations used:

DMPC: dimyristoylphosphatodylcholine

KC: keratinocyte-derived chemokine

LBP: LPS-binding protein

LY: Luciferase Yellow

MCP-1: monocyte chemoattractant peptide 1

MIP-2: macrophage inflammatory protein 2

PLF: peritoneal lavage fluid

PM: peritoneal macrophages

PMN: polymorphonuclear neutrophils

OxPAPC: oxidized 1-palmitoyl-2-arachidonoyl-sn-glycero-3-phosphorylcholine

OxPL: oxidized phospholipids

Support:

This work was in part supported by the Austrian Science Foundation (FWF

P18232-B11) to S.K.

References:

1. Lorber, B., and R. M. Swenson. 1975. The bacteriology of intra-abdominal infections. Surg Clin North Am 55:1349-1354.

2. Holzheimer, R. G., K. H. Muhrer, N. L'Allemand, T. Schmidt, and K. Henneking. 1991. Intraabdominal infections: classification, mortality, scoring and pathophysiology. Infection 19:447-452.

3. Wright, S. D., R. A. Ramos, P. S. Tobias, R. J. Ulevitch, and J. C. Mathison. 1990. CD14, a receptor for complexes of lipopolysaccharide (LPS) and LPS binding protein. Science 249:1431-1433.

4. Poltorak, A., X. He, I. Smirnova, M. Y. Liu, C. V. Huffel, X. Du, D. Birdwell, E. Alejos, M. Silva, C. Galanos, M. Freudenberg, P. Ricciardi-Castagnoli, B. Layton, and B. Beutler. 1998. Defective LPS signaling in C3H/HeJ and C57BL/10ScCr mice: mutations in Tlr4 gene. Science 282:2085-2088.

5. Takeuchi, O., K. Hoshino, T. Kawai, H. Sanjo, H. Takada, T. Ogawa, K. Takeda, and S. Akira. 1999. Differential roles of TLR2 and TLR4 in recognition of gram-negative and gram-positive bacterial cell wall components. Immunity 11:443-451.

6. Akira, S., S. Uematsu, and O. Takeuchi. 2006. Pathogen Recognition and Innate Immunity. Cell 124:783-801.

7. Shimazu, R., S. Akashi, H. Ogata, Y. Nagai, K. Fukudome, K. Miyake, and M. Kimoto.

1999. MD-2, a molecule that confers lipopolysaccharide responsiveness on Toll-like receptor 4. J Exp Med 189:1777-1782.

8. Visintin, A., E. Latz, B. G. Monks, T. Espevik, and D. T. Golenbock. 2003. Lysines 128 and 132 Enable Lipopolysaccharide Binding to MD-2, Leading to Toll-like Receptor-4 Aggregation and Signal Transduction. J. Biol. Chem. 278:48313-48320.

9. Knapp, S., A. F. De Vos, S. Florquin, D. T. Golenbock, and T. Van Der Poll. 2003. Lipopolysaccharide Binding Protein Is an Essential Component of the Innate Immune Response to Escherichia coli Peritonitis in Mice. Infect Immun 71:6747-6753.

10. Zhang, R., M.-L. Brennan, Z. Shen, J. C. MacPherson, D. Schmitt, C. E. Molenda, and S. L. Hazen. 2002. Myeloperoxidase Functions as a Major Enzymatic Catalyst for Initiation of Lipid Peroxidation at Sites of Inflammation. J. Biol. Chem. 277:46116-46122.

11. Subbanagounder, G., J. W. Wong, H. Lee, K. F. Faull, E. Miller, J. L. Witztum, and J. A. Berliner. 2002. Epoxyisoprostane and Epoxycyclopentenone Phospholipids Regulate Monocyte Chemotactic Protein-1 and Interleukin-8 Synthesis. Formation of these Oxidized Phospholipids in Response to Interleukin-1beta. J. Biol. Chem. 277:7271-7281.

12. Bochkov, V. N., and N. Leitinger. 2003. Anti-inflammatory properties of lipid oxidation products. J Mol Med 81:613-626.

13. Leitinger, N. 2003. Oxidized phospholipids as modulators of inflammation in atherosclerosis. Curr Opin Lipidol 14:421-430.

14. Furnkranz, A., A. Schober, V. N. Bochkov, P. Bashtrykov, G. Kronke, A. Kadl, B. R. Binder, C. Weber, and N. Leitinger. 2005. Oxidized phospholipids trigger atherogenic inflammation in murine arteries. Arterioscler Thromb Vasc Biol 25:633-638.

15. Berliner, J. A., and A. D. Watson. 2005. A Role for Oxidized Phospholipids in Atherosclerosis. N Engl J Med 353:9-11.

16. Bochkov, V. N., A. Kadl, J. Huber, F. Gruber, B. R. Binder, and N. Leitinger. 2002. Protective role of phospholipid oxidation products in endotoxin-induced tissue damage. Nature 419:77-81.

17. Wurfel, M. M., B. G. Monks, R. R. Ingalls, R. L. Dedrick, R. Delude, D. Zhou, N. Lamping, R. R. Schumann, R. Thieringer, M. J. Fenton, S. D. Wright, and D. Golenbock. 1997. Targeted deletion of the lipopolysaccharide (LPS)-binding protein gene leads to profound suppression of LPS responses ex vivo, whereas in vivo responses remain intact. J Exp Med 186:2051-2056.

18. Jack, R. S., X. Fan, M. Bernheiden, G. Rune, M. Ehlers, A. Weber, G. Kirsch, R. Mentel, B. Furll, M. Freudenberg, G. Schmitz, F. Stelter, and C. Schutt. 1997. Lipopolysaccharide-binding protein is required to combat a murine gram- negative bacterial infection. Nature 389:742-745.

19. Haziot, A., E. Ferrero, F. Kontgen, N. Hijiya, S. Yamamoto, J. Silver, C. L. Stewart, and S. M. Goyert. 1996. Resistance to endotoxin shock and reduced dissemination of gram-negative bacteria in CD14-deficient mice. Immunity 4:407-414.

20. Hoshino, K., O. Takeuchi, T. Kawai, H. Sanjo, T. Ogawa, Y. Takeda, K. Takeda, and S. Akira. 1999. Cutting edge: Toll-like receptor 4 (TLR4)-deficient mice are hyporesponsive to lipopolysaccharide: evidence for TLR4 as the Lps gene product. J Immunol 162:3749-3752.

21. Moore, K. J., L. P. Andersson, R. R. Ingalls, B. G. Monks, R. Li, M. A. Arnaout, D. T. Golenbock, and M. W. Freeman. 2000. Divergent Response to LPS and Bacteria in CD14-Deficient Murine Macrophages. J Immunol 165:4272-4280.

22. Watson, A. D., N. Leitinger, M. Navab, K. F. Faull, S. Horkko, J. L. Witztum, W. Palinski, D. Schwenke, R. G. Salomon, W. Sha, G. Subbanagounder, A. M. Fogelman, and J. A. Berliner. 1997. Structural Identification by Mass Spectrometry of Oxidized Phospholipids in Minimally Oxidized Low Density Lipoprotein That Induce Monocyte/Endothelial Interactions and Evidence for Their Presence in Vivo. J. Biol. Chem. 272:13597-13607.

23. Renckens, R., J. J. T. H. Roelofs, S. A. J. ter Horst, C. van 't Veer, S. R. Havik, S. Florquin, G. T. M. Wagenaar, J. C. M. Meijers, and T. van der Poll. 2005. Absence of Thrombin-Activatable Fibrinolysis Inhibitor Protects against Sepsis-Induced Liver Injury in Mice. J Immunol 175:6764-6771.

24. Renckens, R., J. J. T. H. Roelofs, S. Florquin, A. F. de Vos, H. R. Lijnen, C. van't Veer, and T. van der Poll. 2006. Matrix Metalloproteinase-9 Deficiency Impairs Host Defense against Abdominal Sepsis. J Immunol 176:3735-3741.

25. Blander, J. M., and R. Medzhitov. 2004. Regulation of phagosome maturation by signals from toll-like receptors. Science 304:1014-1018.

26. Wan, C. P., C. S. Park, and B. H. Lau. 1993. A rapid and simple microfluorometric phagocytosis assay. J Immunol Methods 162:1-7.

27. Weijer, S., M. E. Sewnath, A. F. de Vos, S. Florquin, K. van der Sluis, D. J. Gouma, K. Takeda, S. Akira, and T. van der Poll. 2003. Interleukin-18 Facilitates the Early Antimicrobial Host Response to Escherichia coli Peritonitis. Infect. Immun. 71:5488-5497.

28. Sallusto, F., M. Cella, C. Danieli, and A. Lanzavecchia. 1995. Dendritic cells use macropinocytosis and the mannose receptor to concentrate macromolecules in the major histocompatibility complex class II compartment: downregulation by cytokines and bacterial products. J. Exp. Med. 182:389-400.

29. Beutler, B., and E. T. Rietschel. 2003. Innate immune sensing and its roots: the story of endotoxin. Nat Rev Immunol 3:169-176.

30. Echtenacher, B., W. Falk, D. Mannel, and P. Krammer. 1990. Requirement of endogenous tumor necrosis factor/cachectin for recovery from experimental peritonitis. J Immunol 145:3762-3766.

31. Mercer-Jones, M. A., M. S. Shrotri, M. Heinzelmann, J. C. Peyton, and W. G. Cheadle. 1999. Regulation of early peritoneal neutrophil migration by macrophage inflammatory protein-2 and mast cells in experimental peritonitis. J Leukoc Biol 65:249-255.

32. Peiser, L., P. J. Gough, T. Kodama, and S. Gordon. 2000. Macrophage class A scavenger receptor-mediated phagocytosis of Escherichia coli: role of cell heterogeneity, microbial strain, and culture conditions in vitro. Infect Immun 68:1953-1963.

33. Swanson, J. A., and C. Watts. 1995. Macropinocytosis. Trends in Cell Biology 5:424-428.

34. Racoosin, E., and J. Swanson. 1992. M-CSF-induced macropinocytosis increases solute endocytosis but not receptor-mediated endocytosis in mouse macrophages. J Cell Sci 102:867-880.

35. Kronke, G., V. N. Bochkov, J. Huber, F. Gruber, S. Bluml, A. Furnkranz, A. Kadl, B. R. Binder, and N. Leitinger. 2003. Oxidized phospholipids induce expression of human heme oxygenase-1 involving activation of cAMP-responsive element-binding protein. J Biol Chem 278:51006-51014.

36. Sewnath, M. E., D. P. Olszyna, R. Birjmohun, F. J. ten Kate, D. J. Gouma, and T. van Der Poll. 2001. IL-10-deficient mice demonstrate multiple organ failure and increased mortality during Escherichia coli peritonitis despite an accelerated bacterial clearance. J

Immunol 166:6323-6331.

37. Kadl, A., J. Huber, F. Gruber, V. N. Bochkov, B. R. Binder, and N. Leitinger. 2002. Analysis of inflammatory gene induction by oxidized phospholipids in vivo by quantitative real-time RT-PCR in comparison with effects of LPS. Vascul Pharmacol 38:219-227.

38. Bernheiden, M., J. M. Heinrich, G. Minigo, C. Schutt, F. Stelter, M. Freeman, D. Golenbock, and R. S. Jack. 2001. LBP, CD14, TLR4 and the murine innate immune response to a peritoneal Salmonella infection. J Endotoxin Res 7:447-450.

39. Le Roy, D., F. Di Padova, Y. Adachi, M. P. Glauser, T. Calandra, and D. Heumann. 2001. Critical role of lipopolysaccharide-binding protein and CD14 in immune responses against gram-negative bacteria. J Immunol 167:2759-2765.

40. Opal, S. M., J. E. Palardy, N. Parejo, and R. L. Jasman. 2003. Effect of anti-CD14 monoclonal antibody on clearance of Escherichia coli bacteremia and endotoxemia. Crit Care Med 31:929-932.

41. Ulevitch, R. J., and P. S. Tobias. 1999. Recognition of gram-negative bacteria and endotoxin by the innate immune system. Curr Opin Immunol 11:19-22.

42. Verbon, A., P. E. Dekkers, T. ten Hove, C. E. Hack, J. P. Pribble, T. Turner, S. Souza, T. Axtelle, F. J. Hoek, S. J. van Deventer, and T. van der Poll. 2001. IC14, an anti-CD14 antibody, inhibits endotoxin-mediated symptoms and inflammatory responses in humans. J Immunol 166:3599-3605.

43. Yang, K. K., B. G. Dorner, U. Merkel, B. Ryffel, C. Schutt, D. Golenbock, M. W. Freeman, and R. S. Jack. 2002. Neutrophil influx in response to a peritoneal infection with Salmonella is delayed in lipopolysaccharide-binding protein or CD14-deficient mice. J Immunol 169:4475-4480.

44. Grunwald, U., X. Fan, R. S. Jack, G. Workalemahu, A. Kallies, F. Stelter, and C. Schutt. 1996. Monocytes can phagocytose Gram-negative bacteria by a CD14-dependent mechanism. J Immunol 157:4119-4125.

45. Devitt, A., K. G. Parker, C. A. Ogden, C. Oldreive, M. F. Clay, L. A. Melville, C. O. Bellamy, A. Lacy-Hulbert, S. C. Gangloff, S. M. Goyert, and C. D. Gregory. 2004. Persistence of apoptotic cells without autoimmune disease or inflammation in CD14-/- mice. J. Cell Biol. 167:1161-1170.

46. Miller, Y. I., S. Viriyakosol, C. J. Binder, J. R. Feramisco, T. N. Kirkland, and J. L. Witztum. 2003. Minimally Modified LDL Binds to CD14, Induces Macrophage Spreading via TLR4/MD-2, and Inhibits Phagocytosis of Apoptotic Cells. J. Biol. Chem. 278:1561-1568.

47. Podrez, E. A., E. Poliakov, Z. Shen, R. Zhang, Y. Deng, M. Sun, P. J. Finton, L. Shan, B. Gugiu, P. L. Fox, H. F. Hoff, R. G. Salomon, and S. L. Hazen. 2002. Identification of a Novel Family of Oxidized Phospholipids That Serve as Ligands for the Macrophage Scavenger Receptor CD36. J. Biol. Chem. 277:38503-38516.

48. Stuart, L. M., J. Deng, J. M. Silver, K. Takahashi, A. A. Tseng, E. J. Hennessy, R. A. B. Ezekowitz, and K. J. Moore. 2005. Response to Staphylococcus aureus requires CD36-mediated phagocytosis triggered by the COOH-terminal cytoplasmic domain. J. Cell Biol. 170:477-485.

49. Ott, S. J., N. E. El Mokhtari, M. Musfeldt, S. Hellmig, S. Freitag, A. Rehman, T. Kuhbacher, S. Nikolaus, P. Namsolleck, M. Blaut, J. Hampe, H. Sahly, A. Reinecke, N. Haake, R. Gunther, D. Kruger, M. Lins, G. Herrmann, U. R. Folsch, R. Simon, and S. Schreiber. 2006. Detection of Diverse Bacterial Signatures in Atherosclerotic Lesions of Patients With Coronary Heart Disease. Circulation 113:929-937.

4.1.2. WAVE-1 ANCHORS PKA TO FACILITATE THE DETRIMENTAL EFFECTS OF OXIDIZED PHOSPHOLIPIDS DURING GRAM NEGATIVE SEPSIS

Ulrich Matt[1,2], Omar Sharif[1,2], Tanja Furtner[1,2], Fang Zhang[3], Immanuel Elbau[1,2], Ana Zivkovic[1,2], Karin Stich[2], Olga Oskolkova[4], Bianca Doninger[1,2], Thomas Perkmann[5], Gernot Schabbauer[4], Christoph J. Binder[1,5], Valery N. Bochkov[4], John D. Scott[3], & Sylvia Knapp[1,2]

[1]Research Center for Molecular Medicine (CeMM) of the Austrian Academy of Sciences, Vienna, Austria; [2]Department of Medicine I, Div. of Infectious Diseases and Tropical Medicine, Medical University Vienna, Vienna, Austria; [3]Howard Hughes Medical Institute, Department of Pharmacology, University of Washington School of Medicine, Seattle WA, USA; [4]Institute of Vascular Biology and Thrombosis Research, Center for Biomolecular Medicine and Pharmacology, Medical University Vienna, Vienna, Austria; [5]Department of Medical and Chemical Laboratory Diagnostics, Medical University Vienna, Vienna, Austria

Corresponding Author:

Sylvia Knapp, M.D., Ph.D.

Center for Molecular Medicine of teh Austrian Academy of Sciences; Department of Medicine 1, Div. Of Infectious Diseases and Tropical Medicine, Medical University Vienna

Waehringer Guertel 18-20; 1090 Vienna, Austria

Phone: 0043-1-40400-4954 or 4492 FAX: 0043-1-40400-4498

E-mail: sylvia.knapp@meduniwien.ac.at

Summary

Clearance of invading pathogens is essential to prevent the inflammation and sepsis that are symptomatic of bacterial peritonitis[1-3]. Macrophages participate in this innate immune response by engulfing and digesting pathogens; a process called phagocytosis. Oxidized phospholipids (OxPL) generated in response to infection can prevent the phagocytic clearance of bacteria. We investigated the mechanism underlying OxPL action in macrophages. Exposure to OxPL induced alterations in actin polymerization resulting in spreading of peritoneal macrophages and diminished uptake of *E. coli*. Pharmacological and cell based studies show that an anchored pool of protein kinase A (PKA) mediates these OxPL mediated effects. Gene silencing approaches identified the A-Kinase anchoring protein (AKAP) WAVE-1, as an effector of OxPL action i*n vitro.* Chimeric WAVE1$^{-/-}$ mice survived significantly longer after infection with *E. coli* and OxPL treatment *in vivo*. Collectively these data uncover an unanticipated role for WAVE-1 in innate immunity as a modulator of the response to severe bacterial infections.

Materials & Methods

Phagocytosis assays:

Phagocytosis assays were performed as described previously [5]. Briefly RAW 264.7 cells or primary resident peritoneal macrophages were plated at $0.5x10^6$/ ml in 12-well microtiter plates (Greiner) and allowed to adhere overnight. After washing steps, RPMI was added to wells and macrophages were incubated for 15 min with OxPAPC, DMPC (5µg/ml, unless otherwise indicated), or saline (=control). Subsequently FITC-labeled heat-killed *E. coli* (O18:K1) at a MOI of 100 were added for 1h at 37°C or 4°C, respectively. To remove adherent but not internalized bacteria cells were treated with proteinase K at 50µg/ml for 15 min at room temperature. Immediately thereafter cells were placed on ice, washed, and analyzed using a FACScan (BectonDickinson). The phagocytosis index of each sample was calculated: (mean fluorescence x % positive cells at 37°C) minus (mean fluorescence x % positive cells at 4°C). Pre-treatment with pharmacological inhibitors was performed as indicated.

Phospholipids:

1-palmitoyl-2-arachidonoyl-sn-glycero-3-phosphorylcholine (PAPC) and dimyristoyl-phosphatodyl-choline (DMPC) was obtained from Sigma. DMPC was used as control lipid as it lacks unsaturated fatty acids and thus cannot be oxidized. Oxidized PAPC (OxPAPC) was generated by air oxidation [35], and the extent of oxidation confirmed by electrospray ionization-mass spectrometry [36]. Only preparations showing a reproducible pattern of lipid oxidation products were used, and after testing for biological activity and exclusion of LPS contamination using the Limulus assay.

Mice:

Pathogen free C57BL/6 mice were purchased from Charles River. CD36 mutant oblivious ($CD36^{obl}$) C57BL/6 mice were kindly provided by Bruce Beutler via the Mutant Mouse Regional Resource Centers (MMRC) [37]. WAVE-$1^{-/-}$ mice were generated as described [19] and backcrossed 10 times to a C57BL/6 background. The local animal care committee of the Medical University of Vienna and Ministry of Sciences approved all experiments.

Induction of peritonitis, enumeration of bacteria and monitoring of survival:

Peritonitis was induced by *i.p.* injection of 200µl saline containing 10^4-10^5 CFUs *E.coli* 018:K1 that were harvested at mid-log phase [5]. OxPAPC or DMPC (both at 2.5mg/kg) were administered *i.p.* immediately before bacterial infection. 100µM St-Ht-31 (Promega) was injected i.p. immediately before administering lipids and bacteria. In survival studies, 12 mice/group were inoculated with *E. coli*, and mortality was assessed every 2h. For quantification of bacteria, peritoneal lavage fluid (PLF) and organs were harvested 10h after infection, and processed for bacterial quantification as described [5].

Measurement of oxidized lipids:

Peritoneal lavage fluid (PLF) samples were adjusted to 100 µg/ml protein concentration in PBS containing 0.27 mM EDTA and applied to 96-well MicroFluor microtiter plates (ThermoLabsystems) for overnight incubation at 4°C [25]. Samples were then incubated with isotype control Ab or EO6 (kindly provided by J. L. Witztum UCSD) for 2h at room temperature, followed by a goat-anti-mouse IgM-AP labelled secondary antibody (Sigma; at 1:35,000). For development 25 µl of 33% LumiPhos Plus solution (Lumigen) were added and light emissions were measured as relative light units (RLU) on a WALLAC VIKTOR II luminometer (Perkin Elmer).

Bone marrow transplantation:

Recipient C57/BL6 bone marrow was ablated with a single dose of radiation (9 Gy) using a Cobalt 60 irradiator (MDS Nordion) followed by injection of $2x10^6$ C57/BL6 or WAVE-$1^{-/-}$, respectively, bone marrow cells via the retro-orbital sinus as described [38]. To verify lethal irradiation one mouse from each group (WT or WAVE-$1^{-/-}$ recipients) did not receive bone marrow and was followed over approximately 10d, after which all of them succumbed. After 9 weeks successful reconstitution of donor peritoneal macrophages was verified by checking for WAVE-1 transcripts in freshly isolated peritoneal macrophages of n=3 mice/group.

Confocal microscopy:

Cytoskeletal staining was performed with Alexa-Fluor 488 labelled phalloidin (Invitrogen). Blocking of unspecific background was done with PBS/ 1% BSA for 30 min. Propidium iodide (Sigma) in the presence of 0.1% Triton X-100 was used for nuclear staining. Cells were visualized using a LSM 510 Confocal Laserscanning microscope (Zeiss). Incubations with carrier, DMPC or OxPAPC (10µg/ml) were performed for 30min; pre-treatment with cytochalasin D, H89, PKA inhibitor $amide_{14-22}$ (Calbiochem) and Ht-31 (Promega) was performed as indicated.

PKA kinase assay:

PKA kinase assay (PepTag, Promega) was performed according to the manufacturer's instructions. Briefly, RAW 264.7 were plated at a density of $1x10^7$, treated as indicated, and then scratched off in PKA extraction buffer, homogenized using a 25G needle, centrifuged for 5 min at 14.000 rpm. Controls and sample reaction was prepared according to the manufacturer´s

instructions. After adjustment of protein contents, equal amounts were loaded on a 0.8% agarose gel, and chemiluminescence was recorded with a Bio-Rad UV-transilluminator.

Generation of PKAc and WAVE-1 shRNA cell lines:

PKAc and WAVE-1 gene silencing was carried out by designing short hairpins using the siRNA target designer (Promega,) to nucleotide regions; 930-948 (PKAc, Genbank accession no: NM_008854), and 219-237 (WAVE-1, Genbank accession no: NM_031877). As a control scrambled nucleotide sequences comprising the shRNA to each transcript were used (Supplementary Table 1 online). Nucleotides were annealed and ligated into the PstI site of the psiSTRIKE vector (Promega) and plasmids were transformed into competent DH5-α cells. Purified recombinant DNA (Promega Mmaxiprep kit) (2μg) was transfected into 2 x 10^6 RAW 264.7 cells using the amaxa cell line kit V (Amaxa). Transfected cells were selected with 7μg/ml puromycin and stable cell lines generated.

Western blotting:

Macrophages were washed and lysed as described [39], and 25μg of supernatant were separated by electrophoresis on a 10% SDS polyacrylamide gel. Following electrophoresis, the gels were transferred to polyvinylidene difluoride (PVDF) membranes. Antibodies specific for PKAcα (Santa Cruz) and WAVE-1 (Sigma) were used at a dilution of 1:1000, and β-actin antibody (Sigma) at 1:500. Immunoreactive proteins were detected by the enhanced chemiluminescent protocol (GE Healthcare).

Evaluation of mRNA expression in peritoneal macrophages:

Qiagens RNEasy kit was used for RNA extraction, which included a DNase step, and cDNA was converted using the Superscript III first strand synthesis system as described by the supplier (Invitrogen). RT-PCR was conducted according to the LightCycler FastStart DNA MasterPLUS SYBR Green I system using the Roche Light cycler II sequence detector (Roche Applied Science). Sequences are listed on Supplementary Table 2 online.

Statistical analysis:

Data are presented as the mean ± SEM. Comparisons between groups was assessed using either Mann-Whitney U test or ANOVA followed by Bonferroni´s multiple comparisons analysis, where appropriate. Survival data was analyzed by Gehan-Breslow-Wilcoxon test using GraphPad Prism Software. Differences were considered significant if p-values were < 0.05.

Supplementary Tables:

Table 1

Sequences of nucleotides used for generation of shRNA or scrambled control plasmids (sense orientation only).

	Nucleotide sequence sense (5' → 3')
PKAc shRNA	ACCGGTGGAAGCTCCCTTCATATTCAAGAGATATGAAGGGAGCTTCCACCTTTTTC
WAVE-1shRNA	ACCGGACCGATTGTCTGTTAGTTTCAAGAGAACTAACAGACAATCGGTCCTTTTTC
PKAc SCR	ACCGACGGCAGTGCTTCACATTTTCAAGAGAAATGTGAAGCACTGCCGTCTTTTTC
WAVE1 SCR	ACCGTCTGGCAACGATTTTGGTTTCAAGAGAACCAAAATCGTTGCCAGACTTTTTC

Table 2

Sequences of primers used for RT-PCR

Gene	Sense (5' → 3')	Anti-sense (5' → 3')
WAVE-1	GGAAGCGCCGTCCTCTTG	CTGGGCAGTGCTGTGTGG
AKAP-Lbc	CGCACGTGTCCTGGGTCAT	TGCAGTGATAGAGGGTAGAGCCAGA
Gravin	CGTCGGGAGCAGCTGGAGAT	TGCCCATCCTGGCTTTCCTC
HPRT	GTTAAGCAGTACAGCCCCAAAAG	AAATCCAACAAAGTCTGGCCTGTA

Results

Invasion of bacteria into the peritoneal cavity leads to the immediate initiation of an inflammatory response. Integral to this response are oxygen radicals that are primarily generated to kill microbes. However these agents can also damage host structures through the peroxidation of membrane phospholipids [4]. We have shown that administration of oxidized phospholipids (OxPL) impaired survival during *E. coli* peritonitis by inhibiting phagocytosis of the bacteria [5]. Further investigation of this phenomenon has uncovered a role for endogenously produced OxPL as biologically relevant modulators of *E. coli* infections during peritonitis. Levels of OxPL in the peritoneal lavage fluid (PLF) were significantly increased 10 h after infection with *E. coli* when compared to samples from healthy mice, as measured with a monoclonal antibody that recognizes the phosphocholine headgroup of OxPL (Fig.1a) [6]. More detailed analyses demonstrated that OxPL reduced the uptake of bacteria by peritoneal macrophages in a dose-dependent manner (Fig. 1b, c). Consequently, administration of OxPL led to enhanced bacterial loads in the peritoneal cavity (Fig. 1d). Control experiments confirmed that delivery of native phospholipids did not have this effect (Fig. 1d).

The changes in cell shape associated with phagocytosis require the active remodeling of actin [7]. Delivery of OxPL also affects actin polymerization [8]. Further support for this notion was provided by fluorescent imaging of RAW 264.7 macrophages showing that treatment with OxPL induced cell spreading which is a hallmark of actin reorganization (Fig. 1e). This phenomenon was not observed in control experiments when RAW 264.7 macrophages were treated with unoxidized phospholipids or cytochalasin D, a chemical inhibitor of actin polymerization (Fig. 1e).

Related studies have suggested that this proceeds through a pathway where

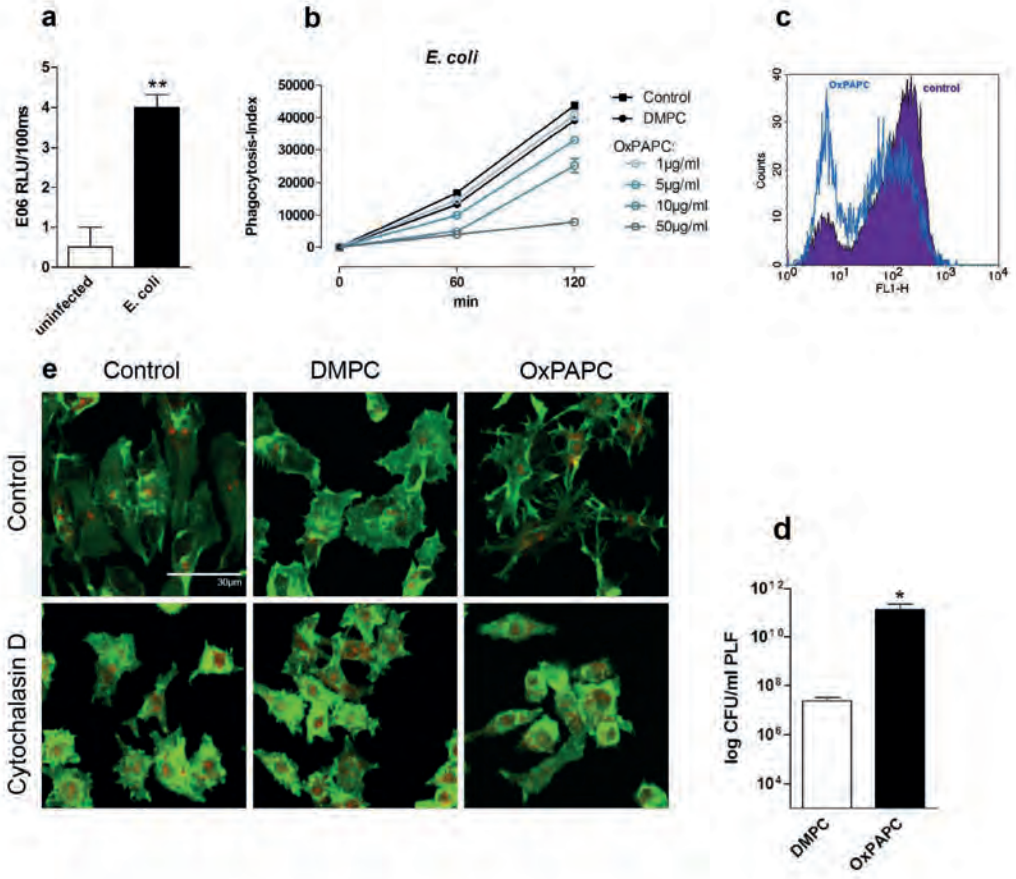

Figure 1: Oxidation of lipids occurs in *E. coli* peritonitis *in vivo,* and leads to an actin-dependent change in cell shape *in vitro*

(a) Endogenous levels of oxidized phosphatidylcholine were measured in peritoneal lavage fluid of healthy mice (n=3) and 10h following induction of bacterial peritonitis (n=8) using the EO6 mAb. (b) RAW 267.4 cells were incubated with indicated doses of OxPAPC or DMPC for 15min, and phagocytosis of *E. coli* was assessed after 60 and 120 min (triplicates, representative of 3 independent experiments). (c) FACS-histogram showing uptake of FITC-labeled *E. coli* by resident peritoneal macrophages pretreated with 10µg/ml of OxPAPC or DMPC after 60min. (d) Mice (n=8/group) were infected with 10^4 CFU *E. coli i.p.* and treated with 2.5mg/kg DMPC or OxPAPC *i.p.* Peritoneal CFU counts were enumerated 10h after infection. Data (a-d) are presented as mean ± SEM; * indicates $p < 0.05$, and ** $p < 0.01$ versus controls. (e) RAW 264.7 cells were incubated with carrier, DMPC, or OxPAPC (10µg/ml; 30min) alone or following incubation with 2µM cytochalasin D (30 min). Cells were subsequently stained for F-actin using phalloidin (green) and propidium-iodide (PI) for nuclei (red); bar 30 µm.

CD36 is a receptor for OxPL [9, 10]. More detailed analyses attempted to assess the contribution of the CD36 scavenger receptor in mediating these OxPL-effects. Interestingly, we could not discern a role for CD36 in OxPL mediated cell spreading when experiments were performed in $CD36^{mut}$ peritoneal macrophages, which harbor a non-functional scavenger receptor (Supplementary Fig. 1a). Further analyses in these cells demonstrated that although the absence of functional CD36 affected phagocytosis of *E. coli* when compared to WT macrophages, this process is still suppressed in the pesence of OxPL (Supplementary Fig. 1b). To exclude the possibility of toxic effects exerted by OxPL, we performed phagocytosis experiments in which phospholipids were removed after pre-incubation, but prior to addition of bacteria. These experiments showed that the inhibitory effects of OxPL were fully reversible over time (Supplementary Fig. 2). Collectively, our data argue against toxic effects or competitive receptor-antagonism between *E. coli* and OxPL. Rather they imply that downstream signaling events account for OxPL-mediated effects on phagocytosis and cell spreading.

Next we focused on assessing the relative contributions of phosphoinositide and cAMP dependent signaling pathways in the control of OxPL-mediated phagocytosis and cell spreading. Activation of phosphoinositide 3-kinase (PI3K) and the concomitant mobilization of Rho family small GTPases have been implicated in actin remodeling events in macrophages [8, 11, 12]. However, treatment with pharmacological agents that target PI3K (wortmannin at 50nM and LY294002 at 10μM) and Rho GTPases (Rho kinase inhibitor Y27632 at 10μM, and Clostridium toxin B at 1ng/ml, which inactivates Rho, Rac and Cdc42) had no effect on OxPL action in macrophages (data not shown). Mobilization of cAMP responsive events is known to suppress receptor-mediated phagocytosis in macrophages [13].

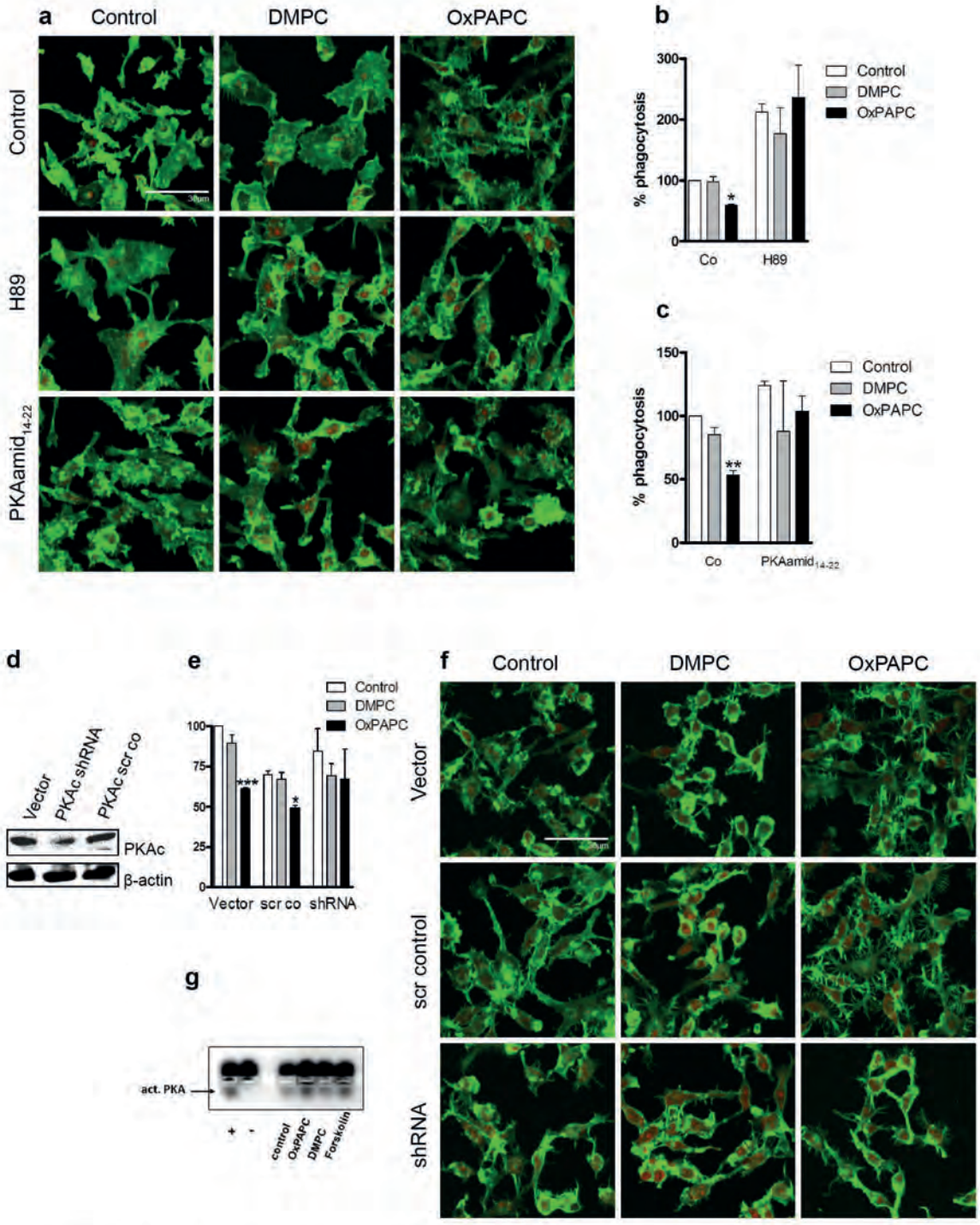

Figure 2: PKA activation mediates OxPAPC-associated cell spread and inhibition of phagocytosis

(a) RAW 264.7 cells were treated with carrier, DMPC or OxPAPC (10µg/ml; 30 min) alone, or following preincubation with H89 (10µM) or PKA amid$_{14-22}$ (20µM) (30 min). Cells were subsequently stained for F-actin (phalloidin; green) and PI (red); bar, 30 µm. (b and c) RAW 264.7 cells were incubated with carrier, DMPC or OxPAPC (5µg/ml) for 15min alone, or after a 30min pretreatment with (b) H89 (10µM), or (c) PKA amid$_{14-22}$ (20µM), respectively. Uptake of FITC-labeled *E. coli* was evaluated after 60 min and is expressed relative to carrier

(representative of 3 independent experiments). Data are mean ± SEM of triplicates; * indicates $p < 0.05$, and ** $p < 0.01$ versus corresponding carrier. (d) RAW 264.7 cells were transfected with shRNA to the α-isoform of PKAc and silencing was verified by Western blot. (e) Control (vector or scrambled control, respectively) and shRNA transfected cells were preincubated with carrier, DMPC or OxPAPC (5μg/ml) for 15 min and phagocytosis of FITC-labeled *E. coli* was examined after 60 min by FACS analysis. Uptake of bacteria is expressed relative to carrier. Data are mean ± SEM of triplicates and representative of 3 independent experiments; * indicates $p < 0.05$, and *** $p < 0.001$ versus corresponding carrier control. (f) For confocal microscopy studies, vector, scrambled-control or shRNA (to PKAc) cells were incubated with carrier, DMPC or OxPAPC (10μg/ml) for 30 min and stained with phalloidin-Alexa 488 (green) and PI (red); bar, 30 μm (representative images of 3 independent experiments are shown).

Accordingly pre-treatment with pharmacological inhibitors of protein kinase A (PKA) abolished OxPL-induced actin spread (Fig. 2a) and completely abrogated the inhibition of phagocytosis (Fig. 2b, c). More definitive results were obtained when experiments were repeated in the presence of the PKA amid$_{14-22}$, a specific inhibitor of this kinase [14, 15] (Fig. 2a-d). Furthermore gene silencing of the α-isoform of the catalytic subunit of PKA using shRNA successfully reversed OxPL-associated inhibition of phagocytosis and reduced OxPL-induced spreading (Fig. 2d-f). These findings led us to hypothesize that OxPL itself activates PKA. Indeed, incubation with OxPL but not native phospholipids (DMPC) increased PKA activity (Fig. 2g). Taken together these results allow us to demonstrate that OxPL activates PKA, which in turn propagates cellular events associated with actin spread and inhibition of phagocytosis.

It is widely acknowledged that PKA phosphorylation events control a plethora of processes and that the specificity of this kinase in different cellular compartments is directed through interaction with A-kinase anchoring proteins (AKAPs) [16, 17]. To investigate if PKA-AKAP interaction is required for OxPL-induced effects, we exploited a cell-permeable AKAP inhibitory peptide (stearated Ht-31) that blocks association of the regulatory subunit RII of PKA with AKAPs [18]. Pre-incubating macrophages with Ht-31 abrogated the change

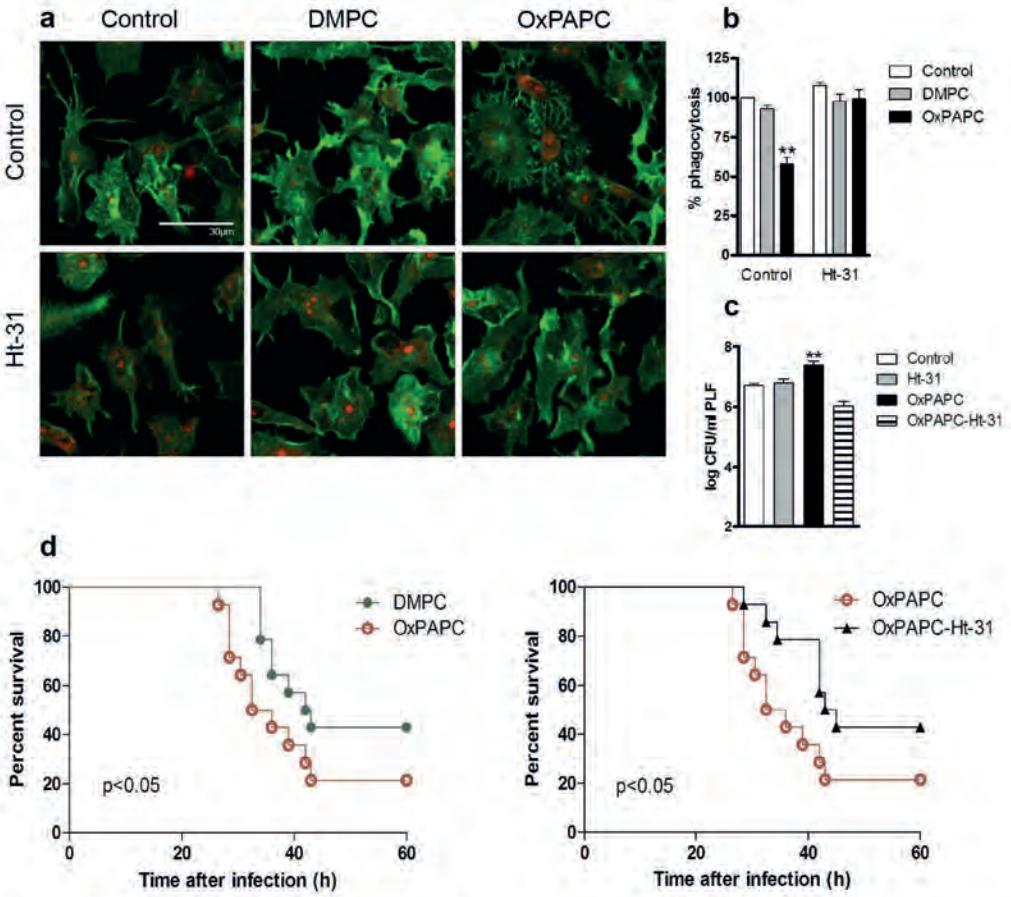

Figure 3: AKAP-inhibition prevents detrimental effects of OxPAPC *in vitro* **and** *in vivo*

(a) RAW 264.7 cells were incubated with carrier, DMPC or OxPAPC (10µg/ml) alone or after treatment with 100µM Ht-31 (30min) and stained with phalloidin (green) and PI (red); bar, 30 µm. (b) RAW 264.7 cells were treated with carrier or phospholipids (5µg/ml; 15min) alone, or after preincubation with Ht-31 (100µM) for 30 min. Phagocytosis of FITC-labeled *E. coli* was analyzed using FACS after 60 min. Uptake is expressed relative to carrier and ** indicates $p < 0.01$. Data are representative mean ± SEM of 3 independent experiments in triplicate. (c) Mice received carrier or 2.5 mg/kg OxPAPC *i.p.*, and/or 100µM of Ht-31, immediately before infection with 10^4 CFU *E. coli*. At t=10h PLF was harvested and bacterial CFUs enumerated. Data are mean ± SEM of 2 independent experiments from n=7-9 mice/group; ** indicates $p < 0.01$ versus carrier. (d) Mice received 2.5 mg/kg DMPC or OxPAPC *i.p.* followed by *i.p.* injection of vehicle or Ht-31 (OxPAPC-Ht-31), after which they were infected with 10^4 CFU *E. coli*. Survival was monitored every 2 h; n=12 mice/group, p value of each experiment is indicated.

in cell shape caused by OxPL (Fig. 3a) and concomitantly prevented OxPL-associated inhibition of phagocytosis (Fig. 3b). Notably, administration of Ht-31 together with OxPL at the onset of *E. coli* peritonitis in mice prevented the increase in bacterial loads caused by OxPL in vivo (Fig. 3c). Survival analysis corroborated these findings, as disruption of PKA anchoring with Ht-31 peptide was able to reverse the detrimental effects of OxPL during *E.coli* peritonitis *in vivo* (Fig. 3d). These data strongly suggest that AKAP interactions contribute to OxPL-induced PKA activation resulting in diminished phagocytosis of bacteria.

Among the 50 AKAPs discovered thus far, only Gravin, AKAP-Lbc, and Wiskott Aldrich syndrome protein-family verprolin-homologous protein 1 (WAVE-1) are thought to interface with the actin cytoskeleton [16]. However, only AKAP-Lbc and WAVE-1 are expressed in RAW 264.7 macrophages (Fig. 4a, b). shRNA mediated gene silencing techniques revealed that knockdown of WAVE-1 suppressed OxPL-associated actin spread and inhibition of phagocytosis (Fig. 4c-e). In contrast, gene silencing of AKAP-Lbc had no effect (data not shown). These results imply that a pool of PKA associated with WAVE-1 modulates cell spreading and inhibition of phagocytosis in macrophages. More definitive support for this concept was provided when similar experiments were performed in primary peritoneal macrophages isolated from WAVE-1$^{-/-}$ mice [19] (Fig. 4f-g). WAVE-1$^{-/-}$ macrophages exhibited neither cell spreading nor impaired bacterial uptake upon OxPL treatment (Fig. 4h-i).

Finally we evaluated the role of WAVE-1 during *E. coli* peritonitis *in vivo*. To exclude the potential influence of the altered size of WAVE1$^{-/-}$ mice [19], we generated chimeric mice on a C57BL/6 background. For this we administered bone marrow of WAVE1$^{-/-}$ or WT littermates to lethally irradiated C57BL/6 mice and ensured complete reconstitution with donor peritoneal macrophages after

nine weeks (Supplementary Fig. 3)[20]. Following *i.p.* injection of either DMPC or OxPL, we infected mice with *E. coli i.p.* and examined their ability to contain bacterial dissemination. OxPL treatment led to enhanced bacterial outgrowth in mice that received WT bone marrow (Fig. 4j-l). In contrast, chimeric mice with WAVE-1$^{-/-}$ peritoneal macrophages appeared resistant to the effects of OxPL (Fig. 4j-l). The CFU count in PLF, liver and blood was similar to the values measured in control mice that received unoxidized lipids. Moreover, WAVE-1$^{-/-}$ macrophages seemed resistant to the OxPL-associated impairment of survival during *E. coli* peritonitis (Fig. 4m). Collectively, these data confirm that WAVE-1 mediates the inhibition of phagocytosis caused by OxPL *in vitro* and *in vivo*.

Figure 4: **WAVE-1 mediates antiphagocytic properties of OxPAPC *in vitro* and *in vivo***

AKAP-Lbc (150bp), WAVE-1 (116bp) and Gravin (136bp) mRNA expression in (a) RAW 264.7 or (b) primary peritoneal macrophages; GAPDH (372bp). (c) Western blot verifying silencing of WAVE-1 (82kD) in RAW 264.7 cells; β-actin control (37kD). (d) Scrambled-control and shRNA (targeting WAVE-1) cells incubated with carrier, DMPC, or OxPAPC (10µg/ml) and stained with phalloidin (green) and PI for nuclei (red); bar, 30 µm. (e) Phagocytosis of *E. coli* (60min) assayed in scrambled-control and shRNA-WAVE-1 cells preincubated with carrier, DMPC or OxPAPC (5µg/ml). Data depicted are mean ± SEM of triplicates, * $p < 0.05$ versus corresponding carrier/DMPC. (f) mRNA expression and (g) western blot for WAVE-1 in WT and WAVE-1$^{-/-}$ primary peritoneal macrophages (WAVE-1 82kD; β-actin 39kD. (h) Primary peritoneal macrophages of WT and WAVE-1$^{-/-}$ mice incubated with carrier, DMPC or OxPAPC (10µg/ml) and stained with phalloidin (green) and PI (red); bar, 30 µm. (i) Phagocytosis of FITC-labeled *E. coli* (60min) by WT and WAVE-1$^{-/-}$ peritoneal macrophages analyzed after prior incubation with DMPC or OxPAPC (5µg/ml). Data are mean ± SEM of triplicates of 2 independent experiments; * $p < 0.01$ versus corresponding DMPC. (j-m) WT and chimeric WAVE-1$^{-/-}$ mice were treated with DMPC or OxPAPC (2.5mg/kg) *i.p.* and infected with 10^{4-5} CFU *E. coli i.p.* (j) Peritoneal, (k) liver and (l) blood CFU counts were enumerated 10h after infection, and (m) survival was monitored every 2h. Data are from n=9-12 mice/group and presented as mean ± SEM; * $p < 0.05$ versus corresponding DMPC control (j-l).

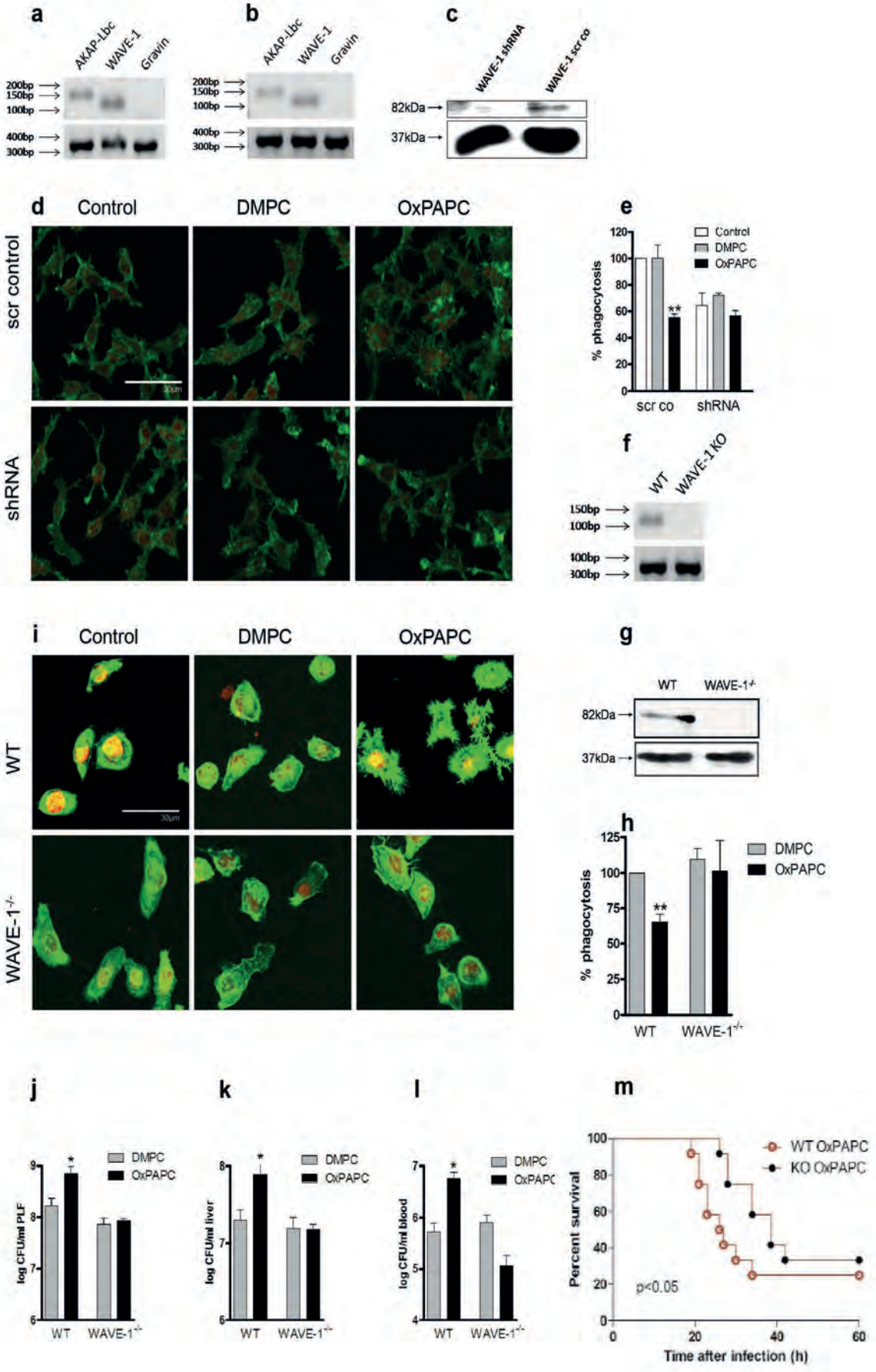
a
AKAP-Lbc
WAVE-1
Gravin
200bp
150bp
100bp
400bp
300bp
b
AKAP-Lbc
WAVE-1
Gravin
200bp
150bp
100bp
400bp
300bp
c
WAVE-1 shRNA
WAVE-1 scr co
82kDa
37kDa
d
Control
DMPC
OxPAPC
scr control
shRNA
30µm
e
Control
DMPC
OxPAPC
% phagocytosis
120
100
80
60
40
20
0
**
scr co
shRNA
f
WT
WAVE-1 KO
150bp
100bp
400bp
300bp
i
Control
DMPC
OxPAPC
WT
WAVE-1-/-
30µm
g
WT
WAVE-1-/-
82kDa
37kDa
h
% phagocytosis
125
100
75
50
25
0
DMPC
OxPAPC
**
WT
WAVE-1-/-
j
log CFU/ml PLF
9
8
7
6
*
DMPC
OxPAPC
WT
WAVE-1-/-
k
log CFU/ml liver
8
7
6
*
DMPC
OxPAPC
WT
WAVE-1-/-
l
log CFU/ml blood
7
6
5
4
*
DMPC
OxPAPC
WT
WAVE-1-/-
m
Percent survival
100
80
60
40
20
0
WT OxPAPC
KO OxPAPC
p<0.05
0
20
40
60
Time after infection (h)

In this study we investigated the mechanism by which OxPL impact phagocytosis during *E. coli* peritonitis. We have discovered a previously unrecognized role of the cytoskeletal associated A-kinase anchoring protein WAVE-1 in macrophages. Our data emphasize the impact of modified lipids during infectious diseases and extend previous reports that documented a role for OxPL in various inflammatory conditions such as atherosclerosis [21, 22] lung inflammation[23-26], or inflammatory brain lesions [27, 28]. Although the precise contribution of OxPL to these diseases or the peritonitis model discussed in this report is not yet fully understood, an important implication of this study is that diminished bacterial clearance is attenuated by interfering with a WAVE-1 associated pool of PKA.

WAVE-1 belongs to the Wiskott-Aldrich syndrome protein (WASP) family that control actin polymerization via the Arp2/3 complex [29]. In contrast to other WASP family members, WAVE-1 also functions to anchor PKA and the Abl tyrosine kinase at sites of actin reorganization [30]. So far, the majority of WAVE-1 action has been studied in the brain. WAVE-1$^{-/-}$ mice exhibit altered synaptic transmission, depleted neuronal migration, behavioral deficits and reduced viability [19, 31]. These electrophysiological and behavioral deficits have been traced back to abnormalities in dynamic actin polymerization and dendritic spine morphology [32]. We have now uncovered an unanticipated role for WAVE-1 and PKA in innate immunity. Three lines of inquire support this claim: 1) inhibition of PKA and disruption of PKA anchoring suppress OxPL induced cell spreading and phagocytosis (**Fig 3**) and 2) WAVE-1 was recently found to be expressed in bone marrow derived macrophages [33] and 3) gene silencing of WAVE-1 or ablation of this AKAP gene in peritoneal macrophages

protect against OxPL challenge in situ and *in vivo* (Fig 4). These findings not only underscore the advantages of PKA anchoring as a means to enhance the selectivity of cAMP responsive events but also unearth an additional role for the WAVE-1 signaling complex. However it is important to note that WAVE-1 affected phagocytosis only in the presence of OxPL, thus indicating a requirement for oxidative stress as seen during serious inflammatory diseases or infections. Nonetheless, the lack of effective therapies to combat sepsis [34] makes it tempting to speculate that targeting OxPL's negative impact on bacterial phagocytosis by WAVE-1 inhibitors might prove to be a promising future direction for therapeutic intervention.

Supplementary Figure 1

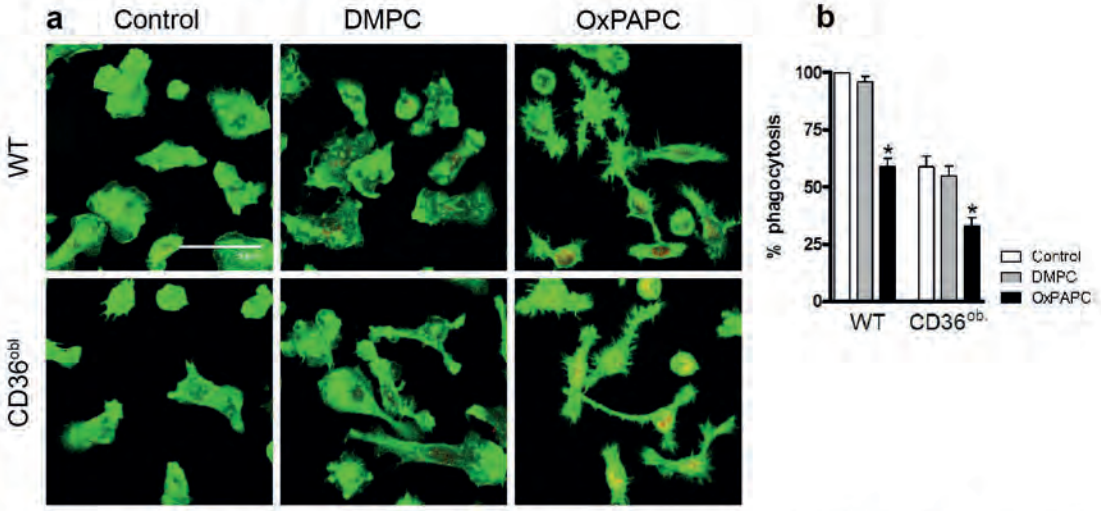

Supplementary Figure 1: OxPAPC induced cell spread and inhibition of phagocytosis is not mediated by CD36

a) Primary peritoneal macrophages of WT and CD36^{obl} mice were incubated with carrier, DMPC, or OxPAPC at 20µg/ml for 30 min. Cells were subsequently fixed and stained for F-actin using Alexa Fluor 488-labelled phalloidin (green) and propidium-iodide (PI) for nuclei (red). Cells were visualized using a LSM 510 confocal laserscanning microscope; bar 30 µm (b) WT and CD36^{obl} peritoneal macrophages were incubated with carrier, DMPC or OxPAPC at 5µg/ml for 15 min, and phagocytosis of FITC-labeled *E. coli* was assayed after 60 min. Uptake is expressed relative to carrier. Data are representative of two independent experiments performed in triplicates; mean ± SEM; * $p < 0.05$ versus carrier.

Supplementary Figure 2

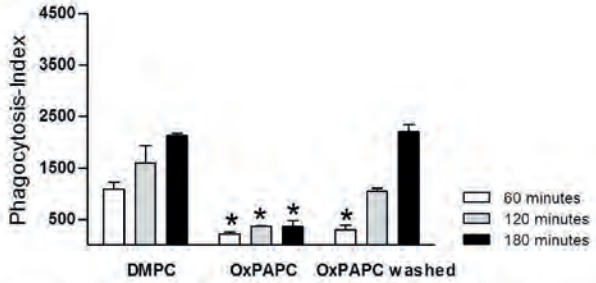

Supplementary Figure 2: OxPAPC-mediated inhibition of phagocytosis is reversible.

RAW 264.7 cells were incubated with DMPC or OxPAPC at 50µg/ml for 15 min. In indicated samples OxPAPC was removed after 15min by thoroughly washing cells with PBS (OxPAPC washed). Cells were then incubated with FITC-labeled *E. coli* and uptake was analyzed by FACS after 60, 120 and 180 min, respectively. Date are presented as phagocytosis-index as described in the Methods section. Depicted data are in duplicate and expressed as mean ± SEM; * $p < 0.05$ compared to DMPC.

Supplementary Figure 3

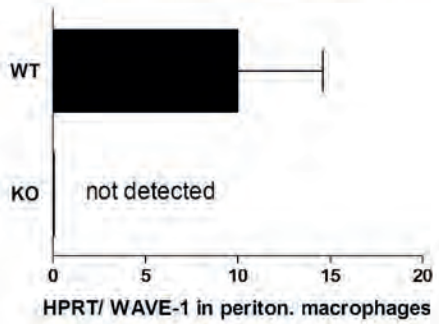

Supplementary Figure 3.

Quantitative WAVE-1 mRNA transcript levels in resident peritoneal macrophages of chimeric mice reconstituted with WT or WAVE1$^{-/-}$ bone marrow cells. Mice were randomly picked (n=3 mice/group); data depicted are mean +/- SEM.

Acknowledgements:

We are grateful to Harald Höger for excellent support in mouse breeding, Rita Böhs for animal care and Edith Pfeiffer for assistance with irradiation. We thank Marion Gröger for technical advice and Julia Schatz for excellent graphical assistance. This work was supported by a grant from the Austrian Science Fund (FWF-P18232-B11 to S.K. and V.B.). J.D.S was supported in part by NIH grant DK54441.

Author contributions:

U.M. designed and performed the majority of experiments, analyzed the data and wrote the manuscript; O.S. designed and performed parts of the experiments; T.F. performed experiments and generated confocal images; I.E., A.Z., K.S., and B.D. performed experiments; O.O. and V.B. provided reagents; G.S. assisted with bone marrow transplantations; T.P. and C.J.B. measured OxPL concentrations; F.Z. and J.D.S. generated and provided WAVE1$^{-/-}$ animals and assisted in the writing of the manuscript; S.K. designed and supervised the project, analyzed the data and wrote the manuscript.

References:

1. Holzheimer, R.G., Muhrer, K.H., L'Allemand, N., Schmidt, T. & Henneking, K. Intraabdominal infections: classification, mortality, scoring and pathophysiology. Infection 19, 447-452. (1991).

2. Wickel, D.J., Cheadle, W.G., Mercer-Jones, M.A. & Garrison, R.N. Poor outcome from peritonitis is caused by disease acuity and organ failure, not recurrent peritoneal infection. Ann. Surg. 225, 744-753; discussion 753-746. (1997).

3. Pinheiro da Silva, F. et al. CD16 promotes Escherichia coli sepsis through an FcR gamma inhibitory pathway that prevents phagocytosis and facilitates inflammation. Nat. Med. 13, 1368-1374 (2007).

4. Hampton, M.B., Kettle, A.J. & Winterbourn, C.C. Inside the neutrophil phagosome: oxidants, myeloperoxidase, and bacterial killing. Blood 92, 3007-3017 (1998).

5. Knapp, S., Matt, U., Leitinger, N. & van der Poll, T. Oxidized phospholipids inhibit phagocytosis and impair outcome in gram-negative sepsis in vivo. J. Immunol. 178, 993-1001 (2007).

6. Friedman, P., Horkko, S., Steinberg, D., Witztum, J.L. & Dennis, E.A. Correlation of antiphospholipid antibody recognition with the structure of synthetic oxidized phospholipids. Importance of Schiff base formation and aldol condensation. J. Biol. Chem. 277, 7010-7020 (2002).

7. Kaksonen, M., Toret, C.P. & Drubin, D.G. Harnessing actin dynamics for clathrin-mediated endocytosis. Nat Rev Mol Cell Biol 7, 404-414 (2006).

8. Miller, Y.I., Worrall, D.S., Funk, C.D., Feramisco, J.R. & Witztum, J.L. Actin polymerization in macrophages in response to oxidized LDL and apoptotic cells: role of 12/15-lipoxygenase and phosphoinositide 3-kinase. Mol. Biol. Cell 14, 4196-4206 (2003).

9. Park, Y.M., Febbraio, M. & Silverstein, R.L. CD36 modulates migration of mouse and human macrophages in response to oxidized LDL and may contribute to macrophage trapping in the arterial intima. J. Clin. Invest. 119, 136-145 (2009).

10. Boullier, A. et al. The binding of oxidized low density lipoprotein to mouse CD36 is mediated in part by oxidized phospholipids that are associated with both the lipid and protein moieties of the lipoprotein. J. Biol. Chem. 275, 9163-9169 (2000).

11. Underhill, D.M. & Ozinsky, A. Phagocytosis of microbes: complexity in action. Annu. Rev. Immunol. 20, 825-852 (2002).

12. Birukov, K.G. et al. Epoxycyclopentenone-containing oxidized phospholipids restore endothelial barrier function via Cdc42 and Rac. Circ. Res. 95, 892-901 (2004).

13. Bryn, T. et al. The cyclic AMP-Epac1-Rap1 pathway is dissociated from regulation of effector functions in monocytes but acquires immunoregulatory function in mature macrophages. J. Immunol. 176, 7361-7370 (2006).

14. Scott, J.D., Fischer, E.H., Demaille, J.G. & Krebs, E.G. Identification of an inhibitory region of the heat-stable protein inhibitor of the cAMP-dependent protein kinase. Proc. Natl. Acad. Sci. U. S. A. 82, 4379-4383 (1985).

15. Scott, J.D., Glaccum, M.B., Fischer, E.H. & Krebs, E.G. Primary-structure requirements for inhibition by the heat-stable inhibitor of the cAMP-dependent protein kinase. Proc. Natl. Acad. Sci. U. S. A. 83, 1613-1616 (1986).

16. Tasken, K. & Aandahl, E.M. Localized effects of cAMP mediated by distinct routes of protein kinase A. Physiol. Rev. 84, 137-167 (2004).

17. Scott, J.D. & Pawson, T. Cell signaling in space and time: where proteins come together and when they're apart. Science 326, 1220-1224 (2009).

18. Carr, D.W., Hausken, Z.E., Fraser, I.D., Stofko-Hahn, R.E. & Scott, J.D. Association of the type II cAMP-dependent protein kinase with a human thyroid RII-anchoring protein. Cloning and characterization of the RII-binding domain. J. Biol. Chem. 267, 13376-13382 (1992).

19. Soderling, S.H. et al. Loss of WAVE-1 causes sensorimotor retardation and reduced learning and memory in mice. Proc. Natl. Acad. Sci. U. S. A. 100, 1723-1728 (2003).

20. Murch, A.R., Grounds, M.D. & Papadimitriou, J.M. Improved chimaeric mouse model confirms that resident peritoneal macrophages are derived solely from bone marrow precursors. J. Pathol. 144, 81-87 (1984).

21. Binder, C.J. et al. Innate and acquired immunity in atherogenesis. Nat. Med. 8, 1218-1226 (2002).

22. Hansson, G.K. & Libby, P. The immune response in atherosclerosis: a double-edged sword. Nat Rev Immunol 6, 508-519 (2006).

23. Yoshimi, N. et al. Oxidized phosphatidylcholine in alveolar macrophages in

idiopathic interstitial pneumonias. Lung 183, 109-121 (2005).

24. Nakamura, T., Henson, P.M. & Murphy, R.C. Occurrence of oxidized metabolites of arachidonic acid esterified to phospholipids in murine lung tissue. Anal. Biochem. 262, 23-32 (1998).

25. Imai, Y. et al. Identification of oxidative stress and Toll-like receptor 4 signaling as a key pathway of acute lung injury. Cell 133, 235-249 (2008).

26. Matt, U. et al. Bbeta(15-42) protects against acid-induced acute lung injury and secondary pseudomonas pneumonia in vivo. Am. J. Respir. Crit. Care Med. 180, 1208-1217 (2009).

27. Newcombe, J., Li, H. & Cuzner, M.L. Low density lipoprotein uptake by macrophages in multiple sclerosis plaques: implications for pathogenesis. Neuropathol. Appl. Neurobiol. 20, 152-162 (1994).

28. Dei, R. et al. Lipid peroxidation and advanced glycation end products in the brain in normal aging and in Alzheimer's disease. Acta Neuropathol 104, 113-122 (2002).

29. Takenawa, T. & Suetsugu, S. The WASP-WAVE protein network: connecting the membrane to the cytoskeleton. Nat Rev Mol Cell Biol 8, 37-48 (2007).

30. Westphal, R.S., Soderling, S.H., Alto, N.M., Langeberg, L.K. & Scott, J.D. Scar/WAVE-1, a Wiskott-Aldrich syndrome protein, assembles an actin-associated multi-kinase scaffold. EMBO J. 19, 4589-4600 (2000).

31. Soderling, S.H. et al. A WAVE-1 and WRP signaling complex regulates spine density, synaptic plasticity, and memory. J. Neurosci. 27, 355-365 (2007).

32. Kim, Y. et al. Phosphorylation of WAVE1 regulates actin polymerization and dendritic spine morphology. Nature 442, 814-817 (2006).

33. Dinh, H., Scholz, G.M. & Hamilton, J.A. Regulation of WAVE1 expression in macrophages at multiple levels. J. Leukoc. Biol. 84, 1483-1491 (2008).

34. Riedemann, N.C., Guo, R.F. & Ward, P.A. The enigma of sepsis. J. Clin. Invest. 112, 460-467 (2003).

35. Bochkov, V.N. et al. Protective role of phospholipid oxidation products in endotoxin-induced tissue damage. Nature 419, 77-81. (2002).

36. Watson, A.D. et al. Structural Identification by Mass Spectrometry of Oxidized Phospholipids in Minimally Oxidized Low Density Lipoprotein That Induce Monocyte/Endothelial Interactions and Evidence for Their Presence in Vivo. J.

Biol. Chem. 272, 13597-13607 (1997).

37. Hoebe, K. et al. CD36 is a sensor of diacylglycerides. Nature 433, 523-527 (2005).

38. Pawlinski, R. et al. Role of tissue factor and protease-activated receptors in a mouse model of endotoxemia. Blood 103, 1342-1347 (2004).

39. Lagler, H. et al. TREM-1 activation alters the dynamics of pulmonary IRAK-M expression in vivo and improves host defense during pneumococcal pneumonia. J. Immunol. 183, 2027-2036 (2009).

4.2. THE FIBRIN DERIVED PEPTIDE Bß$_{15-42}$ IN ACUTE LUNG INJURY

The cleavage of fibrinogen to fibrin and its interaction with platelets are indispensable steps during blood coagulation. Fibrinogen consists of two sets of three different polypeptide chains (Aα-, Bβ-, and γ-chains)[88]. Inflammation activates the coagulation system by releasing tissue factor, which cleaves prothrombin to thrombin[89]. Thrombin then cleaves fibrinogen to fibrinopeptide A and B, ultimately resulting in cross-linked insoluble fibrin. This process is counter- regulated by plasmin, which cleaves fibrin. Thereby, degradation of the C-terminal parts generates D-fragments (D-dimers), whereas the degradation of the N-terminal part leads to the generation of E-fragments.

It is well established, that fibrin induces the release of van-Willebrand factor from endothelial cells[90], and triggers endothelial cells to form capillary sprouts, supporting angiogenesis[91,92]. The terminal fragment of fibrin II, β15-42, a naturally occurring cleavage product of the E1 fragment[93], was found to be responsible for the angiogenic effects of fibrin[94]. Bach *et al.* identified VE-cadherin as the receptor for β15-42[95]. Furthermore, fibrinogen knockout mice have an impaired cell migration during wound healing, in glomerulonephritis and in pulmonary fibrosis[97-99]. Petzelbauer *et al.* consequently uncovered that the N-terminal disulfide knot (NDSK)-II, binds with its α-chain to CD11c/CD18 on monocytes and neutrophils, and with its β-chain to VE-cadherin, thereby building a bridge between leukocytes and endothelial cells, thus facilitating transmigration[35]. Therefore, the administration of the peptide Bβ$_{15-42}$, which lacks the α-chain, and therefore only binds to VE-cadherin, blocked leukocyte transmigration in vitro[35] (Fig. 1). After myocardial infarction, the sudden onset of blood flow upon therapeutic intervention triggers an unfavorable inflammation, which further aggravates myocardial damage[100]. In a model of myocardial reperfusion injury, Petzelbauer *et al.* could demonstrate a beneficial effect of Bβ$_{15-42}$ by virtue of its capacity to reduce leukocyte infiltration[35].

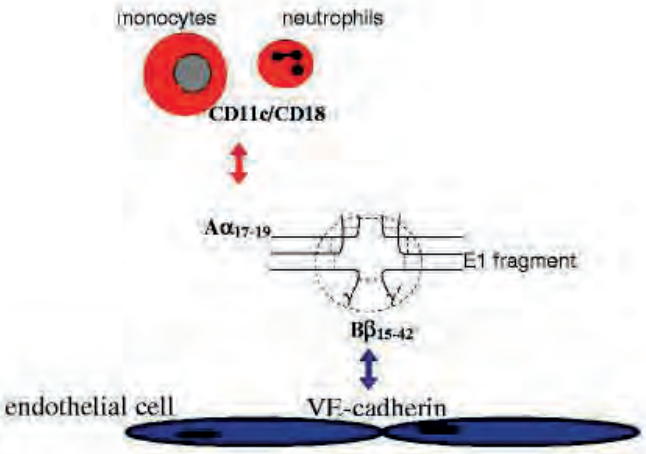

Figure 1. Inhibition of leukocyte migration by $B\beta_{15-42}$. E1-fragments are composed of the N-terminal segments of fibrin, they possess two binding sites: the α-chain to CD11c and CD18 on monocytes and neutrophils, the to VE-cadherin, thereby bridging the endothelium with inflammatory cells. Administration of the β-chain, more precisely the peptide sequence 15-42, which binds to VE-cadherin, therefore results in blockade of leukocyte transmigration (adapted from[101]).

Subsequently it was shown that the administration of $B\beta_{15-42}$ significantly reduced plasma levels of pro-inflammatory cytokines such as TNF-α, IL-1β, or IL-6 after acute myocardial ischemia-reperfusion in mice[102]. This effect was not seen in fibrinogen$^{-/-}$ mice, indicating that the reduced inflammation is due to reduced leukocyte infiltration to the necrotic myocardium[102]. These findings were extended to different organs (liver, small intestine in shock) and animals (pigs)[103-105]. Recently the therapeutic potential of $B\beta_{15-42}$ was studied in a phase-II clinical trial in patients after myocardial infarction (F.I.R.E. study) and the main outcome was a significant reduction of the necrotic core zone[36]. However, biomarkers of myocardial necrosis were unaltered, and there was no significant difference in infarct size after four months.

Aim of the study

The vasculo-protective potential of $B\beta_{15-42}$ prompted us to test its therapeutic potential during acute lung injury, i.e. a condition in which vascular leak plays

an important role. In ALI/ARDS unfavorable inflammation is initiated after insults such as pneumonia, acid aspiration, or systemic inflammation (sepsis or trauma)[28]. After the initial hit, neutrophils are recruited rapidly, supporting inflammation and aggravating the clinical condition[106-108]. We decided to investigate two scenarios: 1. the potential of $B\beta_{15-42}$ to reduce vascular leak and lung injury using two different models of ALI (LPS pneumonitis and acid aspiration injury); and 2. We hypothesized that preexisting lung injury might have harmful effects on subsequent bacterial infection, thus explaining the high rate of ventilator associated pneumonia in ICU patients. Should preexisting ALI impact antibacterial properties within the lungs, prevention of ALI might help sustain a secondary bacterial challenge.

4.2.1. PEPTIDE Bß$_{15-42}$ PRESERVES ENDOTHELIAL BARRIER FUNCTION IN SHOCK

Marion Gröger[1*], Waltraud Pasteiner[2*], George Ignatyev[3#], Ulrich Matt[4], Sylvia Knapp[4], Alena Atrasheuskaya[3], Eugenij Bukin[3], Peter Friedl[2], Daniela Zinkl[1], Renate Hofer-Warbinek[5], Kai Zacharowski[6], Peter Petzelbauer[1] and Sonja Reingruber[2]

[1]Department of Dermatology, Division of General Dermatology, Medical University Vienna, Austria , [2]Fibrex Medical Research & Development GmbH., 1235 Vienna, Austria, [3]State Research Center of Virology and Biotechnology "Vector", Koltsovo, Russia, [#] Present address: State Institute of Standardizing and Control by Name of Tarasevich, Moscow, Russia, [4] Center for Molecular Medicine of the Austrian Academy of Sciences, Vienna, Austria and Department of Medicine 1, Div. of Infectious Diseases and Tropical Medicine, Medical University Vienna, Austria , [5] Department of Vascular Biology and Thrombosis Research, Medical University Vienna, Austria, [6]Molecular, Cardioprotection & Inflammation Group, Department of Anesthesia, University Hospitals Bristol NHS Foundation Trust, Bristol, UK

*equal contribution of MG and WP

Corresponding Author:

Sonja Reingruber, sonja.reingruber@fibrexmedical.com and

Peter Petzelbauer, peter.petzelbauer@meduniwien.ac.at

Abstract

Loss of vascular barrier function causes leak of fluid and proteins into tissues, extensive leak leads to shock and death. Barriers are largely formed by endothelial cell-cell contacts built up by VE-cadherin and are under the control of RhoGTPases. Here we show that a natural plasmin digest product of fibrin, peptide Bß15-42 (also called FX06), significantly reduces vascular leak and mortality in animal models for Dengue shock syndrome. The ability of Bß15-42 to preserve endothelial barriers is confirmed in rats i.v.-injected with LPS. In endothelial cells, Bß15-42 prevents thrombin-induced stress fiber formation, myosin light chain phosphorylation and RhoA activation. The molecular key for the protective effect of Bß15-42 is the src kinase Fyn, which associates with VE-cadherin-containing junctions. Following exposure to Bß15-42 Fyn dissociates from VE-cadherin and associates with p190RhoGAP, a known antagonists of RhoA activation. The role of Fyn in transducing effects of Bß15-42 is confirmed in $Fyn^{-/-}$ mice, where the peptide is unable to reduce LPS-induced lung edema, whereas in wild type littermates the peptide significantly reduces leak. Our results demonstrate a novel function for Bß15-42. Formerly mainly considered as a degradation product occurring after fibrin inactivation, it has now to be considered as a signalling molecule. It stabilizes endothelial barriers and thus could be an attractive adjuvant in the treatment of shock.

Introduction

Capillary leak may be transient, as seen in response to histamine or prolonged as seen in response to thrombin [1]. Extensive leakage often occurs in intensive care patients and is thought to be caused by the exposure of endothelial cells to activated coagulation factors (e.g., thrombin) plus pro-inflammatory stimuli (VEGF, LPS, and others). This results in endothelial cell activation, downregulation of thrombin inhibitors and activation of the small GTPase RhoA. [2–5]. By regulating levels of myosin light chain phosphorylation and actin stress fiber formation RhoA controls cell contraction [1,6–8]. Moreover, it results in a rapid activation and redistribution of the integrin-associated focal adhesion kinase (FAK) to the tips of stress fibers [9] thereby giving anchorage support for cell contraction [10]. Cell contraction and breaking of cell-cell contacts results in gap formation and leak [6,11–13]. VE-cadherin is directly connected to the actin-based cytoskeleton and is one of the key molecules integrating signals for opening and tightening of cell junctions [14–16].

Peptide $B\beta_{15-42}$ interacts with VE-cadherin [17–19]. $B\beta_{15-42}$ is a 28 amino acid cleavage product of fibrin. Following thrombin-induced fibrin formation it is released from fibrin E1 fragments by the action of plasmin and represents a sensitive indicator of fibrinolytic activity [20]. This peptide, also called FX06, was shown to prevent myocardial reperfusion injury and to reduce infarct sizes in animal models for myocardial ischemia/reperfusion [19,21,22]. Also in a multi-centre phase IIa clinical trial FX06 significantly reduced the size of the necrotic core of infarcts in patients with acute myocardial infarction undergoing primary percutaneous coronary intervention (results of the F.I.R.E. study were presented at the ESC congress 2008 in Munich). Parts of this beneficial effect may be explained by the anti-inflammatory properties of FX06 [19]. With VE-cadherin being the molecular target of FX06 we wished to

test the hypothesis that this peptide is also interfering with endothelial barrier function. We therefore selected two different models for capillary leak. First, we used an animal model for Dengue shock syndrome (DSS) [23]. DSS -as a hallmark of the disease- presents with slowly progressive vascular leakage developing within days ultimately leading to death [24,25]. Second, we used a LPS-induced shock model, which rapidly develops leakage within hours [26]. Here we show that FX06 prevents stress-induced RhoA activation. It preserves endothelial barrier function in DSS or LPS-induced shock improves clinical outcomes. As a molecular key for the protective effect of FX06 we identified the src kinase Fyn.

Methods

Ethics statement:

All procedures were carried out in accordance with the *Guide for the Care and Use of Laboratory Animals* (NIH Publication No. 86-23). All experiments were approved by local committees and regional governments on animal experimentation: "Vector" Bioethical Committee (IACUC A5505-01), Russia; Medical University Vienna and Vienna government (MA58).

Peptides and Proteins:

FX06 ($B\beta_{15-42}$; GHRPLDKKREEAPSLRPAPPPISGGGYR, 3039.4D) and random peptide (DRGAPAHRPP RGPISGRSTP EKEKLLPG [19]) were produced by solid-phase peptide synthesis and purified with reversed-phase high performance liquid chromatography using nucleosil 100-10C18 columns (Lonza, Brussels and piChem Forschungs- und Entwicklungs-GmbH, Graz). Thrombin (human) was from Sigma-Aldrich.

Animal models :

Dengue virus infection. Experiments were performed in the BSL-3 facility (SRC VB 'Vector', Russia. The dengue virus DEN-2 (strain P23085) was adapted to adult BALB/c mice (haplotype H-2d) by numbers of sequential intracerebral (*i.c.*) through suckling BALB/c mice followed by intraperitoneal (*i.p.*) passages through immune competent mice at different ages as described [23]; GenBank #AY927231. Six week old male BALB/c mice (14-16g) infected with this virus *i.p.* develop fever, thrombocytopenia, hemoconcentration and virus-induced

death in a dose-dependent fashion [23,49]. Treatment with FX06 or NaCl was initiated at day 3 following virus infection (*i.p.*). The daily doses were splitted into two halves, one injected i.p in the morning the other in the evening. Mice were monitored for signs of morbidity and mortality at least twice daily until day 21. Under methoxyflurane anaesthesia blood was taken from the orbital sinus. Capillary leak was determined at days 3, 5 and 7 by *i.v.* injection of 200 µl of 2% Evan's blue in NaCl. One hour later mice were anesthetised and then perfused with 5 ml PBS through the left cardiac ventricle. Organs were removed and Evan's Blue extravasation was quantified as described [50]. Briefly, following tissue homogenization, centrifugation at 5000 g for 30 min, supernatants were analyzed for absorbance at 620 nm. For comparison, Evan's blue was injected into age matched mice neither infected with dengue nor injected with FX06. Leak was calculated as OD values above that of healthy controls.

The virus load was quantified by titration of serum or brain lysates onto Vero E6 cell cultures as described Diamond (J. Virol. 2000, 74, 7814-7823) and plaque forming units (PFU) per ml serum or per mg organ were determined.

Lipopolysaccaride shock:

Male Spraque Dawley rats (250-280g; Himberg, Austria) were anesthetized with 100 mg/kg sodium thiopentone (Sandoz). Body temperature was kept constant with a homoeothermic blanket. The trachea and the right jugular vein were cannulated. Following fluid replacement (500 µl 0.9% saline *i.v.*) animals were allowed to stabilize for 15 min. Then, 12 mg/kg LPS (*E. coli* serotype 0.127:B8; Sigma-Aldrich) was injected *i.v.* One hour later, 2.4 mg/kg FX06 or NaCl were injected *i.v.* as a bolus. 350 min after LPS injection,

each rat received FluoSpheres® polystyrene microspheres, 1.0 µm, yellow-green fluorescent *i.v.* ($1.2x10^8$ / kg bodyweight), labelled with a yellow-green fluorescent dye (Invitrogen Molecular Probes). Six hours after LPS injection, rats were sacrificed and lungs removed. From the left lung, FluoSpheres® were recovered by washing, digestion in KOH and subsequent fluorescent dye extraction according to manufacturer instructions. Fluorescence was determined at Ex 485/ Em 538 nm. The right lung was fixed in 4% paraformaldehyde, dehydrated in ascending alcohol concentrations (w/o using xylol) and embedded in paraplast. FluoSpheres® were counted in 5 μm sections in 10 high power fields per sample blinded to the conditions.

Lipopolysaccaride pneumonitis:

Female 29S7/SvEvBrd*C57BL/6 wild-type or female 29S7/SvEvBrd*C57BL/6 $Fyn^{-/-}$ mice (The Jackson Laboratory) were anesthetized by inhalation of isoflurane (Abbott Laboratories). LPS (10 µg, *E. coli* O55:B5; Sigma-Aldrich) diluted in 50 µl NaCl was instilled intranasally (*i.n.*), controls received NaCl only. Then, FX06 (2x2.4 mg/kg), random peptide or NaCl were injected *i.p.*, the first dose immediately after LPS challenge, the second 60 min later. 330 min after LPS challenge, mice were anesthetized with ketamine (Pfizer) and Evan's Blue (50 mg/kg; Sigma) was injected *i.v.;* 30 min later, mice were sacrificed, lungs were flushed via the right ventricle using 5 ml cold PBS (pH 7.4), removed and stored in liquid nitrogen. Frozen lungs were homogenized in 300 µl PBS at 4°C followed by incubation in formamide (Calbiochem) at 60°C for 16 h. Absorbance of supernatants was measured at A_{620} and A_{720}. Tissue Evan's Blue content was corrected for heme pigments (A_{720}) and calculated in comparison to a standard curve according to the formula: $A_{620}(\text{corrected}) = A_{620} - (1.426 \times A_{720} + 0.030)$.

Immunofluorescence-staining of endothelial cells in culture. Human Umbilical Vein Endothelial Cells (HUVEC) isolated from umbilical cords derived from the delivery room of the Medical University of Vienna, used at passages 2 to 6, were grown to confluence on chamber slides (Nunc) in IMDM (GIBCO) containing 20 % fetal calf serum, ECGS (50 μg/ml, Promocell) and heparin (5 U/ml) w/o or with FX06 (50 µg/ml), thrombin (5 U/ml) or thrombin+FX06 for indicated times. Following fixation in 4% paraformaldehyde, slides were stained with the following first step antibodies diluted in PBS containing 0.1% TritonX-100 and 1% bovine serum albumin: rabbit anti-phospho-myosin regulatory light chain (3 µg/ml; Chemicon Int.), mouse anti-VE-cadherin (TEA1/ 31, 1 µg/ml; Immunotech), rabbit-anti-β-catenin (1 µg/ml; Sigma-Aldrich) and mouse anti-phospho focal adhesion kinase (pY397, 0.5 µg/ml; BD Transduction Laboratories). Second step Abs were Cy5-labeled goat anti-mouse IgG (Jackson Laboratories) and Alexa488-labeled anti-rabbit IgG (Invitrogen-Molecular Probes). To visualize actin, sections were incubated with TRITC-labelled phalloidin (0.5 µg/ml; Sigma-Aldrich). Sections were then analyzed by a confocal laser scan microscope (LSM 510, Zeiss) with a pinhole of one airy unit, resulting in a section thickness of 0.8 µm.

Evaluation of stress response was performed by 2 independent observers (Fig. 3) and scored as follows:
-parallel actin bundles; absent=0, discrete bundling=1, parallel fibers=2
-myosin light chain phosphorylation; only at junction cross points=0, minimal colocalization with stress fibers=1, strong colocalization with stress fibers=2
-VE-cadherin membrane staining; continuous=0, single discontinuous sites/ cell=1 discontinuous staining=2

FAK staining (Fig. 5A) was scored as follows: weak and cytoplasmic=0, strong and cytoplasmic=1, strong and at tips of stress fibers=2.

RhoA and Rac1 Pull Down:

HUVEC grown to confluence were incubated with FX06 (50 µg/ml), thrombin (5 U/ml) or thrombin+FX06 for indicated times or were left untreated. Active RhoA was pulled down by using Rho Assay Reagent (GST-coupled Rhotekin, Upstate) and active Rac1 by using Rac1 / Cdc42Assay Reagent (GST-coupled Pak-1, Upstate) according to manufactures instructions. Bound proteins were separated on a 15% polyacrylamid gel and blotted on Nitrocellulose-Membrane (Bio-Rad). RhoA was detected with anti-RhoA antibody (clone55; Upstate). Rac1 was detected with anti-Rac1 antibody (clone23A8; Upstate). Total RhoA and Rac1 contents were determined in western blots performed from the same lysates before pull downs were performed.

Immunoprecipitation and Western blotting:

HUVEC grown to confluence were stimulated with FX06 (50 µg/ml), thrombin (5 U/ml) or thrombin + FX06 for indicated times or were left untreated. After washing with PBS (4°C), cells were scrapped into Tris-lysis buffer containing 1% TritonX-100, 1% NP-40 and a protease and phosphatase inhibitory cocktail (Sigma-Aldrich). Cells were kept for 20 min on ice and vortexed every 5 min. Following centrifugation, supernatants were harvested and added to 50 µl sepharose beads (Sigma-Aldrich), which were preincubated with the indicated antibodies. Beads were agitated for 2h at 4°C, washed and incubated with 2x sample buffer at 95°C for 5 min. Beads were removed by centrifugation and supernatants placed onto 10% polyacrylamide gels to separate precipitated proteins. Following blotting onto PVDF (Bio-Rad) membranes, washing with TBS/0.5% TWEEN (TBST), blocking with 1% BSA/TBST for 1h at RT, membranes were incubated with the indicated antibodies in 1% BSA/TBST

over night at 4°C. For detection, HRP-labelled goat anti-mouse or anti-rabbit antibodies (Bio-Rad) in TBST were used and bound Abs were visualized by chemiluminescence (ECL-system, Amersham Corp.) and recorded on film.

For Fyn - p190RhoGAP co-precipitation experiments, membrane fractions were isolated by using the Compartmental Protein Extraction Kit CNMCS (K201301-1-6, Biochain Institute) according to the manufacturer's instructions. Protein concentrations were adjusted to 1 mg protein and samples were added to 5 µg anti-p190RhoGAP antibody (Sigma-Aldrich) or 5 µg anti-Fyn antibody (Santa Cruz) and incubated at 4°C for 12 h. 60 µl Agarose A beads (preincubated with 5% BSA) were added and agitated for 12h at 4°C. Following washing, beads were incubated with 2x sample buffer at 95°C for 5 min. Beads were removed by centrifugation and supernatants placed onto 10% polyacrylamide gels as described above.

Data analysis was done with Dolphin-1D Gel Analysis Software (Wealtec). Protein bands were identified automatically by the program and analysed by comparing the optical densities. Coprecipitated protein bands were normalized to proteins precipitated with the respective antibody.

Results

FX06 improved survival and reduced capillary leak in Dengue-induced shock.

Dengue shock syndrome (DSS) in humans is characterized by progressive capillary leak [24,25]. This progressive loss of vascular barrier function is mimicked in our mouse model. Following Dengue infection *i.p.*, mice developed arching backs, ruffling fur, slowed activity, and finally, at days 5-9, they died in a dose-dependent fashion (Fig. 1A). Moreover, mice presented hemoconcentration and fibrinogen consumption (Fig. 1C) and progressive capillary leak within lungs and the intestine (Fig. 1D).

Animals treated with FX06 (first treatment on day 3 post infection) had significantly improved survival rates (Fig. 1A), significantly reduced capillary leak within lungs and the intestine (Fig.1D) and significantly reduced hemoconcentration and fibrinogen consumption (Fig.1C). Virus loads in serum, liver and brains peaked at day 7 and did not differ between groups (Fig. 1B).

FX06 reduced capillary leak in systemic LPS shock. To further substantiate the finding that FX06 reduced capillary leak, we injected rats with the gram negative toxin LPS *i.v.*. Capillary leak was assessed by quantifying extravasated 1 μm-seized FluoSpheres® within lungs of LPS-exposed animals. FluoSpheres® within lungs were qualitatively analyzed by histology (example shown in Fig. 2A+B), which was indicative for a reduction of beads in FX06-treated rats (Fig 2B). For quantitative evaluation, FluoSpheres® were recovered from the entire left lungs in each animal by tissue homogenization. Retained fluorescence / g tissue was significantly reduced in FX06-treated animals (Fig. 2C). Further evaluation of organ damage revealed elevated

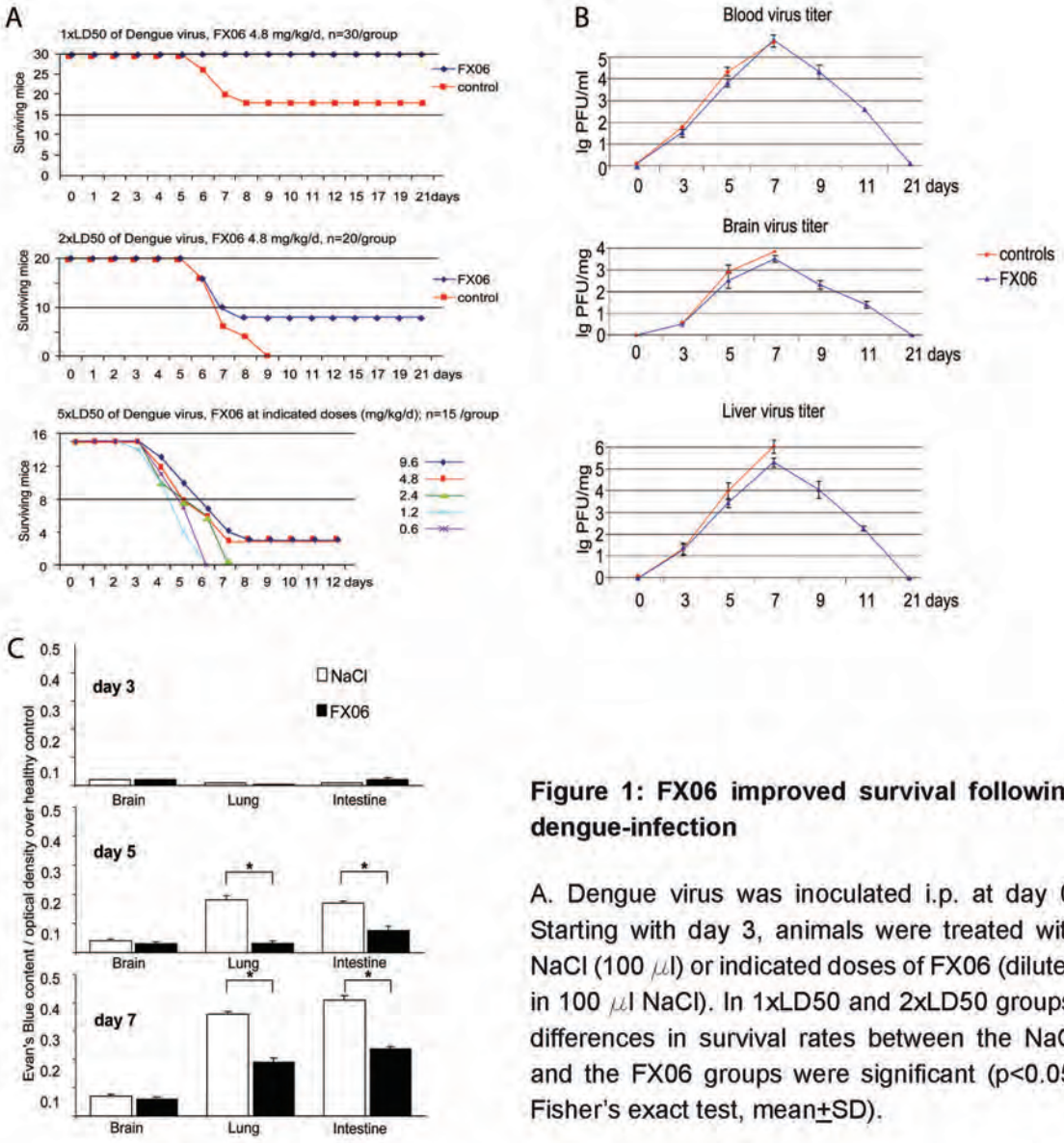

Figure 1: FX06 improved survival following dengue-infection

A. Dengue virus was inoculated i.p. at day 0. Starting with day 3, animals were treated with NaCl (100 μl) or indicated doses of FX06 (diluted in 100 μl NaCl). In 1xLD50 and 2xLD50 groups, differences in survival rates between the NaCl and the FX06 groups were significant ($p<0.05$, Fisher's exact test, mean$\pm$SD).

B. Virus titers following Dengue infection. Mice were infected with 2 xLD50 of Dengue virus *i.p* and treated with NaCl (controls) or FX06 (2.4 mg/kg bodyweight twice daily). The virus load was quantified by titration of serum or brain lysates onto Vero E6 cell cultures as described Diamond (J. Virol. 2000, 74, 7814-7823) and plaque forming units (PFU) per ml serum or per mg organ were determined. n=3 /data point. All control treated animals were dead at day 9.

C. Hematocrit and Fibrinogen following Dengue infection.

D. Organs of 15 animals per time point and group infected with 2xLD50 were analyzed. Treatment started at day 3, mice received NaCl or FX06 (4.8 mg/kg bodyweight in 100 μl NaCl i.p.). Samples at day 3 were taken before treatment was initiated. Evan's blue extravasation was measured as described in Methods and data are presented as optical density above that of healthy controls. At days 5 and 7, in lungs and the intestine, the difference in Evan's blue extravasation between the NaCl and the FX06 group was significant (*$p<0.05$, student's t test, mean$\pm$SD).

serum liver transaminases in LPS-injected rats (AST mean 1013 +/-1016 U/l; ALT mean 649 +/- 835 U/l), which were significantly reduced by FX06 treatment (451 +/-202 U/l and 230 +/- 215 U/l, respectively; n = 10/group; $p<0.05$). Plasma fibrinogen was 139 +/-26 mg/dl in sham treated animals, 44 +/- 16 in LPS-treated and 54 +/- 20 mg/dl in LPS + FX06-treated animals. LPS induced permeability assay was also performed *in vitro* and a decreased permeability of the HUVEC monolayer by 74 + 12% was measured.

FX06 reduced thrombin-induced stress fiber formation. Both dengue and LPS models demonstrated fibrinogen consumption indicative for thrombin activation. Thrombin is known to activate the contractile apparatus of endothelial cells resulting in barrier dysfunction [8,27,28]. We therefore first tested effects of the peptide on thrombin-induced stress fiber formation. As shown in Fig. 3A, thrombin induced pronounced parallel bundling of actin fibers (stress fiber formation), increased phosphorylation of myosin light chain and disrupted the continuous lining of VE-cadherin at endothelial surfaces.

In the presence of FX06 this thrombin effect was reduced, only few stress fibers pervaded the cell. Filamentous actin was mainly located at the cortical band, phosphorylated myosin light chain (pMLC) was found at endothelial cross points and VE-cadherin formed a continuous lining (similar to controls, Fig. 3A). Figure 3B summarizes effects of the peptide on thrombin-induced changes seen in Figure 3A. The peptide alone had no effect on stress fiber formation and phosphorylation of myosin light chain. Random peptide [19] used as an additional control showed identical results as medium control.

In addition, we tested the effects of FX06 on LPS- or TNFalpha-induced stress fiber formation. FX06 prevented actin bundling in both cases (data not shown) indicating that FX06 effects were not restricted to thrombin-mediated stress reactions of endothelial cells.

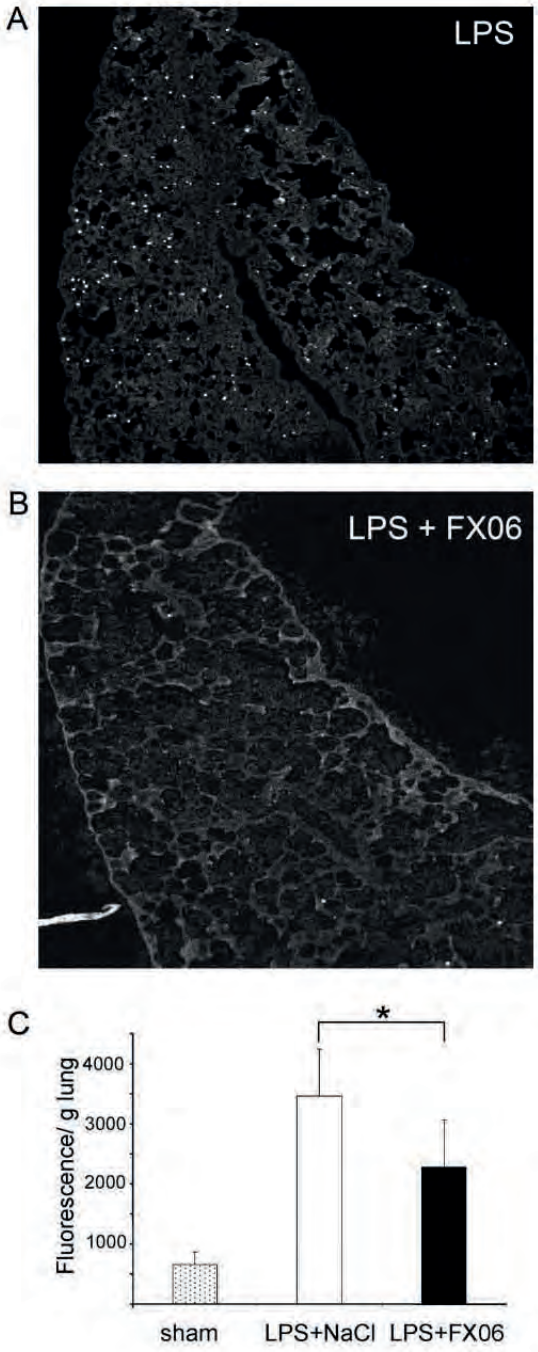

Figure 2: FX06 decreased capillary leak following LPS injection in rats

One hour after LPS injection (*i.v.*, 12 mg/kg), FX06 (2.4 mg/kg) or an equal volume of NaCl (100 μl) were injected *i.v.*; 350 min after LPS injection, FluoSpheres® were injected *i.v.*; 360 min. after LPS injection, rats were sacrificed. The right lung was used for histology and photographed on a laser scan microscope. Examples of images from LPS (A) or LPS + FX06-treated animals(B). From the entire left lung, FluoSpheres® were recovered and fluorescence measured as described in Methods C. The difference between LPS and LPS plus FX06 was significant (n=11 per group; * denotes $p<0.05$, student's t test, mean$\pm$SD).

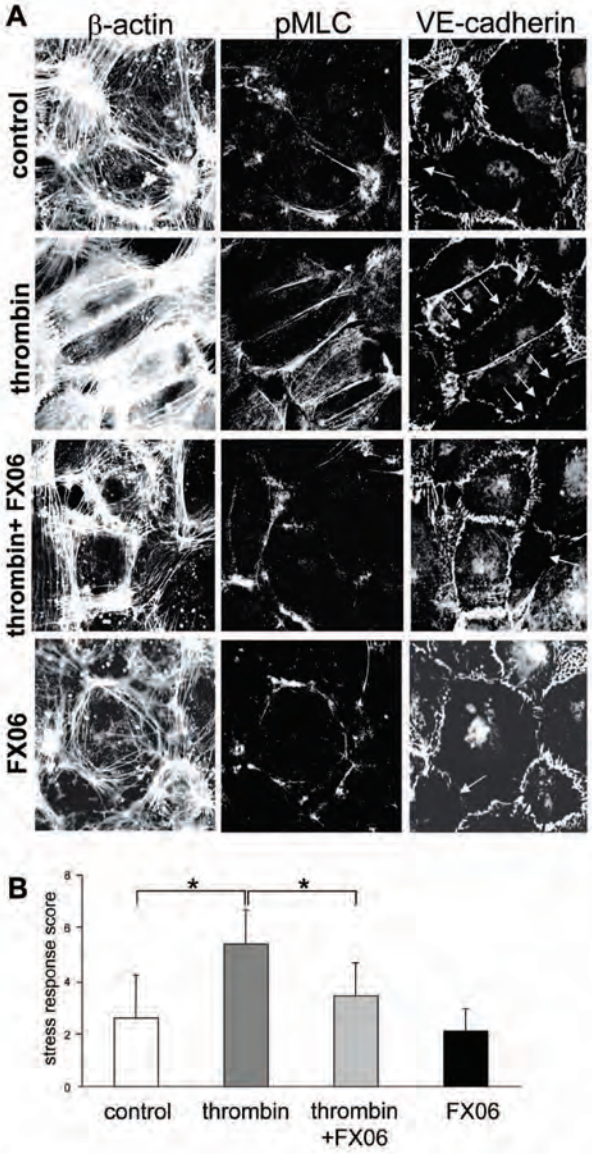

Figure 3: FX06 prevented thrombin-induced actin-bundling and myosin light chain phosphorylation (pMLC)

A. Examples of laser scan images of an immunofluorescence triple staining: actin (left) pMLC (middle), and VE-cadherin (right column). Endothelial cells were exposed to thrombin (5 U/ml), FX06 (50 mg/ml) or thrombin+FX06 for 5 min. Following thrombin, actin formed parallel bundles, pMLC co-localized with parallel actin bundles and VE-cadherin formed a discontinuous band. Arrows denote discontinuous VE-cadherin at the cell margins. FX06 (50 µg/ml) prevented these thrombin-induced changes; staining patterns were comparable to those seen in control cells or FX06-treated cells.

B. The amount and localization of pMLC, the amount of actin bundling and the continuity of VE-cadherin as exemplified in (A) were quantified in 15 randomly photographed LSM images derived from 3 independent experiments by 2 observers blinded to the condition as described in Methods. Thrombin induced a significant raise in scores as compared to controls ($p<0.05$, students t test) and this was significantly reduced by FX06 (* denotes $p<0.05$, mean$\pm$SD).

FX06 inhibited thrombin-induced Focal Adhesion Kinase (FAK) redistribution. It is well documented that for efficient thrombin-induced cell contraction the activation of focal adhesion kinase (FAK) is required. This provides anchorage to the matrix to allow coordinated cell contraction [10,29]. As expected [9], we found that thrombin induced a redistribution of pFAK to the tips of stress fibers (Fig. 4A and B). In contrast, in cells treated with thrombin in the presence of FX06, pFAK remained diffusely distributed in the cytosol comparable to controls (Fig. 4A). Random peptide [19] used as an additional control showed identical result as medium control (data not shown).

FX06 reduced thrombin-induced RhoA activation. Stress fiber formation and myosin light chain activation is under the control of the counteractive balance between RhoA and Rac1 [7,30–33]. As well documented [8], we found thrombin to augment active RhoA and to reduce active Rac1 as determined in pull down assays using GST-coupled Rhotekin and GST-coupled Pak-1 as binding partners for activated GTPases (Fig. 5). Treatment with FX06 alone had reverse effects; it activated Rac1 and decreased the amount of active RhoA (Fig. 5). Combining thrombin with FX06 completely blocked thrombin-induced RhoA activation (Fig. 5).

FX06 dissociated Fyn from VE-cadherin. The only yet known endothelial binding partner of the $B\beta_{15-42}$ sequence of FX06 is VE-cadherin [17–19], which has been described to interfere with the counteractive balance of RhoA and Rac1; VE-cadherin/VE-cadherin engagement reduces RhoA and induces Rac1 activity [33,34]. Since functions of VE-cadherin largely depend on its cytosolic binding partners, we screened effects of the peptide on the composition of the VE-cadherin complex (catenins, VE-PTP, p120cat, c-src, csk and Fyn; data shown for Fyn only). The only significant change observed with FX06 was a rapid dissociation of the src kinase Fyn from VE-cadherin (Fig. 6A). This

was paralleled by association of Fyn with FAK with p190RhoGAP (Fig. 6B). Interestingly, thrombin had no effect on the VE-cadherin / Fyn association, whereas the combination of thrombin + FX06 dissociated Fyn from VE-cadherin (Fig. 6A) and associated Fyn with p190RhoGAP (Fig. 6B-D). This raised the possibility that FX06 protected cells from thrombin-induced cell activation in a Fyn-dependent fashion. We tested this in endothelial cells treated with Fyn shRNA which still responded to thrombin, but FX06 was unable to prevent stress fiber formation (Fig. 1S).

LPS pneumonitis model with wild-type and Fyn$^{-/-}$ mice

As a proof of concept, we tested effects of FX06 in a mouse model of pneumonitis using wild-type and Fyn$^{-/-}$ mice. Intranasal administration of LPS induced pulmonary inflammation as determined by myeloperoxidase (MPO) activity in lung lysates (4753 +/- 1018 pg/ml lung). Moreover, LPS induced capillary leak as determined by Evan's blue accumulation within lungs as compared to sham-treated animals. Leak (Fig. 7) and inflammation (3050 +/-115 pg/ml lung) were significantly diminished in FX06-treated animals. In contrast, no peptide-related reduction of leak (Fig. 7) or reduction of inflammation 4329 +/- 1417 and 4157 +/-1091 pg/ml respectively) was observed in Fyn$^{-/-}$ mice confirming the role of Fyn in mediating protective effects of FX06.

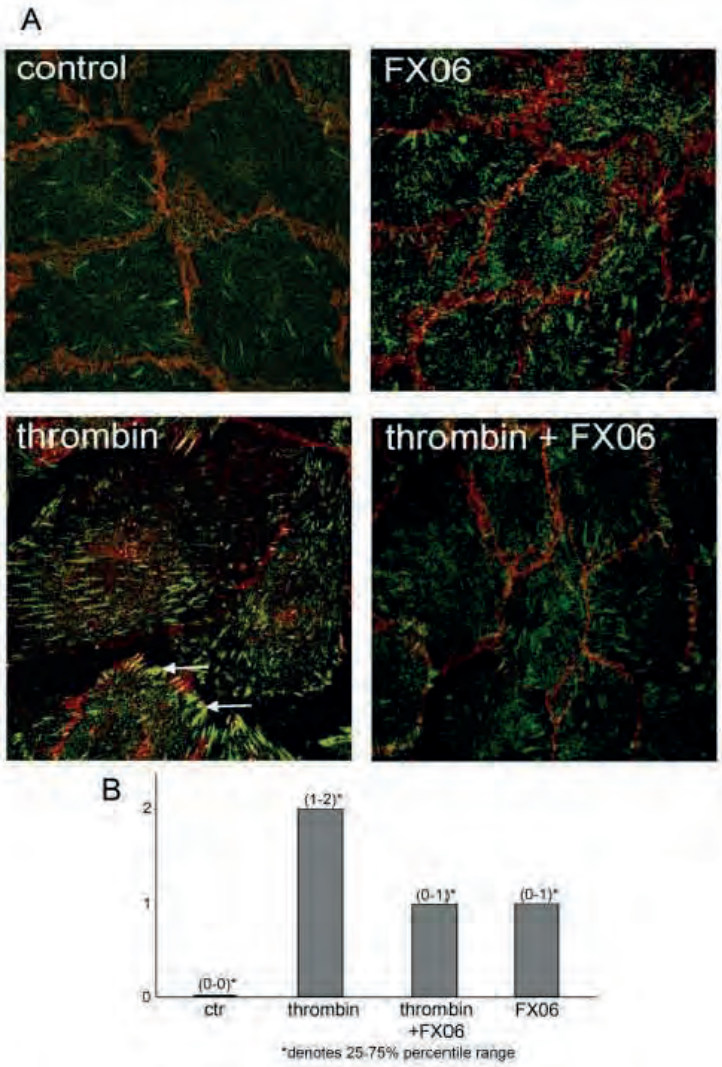

Figure 4: FX06 reduced thrombin-induced FAK activation

A. Immunofluorescence images (anti-ß-catenin Ab in red, anti-phospho-FAK (p397FAK) Ab in green). Endothelial cells were treated as indicated for 5 min. Thrombin induced a robust increase in p397FAK and relocation to cell margins producing a pattern of parallel stripes (arrows) which was not seen in thrombin plus FX06-treated cells.

B. The amount and localization of pFAK as exemplified in (A) was scored in 3 independent experiments by 2 observers blinded to the condition as described in Methods. Thrombin induced a significant raise in scores as compared to random peptide-treated cells (*$p<0.05$) and this was significantly reduced by FX06 (*$p<0.05$).

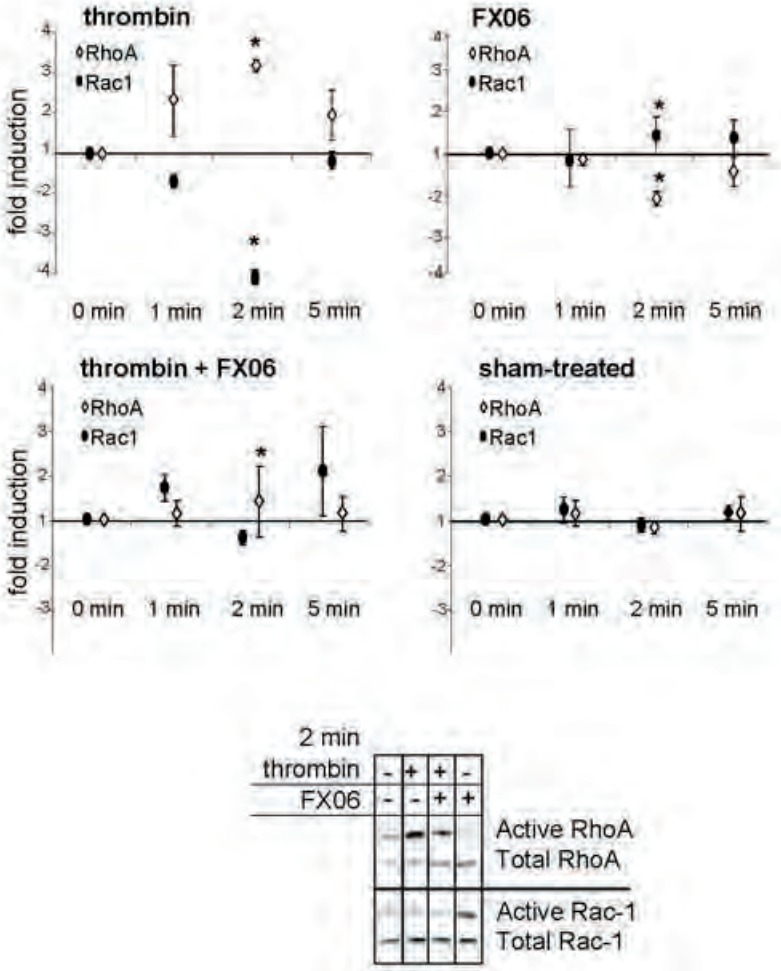

Figure 5: FX06 prevents thrombin-induced RhoA activation

Endothelial cells were exposed to thrombin (5 U/ml), FX06 (50 µg/ml) or thrombin plus FX06 for indicated times. Pull down experiments were performed with GST-coupled Rhotekin (for activated RhoA) or with GST-coupled Pak-1 (for activated Rac1). Graphs depict the mean±SD of 4 independent experiments. Thrombin induced significant elevations of RhoA and reductions of Rac1 activity as indicated by asterisks ($p<0.05$ compared to sham). FX06 alone had the reverse effect (asterisks denote $p<0.05$ compared to sham). In thrombin plus FX06-treated cells, RhoA activation was completely inhibited (asterisks denote $p<0.05$ compared to cells treated with thrombin alone). The Western blot is an example of a pull down experiment 2 minutes after stimulation.

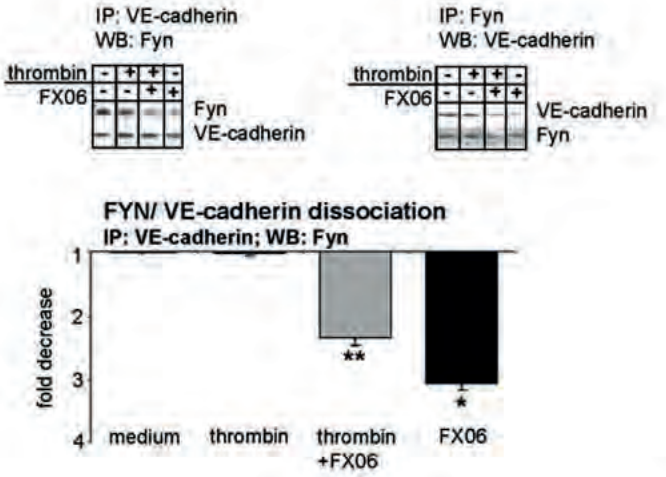

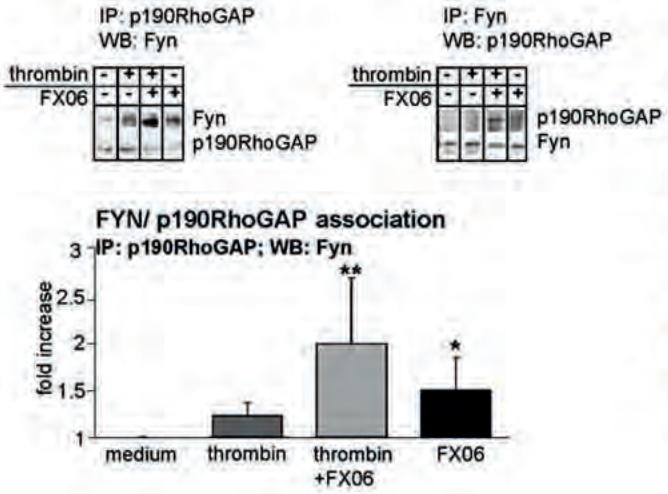

Figure 6: FX06 dissociates Fyn from VE-cadherin and associates Fyn to FAK and RhoGAP

Endothelial cells were treated with thrombin, FX06 or thrombin+FX06 for 1 min. Following lysis, proteins were immunoprecipitated (IP) and co-precipitated proteins detected by western blots (WB) as indicated in (A-D). Mean±SD of three independent experiments; *p<0.05 compared to medium control, **p<0.05 compared to thrombin; representative Western blots are shown at the right side.

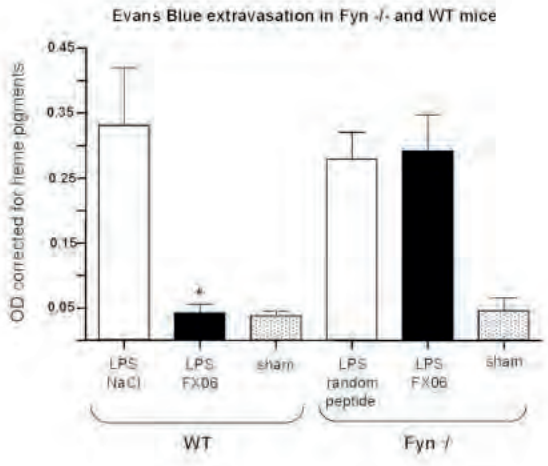

Figure 7: FX06 reduces leak in wild-type but not in Fyn-/- mice

LPS (10 µg) or solvent were instilled intranasally *(i.n.)*. FX06 (2x2.4 mg/kg), random peptide or NaCl were injected *i.p.*, the first dose immediately after LPS challenge, the second dose 60 min later. 330 min after LPS challenge, Evan's Blue was injected *i.v.* 30 min later mice were sacrificed and lungs processed as described in the Methods and analyzed for Evan's blue content; n=8 per group. The difference between LPS and **LPS+FX06 in wild-type mice was significant, *p<0.05.**

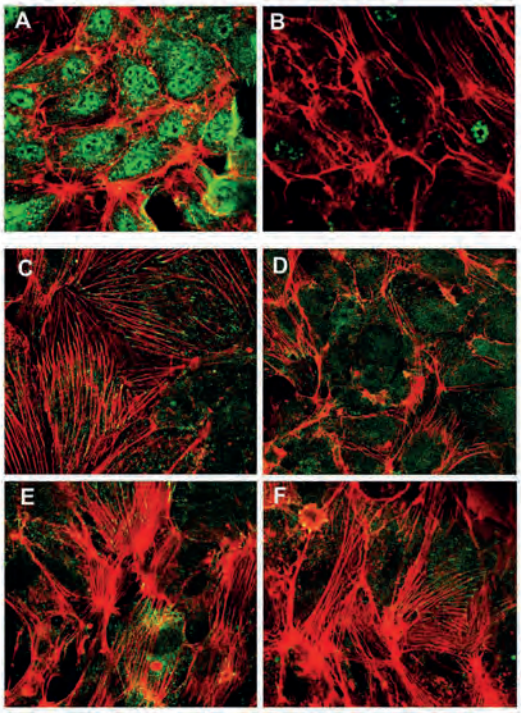

Figure S1

Knock down of Fyn with lentiviral siRNA smart vector in cultured HUVEC; Fyn siRNA and control siRNA were purchased from Dharmacon and used according to the manufacturers instructions. For infection 2 MOI/cell were used. Control staining for Fyn (green) and F-actin (red) in scrambled (A) vs. specific siRNA infected cells (B). C–F: Cytoskeleton formation (red) and pFAK (green) distribution in scrambled (C, D) vs. specific siRNA infected cells (E, F). Cells were treated with 1U Thrombin (C–F) without FX06 (C, E) and with 50 µg/ml FX06 (D, F) for 1 min.

Discussion

Data presented here demonstrate that FX06, a plasmin cleavage product of fibrin, reduces capillary leak during sepsis or lung injury. We have shown this in three models of capillary leak. First, the Dengue shock model, where capillary leak started at day 3 and is slowly progressive thereafter and reaches a maximum at day 7. In this model FX06 significantly reduced leak as determined by Evan's blue extravasation and improved survival. Second, we used an intravenous LPS shock model. Importantly, in this non-recovery model barrier function was measured by extravasation of 1 µm-sized beads, which do not extravasate in subacute models like Dengue. Even in this most severe model for a loss of endothelial barrier function FX06 was able to reduce leakage. Third, we used a pneumonitis model induced by LPS inhalation, where FX06 reduced pulmonary leak.

We have shown previously that FX06 forms low affinity interactions with VE-cadherin and has anti-inflammatory properties [19]. Inflammation and leakage processes are tightly linked and the hierarchy of events difficult to sort out. As reviewed recently by Vestweber [16] mechanisms of leukocyte transmigration go along with vascular permeability and are strongly influenced by VE-cadherin functions. VE-cadherin is a transmembrane molecule crucially involved in the regulation of endothelial barrier function and RhoA activity [15,34,35]. FAK reorganisation, actin stress fiber formation and RhoA activation are established signs of thrombin, LPS or TNF-α-induced vascular hyperpermeability [5,8,36,37]. Indeed, we found that FX06 to reduced FAK reorganisation, actin-bundling and RhoA activation in response to thrombin.

VE-cadherin is organized in a multimeric protein complex called adherens junction. Both, the phosphorylation status of VE-cadherin and the composition of this protein complex are altered in response to factors interfering with

vascular barrier function. FX06 did not change the phosphorylation status of VE-cadherin within 0 to 5 minutes after the addition of the peptide to endothelial cultures (data not shown). Among proteins known to be associated with cadherins are catenins, VE-PTP, p120cat, c-src, csk or Fyn. Thus, in a next step we analyzed whether FX06 altered the composition of the VE-cadherin complex. Among proteins co-precipitated with VE-cadherin, only Fyn was significantly affected. The addition of FX06 to endothelial cells caused an immediate dissociation of Fyn from VE-cadherin.

Fyn is a broadly expressed regulatory src kinase. Fyn knock-out mice are viable and have no apparent phenotype [38–41], most likely due to compensation by other src kinase family proteins [42]. Also overexpression of Fyn has little effects on the phosphorylation status of other proteins [43,44]. Not much is known about the function of Fyn in endothelial cells with one exception, the anti-angiogenic effect of thrombospondin requires Fyn [45]. Fyn has been shown to associate with FAK [40,43,46] and p190RhoGAP [34,47]. We here show that Fyn associates with the VE-cadherin-containing adhesion complex and that FX06 dissociates Fyn from VE-cadherin and associates Fyn to p190RhoGAP, known to inhibit RhoA activation thereby maintaining endothelial barrier function [48]. We therefore postulated that FX06 protected endothelial barriers in a Fyn-dependent fashion. We used $Fyn^{-/-}$ mice in a pneumonitis model, where LPS induced capillary leak in both, wild-type and knock-out mice, but the protective effect of FX06 was seen in wild-type animals only. We have also shown that FX06 can not achieve the protection against thrombin effects in endothelial cells infected with Fyn shRNA. However, thrombin effects seemed to be attenuated in Fyn knock down cells. The mechanism underlying this phenomenon has to be clarified and could be due to the fact, that in the absence of Fyn activation signalling through this molecule is also impaired.

There is an interesting analogy between the effects of FX06 on cadherin-based junctions and the physiological effect of homotypic VE-cadherin / VE-cadherin engagement: both results in a reduction of activated RhoA. In the case of cadherin engagement, this is mediated by a yet not identified src kinase family member [34], in case of FX06, this depends on Fyn. In conclusion, we show that FX06 is a signalling molecule that stabilizes endothelial barriers. Combined with the previously described anti-inflammatory effects of FX06 [19], this peptide appears as an attractive adjuvant in the treatment of inflammatory disorders associated with a break down of vascular barrier function.

Conflict of Interest

PP, SR are founders of Fibrex Medical Inc. www.fibrexmedical.com and own shares, KZ owns stock options of Fibrex, SR, PF and WP are employed by Fibrex.

Acknowledgements

This work was supported by a grant from the Austrian Research Funding Society (FFG) #811037, 'Bridge I' to PP.

We wish to thank the following persons: U.M. Losert and the staff of the Biomedical Sciences Center, Medical University of Vienna, for animal care and assistance in animal experiments; Karin Neumüller, Fahira Basota, Alex Eteleng (Department of Dermatology, Medical University of Vienna, Austria) and Sabine Lehner (Fibrex Vienna) for excellent technical assistance.

References

1. van Hinsbergh V, van Nieuw Amerongen GP (2002) Intracellular signalling involved in modulating human endothelial barrier function. J Anat 200: 549-560.

2. Faust SN, Levin M, Harrison OB, Goldin RD, Lockhart MS, Kondaveeti S, Laszik Z, Esmon CT, Heyderman RS (2001) Dysfunction of endothelial protein C activation in severe meningococcal sepsis. N Engl J Med 345: 408-416.

3. Matsuda N, Hattori Y (2007) Vascular biology in sepsis: pathophysiological and therapeutic significance of vascular dysfunction. J Smooth Muscle Res 43: 117-137.

4. Sohn RH, Deming CB, Johns DC, Champion HC, Bian C, Gardner K, Rade JJ (2005) Regulation of endothelial thrombomodulin expression by inflammatory cytokines is mediated by activation of nuclear factor-kappa B. Blood 105: 3910-3917.

5. Vandenbroucke E, Mehta D, Minshall R, Malik AB (2008) Regulation of endothelial junctional permeability. Ann N Y Acad Sci 1123: 134-145.

6. Garcia JG, Davis HW, Patterson CE (1995) Regulation of endothelial cell gap formation and barrier dysfunction: role of myosin light chain phosphorylation. J Cell Physiol 163: 510-522.

7. Minshall RD, Malik AB (2006) Transport across the endothelium: regulation of endothelial permeability. Handb Exp Pharmacol 107-144.

8. van Nieuw Amerongen GP, Beckers CM, Achekar ID, Zeeman S, Musters RJ, van H, V (2007) Involvement of Rho kinase in endothelial barrier maintenance. Arterioscler Thromb Vasc Biol 27: 2332-2339.

9. Schaphorst KL, Pavalko FM, Patterson CE, Garcia JG (1997) Thrombin-mediated focal adhesion plaque reorganization in endothelium: role of protein phosphorylation. Am J Respir Cell Mol Biol 17: 443-455.

10. Wu MH (2005) Endothelial focal adhesions and barrier function. J Physiol 569: 359-366.

11. Konstantoulaki M, Kouklis P, Malik AB (2003) Protein kinase C modifications of VE-cadherin, p120, and beta-catenin contribute to endothelial barrier dysregulation induced by thrombin. Am J Physiol Lung Cell Mol Physiol 285: L434-L442.

12. Ukropec JA, Hollinger MK, Salva SM, Woolkalis MJ (2000) SHP2 association with VE-cadherin complexes in human endothelial cells is regulated by thrombin. J Biol Chem 275: 5983-5986.

13. Wojciak-Stothard B, Potempa S, Eichholtz T, Ridley AJ (2001) Rho and Rac but not Cdc42 regulate endothelial cell permeability. J Cell Sci 114: 1343-1355.

14. Broman MT, Mehta D, Malik AB (2007) Cdc42 regulates the restoration of endothelial adherens junctions and permeability. Trends Cardiovasc Med 17: 151-156.

15. Dejana E, Spagnuolo R, Bazzoni G (2001) Interendothelial junctions and their role in the control of angiogenesis, vascular permeability and leukocyte transmigration. Thromb Haemost 86: 308-315.

16. Vestweber D (2008) VE-cadherin: the major endothelial adhesion molecule controlling cellular junctions and blood vessel formation. Arterioscler Thromb Vasc Biol 28: 223-232.

17. Bach TL, Barsigian C, Yaen CH, Martinez J (1998) Endothelial cell VE-cadherin functions as a receptor for the beta15-42 sequence of fibrin. J Biol Chem 273: 30719-30728.

18. Gorlatov S, Medved L (2002) Interaction of fibrin(ogen) with the endothelial cell receptor VE-cadherin: mapping of the receptor-binding site in the NH2-terminal portions of the fibrin beta chains. Biochemistry 41: 4107-4116.

19. Petzelbauer P, Zacharowski PA, Miyazaki Y, Friedl P, Wickenhauser G, Castellino FJ, Groger M, Wolff K, Zacharowski K (2005) The fibrin-derived peptide Bbeta15-42 protects the myocardium against ischemia-reperfusion injury. Nat Med 11: 298-304.

20. Fareed J, Hoppensteadt DA, Leya F, Iqbal O, Wolf H, Bick R (1998) Useful laboratory tests for studying thrombogenesis in acute cardiac syndromes. Clin Chem 44: 1845-1853.

21. Roesner JP, Petzelbauer P, Koch A, Mersmann J, Zacharowski PA, Boehm O, Reingruber S, Pasteiner W, Mascher D, Wolzt M, Barthuber C, Noldge-Schomburg GE, Scheeren TW, Zacharowski K (2007) The fibrin-derived peptide Bbeta15-42 is cardioprotective in a pig model of myocardial ischemia-reperfusion injury. Crit Care Med 35: 1730-1735.

22. Zacharowski K, Zacharowski PA, Friedl P, Mastan P, Koch A, Boehm O, Rother RP, Reingruber S, Henning R, Emeis JJ, Petzelbauer P (2007) The effects of the fibrin-derived peptide Bbeta(15-42) in acute and chronic rodent models of myocardial ischemia-reperfusion. Shock 27: 631-637.

23. Atrasheuskaya A, Petzelbauer P, Fredeking TM, Ignatyev G (2003) Anti-TNF antibody treatment reduces mortality in experimental dengue virus infection. FEMS Immunol Med Microbiol 35: 33-42.

24. Srikiatkhachorn A, Krautrachue A, Ratanaprakarn W, Wongtapradit L, Nithipanya N, Kalayanarooj S, Nisalak A, Thomas SJ, Gibbons RV, Mammen MP, Jr., Libraty DH, Ennis FA, Rothman AL, Green S (2007) Natural history of plasma leakage in dengue hemorrhagic fever: a serial ultrasonographic study. Pediatr Infect Dis J 26: 283-290.

25. Halstead SB (2007) Dengue. Lancet 370: 1644-1652.

26. Bannerman DD, Goldblum SE (1999) Direct effects of endotoxin on the endothelium: barrier function and injury. Lab Invest 79: 1181-1199.

27. Coughlin SR (1999) How the protease thrombin talks to cells. Proc Natl Acad Sci U S A 96: 11023-11027.

28. Vu TK, Wheaton VI, Hung DT, Charo I, Coughlin SR (1991) Domains specifying thrombin-receptor interaction. Nature 353: 674-677.

29. Parsons JT, Martin KH, Slack JK, Taylor JM, Weed SA (2000) Focal adhesion kinase: a regulator of focal adhesion dynamics and cell movement. Oncogene 19: 5606-5613.

30. Brunton VG, MacPherson IR, Frame MC (2004) Cell adhesion receptors, tyrosine kinases and actin modulators: a complex three-way circuitry. Biochim Biophys Acta 1692: 121-144.

31. Ohkawara H, Ishibashi T, Sakamoto T, Sugimoto K, Nagata K, Yokoyama K, Sakamoto N, Kamioka M, Matsuoka I, Fukuhara S, Sugimoto N, Takuwa Y, Maruyama Y (2005) Thrombin-induced rapid geranylgeranylation of RhoA as an essential process for RhoA activation in endothelial cells. J Biol Chem 280: 10182-10188.

32. Vouret-Craviari V, Boquet P, Pouyssegur J, Van Obberghen-Schilling E (1998) Regulation of the actin cytoskeleton by thrombin in human endothelial cells: role of Rho proteins in endothelial barrier function. Mol Biol Cell 9: 2639-2653.

33. Yap AS, Kovacs EM (2003) Direct cadherin-activated cell signaling: a view from the plasma membrane. J Cell Biol 160: 11-16.

34. Noren NK, Arthur WT, Burridge K (2003) Cadherin engagement inhibits RhoA via p190RhoGAP. J Biol Chem 278: 13615-13618.

35. Nelson CM, Pirone DM, Tan JL, Chen CS (2004) Vascular endothelial-cadherin regulates cytoskeletal tension, cell spreading, and focal adhesions by stimulating RhoA. Mol Biol Cell 15: 2943-2953.

36. van Nieuw Amerongen GP, Natarajan K, Yin G, Hoefen RJ, Osawa M, Haendeler J, Ridley AJ, Fujiwara K, van H, V, Berk BC (2004) GIT1 mediates thrombin signaling in endothelial cells: role in turnover of RhoA-type focal adhesions. Circ Res 94: 1041-1049.

37. van Nieuw Amerongen GP, Musters RJ, Eringa EC, Sipkema P, van H, V (2008) Thrombin-induced endothelial barrier disruption in intact microvessels: role of RhoA/Rho kinase-myosin phosphatase axis. Am J Physiol Cell Physiol 294: C1234-C1241.

38. Beggs HE, Soriano P, Maness PF (1994) NCAM-dependent neurite outgrowth is inhibited in neurons from Fyn-minus mice. J Cell Biol 127: 825-833.

39. Grant SG, O'Dell TJ, Karl KA, Stein PL, Soriano P, Kandel ER (1992) Impaired long-term potentiation, spatial learning, and hippocampal development in fyn mutant mice. Science 258: 1903-1910.

40. Grant SG, Karl KA, Kiebler MA, Kandel ER (1995) Focal adhesion kinase in the brain: novel subcellular localization and specific regulation by Fyn tyrosine kinase in mutant mice. Genes Dev 9: 1909-1921.

41. Stein PL, Lee HM, Rich S, Soriano P (1992) pp59fyn mutant mice display differential signaling in thymocytes and peripheral T cells. Cell 70: 741-750.

42. Stein PL, Vogel H, Soriano P (1994) Combined deficiencies of Src, Fyn, and Yes tyrosine kinases in mutant mice. Genes Dev 8: 1999-2007.

43. Cobb BS, Schaller MD, Leu TH, Parsons JT (1994) Stable association of

pp60src and pp59fyn with the focal adhesion-associated protein tyrosine kinase, pp125FAK. Mol Cell Biol 14: 147-155.

44. Schaller MD, Hildebrand JD, Parsons JT (1999) Complex formation with focal adhesion kinase: A mechanism to regulate activity and subcellular localization of Src kinases. Mol Biol Cell 10: 3489-3505.

45. Jimenez B, Volpert OV, Crawford SE, Febbraio M, Silverstein RL, Bouck N (2000) Signals leading to apoptosis-dependent inhibition of neovascularization by thrombospondin-1. Nat Med 6: 41-48.

46. Cary LA, Chang JF, Guan JL (1996) Stimulation of cell migration by overexpression of focal adhesion kinase and its association with Src and Fyn. J Cell Sci 109 (Pt 7): 1787-1794.

47. Liang X, Draghi NA, Resh MD (2004) Signaling from integrins to Fyn to Rho family GTPases regulates morphologic differentiation of oligodendrocytes. J Neurosci 24: 7140-7149.

48. Holinstat M, Knezevic N, Broman M, Samarel AM, Malik AB, Mehta D (2006) Suppression of RhoA activity by focal adhesion kinase-induced activation of p190RhoGAP: role in regulation of endothelial permeability. J Biol Chem 281: 2296-2305.

49. Bukin EK, Otrashevskaia EV, Vorob'eva MS, Ignat'ev GM (2007) [Comparative study of hemostasis and cytokine production in experimental Dengue virus infection]. Vopr Virusol 52: 32-36.

50. Green TP, Johnson DE, Marchessault RP, Gatto CW (1988) Transvascular flux and tissue accrual of Evans blue: effects of endotoxin and histamine. J Lab Clin Med 111: 173-183.

4.2.2. $B\beta_{15-42}$ PROTECTS AGAINST ACID-INDUCED ACUTE LUNG INJURY AND SECONDARY *PSEUDOMONAS PNEUMONIA IN VIVO*

Ulrich Matt[1,2], Joanna Maria Warszawska[1,2], Michael Bauer[3], Wolfgang Dietl[3], Ildiko Mesteri[4], Bianca Doninger[1,2], Isabella Haslinger[2], Gernot Schabbauer[5], Thomas Perkmann[6], Christoph J. Binder[1,6], Sonja Reingruber[7], Peter Petzelbauer[8] & Sylvia Knapp[1,2]

[1]Research Center for Molecular Medicine of the Austrian Academy of Sciences (CeMM), Vienna, Austria; [2]Department of Medicine I, Div. of Infectious Diseases and Tropical Medicine, Medical University Vienna, Vienna, Austria; [3]Ludwig Boltzmann Cluster for Cardiovascular Research, Department of Biomedical Research, Medical University Vienna, Austria; [4]Department of Pathology, Medical University Vienna, Vienna, Austria; [5]Institute of Vascular Biology and Thrombosis Research, Center for Biomolecular Medicine and Pharmacology, Medical University Vienna, Vienna, Austria; [6]Department of Medical and Chemical Laboratory Diagnostics, Medical University Vienna, Vienna, Austria; [7]Fibrex Medical Research & Development GmbH., Vienna, Austria; [8]Department of Dermatology, Division of General Dermatology, Medical University Vienna, Vienna, Austria

Corresponding Author:

Sylvia Knapp, M.D., Ph.D.

Center for Molecular Medicine of teh Austrian Academy of Sciences, Department of Medicine 1, Div. Of Infectious Diseases and Tropical Medicine, Medical University Vienna

Waehringer Guertel 18-20; 1090 Vienna, Austria

Phone: 0043-1-40400-4954 or 4492 FAX: 0043-1-40400-4498
E-mail: sylvia.knapp@meduniwien.ac.at

Running title: fibrin-derived peptide $B\beta_{15-42}$ dampens inflammation in acute lung injury

Descriptor number: 1. Acute respiratory distress syndrome (ARDS) and acute lung injury (ALI): experimental models

Financial support: This work was in part supported by a grant from the Austrian Research

Funding Society: (FFG #811037, 'Bridge I')

At a glance commentary:

Scientific Knowledge on the Subject:

Vascular leak and neutrophil migration are hallmarks of acute lung injury. In spite of high mortality rates, specific therapies to prevent lung injury and inflammation are not available.

What This Study Adds to the Field:

The fibrin-derived peptide $B\beta_{15-42}$ prevents vascular leak and protects mice from acute lung injury and secondary *Pseudomonas aeruginosa* pneumonia *in vivo*.

Keywords: acute lung injury, inflammation, pneumonia, *Pseudomonas aeruginosa*

Abstract

Rationale: Acute lung injury is a serious condition in critically ill patients that predisposes to secondary bacterial pneumonia. Vascular leak is a hallmark in the pathogenesis of acute lung injury. The fibrin-derived peptide $B\beta_{15-42}$ was shown to preserve endothelial barriers, thereby reducing vascular leak. The potential therapeutic role of $B\beta_{15-42}$ in acute lung injury was not addressed so far.

Objectives: To investigate the therapeutic potential of $B\beta_{15-42}$ in acute lung injury and secondary pneumonia induced by *Pseudomonas aeruginosa*.

Methods: The effect of the fibrin derived peptide $B\beta_{15-42}$ was studied in models of acute lung injury, induced either by pulmonary administration of LPS or hydrochloric acid. Lung inflammation was analyzed by quantifying cell-influx, cytokine levels and oxidized lipids. Vascular leak was determined by Evans Blue extravasations and alveolar protein content. In subsequent two-hit studies, mice were infected with *Pseudomonas aeruginosa* 24h after induction of aspiration pneumonitis and effects of $B\beta_{15-42}$ on inflammation, bacterial clearance and survival were evaluated.

Results: After LPS or acid inhalation proinflammatory cytokine levels, neutrophil influx and vascular leak were found diminished in mice treated with $B\beta_{15-42}$. Acid aspiration impaired macrophage functions and rendered mice more susceptible to subsequent *Pseudomonas aeruginosa* infection, whereas mice that received $B\beta_{15-42}$ during acid aspiration and were subsequently challenged with bacteria, displayed reduced inflammation, enhanced bacterial clearance, and ultimately improved survival.

Conclusions: The fibrin-derived peptide $B\beta_{15-42}$ exerted protective effects during acute lung injury, resulting in diminished lung injury and preserved antibacterial properties of macrophages, which improved outcome during subsequent *Pseudomonas aeruginosa* pneumonia.

Introduction

Acute lung injury (ALI) is a serious condition defined as rapid-onset bilateral pulmonary infiltrates and hypoxemia of non-cardiac origin (1, 2). Acute respiratory distress syndrome (ARDS) is the most severe form of ALI. With a reported incidence of 79 per 100.000 and an in-hospital mortality of 40 percent, ALI represents a serious problem among intensive care unit (ICU) patients (3). ALI can develop as a result of direct injury to the lungs, such as during pneumonia, or aspiration of gastric contents, or occur in the course of systemic inflammation such as during sepsis or following trauma (4). Despite these different etiologies, the pathological features observed in ALI share common findings like protein-rich edema and accumulation of neutrophils (4, 5).

To investigate the molecular mechanisms leading to ALI, a number of animal models have been established. Among them, LPS- and hydrochloric acid (HCl) induced ALI are known to yield very reproducible results and are characterized by a rapid influx of polymorphonuclear leukocytes (PMNs), and release of proinflammatory cytokines. While both models ultimately lead to the disruption of endothelial barriers, LPS seems to primarily target the endothelium, whereas HCl has been reported to initially damage epithelial cells (6). Acid aspiration is a widely used model of ALI in mice, as it ideally imitates the pathophysiologic events observed in humans (7-9) by mimicking the clinically relevant event of aspiration of gastric contents in patients with reduced consciousness, referred to as aspiration pneumonitis (10).

Secondary bacterial infection is a frequent and dreaded complication in critically ill patients suffering from ALI (10). *Pseudomonas aeruginosa* (*P. aeruginosa*) is one of the most common pathogens causing nosocomial pneumonia, particularly in ICUs, where intubation favors its colonization, and antibiotic therapy selects multiresistant strains (11). Experimentally it was shown that preceding acid aspiration primes for an exaggerated, and thereby

harmful inflammation to subsequent administration of LPS (12) or bacteria (13). In both reports, administration of LPS or bacteria after instillation of acid led to a dramatic increase in proinflammatory cytokines such as IL-6, IL-1β, KC or MIP-2 (13). Westerloo *et al.* nicely demonstrated that clearance of *Klebsiella pneumoniae* was greatly impaired in mice suffering from preceding acid aspiration (13). In addition, others reported that acid aspiration enhanced bacterial adherence (14) and that gastric acid and particulate aspiration impaired pulmonary bacterial clearance (15). Hence, while ALI itself is considered a life-threatening condition, it furthermore predisposes to nosocomial pneumonia, thus underlining the urgent need for better treatment of ALI.

In 2005 a naturally occurring peptide derived from the N-terminus of the beta-chain of fibrin, $B\beta_{15-42}$, was shown to protect from myocardial reperfusion injury in rats due to its capacity to prevent leukocyte migration (16). In a subsequently installed multi-center phase IIa clinical trial, these findings could be confirmed in patients suffering from acute myocardial infarction (17). $B\beta_{15-42}$ significantly reduced the size of necrotic zones in patients with acute myocardial infarction undergoing primary percutaneous coronary intervention (17). In another series of experiments, $B\beta_{15-42}$ was shown to be vasculoprotective in models of vascular leak, such as Dengue hemorrhagic shock or LPS-shock (18). It improved survival and reduced vascular leak in a Fyn-dependent manner (18). The anti-inflammatory and vasculoprotective features of the peptide prompted us to test its therapeutic potential in the lung.

Although our understanding of pathophysiological mechanisms underlying ALI has improved substantially over the last years, therapeutic advances are missing and treatment recommendations are limited to protective ventilation and supportive care (19). The high lethality and great clinical importance of ALI prompted us to explore the therapeutic potential of $B\beta_{15-42}$ during ALI and secondary bacterial pneumonia.

Materials and Methods:

Animals:

Pathogen-free 9-11 week-old male C57BL/6 mice were purchased from Charles River. All experiments were approved by the local Ethics committee of the Medical University Vienna and the Ministry of Sciences.

Induction of ALI and pneumonia:

Acute lung inflammation and pneumonia was induced as described previously (20). Briefly, mice were short-term anesthetized by inhalation of isoflurane (Abbott Laboratories), and 50µl of LPS (*E. coli* O55:B5, 100ng, Sigma, St. Louis, MO) or *P. aeruginosa* (PA103) at indicated amounts was instilled intranasally (*i.n.*). For the induction of acid-induced lung injury mice were anaesthetized using ketamine and xylazine and 50µl of 0.1N endotoxin-free HCl (Sigma) was injected intratracheally. For more detailed information see the online supplement.

Peptide preparation and administration:

$B\beta_{15\text{-}42\text{-}NH2}$ (GHRPLDKKREEAPSLRPAPPPISGGGYR-NH2) was used as a proteolytically stable analogue of $B\beta_{15\text{-}42}$; random peptide or saline was used as control. Peptides were produced by solid-phase peptide synthesis and purified with reverse-phase high-performance liquid chromatography using nucleosil 100-10C18 columns (Lonza, Brussels, Belgium, and piChem Forschungs- und Entwicklungs-GmbH, Graz, Austria) (16). Mice were treated with 4.8 mg/kg i.p. at t=0 and t=+1h after LPS or acid-challenge, respectively. In all experiments

lasting longer than 24h mice received a third dose at t=+6h.

Lung sampling and quantification of CFUs:

Whole lungs were harvested and processed as described (21, 22), determination of lung CFUs is described in the online supplement.

Determination of vascular permeability, edema and histology:

Vascular leak was determined using Evans Blue extravasations as described (23). Edema was quantified by determining total protein concentration in broncho-alveolar lavage fluid (BALF) using a protein assay kit (Pierce, Rockford, Ill.). For lung-histology the left lobe was removed and processed as described earlier (21), paraffin sections were stained with Hematoxylin & Eosin. The degree of inflammation was scored based on the size of the infiltrate, presence of edema, bronchitis, thrombi, endothelitis, pleuritis and perivascular infiltrates by a pathologist blinded for groups. Immunohistochemical staining of interleukin-1 receptor associated kinase (IRAK)-M was done as described (24). Further details are outlined in the online supplement.

Broncho-alveolar lavage and differential cell count:

BAL was performed as described previously (21). Cells were enumerated using a hemocytometer and differential cell counts were performed on cytospin preparations stained with Giemsa. The BALF was stored at -70°C for determination of cytokines, protein content and oxidized lipids.

Protein, oxidized phospholipids and myeloperoxidase assays:

TNF-α, IL-1β, IL-6, IL-10, keratinocyte-derived chemokine (KC), macrophage-

inflammatory protein (MIP-2) and myeloperoxidase (MPO) were quantified in BALF and lung homogenates using specific ELISAs (R&D Systems, Minneapolis, MN and HyCult, Uden, the Netherlands) according to the manufacturers' instructions. Oxidized lipids were measured as described (25). More detailed information are provided in the online supplement.

Phagocytosis assay:

Phagocytosis of heat killed P. aeruginosa (PA103) was assessed in essence as described (26), and is further outlined in the online supplement.

Evaluation of mRNA levels in whole lung preparations:

Semi-quantitative mRNA analysis for IRAK-M transcripts in whole lung preparations was done as described (24), and is further outlined in the online supplement.

Statistics:

Values are expressed as mean±SEM. Data between 2 groups were analyzed using unpaired Student's t-test; for >2 groups one way ANOVA followed by Tukey´s multiple comparison test was used. Differences in CFU counts (non-parametric) were calculated using Mann-Whitney test (2 groups) or Kruskal-Wallis test followed by Dunn´s multiple comparison test (> 2 groups). Survival data were analyzed by Kaplan-Meier followed by log-rank test. Criteria for significance for all experiments were $p < 0.05$.

Results

$B\beta_{15\text{-}42\text{-}NH2}$ exerts anti-inflammatory properties within the lungs

We first analyzed the effects of $B\beta_{15\text{-}42\text{-}NH2}$ during acute pulmonary inflammation and challenged mice with 100ng LPS i.n. and administered 4.8 mg/kg of the peptide intraperitoneally (*i.p.*) immediately after LPS-challenge and one hour later. Control animals received saline or control peptides, respectively. After six hours we enumerated cells in BALF where we found significantly reduced numbers of neutrophils in mice treated with the peptide (Fig. 1A). In line with the decreased influx of PMNs we observed significantly reduced levels of proinflammatory cytokines and chemokines in BALF (Fig. 1B) and lungs (Fig. 1C) from $B\beta_{15\text{-}42\text{-}NH2}$ treated mice. While TNFα levels were significantly diminished in the broncho-alveolar compartment, IL-10 concentrations were elevated in lungs of $B\beta_{15\text{-}42\text{-}NH2}$ treated animals (Fig 1C). Because vascular leak is considered a hallmark of ALI, we also measured total protein contents in BALF of LPS-challenged mice and detected lower protein amounts in $B\beta_{15\text{-}42\text{-}NH2}$ treated animals (Fig. 1D). Finally, we were able to confirm that $B\beta_{15\text{-}42\text{-}NH2}$ treatment reduced vascular leak within the pulmonary compartment by illustrating diminished Evans-Blue extravasations during LPS-induced ALI (Fig. 1E). Hence, these data demonstrate that $B\beta_{15\text{-}42\text{-}NH2}$ exerts potent anti-inflammatory effects within the respiratory tract and attenuates vascular leak during ALI *in vivo*.

$B\beta_{15\text{-}42\text{-}NH2}$ dampens acid induced lung inflammation.

Having established that $B\beta_{15\text{-}42\text{-}NH2}$ reduces inflammation and improves vascular barrier function during LPS-pneumonitis *in vivo*, we next aimed for a model in which afore described findings could be utilized for therapeutic purposes

and decided to extend our studies to acid-induced ALI, which more closely reflects the situation seen in ICU patients. For this purpose we administered 50µl of endotoxin-free 0.1N HCl intratracheally, treated mice with $B\beta_{15\text{-}42\text{-}NH2}$ or saline as described above, and evaluated mice every 2h up to 8h. As depicted in Fig. 2A to D, $B\beta_{15\text{-}42\text{-}NH2}$ treatment resulted in a diminished PMN influx to the broncho-alveolar compartment, reduced levels of proinflammatory cytokines, and decreased total protein concentration in BALF. To investigate the inflammatory response and impact of $B\beta_{15\text{-}42\text{-}NH2}$ in more detail we then focused on 6h after instillation of acid and revealed that treatment with the peptide markedly contained the rise of leucocytes (Fig. 2E). A similar pattern was observed for levels of the proinflammatory cytokines in BALF and lung tissue (Fig. 2F and 2G). In line with a previous report, which delineated IL-6 as a crucial mediator of acid induced lung inflammation (25), we found IL-6 highly elevated upon acid aspiration whereas $B\beta_{15\text{-}42\text{-}NH2}$ treatment resulted in diminished IL-6 levels (Fig. 2F and 2G). IL-1β was significantly reduced in lungs of mice that received $B\beta_{15\text{-}42\text{-}NH2}$ (Fig. 2G), which is noteworthy as an earlier report discovered that IL-1R gene deficient mice exhibited an improved bacterial clearance during *P. aeurginosa* pneumonia (27). Similar to what we observed during LPS-pneumonitis, $B\beta_{15\text{-}42\text{-}NH2}$ treatment led to enhanced levels of the anti-inflammatory cytokine IL-10; significantly higher IL-10 concentrations were discovered in BALF from the treatment group, and IL-10 levels obtained from lung-homogenates were modestly elevated although differences did not reach significance ($p=0.055$) (Fig. 2F and 2G). Furthermore, the inhibitory effects of $B\beta_{15\text{-}42\text{-}NH2}$ on vascular leak during acid aspiration were confirmed by showing reduced total protein concentrations in BALF and diminished Evans Blue extravasations (Fig. 2H and 2I). Because acid aspiration-associated generation of reactive oxygen species and subsequent oxidation of pulmonary phospholipids were shown recently to perpetuate ALI

in vivo (25), we measured BALF-levels of oxidized phospholipids using the well-described antibody E06 (28). In accordance with diminished pulmonary inflammation, we observed a tendency towards reduced levels of oxidative epitopes in $B\beta_{15\text{-}42\text{-}NH2}$ treated animals (Fig. 2J), although differences did not reach significance (p=0.07). Together, $B\beta_{15\text{-}42\text{-}NH2}$ was able to attenuate lung injury following acid aspiration *in vivo*.

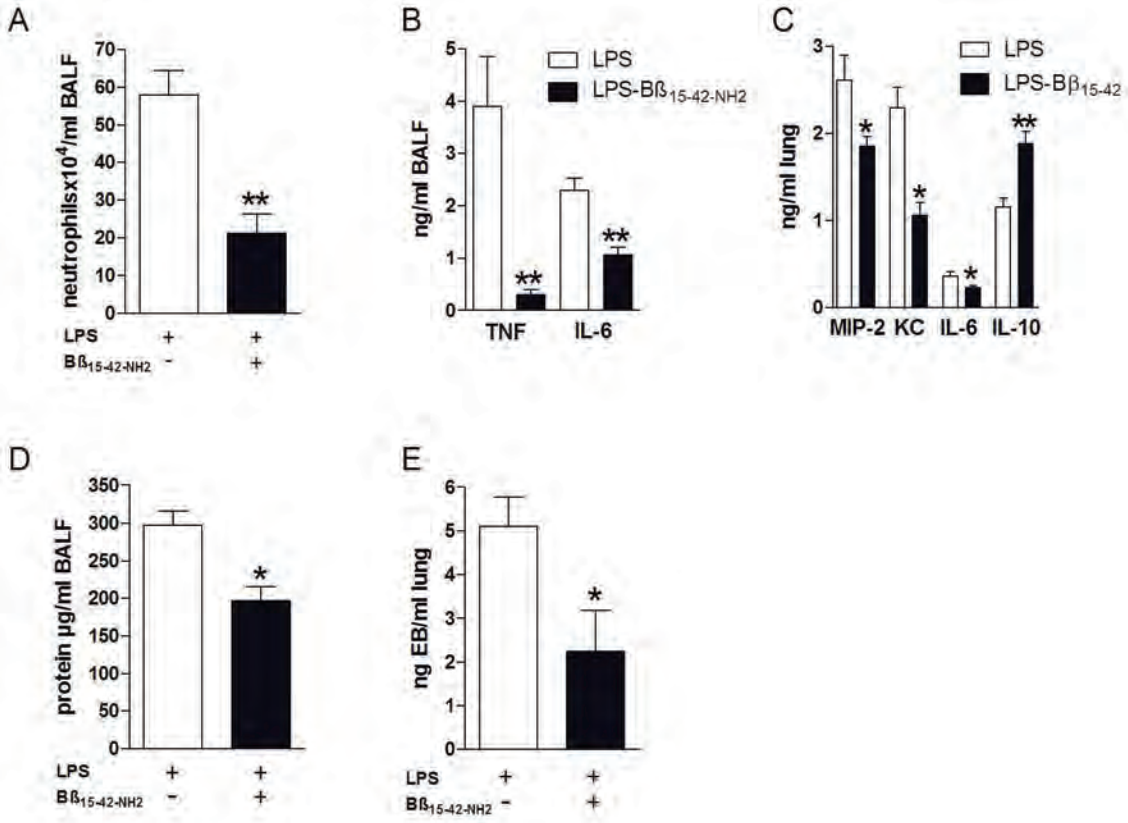

Figure 1. $B\beta_{15\text{-}42\text{-}NH2}$ exerts anti-inflammatory properties in the lung

Mice received 100ng LPS *i.n.* and $B\beta_{15\text{-}42\text{-}NH2}$ or carrier (NaCl), respectively, *i.p.* at t=0 and t=+1h. After 6h PMN influx was assessed by cytospin preparations of BALF (A), cytokines were measured in BALF (B) and lung homogenates (C), and total protein content in the BALF (D). For measurement of Evans Blue (EB) extravasations mice received 10µg LPS *i.n.* and $B\beta_{15\text{-}42\text{-}NH2}$ or NaCl treatment, respectively, as described above (E). (A-D): n=6 mice/group, (E): n=4 mice/group. Depicted are representative data out of 3 independent experiments. Data are mean ± SEM; *p < 0.05, **p < 0.01.

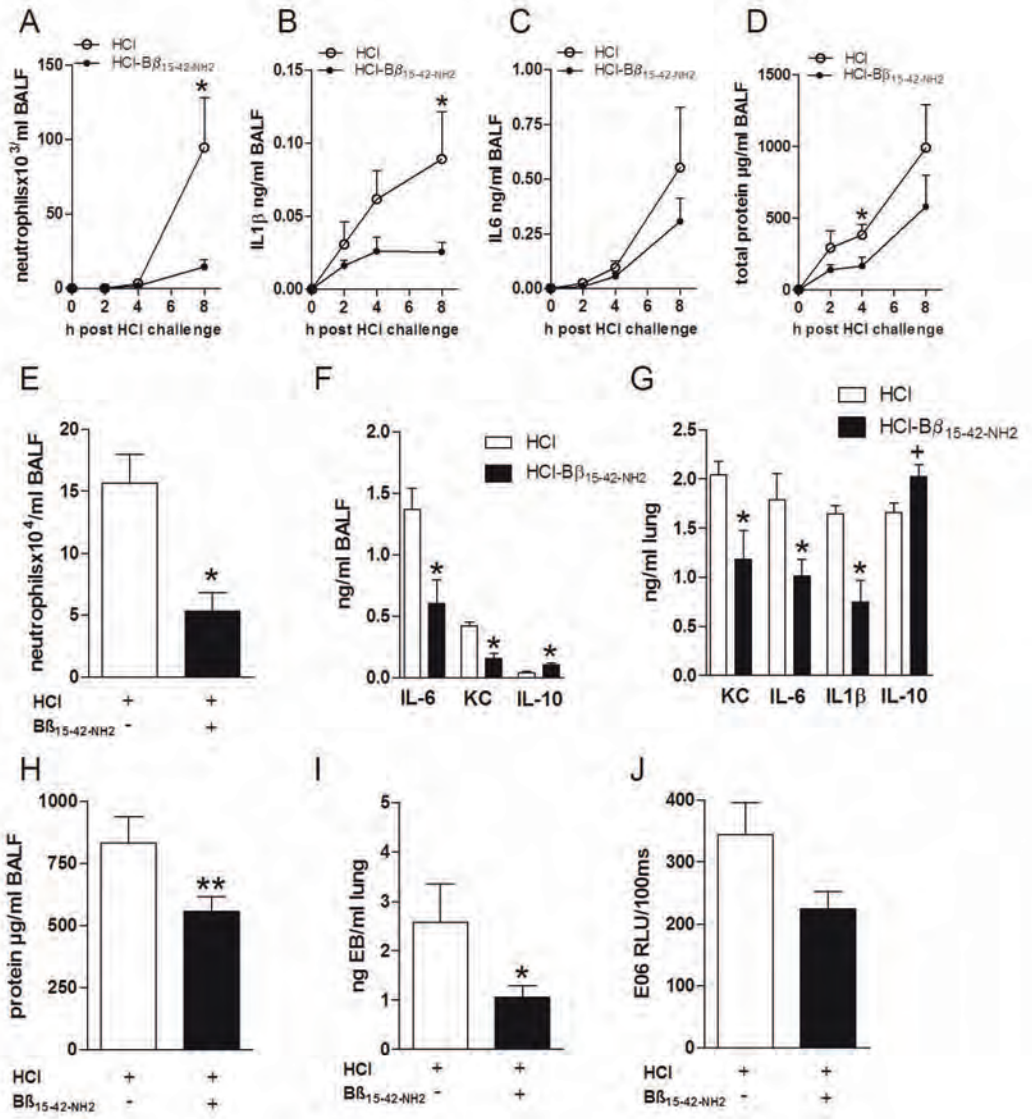

Figure 2. Bß$_{15\text{-}42\text{-}NH2}$ dampens acid induced lung inflammation

Endotoxin-free 0.1N HCl (50µl) was instilled intratracheally in mice followed by *i.p.* injection of Bß$_{15\text{-}42\text{-}NH2}$ or carrier (NaCl) at t=0 and t=+1h. Time course analysis for PMN influx (A), IL1β (B), IL6 levels (C) and total protein concentration (D) in BALF are depicted. After 6h PMN influx in BALF was assessed on cytospin preparations (E), cytokines and chemokines were measured in BALF (F) and lung homogenates (G). Total protein content was measured in BALF (H). Evans Blue extravasations were quantified in lung homogenates (I) and oxidation epitopes (E06) in BALF (J). (A-I): n=6-8 mice/group; (J): pooled data of 2 experiments (n=11-13 mice/group). Data shown are 1 out of 2 independent experiments and depicted as mean ± SEM; *$p < 0.05$, **$p < 0.01$.

Preceding acid aspiration impairs bacterial clearance during *P. aeruginosa* pneumonia

Arguing that pre-existing acid-induced lung damage predisposes patients for subsequent bacterial pneumonia, we hypothesized that attenuation of acid induced lung injury might improve outcome during secondary bacterial respiratory tract infection. To test this concept we first attempted to establish that acid aspiration would alter the course of secondary pneumonia induced by *P. aeruginosa*, the most frequently isolated pathogen in hospital-acquired pneumonia (29). For this purpose we induced acid aspiration or administered saline, respectively, and infected all mice *i.n.* with *P. aeruginosa* after 24h. This specific infection time point was chosen after we had determined that acid induced lung inflammation gradually resolved by 24h. Mice were then sacrificed 16h after secondary intranasal infection with *P. aeruginosa* and the inflammatory response and bacterial clearance was evaluated. As anticipated, preceding acid aspiration was associated with highly elevated lung-levels of pro-inflammatory cytokines such as KC, IL-6, IL-1β or TNF-α compared to control animals (Fig. 3A). Neutrophil influx, which was assessed by measuring lung MPO concentrations, was significantly higher in mice that underwent acid aspiration before pneumonia as compared to saline-treated mice (Fig. 3B). Furthermore, despite this exaggerated inflammatory response, bacterial clearance was greatly impaired, leading to almost 1000-fold increased bacterial counts in lungs from mice of the acid-aspiration group, as compared to control animals (Fig. 3C). Therefore, preceding acid aspiration impairs host defense mechanisms against secondary *P. aeruginosa* infection.

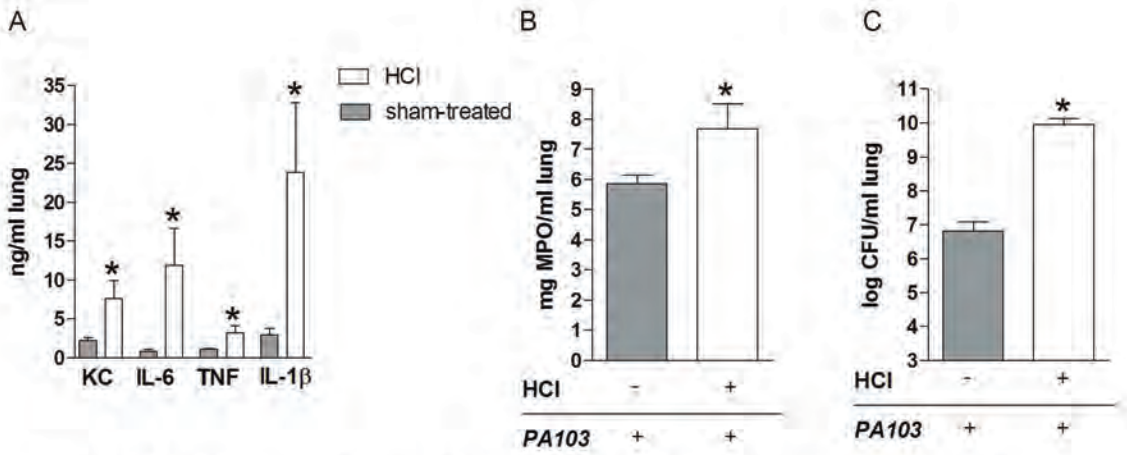

Figure 3. Acid aspiration impairs host response to *P. aeruginosa* pneumonia

Mice received 50µl of 0.1N HCl (HCl group) or sterile NaCl (sham group) and 24h later $1x10^4$ CFU *P. aeruginosa i.n.*. Mice were sacrificed 16h after bacterial infection and lung cytokines, chemokines and MPO were evaluated (A, B). Serial dilutions of lung homogenates were plated on blood agar plates to determine bacterial CFUs (C). Data are from n=8 mice/group, and represent mean ± SEM. *$p < 0.05$.

$B\beta_{15\text{-}42\text{-}NH2}$ diminishes the unfavorable, exaggerated immune response to *P. aeruginosa* after acid aspiration

We next tested our hypothesis that $B\beta_{15\text{-}42\text{-}NH2}$ treatment would reduce acid induced lung injury and thus attenuate detrimental effects on the host response to subsequent bacterial pneumonia. For this purpose we repeated before described experiments, challenged mice with HCl or saline (sham group), respectively, and treated one group of mice that received HCl i.t. with $B\beta_{15\text{-}42\text{-}NH2}$ i.p. at t=0h, +1h, and +6h after intratracheal acid administration. Twenty four h later we ensured gradual resolution of acid-induced lung inflammation and observed that inflammatory markers did not differ between the sham group and HCl-mice that received $B\beta_{15\text{-}42\text{-}NH2}$ (Table 1).

Lung	Sham	HCl	HCl-Bß$_{15-42-NH2}$
MPO mg/ml	1.2 ± 0.08	1.5 ± 0.02*	1.1 ± 0.01
IL-6 ng/ml	0.28 ± 0.02	0.53 ± 0.13	0.31 ± 0.03
KC ng/ml	1.64 ± 0.06	2.7 ± 0.12*	1.24 ± 0.02
TNF ng/ml	0.23 ± 0.01	0.23 ± 0.02	0.21 ± 0.03
E06 RLU/100ms	6108 ± 2085	15947 ± 4190	5453 ± 887

Table 1. Pulmonary inflammation markers 24h after acid aspiration

Mice underwent NaCl (sham) or acid aspiration (HCl) with subsequent Bß$_{15-42-NH2}$ treatment (HCl-Bß$_{15-42-NH2}$). Pulmonary inflammation markers were evaluated after 24h. Shown are mean ± SEM of n=3 mice/group; *$p < 0.05$ versus sham and HCl-Bß$_{15-42-NH2}$ group.

Next we aimed to evaluate the effects of these differences on a second hit pneumonia with *P. aeruginosa*. We therefore inoculated mice intranasallay twenty-four h after acid aspiration or sham surgery, respectively, with *P. aeruginosa* and evaluated the host inflammatory response 16h thereafter (i.e. 24h acid aspiration + 16h infection). Upon analysis of pulmonary cytokine and chemokine levels, we discovered that Bß$_{15-42-NH2}$ treatment of mice that received HCl resulted in almost identical lung concentrations of MPO, KC, IL-6, TNF-α and IL-1β as those found in mice that received saline instead of HCl (Fig. 4A-C). While acid aspiration followed by *P. aeruginosa* infection led to an enhanced inflammatory response, sham treated mice (i.e. NaCl instead of HCl) and Bß$_{15-42-NH2}$ treated mice (i.e. HCl and Bß$_{15-42-NH2}$) displayed significantly reduced concentrations of proinflammatory mediators and MPO levels. In parallel, the anti-inflammatory cytokine IL-10 showed the opposite feature, with lowest levels found in mice that underwent acid aspiration before infection (Fig. 4D). When enumerating lung CFUs we observed striking differences: Bß$_{15-42-NH2}$ treated mice that underwent acid aspiration showed an identical bacterial load as sham-treated control animals (NaCl aspiration), whereas in mice that underwent acid aspiration followed by bacterial infection approximately 4-log higher numbers of bacteria were recovered from lungs (Fig. 4E). Likewise, systemic bacterial dissemination was found reduced in Bß$_{15-42-}$

$_{NH2}$ treated mice. While 33% of blood cultures were positive in acid aspiration mice, only 8% and 13% of control or Bß$_{15\text{-}42\text{-}NH2}$ treated mice, respectively, displayed systemic bacterial spread. To finally test if administration of Bß$_{15\text{-}42\text{-}NH2}$ after onset of lung injury still exerts therapeutic effects, we repeated the second hit study and started peptide treatment at t=0h, t=+1h, or t=+2h after acid aspiration. Identical to earlier experiments, all mice received additional doses of Bß$_{15\text{-}42\text{-}NH2}$ 1h and 6h after the first application and *P. aeruginosa* was administered 24h after acid aspiration. As depicted in Fig. 4F, Bß$_{15\text{-}42\text{-}NH2}$ treatment 1h after the initial injury still exerted beneficial effects and resulted in significantly improved bacterial clearance.

In line with enhanced bacterial outgrowth and proinflammatory cytokine levels, mice of the acid aspiration and infection group exhibited significantly more pronounced signs of lung inflammation and injury as assessed by histopathological scoring of lung slides (Fig. 5). Lungs from both control and Bß$_{15\text{-}42\text{-}NH2}$ treated mice showed only residual signs of inflammation. Therefore, improvement of lung barrier function during acid aspiration attenuated detrimental effects of subsequent *P. aeruginosa* challenge *in vivo*.

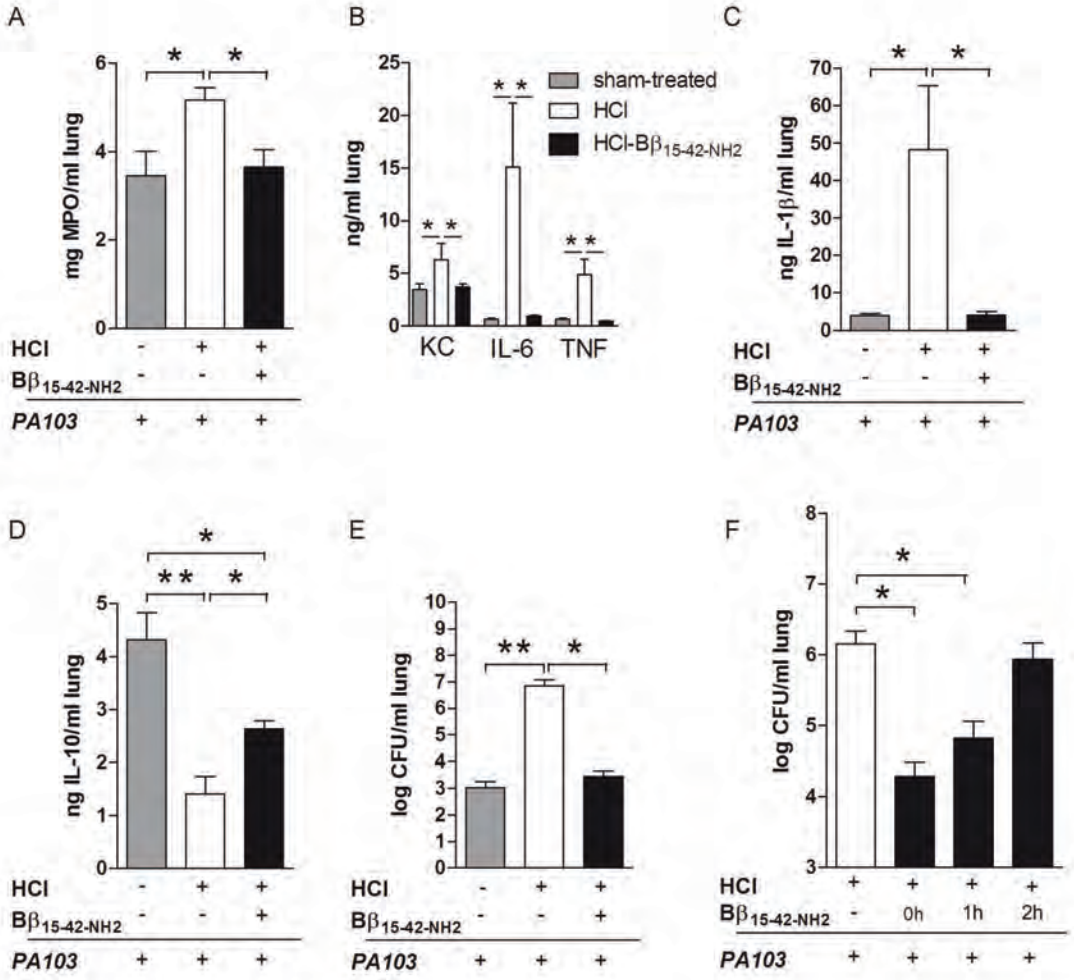

Figure 4. Bß$_{15\text{-}42\text{-}NH2}$ treatment of aspiration-induced ALI dampens inflammation during secondary *P. aeruginosa* pneumonia

Endotoxin-free 0.1N HCl (50µl) was instilled intratracheally in mice followed by *i.p.* injection of Bß$_{15\text{-}42\text{-}NH2}$ (HCl-Bß$_{15\text{-}42\text{-}NH2}$) or sterile NaCl (HCl) at t=0, t=+1h and t=+6h. Sham-treated animals received sterile NaCl intratracheally and *i.p.* (sham group). After 24h all three groups were infected with 1x10^4 CFU *P. aeruginosa i.n.*. Sixteen h after infection mice were sacrificed and MPO, cytokines and chemokines in lung homogenates were evaluated (A-D). Lung CFUs were determined on blood agar plates (E). Depicted is 1 out of 3 independent experiments of n=6-9 mice/group. In (F) mice were treated as described above with the exception that Bβ$_{15\text{-}42\text{-}NH2}$ treatment was started at t=0h, t=+1h or t=+2h after acid aspiration (black bars). Control mice (white bar) did not receive any Bβ$_{15\text{-}42\text{-}NH2}$. All mice were infected with P. aeruginosa 24h after acid aspiration. (A-F) Data are mean ± SEM; *p < 0.05, **p < 0.01.

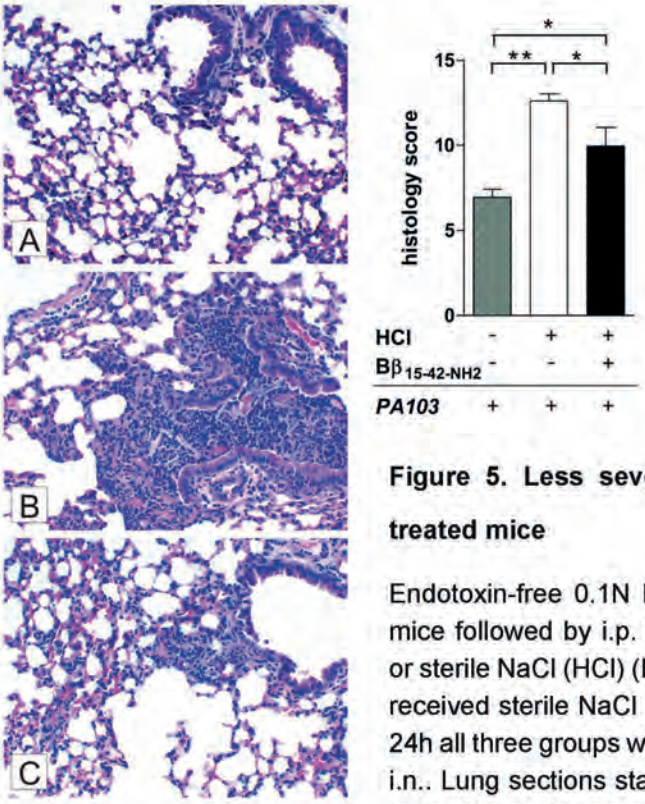

Figure 5. Less severe pulmonary infiltrates in Bß$_{15-42-NH2}$ treated mice

Endotoxin-free 0.1N HCl (50µl) was instilled intratracheally in mice followed by i.p. injection of Bß$_{15-42-NH2}$ (HCl-Bß$_{15-42-NH2}$) (C) or sterile NaCl (HCl) (B) at t=0, t=+1h and t=+6h. Control groups received sterile NaCl intratracheally and i.p. (Control) (A). After 24h all three groups were infected with 1x10^4 CFU *P. aeruginosa* i.n.. Lung sections stained with H&E were scored as described in the Methods section by a pathologist blinded for groups and are expressed as inflammation score. Representative slides are shown; magnification x 20. Depicted is 1 out of 3 independent experiments of n=6-9 mice/group; data are mean ± SEM; *p < 0.05, **p < 0.01.

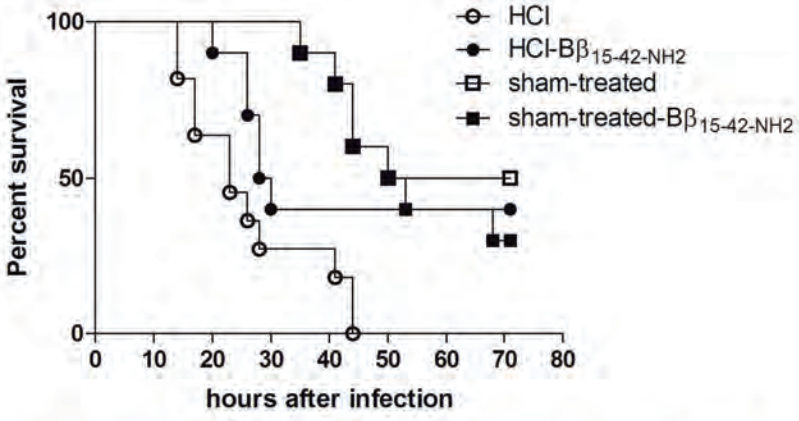

Figure 6. Bß$_{15-42-NH2}$ improves survival during secondary *P. aeruginosa* pneumonia

Endotoxin-free 0.1N HCl (50µl) was instilled intratracheally in mice followed by *i.p.* injection of Bß$_{15-42-NH2}$ (HCl-Bß$_{15-42-NH2}$) or sterile NaCl (HCl) at t=0, t=+1h and t=+6h. Control groups received sterile NaCl intratracheally and *i.p.* (sham-treated) or NaCl intratracheally and Bß$_{15-42-NH2}$ *i.p.* (sham-treated-Bß$_{15-42-NH2}$). After 24h all four groups were *i.n.* infected with 1x10^4 CFU *P. aeruginosa*. Survival of n=9-11 mice/group was monitored over 72h. Control and Bß$_{15-42-NH2}$ treated animals displayed an improved survival compared to the HCl-group ($p < 0.05$).

Bß$_{15\text{-}42\text{-}NH2}$ treatment reduces mortality due to secondary *P. aeruginosa* pneumonia.

To ultimately verify the potential therapeutic benefit of Bß$_{15\text{-}42\text{-}NH2}$ treatment during acid-induced ALI followed by bacterial infection, we induced acid or NaCl aspiration in mice, treated one HCl group with Bß$_{15\text{-}42\text{-}NH2}$, followed by *P. aeruginosa* infection and monitored survival over 4 days. To exclude any potential effect of Bß$_{15\text{-}42\text{-}NH2}$ on the course of bacterial infection itself, we included a second sham-group that received Bß$_{15\text{-}42\text{-}NH2}$ together with NaCl aspiration (sham-treated- Bß$_{15\text{-}42\text{-}NH2}$). Survival data clearly demonstrated the impact of preceding acid aspiration on secondary pneumonia, as well as the therapeutic role of Bß$_{15\text{-}42\text{-}NH2}$ herein. While all mice undergoing acid aspiration succumbed to bacterial infection within 44h, 50% of control animals (i.e. NaCl aspiration) and 40% of Bß$_{15\text{-}42\text{-}NH2}$ treated acid aspiration mice survived secondary *P. aeruginosa* pneumonia (both control groups and HCl-Bß$_{15\text{-}42\text{-}NH2}$ mice $p<0.05$ versus HCl) (Fig. 6). Bß$_{15\text{-}42\text{-}NH2}$ administration to sham-treated mice had no effect on the course of bacterial infection. Hence, Bß$_{15\text{-}42\text{-}NH2}$ treatment clearly improved the acid-aspiration induced impairment in host defense mechanisms and decreased death from secondary bacterial pneumonia.

Preceding acid aspiration impairs antibacterial properties of alveolar macrophages

In our efforts to understand how Bß$_{15\text{-}42\text{-}NH2}$ treatment improved bacterial clearance during secondary pneumonia despite decreased inflammation, we hypothesized that prevention of acute lung injury might preserve antibacterial properties of phagocytes at the onset of infection. To test this idea we first investigated if acid aspiration per se impaired the phagocytic properties of

macrophages and repeated acid aspiration studies to isolate primary alveolar macrophages 24h after mice received HCl alone or in combination with $B\beta_{15\text{-}42\text{-}NH2}$ (i.e. at the time when we challenged mice with *P. aeruginosa* in earlier experiments). Isolated primary alveolar macrophages were then studied for their ability to phagocytose *P. aeruginosa* ex vivo. As shown in Fig. 7A, preceding acid aspiration significantly impaired phagocytosis of bacteria by alveolar macrophages ($p<0.001$ versus sham-treated mice), whereas treatment with $B\beta_{15\text{-}42\text{-}NH2}$ completely prevented this effect ($p<0.001$ versus HCl group). Hence, preceding acid aspiration itself led to impaired antimicrobial properties of alveolar macrophages and attenuation of pulmonary inflammation (as seen in $B\beta_{15\text{-}42\text{-}NH2}$ treated animals) restored the phagocytic functions of alveolar macrophages. In order to understand how preceding lung injury interfered with bactericidal properties of phagocytes, we hypothesized that expression of negative regulators, which are required for resolution of inflammation, might concurrently impact the antimicrobial functions of macrophages. We therefore quantified expression levels of IRAK-M in lung homogenates 24h after induction of acid aspiration and indeed found significantly enhanced IRAK-M transcript levels in lungs from mice that received HCl, as compared to sham-treated or HCl-$B\beta_{15\text{-}42\text{-}NH2}$ animals (Fig. 7B). In addition, immunhohistochemical studies on primary alveolar macrophages disclosed strongest IRAK-M protein expression in cells from HCl-treated mice as compared to HCl-$B\beta_{15\text{-}42\text{-}NH2}$ animals (Fig. 7C). Together, we demonstrated that preceding lung injury increased expression of negative regulators such as IRAK-M, which was associated with impaired bactericidal properties of alveolar macrophages at the onset of bacterial infection (i.e. 24h after HCl administration) and might thus explain worsened outcome during subsequent *Pseudomonas* pneumonia.

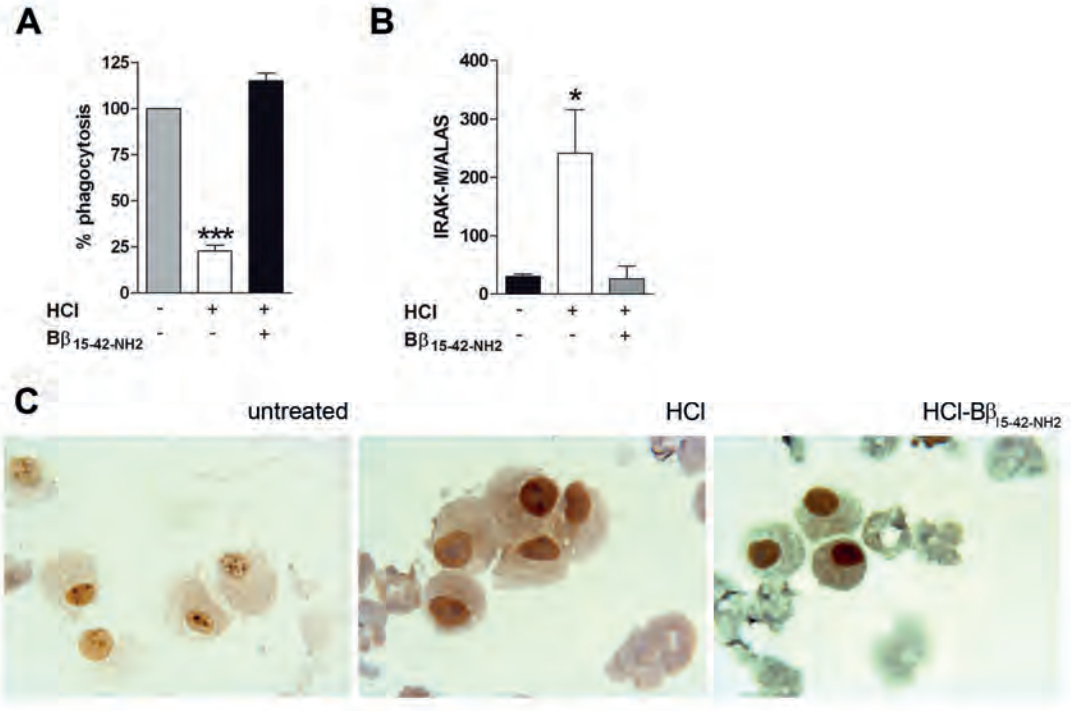

Figure 7. Acid-induced inflammation impairs bacterial phagocytosis by alveolar macrophages

Endotoxin-free 0.1N HCl (50µl) was instilled intratracheally in mice followed by i.p. injection of $B\beta_{15\text{-}42\text{-}NH2}$ (HCl-$B\beta_{15\text{-}42\text{-}NH2}$) or sterile NaCl (HCl) at t=0, t=+1h and t=+6h. Control groups received sterile NaCl intratracheally and i.p. (sham-treated). (A) After 24h alveolar macrophages were harvested, and uptake of FITC-labeled *P. aeruginosa* was assessed by FACS; (n=7 mice/ group). (B) Lungs were harvested after 24h to conduct RT-PCR on IRAK-M; (n=3 mice/ group). (C) Representative slides from immunohistochemical staining of IRAK-M on alveolar macrophages 24 h after acid aspiration. Values are expressed as mean ± SEM; *$p < 0.05$, ***$p < 0.001$.

Discussion

Vascular leak, neutrophil influx, and rise in cytokines at the site of injury are hallmarks of ALI in humans and animals (5, 6, 30). Although important progress has been made in understanding the pathogenesis of ALI over the last years, significant therapeutic implications are still missing. In order to fill this gap we decided to investigate the potential role of a peptide that has been shown earlier to prevent transmigration of neutrophils and vascular leak in models of myocardial reperfusion injury. This peptide is called $B\beta_{15-42,}$ consists of 28aa and is a natural plasmin digest of fibrin (16). For studies shown here we have used a proteolytically stable analogue, $B\beta_{15-42-NH2.}$ We studied different models of ALI and show that treatment with $B\beta_{15-42-NH2}$ diminished lung inflammation in vivo. Furthermore, we were able to illustrate that acid-induced ALI impaired antibacterial defense mechanisms and thus primed for an exaggerated inflammatory response to secondary bacterial infection by P. aeruginosa and that treatment with $B\beta_{15-42-NH2}$ could attenuate the detrimental effects of preceding ALI *in vivo*. The net result was improved survival from secondary P. aeruginosa pneumonia. We suggest that reduced inflammation throughout the course of acid aspiration in animals treated with the peptide, and therefore accelerated regeneration from this injurious event (see Table1) with restored antimicrobial properties (Fig. 7A), is responsible for the improved outcome in the second hit model. As to our knowledge, this is the first report that explicitly demonstrates a therapeutic strategy to improve outcome during secondary bacterial pneumonia by diminishing ALI *in vivo*.

Endothelial cells play a central role in the pathogenesis of acute lung injury (31). The biological properties of $B\beta_{15-42}$ were first described in 2005, when anti-inflammatory features of the peptide were identified (16). We have extended these studies and could show recently that $B\beta_{15-42}$ antagonizes stress

induced RhoA activation (18), which is an integral regulator of endothelial cell contraction by regulating levels of myosin light chain phosphorylation (32-34). Cell contraction and breaking of cell-cell contacts results in gap formation and leak (32, 35, 36). Earlier studies thoroughly investigated the role of myosin light chain kinase 210 (MLCK210), which is abundantly present in endothelial cells, during sepsis and LPS-induced ALI. Using MLCK210 gene-deficient mice or a small-molecule inhibitor approach, respectively, two reports demonstrated diminished lung injury in response to sepsis or LPS and mechanical ventilation *in vivo* (37, 38). Furthermore, genetic studies revealed single nucleotide polymorphisms of the MLCK210 gene to confer susceptibility to sepsis- and trauma-associated ALI in humans (39, 40). These findings are in line with the proposed mode of action of $B\beta_{15-42}$, namely inhibiting RhoA activation with subsequently reduced myosin light chain phosphorylation (18). The functional importance of this finding was conclusively confirmed by showing reduced vascular leak in LPS-challenged mice that have received $B\beta_{15-42}$. We hereby extended these findings and focused on the potential therapeutic role of $B\beta_{15-42}$ during ALI *in vivo*. Employing two distinct mouse models of ALI enabled us to show that early treatment with $B\beta_{15-42}$ efficiently preserved the endothelial barrier and diminished pulmonary inflammation following LPS or hydrochloric acid administration.

Aspiration of acid represents a clinically relevant and useful tool to study ALI (6), as aspiration of gastric contents is a major cause of ALI and associated with high mortality rates (27, 41). Adding to the poor prognosis, patients with ALI that require mechanical ventilation are at increased risk for secondary bacterial infection (42). The chemical injury by HCl is thought to directly damage airway epithelia, which in turn triggers an inflammatory response followed by edema formation and influx of neutrophils (5, 43-47). Experimentally it has been shown that prior lung injury caused by acid aspiration or during sepsis

primes for fatal secondary pneumonia (13, 48). Westerloo *et al.* observed acid-induced enhanced inflammation to result in worsened outcome during secondary *Klebsiella* pneumonia. In line with these findings, we also observed a tremendously enhanced inflammatory response and impaired bacterial clearance in a model of secondary bacterial pneumonia induced by *P. aeruginosa* after acid aspiration. We moreover disclosed that acid aspiration resulted in impaired bacterial clearance, which was associated with enhanced pulmonary expression of the negative regulator IRAK-M (Fig. 7B and 7C). IRAK-M is an inhibitor of TLR-signaling, and involved in the resolution of inflammation (49). Deng *et al.* demonstrated the crucial role of IRAK-M in bacterial clearance of *P. aeruginosa* earlier using a model of sublethal cecal ligation puncture followed by secondary bacterial pneumonia (48). We hereby confirmed and extended these observations by demonstrating that $B\beta_{15\text{-}42\text{-}NH2}$ treatment was able to reduce lung injury, diminish IRAK-M expression and thus restore antimicrobial properties of alveolar macrophages.

Time-course studies revealed the immediate leakage of proteins into the alveolar compartment and therefore suggest an early involvement of endothelial cells. In parallel, beneficial effects of $B\beta_{15\text{-}42\text{-}NH2}$ were discernable 2h after induction of lung injury and ultimately resulted in less pronounced inflammation and thus accelerated resolution. It therefore seems likely that increased IL-10 levels 6h after acid aspiration already reflected the early resolution phase, since increased phagocytosis by macrophages of spent cells is associated with release of IL-10 (50). This concept was further confirmed by reduced IRAK-M transcript levels in $B\beta_{15\text{-}42\text{-}NH2}$ treated animals after 24h. Hence, $B\beta_{15\text{-}42\text{-}NH2}$ associated attenuation of lung injury expedited resolution and recovery.

To our current knowledge, VE-cadherin is the only transmembrane ligand of $B\beta_{15\text{-}42.}$ VE-cadherin is expressed on endothelial cells and is of integral

importance in regulating endothelial barrier function and inflammation (51). The reduced cytokine levels seen after treatment with $B\beta_{15-42}$ could be a secondary effect of vascular integrity *in vivo*, as incubation of $B\beta_{15-42}$ with LPS-stimulated monocytes, alveolar macrophages or endothelial cells *in vitro* did not result in an altered release of proinflammatory cytokines (data not shown). Moreover, we could clearly illustrate that $B\beta_{15-42}$ administration to sham-treated mice did not affect host defense mechanisms against *P. aeruginosa in vivo*. Of interest is the observation that even mice that were treated one hour after acid aspiration showed improved bacterial clearance in a second hit model (Fig. 4F). Apart from endothelial cells, alveolar epithelial cells importantly contribute to the integrity of the alveolar barrier and are crucially involved in formation and clearance of ALI (52). Although it is tempting to speculate that $B\beta_{15-42}$ also acts on epithelial cells, we currently have no data that would imply a role for $B\beta_{15-42}$ in specifically affecting the epithelial barrier function.

In conclusion, we hereby established tissue protective properties of $B\beta_{15-42}$ within the pulmonary compartment by investigating two distinct models of ALI. Our data furthermore indicate that mitigation of ALI can restore antimicrobial properties of alveolar macrophages and thus improve outcome during secondary bacterial pneumonia. Together these results as well as recently published data on the tolerability and efficacy of $B\beta_{15-42}$ in patients undergoing coronary intervention (17) suggest that $B\beta_{15-42}$ might be an attractive therapy to abate harmful consequences of ALI.

Acknowledgments

We would like to thank Peter Haslinger for graphical assistance.

Conflict of interest statement

PP and SR are founders and shareholders of Fibrex Medical Inc.; SR is employed by Fibrex. www.fibrexmedical.com.

References:

1. Herridge, M. S., and D. C. Angus. 2005. Acute lung injury--affecting many lives. N Engl J Med 353(16):1736-8.
2. Bernard, G. R., A. Artigas, K. L. Brigham, J. Carlet, K. Falke, L. Hudson, M. Lamy, J. R. Legall, A. Morris, and R. Spragg. 1994. The American-European Consensus Conference on ARDS. Definitions, mechanisms, relevant outcomes, and clinical trial coordination. Am J Respir Crit Care Med 149(3 Pt 1):818-24.
3. Rubenfeld, G. D., E. Caldwell, E. Peabody, J. Weaver, D. P. Martin, M. Neff, E. J. Stern, and L. D. Hudson. 2005. Incidence and outcomes of acute lung injury. N Engl J Med 353(16):1685-93.
4. Ware, L. B., and M. A. Matthay. 2000. The acute respiratory distress syndrome. N Engl J Med 342(18):1334-49.
5. Matthay, M. A., and G. A. Zimmerman. 2005. Acute lung injury and the acute respiratory distress syndrome: four decades of inquiry into pathogenesis and rational management. Am J Respir Cell Mol Biol 33(4):319-27.
6. Matute-Bello, G., C. W. Frevert, and T. R. Martin. 2008. Animal models of acute lung injury. Am J Physiol Lung Cell Mol Physiol 295(3):L379-99.
7. Imai, Y., J. Parodo, O. Kajikawa, M. de Perrot, S. Fischer, V. Edwards, E. Cutz, M. Liu, S. Keshavjee, T. R. Martin, J. C. Marshall, V. M. Ranieri, and A. S.

Slutsky. 2003. Injurious mechanical ventilation and end-organ epithelial cell apoptosis and organ dysfunction in an experimental model of acute respiratory distress syndrome. Jama 289(16):2104-12.

8. Imai, Y., K. Kuba, S. Rao, Y. Huan, F. Guo, B. Guan, P. Yang, R. Sarao, T. Wada, H. Leong-Poi, M. A. Crackower, A. Fukamizu, C. C. Hui, L. Hein, S. Uhlig, A. S. Slutsky, C. Jiang, and J. M. Penninger. 2005. Angiotensin-converting enzyme 2 protects from severe acute lung failure. Nature 436(7047):112-6.

9. Nagase, T., N. Uozumi, S. Ishii, K. Kume, T. Izumi, Y. Ouchi, and T. Shimizu. 2000. Acute lung injury by sepsis and acid aspiration: a key role for cytosolic phospholipase A2. Nat Immunol 1(1):42-6.

10. Marik, P. E. 2001. Aspiration pneumonitis and aspiration pneumonia. N Engl J Med 344(9):665-71.

11. Sadikot, R. T., T. S. Blackwell, J. W. Christman, and A. S. Prince. 2005. Pathogen-host interactions in Pseudomonas aeruginosa pneumonia. Am J Respir Crit Care Med 171(11):1209-23.

12. Yamada, H., H. Miyazaki, T. Kikuchi, J. Fujimoto, and I. Kudoh. 2000. Acid instillation enhances the inflammatory response to subsequent lipopolysaccharide challenge in rats. Am J Respir Crit Care Med 162(4 Pt 1):1366-71.

13. van Westerloo, D. J., S. Knapp, C. van't Veer, W. A. Buurman, A. F. de Vos, S. Florquin, and T. van der Poll. 2005. Aspiration pneumonitis primes the host for an exaggerated inflammatory response during pneumonia. Crit Care Med 33(8):1770-8.

14. Mitsushima, H., K. Oishi, T. Nagao, A. Ichinose, M. Senba, T. Iwasaki, and T. Nagatake. 2002. Acid aspiration induces bacterial pneumonia by enhanced bacterial adherence in mice. Microb Pathog 33(5):203-10.

15. Rotta, A. T., K. T. Shiley, B. A. Davidson, J. D. Helinski, T. A. Russo, and P. R. Knight. 2004. Gastric acid and particulate aspiration injury inhibits pulmonary bacterial clearance. Crit Care Med 32(3):747-54.

16. Petzelbauer, P., P. A. Zacharowski, Y. Miyazaki, P. Friedl, G. Wickenhauser, F.

J. Castellino, M. Groger, K. Wolff, and K. Zacharowski. 2005. The fibrin-derived peptide Bbeta15-42 protects the myocardium against ischemia-reperfusion i njury. Nat Med 11(3):298-304.

17. Atar, D., P. Petzelbauer, J. Schwitter, K. Huber, B. Rensing, J. D. Kasprzak, C. Butter, L. Grip, P. R. Hansen, T. Suselbeck, P. M. Clemmensen, M. Marin-Galiano, B. Geudelin, and P. T. Buser. 2009. Effect of intravenous FX06 as an adjunct to primary percutaneous coronary intervention for acute ST-segment elevation myocardial infarction results of the F.I.R.E. (Efficacy of FX06 in the Prevention of Myocardial Reperfusion Injury) trial. J Am Coll Cardiol 53(8):720-9.

18. Gröger, M., W. Pasteiner, G. Ignatyev, U. Matt, S. Knapp, A. Atrasheuskaya, E. Bukin, P. Friedl, D. Zinkl, R. Hofer-Warbinek, K. Zacharowski, P. Petzelbauer, and S. Reingruber. 2009. Peptide Bb15-42 Preserves Endothelial Barrier Function in Shock. PLoS ONE 4(4):e5391.

19. McIntyre, R. C., Jr., E. J. Pulido, D. D. Bensard, B. D. Shames, and E. Abraham. 2000. Thirty years of clinical trials in acute respiratory distress syndrome. Crit Care Med 28(9):3314-31.

20. Knapp, S., C. W. Wieland, S. Florquin, R. Pantophlet, L. Dijkshoorn, N. Tshimbalanga, S. Akira, and T. van der Poll. 2006. Differential roles of CD14 and toll-like receptors 4 and 2 in murine Acinetobacter pneumonia. Am J Respir Crit Care Med 173(1):122-9.

21. Knapp, S., C. W. Wieland, C. van 't Veer, O. Takeuchi, S. Akira, S. Florquin, and T. van der Poll. 2004. Toll-like receptor 2 plays a role in the early inflammatory response to murine pneumococcal pneumonia but does not contribute to antibacterial defense. J Immunol 172(5):3132-8.

22. Knapp, S., J. C. Leemans, S. Florquin, J. Branger, N. A. Maris, J. Pater, N. van Rooijen, and T. van der Poll. 2003. Alveolar macrophages have a protective antiinflammatory role during murine pneumococcal pneumonia. Am J Respir Crit Care Med 167(2):171-9.

23. Wang le, F., M. Patel, H. M. Razavi, S. Weicker, M. G. Joseph, D. G. McCormack, and S. Mehta. 2002. Role of inducible nitric oxide synthase in

pulmonary microvascular protein leak in murine sepsis. Am J Respir Crit Care Med 165(12):1634-9.

24. Lagler, H., O. Sharif, I. Haslinger, U. Matt, K. Stich, T. Furtner, B. Doninger, K. Schmid, R. Gattringer, A. F. de Vos, and S. Knapp. 2009. TREM-1 activation alters the dynamics of pulmonary IRAK-M expression in vivo and improves host defense during pneumococcal pneumonia. J Immunol 183(3):2027-36.

25. Imai, Y., K. Kuba, G. G. Neely, R. Yaghubian-Malhami, T. Perkmann, G. van Loo, M. Ermolaeva, R. Veldhuizen, Y. H. Leung, H. Wang, H. Liu, Y. Sun, M. Pasparakis, M. Kopf, C. Mech, S. Bavari, J. S. Peiris, A. S. Slutsky, S. Akira, M. Hultqvist, R. Holmdahl, J. Nicholls, C. Jiang, C. J. Binder, and J. M. Penninger. 2008. Identification of oxidative stress and Toll-like receptor 4 signaling as a key pathway of acute lung injury. Cell 133(2):235-49.

26. Knapp, S., U. Matt, N. Leitinger, and T. van der Poll. 2007. Oxidized phospholipids inhibit phagocytosis and impair outcome in gram-negative sepsis in vivo. J Immunol 178(2):993-1001.

27. Schultz, M. J., A. W. Rijneveld, S. Florquin, C. K. Edwards, C. A. Dinarello, and T. van der Poll. 2002. Role of interleukin-1 in the pulmonary immune response during Pseudomonas aeruginosa pneumonia. Am J Physiol Lung Cell Mol Physiol 282(2):L285-90.

28. Friedman, P., S. Horkko, D. Steinberg, J. L. Witztum, and E. A. Dennis. 2002. Correlation of antiphospholipid antibody recognition with the structure of synthetic oxidized phospholipids. Importance of Schiff base formation and aldol condensation. J Biol Chem 277(9):7010-20.

29. Hoffken, G., and M. S. Niederman. 2002. Nosocomial pneumonia: the importance of a de-escalating strategy for antibiotic treatment of pneumonia in the ICU. Chest 122(6):2183-96.

30. Park, W. Y., R. B. Goodman, K. P. Steinberg, J. T. Ruzinski, F. Radella, 2nd, D. R. Park, J. Pugin, S. J. Skerrett, L. D. Hudson, and T. R. Martin. 2001. Cytokine balance in the lungs of patients with acute respiratory distress syndrome. Am J Respir Crit Care Med 164(10 Pt 1):1896-903.

31. Maniatis, N. A., and S. E. Orfanos. 2008. The endothelium in acute lung injury/ acute respiratory distress syndrome. Curr Opin Crit Care 14(1):22-30.

32. Garcia, J. G., H. W. Davis, and C. E. Patterson. 1995. Regulation of endothelial cell gap formation and barrier dysfunction: role of myosin light chain phosphorylation. J Cell Physiol 163(3):510-22.

33. Minshall, R. D., and A. B. Malik. 2006. Transport across the endothelium: regulation of endothelial permeability. Handb Exp Pharmacol(176 Pt 1):107-44.

34. van Nieuw Amerongen, G. P., C. M. Beckers, I. D. Achekar, S. Zeeman, R. J. Musters, and V. W. van Hinsbergh. 2007. Involvement of Rho kinase in endothelial barrier maintenance. Arterioscler Thromb Vasc Biol 27(11):2332-9.

35. Konstantoulaki, M., P. Kouklis, and A. B. Malik. 2003. Protein kinase C modifications of VE-cadherin, p120, and beta-catenin contribute to endothelial barrier dysregulation induced by thrombin. Am J Physiol Lung Cell Mol Physiol 285(2):L434-42.

36. Wojciak-Stothard, B., S. Potempa, T. Eichholtz, and A. J. Ridley. 2001. Rho and Rac but not Cdc42 regulate endothelial cell permeability. J Cell Sci 114(Pt 7):1343-55.

37. Rossi, J. L., A. V. Velentza, D. M. Steinhorn, D. M. Watterson, and M. S. Wainwright. 2007. MLCK210 gene knockout or kinase inhibition preserves lung function following endotoxin-induced lung injury in mice. Am J Physiol Lung Cell Mol Physiol 292(6):L1327-34.

38. Wainwright, M. S., J. Rossi, J. Schavocky, S. Crawford, D. Steinhorn, A. V. Velentza, M. Zasadzki, V. Shirinsky, Y. Jia, J. Haiech, L. J. Van Eldik, and D. M. Watterson. 2003. Protein kinase involved in lung injury susceptibility: evidence from enzyme isoform genetic knockout and in vivo inhibitor treatment. Proc Natl Acad Sci U S A 100(10):6233-8.

39. Gao, L., A. Grant, I. Halder, R. Brower, J. Sevransky, J. P. Maloney, M. Moss, C. Shanholtz, C. R. Yates, G. U. Meduri, M. D. Shriver, R. Ingersoll, A. F. Scott, T. H. Beaty, J. Moitra, S. F. Ma, S. Q. Ye, K. C. Barnes, and J. G. Garcia. 2006. Novel polymorphisms in the myosin light chain kinase gene confer risk for acute lung injury. Am J Respir Cell Mol Biol 34(4):487-95.

40. Christie, J. D., S. F. Ma, R. Aplenc, M. Li, P. N. Lanken, C. V. Shah, B. Fuchs, S. M. Albelda, C. Flores, and J. G. Garcia. 2008. Variation in the myosin light chain kinase gene is associated with development of acute lung injury after major trauma. Crit Care Med 36(10):2794-800.

41. Doyle, R. L., N. Szaflarski, G. W. Modin, J. P. Wiener-Kronish, and M. A. Matthay. 1995. Identification of patients with acute lung injury. Predictors of mortality. Am J Respir Crit Care Med 152(6 Pt 1):1818-24.

42. Chastre, J., and J.-Y. Fagon. 2002. Ventilator-associated Pneumonia. Am J Respir Crit Care Med 165(7):867-903.

43. Kennedy, T. P., K. J. Johnson, R. G. Kunkel, P. A. Ward, P. R. Knight, and J. S. Finch. 1989. Acute acid aspiration lung injury in the rat: biphasic pathogenesis. Anesth Analg 69(1):87-92.

44. Holter, J. F., J. E. Weiland, E. R. Pacht, J. E. Gadek, and W. B. Davis. 1986. Protein permeability in the adult respiratory distress syndrome. Loss of size selectivity of the alveolar epithelium. J Clin Invest 78(6):1513-22.

45. Weiland, J. E., W. B. Davis, J. F. Holter, J. R. Mohammed, P. M. Dorinsky, and J. E. Gadek. 1986. Lung neutrophils in the adult respiratory distress syndrome. Clinical and pathophysiologic significance. Am Rev Respir Dis 133(2):218-25.

46. Abraham, E. 2003. Neutrophils and acute lung injury. Crit Care Med 31(4 Suppl):S195-9.

47. Zarbock, A., K. Singbartl, and K. Ley. 2006. Complete reversal of acid-induced acute lung injury by blocking of platelet-neutrophil aggregation. J Clin Invest 116(12):3211-9.

48. Deng, J. C., G. Cheng, M. W. Newstead, X. Zeng, K. Kobayashi, R. A. Flavell, and T. J. Standiford. 2006. Sepsis-induced suppression of lung innate immunity is mediated by IRAK-M. J Clin Invest 116(9):2532-42.

49. Kobayashi, K., L. D. Hernandez, J. E. Galan, C. A. Janeway, Jr., R. Medzhitov, and R. A. Flavell. 2002. IRAK-M is a negative regulator of Toll-like receptor signaling. Cell 110(2):191-202.

50. Voll, R. E., M. Herrmann, E. A. Roth, C. Stach, J. R. Kalden, and I. Girkontaite. 1997. Immunosuppressive effects of apoptotic cells. Nature 390(6658):350-1.

51. Vestweber, D. 2008. VE-cadherin: the major endothelial adhesion molecule controlling cellular junctions and blood vessel formation. Arterioscler Thromb Vasc Biol 28(2):223-32.

52. Gropper, M. A., and J. Wiener-Kronish. 2008. The epithelium in acute lung injury/acute respiratory distress syndrome. Curr Opin Crit Care 14(1):11-5.

4.3. THE ROLE OF PTEN IN BACTERIAL PNEUMONIA

PI3K: classification, main functions, and research tools

Phosphoinositide 3-kinases (PI3K) are a family of lipid kinases consisting of 3 different families (Class I-III). PI3K phosphorylates phosphoinositides at the D-3 position of the inositol ring. This leads to recruitment of downstream effector kinases such as Akt, which bear the pleckstrin homology domain, to the plasma membrane, initiating signaling events that govern such diverse and crucial processes as cell survival pathways, cell metabolism and growth, cytoskeletal rearrangements, motility and migration, adhesion, inflammation and phagocytosis (Fig. 1).

PI3K hyperactivation contributes to human cancer development, and defects in the pathway support type II diabetes signaling[109,110]. The well described class I family consists of class IA kinases (α, β, δ), which are activated in response to growth factors and the class IB enzyme PI3Kγ, which is activated by G-protein coupled receptors. Class IA kinases are all heterodimers consisting of a regulatory subunit p85 (p101 and p84 for for PI3Kγ), which controls their regulation and localization[111], and a catalytic subunit (Class I: p110α, p110β, p110γ or Class II: p84, p101). PI3Kγ and PI3Kδ are primarily found in leukocytes, whereas PI3Kα and PI3Kβ are ubiquitously expressed. Inactivation of PI3K is regulated by two distinct types of phosphatases: SHIP1 and SHIP2 dephosphorylate the 5 position of the $PI(3,4,5)P_3$, whereas PTEN dephosphorylates the 3 position of the inositol ring. Loss of SHIP2 causes a dramatic increase in insulin sensitivity[112], and loss of PTEN is reported in a number of advanced human tumors, as reduced PTEN protein expression occurs in approximately 50% of all tumors[113].

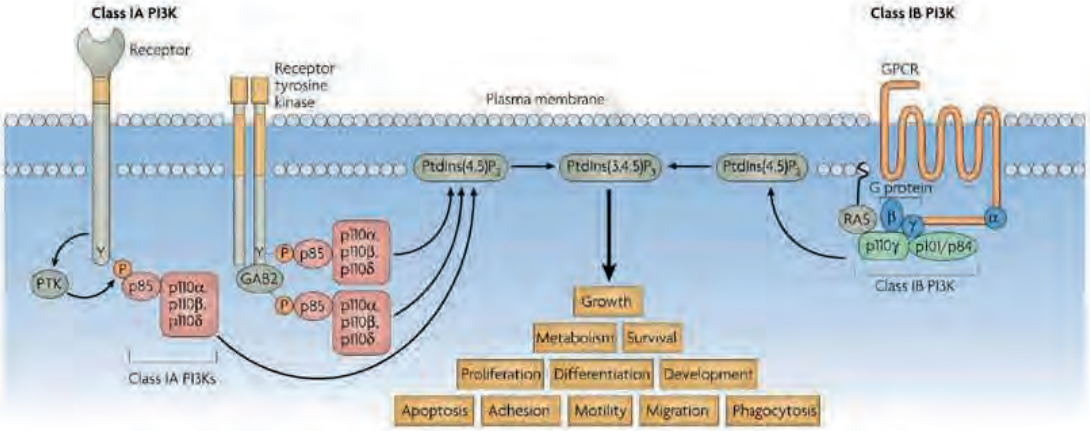

Figure 1. Overview of PI3K signaling. Class IA PI3K isoforms (p110α, p110β and p110δ) bind directly or indirectly to receptors through the interaction of their regulatory subunits (p85) with tyrosine-phosphorylated recognition motifs on the receptor cytoplasmic domains. The only class IB PI3K isoform, PI3Kγ, is recruited to G-protein-coupled receptors (GPCRs) by direct interaction with G-protein βγ subunits, through both the catalytic p110 and the regulatory subunits (adapted from[111]).

To study PI3K function, two inhibitors are widely used: Wortmannin and LY294002. These two inhibitors not only block all class I isoforms, but also class II and class III PI3Ks. Genetic deletion of the major catalytic subunit p85, or the ubiquitously expressed p110α or p110β results in embryonic lethality in mice. By contrast, mice lacking the leukocyte specific PI3Kδ or PI3Kγ are viable and show no apparent phenotype. But their important and also pleiotropic role in inflammation leads to altered phenotypes in different inflammatory settings, having a role in T-cell and B-cell signaling[114], and in innate immune responses[115]. More recently, orally active small molecule inhibitors could confirm some of the previous genetic studies[111]. Deletion of PTEN also resulted in embryonic lethality, and heterozygous mice have a high incidence of tumours[116].

PI3K and PTEN in innate immunity

PI3K affects innate immune functions on three different levels: leukocyte recruitment, bactericidal properties and modulation of inflammation. The role of PI3K in inflammation is debated, since some reports using pharmacological inhibitors suggested a pro-inflammatory role[117-119], whereas others claim PI3K to mediate anti-inflammatory pathways[120-124]. A number of independent studies in p85 deficient animals showed that activation of various TLRs led to an increased pro-inflammatory response[125-128]. Martin *et al.* demonstrated that TLR activation led to PI3K-mediated inactivation of GSK3β and thereby NF-κB down-regulation, ultimately resulting in increased IL-10 and decreased levels of pro-inflammatory cytokines TNF, IL-6 and IL-12[129]. Thus, increasing evidence suggests that PI3K is capable of limiting the inflammatory response to various TLR-ligands.

PI3K is a crucial pathway in phagocytosis[130], uptake of large particles seems to be more dependent on PI3K than ingestion of smaller ones[131]. PI3K controls cell polarity and motility by generating pools of PtdIns(3,4,5)P3 that promote actin polymerization at the leading edge of leukocytes, thus allowing pseudopod extension[132]. Furthermore several reports indicate a role for PI3K in phagosome maturation[133-135], as levels of $PtdInsP_3$ were shown to rise substantially in the phagosomal membrane, leading to the recruitment of signaling proteins involved in phagosome maturation[133]. In terms of bactericidal properties, oxidative burst in neutrophils requires proper PI3Kγ-signalling[136]. PI3Kγ deficient neutrophils, macrophages and dendritic cells were shown to have defects in migration to the site of inflammation[137-140]. Maus *et al.* showed in a model of pneumococcal pneumonia, that genetic deletion and pharmacological inhibition of PI3Kγ in mice resulted in impaired macrophage recruitment, but interestingly unaltered neutrophil attraction to the lung[141]. PI3Kγ

deficient animals moreover exhibited defective bacterial clearance, and ultimately impaired survival[141].

Neutrophils obtained from mice lacking myeloid PTEN (as described above) displayed higher Akt phosphorylation and actin polymerization, resulting in a small defect in directionality and increased cell spread, but without impairing overall chemotaxis *in vitro*[142]. By contrast migration of neutrophils *in vivo* was increased upon thioglycollate or *E. coli* challenge in the peritoneal cavity[142]. Furthermore PTEN$^{-/-}$ neutrophils displayed increased and prolonged superoxide production[142]. Neutrophils were shown to prioritize the end-target chemoattracant, i.e. fMLP of bacteria[143]. Heit *et al.* demonstrated that neutrophils deficient in PTEN fail to prioritize chemotactic cues, and were therefore distracted by other chemoattractants[144]. This resulted in delayed clearance of bacteria in a *Staphylococcus aureus* infection model, and reduced swelling in an arthritis model in mice lacking PTEN specifically in neutrophils. Recently it was shown, that myeloid PTEN depletion in mice led to impaired survival in a model of *E.coli* pneumonia, due to enhanced neutrophil recruitment, but improved survival in *E. coli* pneumonia in neutropenic mice[145]. Inhalation of LPS or bacteria also resulted in higher neutrophil levels in these mice. In terms of cytokine production they observed decreased TNFα and IL-6 secretion upon LPS stimulation in alveolar macrophages. Importantly the same group demonstrated that loss of PTEN in neutrophils delays their spontaneous death[145,146]. Another report previously demonstrated increased phagocytosis by PTEN deficient murine peritoneal macrophages[147]. Using a pharmacological PTEN inhibitor, Canetti *et al.* also showed the involvement of PTEN in inhibition of phagocytosis and bacterial killing by alveolar macrophages[148].

Thus, PI3K activity has pleiotropic and fundamental roles in innate immunity, but data on bacterial infections are limited. In terms of phagocytosis, bacterial

killing, and leukocyte recruitment PTEN deficiency seems to mostly reflect increased PI3K activity by having opposite effects than PI3K inhibition. But reports on PTEN mediated effects independent of its PI3K antagonism in this context point towards a higher complexity, as it was shown that PTEN is able to prevent leukocyte migration independent of its phosphatase activity[149,93].

Aim of the project

Since the PI3K/PTEN pathway has important roles in regulation of the inflammatory response, but data on bacterial infections are limited, we were interested to study this pathway herein. Moreover the increasing number on patents and clinical trials on drugs targeting the PI3K/PTEN pathway underline the urgent need of deciphering its role in clinically relevant infections[150]. We decided to focus on the role of myeloid PTEN to the clinically relevant pathogens *Streptococcus pneumoniae* and *Acinetobacter baumannii*. As PI3K affects major defense mechanisms to bacterial infections, we hypothesized that myeloid deletion of PTEN might alter the course of infection significantly. Our goal was to uncover potential differences in terms of cytokine secretion, bactericidal properties and leukocyte recruitment specifically in the context of clinically relevant pneumonias.

4.3.1. MYELOID PTEN PROMOTES INFLAMMATION BUT IMPAIRS BACTERICIDAL ACTIVITIES DURING MURINE PNEUMOCOCCAL PNEUMONIA

Gernot Schabbauer *[1], Ulrich Matt †[1], Philipp Günzl*, Joanna Warszawska†‡, Tanja Furtner†‡, Eva Hainzl*, Immanuel Elbau†‡, Ildiko Mesteri§, Bianca Doninger†, Bernd R. Binder* and Sylvia Knapp †‡

*Department of Vascular Biology and Thrombosis Research, Center for Biomolecular Medicine and Pharmacology, Medical University of Vienna, Vienna, 1090, Austria; †Research Center for Molecular Medicine of the Austrian Academy of Sciences (CeMM), Vienna, 1090, Austria; ‡Department of Medicine I, Div. of Infectious Diseases and Tropical Medicine, Medical University of Vienna, Vienna, 1090, Austria §Institute for Clinical Pathology, Medical University of Vienna, Vienna, 1090, Austria
[1] **Authors contributed equally to this work**

Running title: PTEN modulates the immune response during bacterial pneumonia. This work was in part supported by grants from the Austrian Science Fund (FWF P19850-B12) (to G.S.).

Keywords: pneumonia, PI3K, PTEN, inflammation, macrophage

Corresponding authors:

Gernot Schabbauer Ph.D.

Department of Vascular Biology and Thrombosis Research, Center for Biomolecular Medicine and Pharmacology, Medical University of Vienna

Schwarzspanierstrasse 17; 1090 Wien, Austria

Phone: 0043-1-4277-62508 FAX: 0043-1-4277-9625
E-mail: gernot.schabbauer@meduniwien.ac.at

Sylvia Knapp, M.D., Ph.D.

Center for Molecular Medicine of teh Austrian Academy of Sciences, Department of Medicine 1, Div. Of Infectious Diseases and Tropical Medicine, Medical University Vienna

Waehringer Guertel 18-20; 1090 Vienna, Austria

Phone: 0043-1-40400-4954 or 4492 FAX: 0043-1-40400-4498

E-mail: sylvia.knapp@meduniwien.ac.at

Abstract:

PI3K has been described as an essential signaling component involved in the chemotactic cell influx that is required to eliminate pathogens. At the same time, PI3K was reported to modulate the immune response thus limiting the magnitude of acute inflammation. The precise role of the PI3K pathway and its endogenous antagonist PTEN during clinically relevant bacterial infections is still poorly understood.

Utilizing mice lacking myeloid cell-specific PTEN we studied the impact of PTEN on the immune response to *S. pneumoniae*. Survival analysis disclosed that PTEN-deficient mice displayed less severe signs of disease and prolonged survival. The inflammatory response to *S. pneumoniae* was greatly reduced in macrophages *in vitro* and *in vivo*. Unexpectedly neutrophil influx to the lungs was significantly impaired in animals lacking myeloid-cell PTEN, whereas the additional observation of improved phagocytosis by alveolar macrophages lacking PTEN ultimately resulted in unaltered lung CFUs following bacterial infection.

Together, the absence of myeloid cell-associated PTEN and consecutively enhanced PI3K activity dampened pulmonary inflammation, reduced neutrophil influx and augmented phagocytic properties of macrophages, which ultimately resulted in decreased tissue injury and improved survival during murine pneumococcal pneumonia.

Introduction:

Infectious diseases are a major burden for our society with respiratory tract infections being a leading cause of morbidity and mortality worldwide. *Streptococcus pneumoniae* (*S. pneumoniae*) is the most frequent causative pathogen of community acquired pneumonia, affecting more than 500.000 people in the United States annually (1,2). The worldwide increase in antibiotic resistance among *S. pneumoniae* strains underlines the urgent need for a better understanding of molecular mechanisms associated with pneumococcal pneumonia (3).

The Phosphatase and Tensin homologue deleted on chromosome 10 (PTEN) is a well described tumor suppressor gene and multifunctional phosphatase that antagonizes PI3K's enzymatic activity by dephosphorylating phosphatidylinositol (3,4,5)-trisphosphate (PtdIns (3,4,5)P_3) to generate PtdIns (4,5)P_2. PI3K's enzymatic activity is warranted by two distinct subclasses, namely class Ia (p110α, β, δ) and class Ib (p110γ) (4). PTEN efficiently limits PI3K activity and downstream Akt signaling. PI3K/PTEN has been shown to play a prominent role in a variety of cellular mechanisms such as survival, migration and growth (5). However, little is known about the biological role of PTEN in inflammation and in particular during infectious diseases. The PI3K/ Akt signaling axis is crucial for site directed migration and diapedesis of immune effector cells such as neutrophils and monocytes to the site of inflammation and infection (6-10). In contrast to the conception that PI3K mediates pro-inflammatory signals, several studies indicate that the PI3K/PTEN pathway modulates the inflammatory response to bacterial cell wall components (11-15). Making use of a combination of pharmacologic and genetic means, we and others could previously show that the PI3K pathway provides beneficial anti-inflammatory properties in mouse models of endotoxemia and sepsis. These

observations have been further supported by Martin *et al.*, who intriguingly demonstrated that TLR-induced PI3K/Akt activation phosphorylated - and thereby inactivated - downstream glycogen synthase kinase (GSK) 3β, which in turn resulted in diminished nuclear factor (NF)-κB driven pro-inflammatory gene expression in monocytic cells (16).

The precise function of PI3K signaling during infections with viable bacteria is less well understood. Maus *et al.* published a report that investigated the contribution of the γ-catalytic subunit of PI3K (p110γ) during pneumococcal pneumonia (17). They hereby demonstrated that p110γ, which is generally thought to be responsible for the G-protein coupled receptor (GPCR)-induced chemotactic response of neutrophils and monocytes, was not required for neutrophil influx following pulmonary inoculation of pneumolysin or whole bacteria *in vivo* (17). However, p110γ deficient mice displayed an impaired bacterial clearance and delayed recruitment of exudate macrophages (17).

Still the role of myeloid cell associated PTEN upon infection with clinically relevant pathogens in healthy mice, such as community-acquired pneumonia by *S. pneumoniae*, is incompletely understood. The increasing number of patients and clinical trials applying drugs targeting the PI3K/PTEN pathway, highlight the urgent need for a better comprehension of PI3K/PTEN signaling during clinically relevant infections (18). To elucidate the contribution of myeloid cell associated PI3K/PTEN during *S. pneumoniae* infection we therefore made use of a conditional knockout strategy to specifically eliminate PTEN expression in myeloid cells (we hereafter refer to these mice as $PTEN^{MC\text{-}KO}$ animals and $PTEN^{MC\text{-}Wt}$ littermate controls, respectively). Pneumococcal pneumonia was then induced in $PTEN^{MC\text{-}KO}$ mice, which displayed enhanced PI3K activity, and littermate $PTEN^{MC\text{-}Wt}$ controls after which the inflammatory response was investigated.

Methods:

Mice

Floxed PTEN mice were kindly provided by T.W. Mak (19), LysM cre recombinase transgenic mice were a kind gift from R. Johnson (20). PI3Kγ (p110γ) mice were obtained from J.M. Penninger (21). Intercrossed mice were backcrossed to a C57BL/6J background for at least 8 generations. Littermate-controlled experiments were performed using 8-12 week old male mice. For genotyping murine tissue was lysed in PCR-lysis buffer and direct PCR was performed using GoTaq™ DNA Polymerase (Promega). All animal studies were approved and comply with institutional guidelines (BMWF-66.009/0103-C/GT/2007).

Harvest of primary cells

Thioglycollate-elicited peritoneal macrophages were isolated from $PTEN^{MC\text{-}KO}$ and $PTEN^{MC\text{-}Wt}$ controls as described previously (22). Alveolar macrophages were isolated by bilateral bronchoalveolar lavage (BAL) as described elsewhere (23,24). Bone marrow was isolated from femurs and tibias of healthy $PTEN^{MC\text{-}KO}$ and $PTEN^{MC\text{-}Wt}$ mice. Bone marrow cells were incubated with conditioned media from L929 cells (20% in RPMI) for 10 days to allow differentiation and maturation of macrophages.

Western Blotting

Macrophage cell lysates were separated by SDS-PAGE, blotted to membrane (Immobilon PVDF Transfer Membrane; Millipore), probed with rabbit primary Abs against PTEN, AKT, phospho-AKT(Ser473), phospho-GSK3ß(Ser9) (Cell Signaling Technology), β-Actin (Sigma), IL-6 (R&D Systems) and inducible

nitric oxide synthase (iNOS) (NEB). For detection a goat anti-rabbit secondary Ab conjugated with horseradish peroxidase (Amersham) was used.

NO generation assay

iNOS activity was measured by the generation of nitrite (Sigma) in supernatants of $PTEN^{MC\text{-}KO}$ and $PTEN^{MC\text{-}Wt}$ littermate control macrophages incubated with heat-killed S. pneumonia (ATCC 6303) for 24h. Assays were performed according to the manufacturer's protocol (25).

Phagocytosis and killing assays

Primary alveolar macrophages were incubated with FITC-labeled heat-killed *S. pneumoniae* (ATCC 6303) at a multiplicity of infection (MOI) of 100 for 30 min at 37°C. After washing steps, lysosomes were stained with Lysotracker red and nuclei with DAPI (Invitrogen), followed by visualization using confocal laser scanning microscopy (LSM 510, Zeiss). The ratio of engulfed bacteria (as determined by overlay of green bacteria and red lysosomes) were quantified by an independent researcher from 300-400 counted cells per well and are expressed as percentage of cells that contain bacteria. In addition, a FACS-based phagocytosis assay was performed exactly as described earlier (26). In brief, primary alveolar macrophages were allowed to adhere over night before being incubated with FITC-labeled *S. pneumoniae* at 37°C or 4°C, respectively. Uptake of bacteria was quantified by FACS and the phagocytosis-index was calculated as follows: (mean fluorescence x % positive cells at 37°C) minus (mean fluorescence x % positive cells at 4°C). Bacterial killing was performed as described (26). In brief, alveolar macrophages were isolated, plated at a density of $2x10^5$ cells/well and allowed to adhere. *S. pneumoniae* were added

at a MOI of 100 and plates were placed at 37C for 10min. Each well was then washed 5 times with ice-cold PBS to remove extracellular bacteria. To determine bacterial uptake after 10min, triplicate of wells were lysed with sterile H_2O and designated as t=0. Pre-warmed SF-RPMI was added to remaining wells and plates were placed at 37C for 10, 30, 60 or 90min after which cells were again washed 5 times with ice-cold PBS and lysed as described above. Cell-lysates were plated in serial-fold dilutions on blood agar plates and bacterial counts were enumerated after 16h. Bacterial killing was expressed as the percentage of killed bacteria in relation to t=0 (percent killing = 100 – {(# CFU at time x / # CFU at time 0) x 100}).

Pneumonia experiments:

Pneumococcal pneumonia was induced as described previously (27-29). Briefly *S. pneumoniae* serotype 3 was obtained from American Type Culture Collection (ATCC 6303, Rockville, MD) and grown to log-phase. Mice were short-term anesthetized with isoflurane (Forene, Abbott) and 50 µl of the bacterial suspension (approximately $5x10^4$ CFUs) was inoculated intranasally. For survival analysis infected mice were observed every 3h. At indicated time points mice were sacrificed; BAL was performed, blood and lungs were collected and processed as described (28,30). CFUs were determined from serial dilutions of lung homogenates, blood and BAL fluid (BALF), plated on blood agar plates and incubated at 37°C for 16h before colonies were counted. Cytokines and chemokines were quantified in lung homogenates and BALF. TNF-α, IL-6, keratinocyte-derived chemokine (KC), MCP-1 and macrophage inflammatory protein (MIP)-2 were measured using ELISAs (R&D Systems), as was myeloperoxidase (MPO) (HyCult Biotechnology) and IL-10 (Bender Medsystems). Detection limits were: 15ng/ml for TNF-α; 16pg/ml for IL-6;

12pg/ml for KC; 4pg/ml for MCP-1; 94pg/ml for MIP-2; and 15pg/ml for IL-10. Differential cell counts were determined using counting chambers and cytospin preparations stained with Giemsa.

Histology

Lungs were fixed in formalin and embedded in paraffin; 4µm sections were stained in H&E, and analyzed by a blinded pathologist. The lung was scored with respect to the following parameters: interstitial inflammation, edema, endothelitis, bronchitis, pleuritis and thrombi formation. Each parameter was graded on a scale of 0 to 3, with 0: absent, 1: mild, 2: moderate and 3: severe. The total "lung inflammation score" was expressed as the sum of the scores for each parameter, the maximum being 18. Granulocyte immunostaining was performed on paraffin-embedded lungs as described (28). After antigen retrieval using pepsin, tissue sections were incubated with FITC rat anti-mouse Ly-6G (BD Bioscience) or corresponding Isotype control IgG (Cemfret Analytics), followed by rabbit anti-FITC Ab (ZYMED) in normal mouse serum. Finally slides were incubated with polyclonal anti-rabbit-HRP Ab (Immunologic), and visualized using 3,3-diaminobenzidin-tetra-hydrochloride (DAB, Vector Lab). Counterstaining was done with hemalaun solution.

Statistical Analysis

Data were analyzed by GraphPad Prism 4 software using unpaired Student's t-test or one way ANOVA followed by post hoc tests, when appropriate. Bacterial killing data were calculated by two-way ANOVA. Survival data were analyzed by Kaplan Meier followed by log-rank test. Criteria for significance for all experiments were $p<0.05$.

Results:

PTEN depletion is associated with enhanced PI3K activity in macrophages

To investigate the role of myeloid cell-derived PTEN during the inflammatory response to bacterial infections we generated conditional pten knockout mice in which PTEN expression was controlled by LysM, a myeloid cell specific promoter (20). Depending on the presence of LysM cre recombinase, double floxed ($pten^{flox/flox}$) mice are referred to as $PTEN^{MC\text{-}KO}$ or $PTEN^{MC\text{-}Wt}$ mice, respectively (Fig. 1A). Deletion of PTEN was confirmed in primary macrophages (Fig. 1B) and resulting downstream effects of constitutively active PI3K were reflected by greatly elevated baseline levels of phospho-Akt and phospho-GSK3ß in $PTEN^{MC\text{-}KO}$ macrophages (Fig.1C). These findings also indicate that alternative lipid phosphatases such as SHIP1 and SHIP2, which are known to influence $PI(3,4,5)P_3$ plasma membrane content (31), do not sufficiently limit PI3K activity in macrophages or compensate for the loss of PTEN.

In order to characterize PTEN-associated properties of macrophages during bacterial infection, we next examined kinase phosphorylation downstream of PI3K in $PTEN^{MC\text{-}Wt}$ and $PTEN^{MC\text{-}KO}$ macrophages upon stimulation with *S. pneumoniae*. Bacterial challenge led to Akt and GSK3ß phosphorylation in $PTEN^{MC\text{-}Wt}$ cells with highest levels 60 minutes post activation (Fig. 1D). While Akt phosphorylation only modestly increased over baseline levels upon S. pneumoniae stimulation in PTEN-deficient macrophages, GSK3ß phosphorylation was found markedly enhanced in these cells (Fig. 1D). These data illustrate that the innate immune response to *S. pneumoniae* involves downstream PI3K pathway activation.

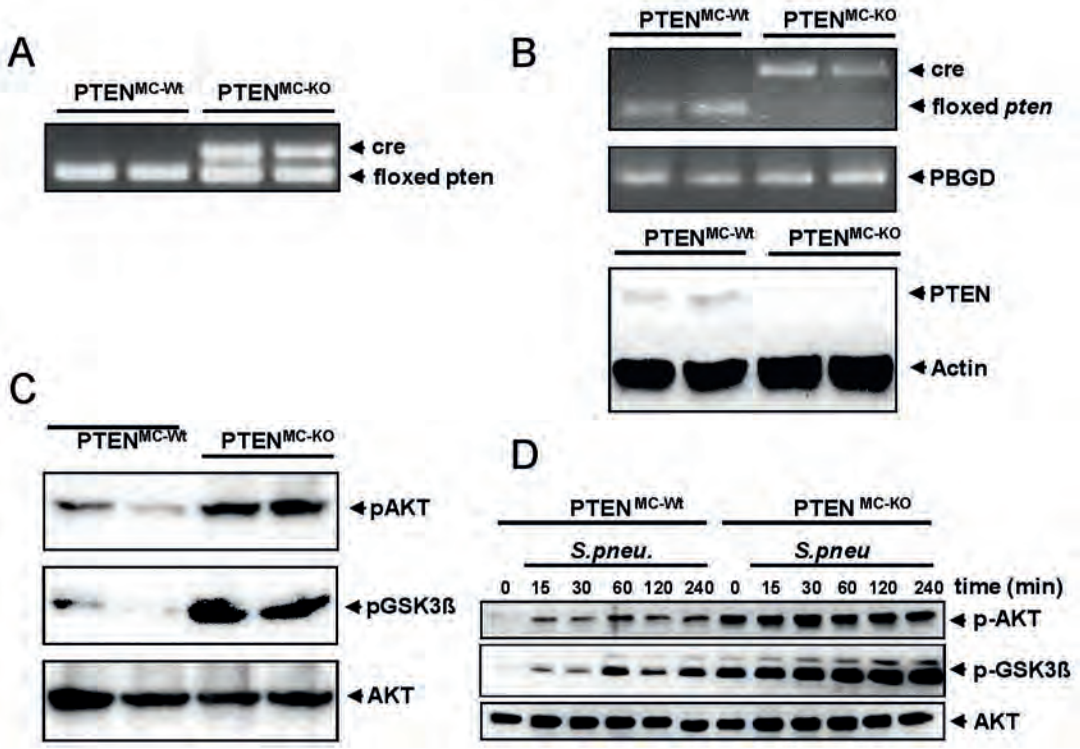

Figure 1: PTEN deficiency in myeloid cells.

(A) Genomic DNA PCR analysis of the pten and cre allele was performed on tissue from fl/fl pten, lysM cre positive or negative mice. (B) Excision of the pten allele was detected by PCR analysis of macrophage genomic DNA; pbgd was used as internal control. PTEN deficiency of peritoneal macrophages derived from two mice per genotype was analyzed by Western blotting using a PTEN-specific antibody. Cell lysates derived from two mice of each genotype are shown. (C) Constitutive PI3K/PTEN dependent signaling was determined in resting macrophages derived from two mice per genotype using phospho-Akt and phospho-GSK3ß Abs. Total-Akt was used as loading control. (D) Time course analysis of PI3K/PTEN-dependent signaling in S. pneumoniae stimulated macrophages. Phosphorylation of Akt and GSK3ß was determined by Western blotting. Total Akt was used as loading control.

Improved survival of PTEN^{MC-KO} mice infected with *S. pneumoniae*

To test whether PTEN deficiency in myeloid cells might impact the outcome of pneumococcal pneumonia in vivo, we infected PTEN^{MC-KO} and PTEN^{MC-Wt} mice with $5x10^4$ CFUs *S. pneumoniae* and monitored survival over seven days. Already two days after infection, we found PTEN^{MC-KO} mice to show less severe signs of disease, which was quantified using a clinical severity score (data not shown). PTEN^{MC-Wt} animals rapidly displayed signs of serious infection

and all mice succumbed within 107h after induction of pneumonia – at a time when more than 50% of PTEN^{MC-KO} animals were still alive (Fig. 2). Together, myeloid-cell specific PTEN-deficiency was associated with less severe signs of disease and significantly improved survival during pneumococcal pneumonia *in vivo*.

A

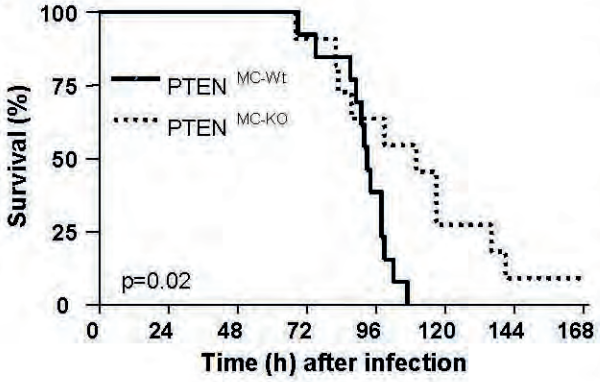

Figure 2: Improved survival of pneumococci infected PTEN^{MC-KO} mice.

(A) PTEN^{MC-KO} and PTEN^{MC-Wt} littermate controls were infected intranasally with *S. pneumoniae* (CFU 4x10^5) and monitored over 7 days (n=11-13 per group); statistical analysis was performed by log-rank test; the p value is depicted in the graph.

PTEN enhanced the inflammatory response and attenuated bactericidal properties *in vitro*

In our effort to elucidate the detrimental role of PTEN during pneumococcal pneumonia, we investigated PTEN's contribution to basic functional properties of myeloid cells such as cytokine secretion, or bacterial phagocytosis and killing. Upon stimulation of bone marrow-derived macrophages (BMDM) and primary alveolar macrophages (AM) from PTEN^{MC-KO} and PTEN^{MC-Wt} mice with *S. pneumoniae* we observed a significantly reduced TNF-α release by PTEN^{MC-KO} macrophages compared to PTEN^{MC-Wt} cells, whereas KC levels did not differ significantly (Fig. 3A, B). To study effector molecules importantly associated with bactericidal mechanisms we next investigated the pathogen-induced expression of inducible NO synthase (iNOS) in AMs and BMDMs. Surprisingly, we hereby discovered that PTEN^{MC-KO} BMDM stimulated with

S. pneumoniae expressed significantly higher iNOS levels 8h post induction (data not shown) while iNOS expression was diminished in PTEN-deficient AMs (Fig. 3C). We furthermore confirmed that decreased iNOS expression correlated with suppressed NO production by quantifying nitrite in supernatants of AMs (Fig. 3C).

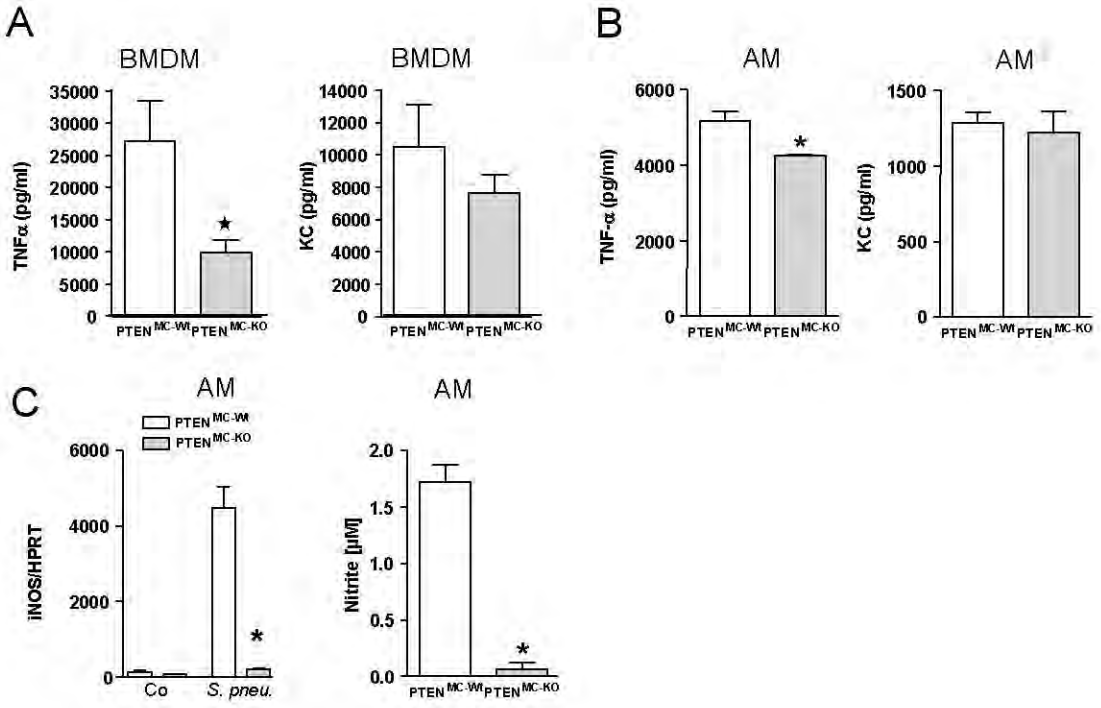

Figure 3: Role of PTEN in inflammation *in vitro*.

(A) BMDM and (B and C) AM were stimulated with *S. pneumoniae* (10^7CFU/ml) for 6h and TNF-α and KC release was measured in supernatants (A and B). (C) iNOS expression was assessed by RT-PCR and NO release was quantified in supernatants. Data are representative of two independent experiments and show mean ± SEM of n=3/genotype for BMDM and n=4/ genotype for AM. *indicates $p<0.05$ versus $PTEN^{MC\text{-}Wt}$.

We then isolated primary alveolar macrophages from PTEN$^{MC\text{-}Wt}$ and PTEN$^{MC\text{-}KO}$ mice and explored their ability to phagocytose *S. pneumoniae* using confocal microscopy as well as a FACS-based phagocytosis assay. By quantifying the proportion of macrophages that contained intracellular bacteria, we discovered a significantly increased uptake of *S. pneumoniae* by PTEN$^{MC\text{-}KO}$ cells (Fig. 4A, B), $p<0.05$ versus wild type cells). Furthermore, performing a killing assay enabled us to demonstrate enhanced bacterial killing by AM from PTEN$^{MC\text{-}KO}$ mice (Fig. 4C).

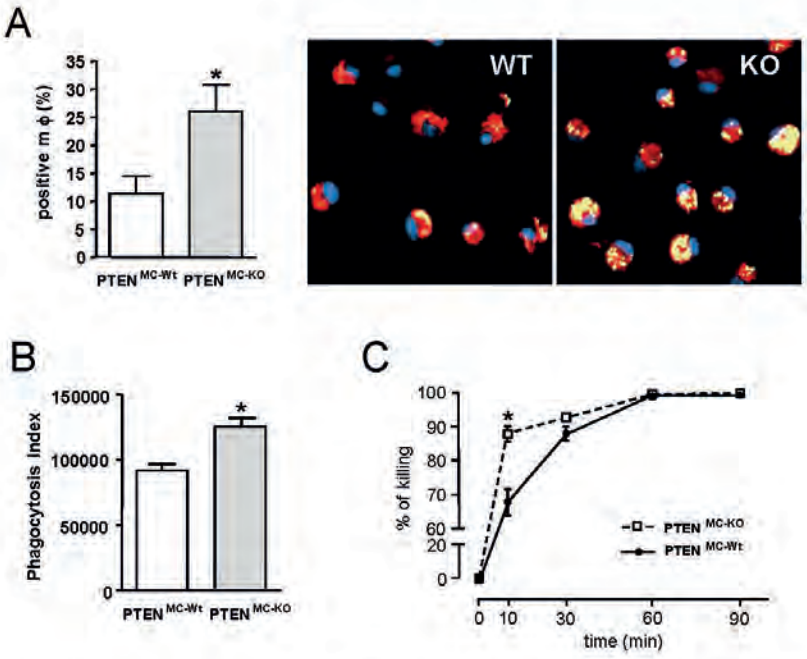

Figure 4: Role of PTEN in bacterial uptake and killing in alveolar macrophages.

AM from PTEN$^{MC\text{-}KO}$ and PTEN$^{MC\text{-}Wt}$ littermate control mice were incubated with FITC-labeled *S. pneumoniae* for 30 min and uptake of bacteria was quantified. (A) Bacterial uptake was quantified as described in the Methods section. The percentage of macrophages that contained bacteria is shown. Representative confocal microscopy images of AM of n= 3 per group are depicted: PTEN$^{MC\text{-}Wt}$ (left image) and PTEN$^{MC\text{-}KO}$ (right image); magnification 100x objective. Nuclei are stained with DAPI (blue), ingested bacteria (green) are defined by co-localization with lysosomes (red) and appear yellow. (B) Uptake of FITC-labeled bacteria was analyzed by FACS. (C) Bacterial killing by AM was analyzed over time. Data are presented as mean ± SEM. * indicates $p<0.05$ versus PTEN$^{MC\text{-}Wt}$.

Hence, these data illustrate that PTEN activity strongly impacted functional properties attributed to macrophages. While constitutively active PI3K signaling counteracted the proinflammatory TNF-α and iNOS response, it augmented the phagocytic and bactericidal properties of primary AM upon challenge with *S. pneumoniae in vitro.*

Anti-inflammatory phenotype and reduced neutrophil influx early during pneumococcal pneumonia in PTEN^{MC-KO} mice

To discern the in vivo impact of myeloid-cell associated PTEN on inflammation during bacterial infection we then asked how above described findings would translate into the immediate host response during bacterial pneumonia *in vivo.* For this purpose we infected PTEN^{MC-KO} and PTEN^{MC-Wt} mice with *S. pneumoniae* and studied the early inflammatory response after 6h. In line with *in vitro* data depicted in Fig.3, PTEN^{MC-KO} animals exhibited a diminished pro-inflammatory cytokine response, illustrated by significantly lower TNF-α concentrations in BALF of these mice ($p<0.01$ versus PTEN^{MC-Wt} mice; Fig. 5A). At the same time, the anti-inflammatory cytokine IL-10 was found significantly increased in lungs of PTEN^{MC-KO} mice as compared to wild type animals (Fig. 5B), indicating that the constitutive activation of myeloid cell-derived PI3K pathways dampened the inflammatory response *in vivo.*

Host defense against respiratory tract infections critically depends on the effective influx of neutrophils. Because PI3K activation has been repeatedly shown to promote neutrophil chemotaxis (10) and in light of a recent publication that highlighted the role of myeloid PTEN as a suppressor of neutrophil migration (32), we expected PTEN^{MC-KO} mice to exhibit an enhanced recruitment of neutrophils to the alveolar compartment. When enumerating

the number of cells attracted to the alveolar compartment 6h after induction of pneumococcal pneumonia we surprisingly found a significantly impaired influx of neutrophils in the absence of PTEN (Fig. 5C-D). Despite this reduced neutrophil attraction and diminished TNF-α response, bacterial outgrowth in lungs and BALF of PTEN^{MC-KO} mice was not affected at this early time point (Fig. 5E, F). Together, PTEN-deficiency dampened the early inflammatory response during bacterial pneumonia.

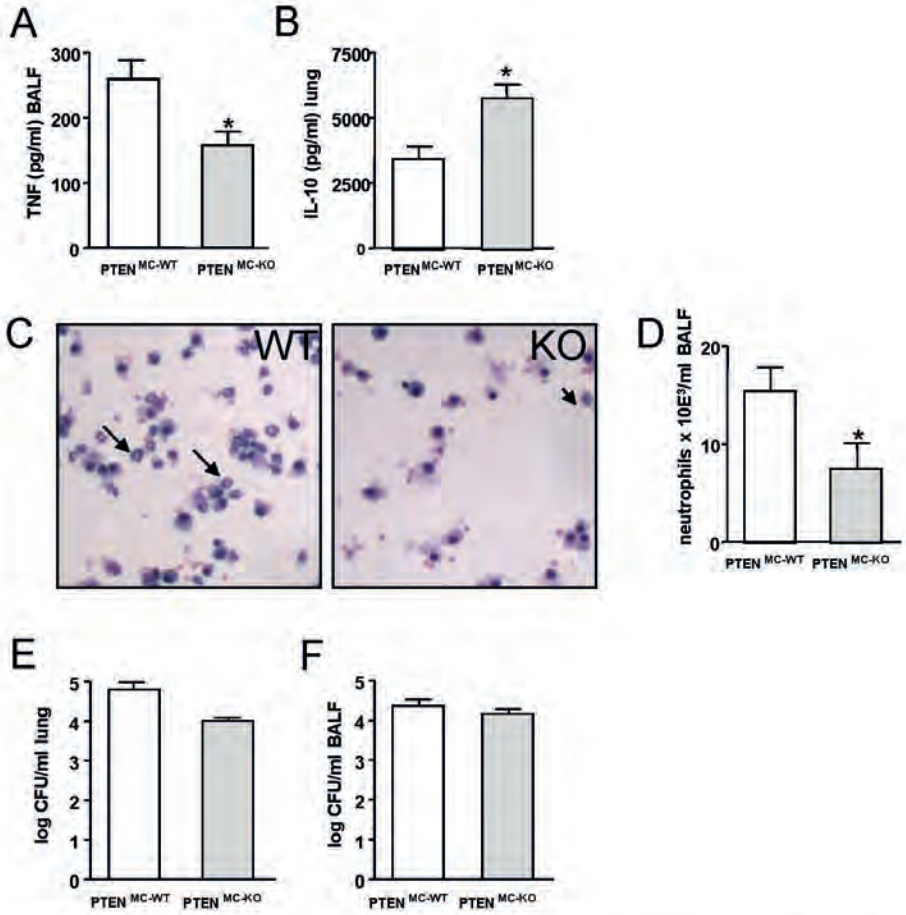

Figure 5: Role of PTEN early after induction of pneumonia (6h).

PTEN^{MC-KO} and PTEN^{MC-Wt} mice were infected intranasally with *S. pneumoniae* (4x10^5 CFUs), BALF and lungs were harvested 6h post infection. (A) TNFα levels in BALF and (B) lung IL-10 concentrations were determined by ELISA. Representative BALF cytospins stained with Giemsa are depicted in (C); (neutrophils are indicated by arrows; magnification 20x objective). Enumeration of neutrophils in BALF (D). Bacterial CFU counts were determined in lung homogenates (E) and BALF (F). Data are presented as mean ± SEM of n=6-7 mice/ group; * indicates $p < 0.05$.

PTEN^{MC-KO} mice exhibit a diminished inflammatory response and modestly enhanced bacterial burden 48h after induction of pneumonia

Having established PTEN's pro-inflammatory contribution to the induction-phase of *S. pneumoniae* infection *in vivo*, we then explored PTEN's impact over the course of pneumococcal pneumonia and investigated mice 48h after infection. At this later time-point, we continued to observe reduced levels of pro-inflammatory mediators in BALF and lungs of mice lacking PTEN. As depicted in Table 1, BALF concentrations of TNF-α, KC and MCP-1 were significantly decreased whereas IL-6 showed a modest but non-significant reduction in PTEN^{MC-KO} versus PTEN^{MC-Wt} mice. In contrast to the alveolar compartment, TNF-α and IL-6 levels did not differ in lung homogenates (data not shown), whereas KC concentrations were considerably decreased, and IL-10 levels significantly increased in lungs from PTEN^{MC-KO} mice as compared to PTEN^{MC-Wt} animals (Fig. 6A, B). In line with this diminished chemokine release, PTEN^{MC-KO} animals displayed an impaired ability to attract neutrophils to the site of infection, as illustrated by a significantly decreased proportion of neutrophils in BALF (Table 2) as well as reduced myeloperoxidase (MPO) levels in lungs from PTEN^{MC-KO} mice (Fig. 6C) 48h after infection. The reduction in pro-inflammatory mediators and neutrophil influx was accompanied by modestly increased bacterial counts in the alveolar compartment of PTEN^{MC-KO} mice 48h after infection with *S. pneumoniae* (Fig. 6D), while CFU counts in lung homogenates did not differ between the mouse strains (Fig. 6E).

Since PI3K activation has been repeatedly shown to promote migration of neutrophils (7,8,21,33), the continual observation of impaired pulmonary neutrophil recruitment in PTEN^{MC-KO} mice was unanticipated (Fig. 5C,D, 6C). Based on a recent report, which illustrated PTEN's suppressive function on neutrophil migration during *E.coli* peritonitis and sterile peritoneal inflammation

(32), we wondered whether these contradicting results were due to pathogen- or organ-specific differences that have never been investigated before. To answer this question we injected *S. pneumoniae* intraperitoneally in PTEN^{MC-KO} mice and PTEN^{MC-Wt} littermate controls and enumerated peritoneal neutrophil counts after 6h. In contrast to the diminished alveolar neutrophil influx during pneumonia we found an enhanced peritoneal recruitment of neutrophils in animals lacking myeloid-cell associated PTEN (Fig. 7A). These findings indicate that organ-specific differences could explain our observation of diminished neutrophil migration in PTEN^{MC-KO} mice suffering from pneumococcal pneumonia *in vivo* and argue against a fundamental cellular defect of PTEN-deficient neutrophils. To understand organ-specific differences we additionally studied the inflammatory cytokine and chemokine response of primary peritoneal macrophages upon *S. pneumoniae* stimulation *in vitro*. Comparable to our observations from BMDM and AM (Fig. 3), we discovered reduced TNF-α secretion by peritoneal PTEN^{MC-KO} macrophages (Fig. 7B). However, in strong contrast to BMDM or AM, peritoneal macrophages that lacked PTEN released significantly more KC than PTEN^{MC-Wt} cells (Fig. 7C). This enhanced chemokine release by PTEN^{MC-KO} peritoneal macrophages provides a potential explanation for the augmented PMN influx into the peritoneal cavity.

Constitutively active PI3K does not impact clearance of *S. pneumoniae* 65h after infection

In an attempt to identify the contributing factors that ultimately led to improved outcome of PTEN^{MC-KO} mice suffering from pneumococcal pneumonia, we repeated the pneumonia study and sacrificed mice after 65h, i.e. right before animals started to succumb to infection. We hereby observed significantly decreased IL-6 levels and modestly reduced TNF-α and KC concentrations in

BALF of PTEN^{MC-KO} (Table 3). In line with above described findings at 6h and 48h after infection, we continued to detect significantly higher IL-10 levels in lung homogenates of mice lacking myeloid PTEN (Fig. 8A). When analyzing the cellular composition in BALF, we found a predominance of monocytes/ macrophages in PTEN^{MC-KO} mice, whereas neutrophil numbers exceeded monocytes/macrophages in PTEN^{MC-Wt} littermates (Fig. 8B, C). In accordance, histological evaluation of lung slides disclosed significantly more pronounced signs of inflammation in PTEN^{MC-Wt} mice than PTEN^{MC-KO} animals (Fig. 8D). However, when enumerating bacterial counts in BALF and lungs we did not discover any differences between wild-type and PTEN-deficient mice 65h after infection (Fig. 8E). Furthermore blood cultures did not reveal any differences between groups (data not shown).

Hence, these data indicate that the continuous activation of PI3K, as seen in PTEN^{MC-KO} mice, beneficially modulated the inflammatory response to S. pneumoniae, thus allowing for accelerated resolution of pneumonia without impairing bacterial clearance *in vivo*.

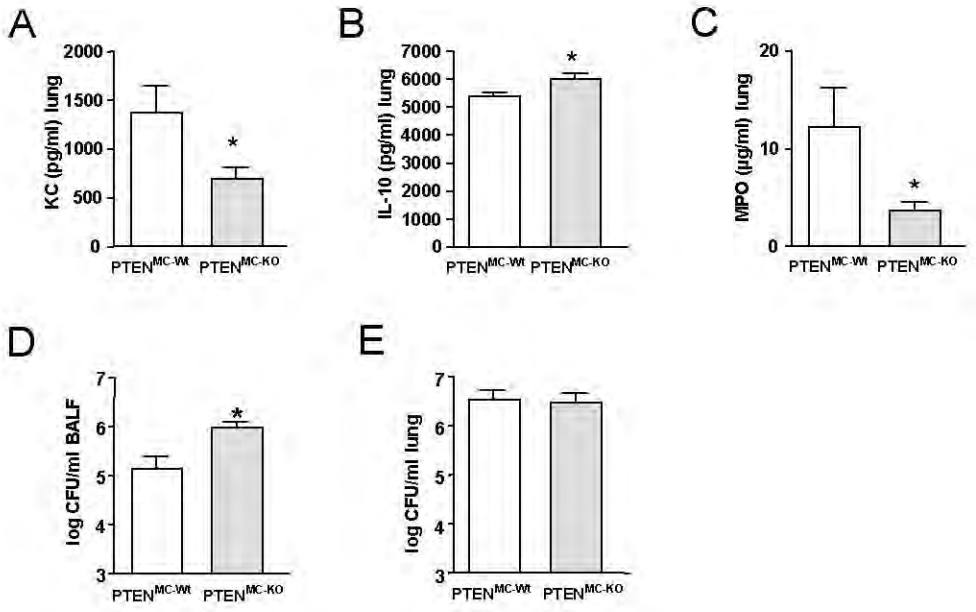

Figure 6: Role of PTEN 48h after induction of pneumococcal pneumonia.

PTENMC-KO and littermate PTENMC-Wt mice were infected intranasally with 4x105 CFUs *S. pneumoniae* and sacrificed after 48h (n=7-9/group). (A) KC, (B) IL10, and (C) MPO concentrations were determined in lung homogenates by ELISA. Bacterial CFUs were enumerated by plating serial dilutions of (D) BALF and (E) lung homogenates. Data are presented as mean ± SEM; * indicates p <0.05.

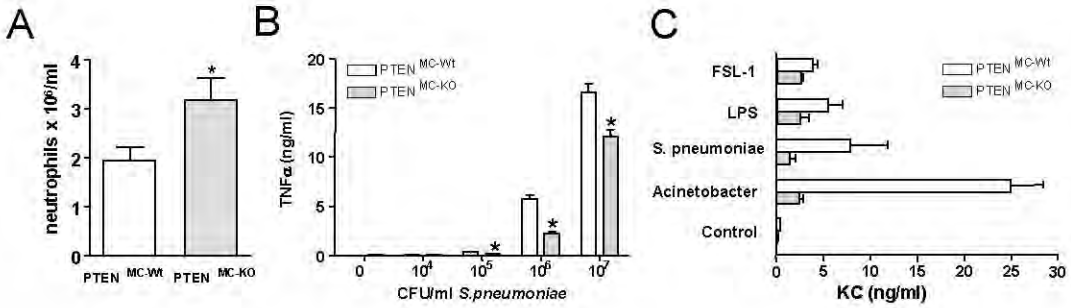

Figure 7: Immune-modulatory properties of PTEN in peritoneal inflammation.

PTEN^{MC-KO} and PTEN^{MC-Wt} littermates were infected intraperitoneally with *S. pneumoniae* (CFU 4x10^5). Peritoneal lavage was performed after 6h and (A) neutrophils were enumerated (n=6-7mice/group). (B, C) Dose-dependent (10^3/ml to 10^7/ml; heat-killed S. pneumoniae) TNF-α release and KC secretion in response to TLR2/4 ligands (LPS 100ng/ml; FSL-1 10ng/ml;) and heat killed bacteria (10^7/ml) was determined in supernatants of PTEN^{MC-KO} and PTEN^{MC-Wt} macrophages after 12h; (n=9 per genotype). Data are presented as mean ± SEM; * indicates p <0.05.

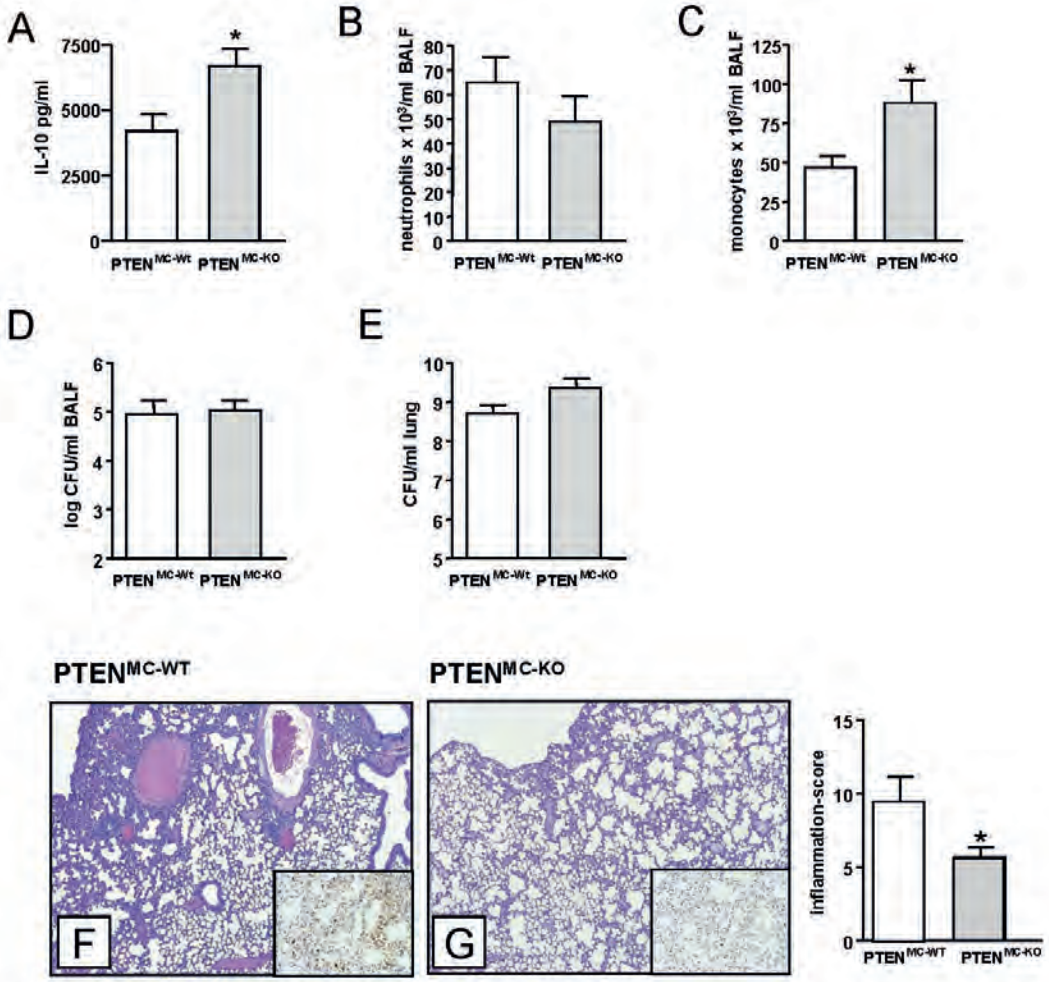

Figure 8: Unaltered bacterial counts despite reduced inflammation in PTEN^{MC-KO} mice 65h after infection.

PTEN^{MC-KO} and PTEN^{MC-Wt} littermates were infected with *S. pneumoniae* (CFU 4x10^5) and sacrificed after 65h. (A) Whole lung IL-10 concentrations were determined by ELISA. Neutrophil (B) and monocyte/macrophage (C) influx into the broncho-alveolar compartment was determined on cytospins. Bacterial CFUs in BALF (D) and lungs (E) were quantified by plating serial dilutions on blood agar plates. (F) Representative lung histology images of PTEN^{MC-Wt} and PTEN^{MC-KO} mice 65 hours after infection with 4x10^5 CFU S. pneumoniae. Lung sections stained with H&E were scored (as described in the Methods section) by a trained pathologist blinded for groups and are expressed as inflammation score. The insets are representative pictures of immunostaining for granulocytes, confirming reduced neutrophil influx in PTEN^{MC-KO} mice. H&E staining: magnification 4x objective; inset (Ly6-staining): magnification 20x objective. Data are presented as mean ± SEM of n=7-8 mice/group. Statistical significance ($p < 0.05$) is indicated by *.

Table 1

BALF	PTEN $^{MC-Wt}$	PTEN $^{MC-KO}$
TNFα	1566 ± 586	206 ± 60 *
IL6	379 ± 191	104 ± 15
KC	162 ± 41	85 ± 18 *
MCP-1	929 ± 393	229 ± 128 *

BALF cytokine and chemokine levels (pg/ml) in PTEN^{MC-KO} and PTEN^{MC-Wt} mice 48h post *S. pneumoniae* infection. Data are presented as mean ± SEM of n=9-10 mice/group; * indicates p value <0.05.

Table 2

BALF	PTEN $^{MC-Wt}$	PTEN $^{MC-KO}$
Total cells x 10^4/ml	11 ± 4.6	12.8 ± 7.7
Neutrophils (%)	61.3 ± 5.9	47.7 ±10.5*
Monocytes/ Macrophages (%)	38.2 ± 5.8	52.8 ± 10.6*

BALF cellular composition (%) in PTEN^{MC-KO} and PTEN^{MC-Wt} mice 48h post *S. pneumoniae* infection. Data are presented as mean ± SEM of n=9-10 mice/group; * indicates p value <0.05.

Table 3

BALF	PTEN $^{MC-Wt}$	PTEN $^{MC-KO}$
TNFα	201 ± 63	107 ± 35
IL6	547 ± 115	199 ± 59*
KC	259 ± 114	119 ± 49

BALF cytokine and chemokine levels (pg/ml) in PTENMC-KO and PTENMC-Wt mice 65h post *S. pneumoniae* infection. Data are presented as mean ± SEM of n=7-8 mice/group; * indicates p value <0.05.

Discussion:

The role of PI3K pathways in the inflammatory response is a controversial matter as published reports suggested either pro-inflammatory or anti-inflammatory properties (15,34,35). We and others demonstrated earlier that PI3K activation exerts protective immunomodulatory effects in murine models of endotoxemia and sepsis (16,36,37). These findings have been partly attributed to PI3K's ability to modulate the transcriptional activity of NFκB and to efficiently limit pro-inflammatory signaling cascades induced via MAP kinase pathways (11,35). Given that PTEN is a key regulator of PI3K activity, we hypothesized that PTEN might act as a critical modulator of the inflammatory response during bacterial infection. To investigate this idea in a clinically relevant model, we studied the role of PTEN during *S. pneumoniae* pneumonia *in vivo* and discovered that myeloid cell-specific PTEN-deficiency exerted beneficial effects. PTEN-deficiency was associated with diminished TNF-α and increased IL-10 responses, enhanced macrophage phagocytosis, reduced neutrophil migration to lungs and ultimately improved survival.

Modulation of PI3K activity by cell-type specific pten gene ablation disclosed a markedly reduced TNF-α response by various primary macrophage subsets that were stimulated with *S. pneumoniae*. These findings correlated with earlier observations by us and other investigators who showed that LPS-challenged PTEN-deficient macrophages displayed a profoundly reduced TNF-α release and diminished activation of MAP kinases (15,38). We concurrently discovered the enhanced phosphorylation of GSK3β in PTEN-deficient macrophages. GSK3β is a constitutively active serine/threonine kinase and downstream target of PI3K that can be inactivated through phosphorylation by Akt (39). The biological significance of GSK3β during inflammation was discovered by Martin et al., who revealed that GSK3β inhibition led to a diminished inflammatory

response towards various TLR agonists, which was illustrated by reduced TNFα and enhanced IL-10 releases (16). In striking agreement with this report, we hereby observed decreased levels of pro-inflammatory cytokines such as TNFα, and elevated concentrations of the anti-inflammatory cytokine IL-10 in lungs of *S. pneumoniae* infected PTEN^{MC-KO} animals. Therefore, enhanced phosphorylation and consecutive inactivation of GSK3β activity in macrophages of PTEN^{MC-KO} animals might explain our *in vivo* findings of a dampened inflammatory response in these mice.

The most unanticipated finding of our studies was the diminished pulmonary neutrophil influx in PTEN^{MC-KO} mice suffering from pneumococcal pneumonia. Importantly though, this observation was not related to constitutively reduced neutrophil numbers in this specific mouse strain, since we previously showed that blood neutrophil numbers were even higher in healthy PTEN^{MC-KO} animals as compared to wild type mice (15). In support of the general notion of PI3K being a key player in cell migration (6-8,10,19), the migratory capacity of PTEN deficient neutrophils was found enhanced in earlier reports (32). Furthermore, increased neutrophil recruitment was observed in PTEN^{MC-KO} animals using models of thioglycollate or *E. coli* induced peritonitis *in vivo* (32). Although we were able to confirm these data as we also observed enhanced peritoneal neutrophil influx following thioglycollate administration in PTEN^{MC-KO} mice (data not shown), we consistently observed reduced alveolar neutrophil migration during pneumococcal pneumonia in PTEN^{MC-KO} animals. To exclude the possibility of pathogen-specific differences, we challenged mice intraperitoneally with *S. pneumoniae* and observed enhanced peritoneal neutrophil recruitment in PTEN^{MC-KO} mice (Fig. 6A). Since neutrophil attraction to sites of infection critically depends on the effective release of chemokines such as KC (40,41), we investigated if organ-specific differences in neutrophil migration in PTEN^{MC-KO} animals were a consequence of altered chemokine

release by resident macrophages. Indeed, when measuring KC concentrations in supernatants of alveolar and peritoneal macrophages that were stimulated with *S. pneumoniae in vitro* we discovered an enhanced KC release by peritoneal but not alveolar $PTEN^{MC-KO}$ macrophages. Beside macrophages, respiratory epithelial cells are a major source of KC within the lungs *in vivo* and release of this chemokine is largely triggered by macrophage-derived pro-inflammatory cytokines such as TNF-α (42). The fact that we identified reduced KC levels in lung-homogenates from infected $PTEN^{MC-KO}$ mice *in vivo* (Table 1) might therefore result from the attenuated macrophage-associated (e.g. TNF-α mediated) activation of airway epithelial cells in vivo, ultimately resulting in reduced neutrophil recruitment. In contrast to our observations, Li *et al.* disclosed increased pulmonary KC concentrations and enhanced neutrophil migration in PTEN-deficient mice suffering from *E. coli* pneumonia (43). It therefore seems that PTEN differentially regulates the attraction of neutrophils, depending on either the affected organ and/or the inducing agent.

Unlike neutrophils, cells of monocytic origin (infiltrating monocytes/ macrophages) were recruited in increased numbers to lungs of healthy and *S. pneumoniae* infected $PTEN^{MC-KO}$ mice (data not shown and Table 1). This result is in agreement with a report by Maus *et al.*, who showed that monocyte/ macrophage recruitment in pneumoccocal pneumonia is critically depended on proper p110γ signal transduction (17). Alveolar macrophages crucially contribute to host defense during murine pneumococcal pneumonia (29). We recently demonstrated that alveolar macrophages exert an important role in the resolution of pneumococcal pneumonia by virtue of their capacity to eliminate apoptotic neutrophils (29). This idea is strengthened by data obtained in p110γ deficient mice in which the recruitment of monocytes/macrophages was found impaired (17)(and data not shown). PI3Kγ-KO mice showed substantial lung

infiltrates and tissue injury during pneumococcal pneumonia (data not shown), whereas $PTEN^{MC\text{-}KO}$ mice, embracing significantly increased numbers of (alveolar) macrophages, showed less severe signs of tissue damage (Fig.8). We in addition discovered an increased phagocytic potential of alveolar macrophages in the absence of PTEN. The enhanced phagocytic properties of PTEN-deficient macrophages might have compensated for the reduced number of infiltrating neutrophils. However, the precise role of neutrophils during pneumococcal pneumonia has been challenged recently by a report showing unaltered bacterial clearance and improved survival in neutrophil-depleted animals that were infected with *S. pneumoniae* (44). It seems that enhanced neutrophil numbers prolong inflammation and ultimately fuel tissue damage, thus resulting in worsened outcome. It is therefore tempting to hypothesize that lower neutrophil counts and simultaneously increased numbers of macrophages in $PTEN^{MC\text{-}KO}$ animals improved bacterial clearance and augmented the resolution of inflammation, thus contributing to diminished tissue damage and favorable outcome in these animals.

In conclusion, our findings demonstrate that enhanced PI3K activity in PTEN deficient mice resulted in an improved outcome during pneumococcal pneumonia. These findings implicate a crucial role for PTEN in the homeostasis of pro- and anti-inflammatory mechanisms evoked during a relevant bacterial infection. Thus, interfering with PI3K signaling might have tremendous implications on the course of pneumococcal pneumonia: while blockade of PTEN might be beneficial, reduced PI3K activity might prove detrimental.

Acknowledgement:

All authors declare no financial conflict of interest relevant to this article. We thank Erhart L. and Raim R. for excellent technical assistance.

Footnotes:

Non-standard abbreviations:

AKT...protein kinase B

AM ...alveolar macrophage

BAL...broncho-alveolar lavage

BMDM ...bone marrow derived macrophage

GSK...glycogen synthase kinase

iNOS...inducible NO synthase

KC...keratinocyte-derived chemokine

LysM...lysozyme M

MPO...myeloperoxidase

$PI(3,4,5)P_3$ ...phosphatidylinositol (3,4,5) triphosphate

PTEN...phosphatase and tensin homologue

Reference List

1. National Immunization Program.Centers for Disease Control and Prevention and U.S.Department of Health and Human Services. 2007. Epidemiology and Prevention of Vaccine-Preventable Diseases.
2. Ortqvist, A., J. Hedlund, and M. Kalin. 2005. Streptococcus pneumoniae: epidemiology, risk factors, and clinical features. Semin. Respir. Crit Care Med. 26:563-574.
3. Appelbaum, P. C. 2002. Resistance among Streptococcus pneumoniae: Implications for drug selection. Clin. Infect. Dis. 34:1613-1620.
4. Tamguney, T. and D. Stokoe. 2007. New insights into PTEN. J. Cell Sci. 120:4071-4079.
5. Cantley, L. C. 2002. The phosphoinositide 3-kinase pathway. Science 296:1655-1657.

6. Curnock, A. P., M. K. Logan, and S. G. Ward. 2002. Chemokine signalling: pivoting around multiple phosphoinositide 3-kinases. Immunology 105:125-136.

7. Hirsch, E., V. L. Katanaev, C. Garlanda, O. Azzolino, L. Pirola, L. Silengo, S. Sozzani, A. Mantovani, F. Altruda, and M. P. Wymann. 2000. Central role for G protein-coupled phosphoinositide 3-kinase gamma in inflammation. Science 287:1049-1053.

8. Li, Z., H. Jiang, W. Xie, Z. Zhang, A. V. Smrcka, and D. Wu. 2000. Roles of PLC-beta2 and -beta3 and PI3Kgamma in chemoattractant-mediated signal transduction. Science 287:1046-1049.

9. Sasaki, T., J. Irie-Sasaki, R. G. Jones, A. J. Oliveira-dos-Santos, W. L. Stanford, B. Bolon, A. Wakeham, A. Itie, D. Bouchard, I. Kozieradzki, N. Joza, T. W. Mak, P. S. Ohashi, A. Suzuki, and J. M. Penninger. 2000. Function of PI3Kgamma in thymocyte development, T cell activation, and neutrophil migration. Science 287:1040-1046.

10. Stephens, L., C. Ellson, and P. Hawkins. 2002. Roles of PI3Ks in leukocyte chemotaxis and phagocytosis. Curr. Opin. Cell Biol. 14:203-213.

11. Fukao, T. and S. Koyasu. 2003. PI3K and negative regulation of TLR signaling. Trends Immunol. 24:358-363.

12. Ruse, M. and U. G. Knaus. 2006. New players in TLR-mediated innate immunity: PI3K and small Rho GTPases. Immunol. Res. 34:33-48.

13. Guha, M. and N. Mackman. 2002. The phosphatidylinositol 3-kinase-Akt pathway limits lipopolysaccharide activation of signaling pathways and expression of inflammatory mediators in human monocytic cells. J. Biol. Chem. 277:32124-32132.

14. Gunzl, P. and G. Schabbauer. 2008. Recent advances in the genetic analysis of PTEN and PI3K innate immune properties. Immunobiology 213:759-765.

15. Luyendyk, J. P., G. A. Schabbauer, M. Tencati, T. Holscher, R. Pawlinski, and N. Mackman. 2008. Genetic analysis of the role of the PI3K-Akt pathway in lipopolysaccharide-induced cytokine and tissue factor gene expression in monocytes/macrophages. J. Immunol. 180:4218-4226.

16. Martin, M., K. Rehani, R. S. Jope, and S. M. Michalek. 2005. Toll-like receptor-mediated cytokine production is differentially regulated by glycogen synthase kinase 3. Nat. Immunol. 6:777-784.

17. Maus, U. A., M. Backi, C. Winter, M. Srivastava, M. K. Schwarz, T. Ruckle, J. C. Paton, D. Briles, M. Mack, T. Welte, R. Maus, R. M. Bohle, W. Seeger, C. Rommel, E. Hirsch, J. Lohmeyer, and K. T. Preissner. 2007. Importance of phosphoinositide 3-kinase gamma in the host defense against pneumococcal infection. Am. J. Respir. Crit Care Med. 175:958-966.

18. Marone, R., V. Cmiljanovic, B. Giese, and M. P. Wymann. 2008. Targeting phosphoinositide 3-kinase: moving towards therapy. Biochim. Biophys. Acta 1784:159-185.

19. Suzuki, A., M. T. Yamaguchi, T. Ohteki, T. Sasaki, T. Kaisho, Y. Kimura, R.

Yoshida, A. Wakeham, T. Higuchi, M. Fukumoto, T. Tsubata, P. S. Ohashi, S. Koyasu, J. M. Penninger, T. Nakano, and T. W. Mak. 2001. T cell-specific loss of Pten leads to defects in central and peripheral tolerance. Immunity. 14:523-534.

20. Peyssonnaux, C., V. Datta, T. Cramer, A. Doedens, E. A. Theodorakis, R. L. Gallo, N. Hurtado-Ziola, V. Nizet, and R. S. Johnson. 2005. HIF-1alpha expression regulates the bactericidal capacity of phagocytes. J. Clin. Invest 115:1806-1815.

21. Sasaki, T., J. Irie-Sasaki, R. G. Jones, A. J. Oliveira-dos-Santos, W. L. Stanford, B. Bolon, A. Wakeham, A. Itie, D. Bouchard, I. Kozieradzki, N. Joza, T. W. Mak, P. S. Ohashi, A. Suzuki, and J. M. Penninger. 2000. Function of PI3Kgamma in thymocyte development, T cell activation, and neutrophil migration. Science 287:1040-1046.

22. Davies, J. Q. and S. Gordon. 2005. Isolation and culture of murine macrophages. Methods Mol. Biol. 290:91-103.

23. Knapp, S., S. Florquin, D. T. Golenbock, and P. T. van der. 2006. Pulmonary lipopolysaccharide (LPS)-binding protein inhibits the LPS-induced lung inflammation in vivo. J. Immunol. 176:3189-3195.

24. Lagler, H., O. Sharif, I. Haslinger, U. Matt, K. Stich, T. Furtner, B. Doninger, K. Schmid, R. Gattringer, A. F. de Vos, and S. Knapp. 2009. TREM-1 activation alters the dynamics of pulmonary IRAK-M expression in vivo and improves host defense during pneumococcal pneumonia. J. Immunol. 183:2027-2036.

25. LeBel, C. P., H. Ischiropoulos, and S. C. Bondy. 1992. Evaluation of the probe 2',7'-dichlorofluorescin as an indicator of reactive oxygen species formation and oxidative stress. Chem. Res. Toxicol. 5:227-231.

26. Knapp, S., U. Matt, N. Leitinger, and P. T. van der. 2007. Oxidized phospholipids inhibit phagocytosis and impair outcome in gram-negative sepsis in vivo. J. Immunol. 178:993-1001.

27. Knapp, S., L. Hareng, A. W. Rijneveld, P. Bresser, J. S. van der Zee, S. Florquin, T. Hartung, and P. T. van der. 2004. Activation of neutrophils and inhibition of the proinflammatory cytokine response by endogenous granulocyte colony-stimulating factor in murine pneumococcal pneumonia. J. Infect. Dis. 189:1506-1515.

28. Knapp, S., C. W. Wieland, '. van, V, O. Takeuchi, S. Akira, S. Florquin, and P. T. van der. 2004. Toll-like receptor 2 plays a role in the early inflammatory response to murine pneumococcal pneumonia but does not contribute to antibacterial defense. J. Immunol. 172:3132-3138.

29. Knapp, S., J. C. Leemans, S. Florquin, J. Branger, N. A. Maris, J. Pater, R. N. van, and P. T. van der. 2003. Alveolar macrophages have a protective antiinflammatory role during murine pneumococcal pneumonia. Am. J. Respir. Crit Care Med. 167:171-179.

30. Dessing, M. C., S. Knapp, S. Florquin, A. F. de Vos, and P. T. van der. 2007. CD14 facilitates invasive respiratory tract infection by Streptococcus pneumoniae. Am. J. Respir. Crit Care Med. 175:604-611.

31. Sly, L. M., V. Ho, F. Antignano, J. Ruschmann, M. Hamilton, V. Lam, M. J. Rauh,

and G. Krystal. 2007. The role of SHIP in macrophages. Front Biosci. 12:2836-2848.

32. Subramanian, K. K., Y. Jia, D. Zhu, B. T. Simms, H. Jo, H. Hattori, J. You, J. P. Mizgerd, and H. R. Luo. 2007. Tumor suppressor PTEN is a physiologic suppressor of chemoattractant-mediated neutrophil functions. Blood 109:4028-4037.

33. Liu, L., K. D. Puri, J. M. Penninger, and P. Kubes. 2007. Leukocyte PI3Kgamma and PI3Kdelta have temporally distinct roles for leukocyte recruitment in vivo. Blood 110:1191-1198.

34. Strassheim, D., J. Y. Kim, J. S. Park, S. Mitra, and E. Abraham. 2005. Involvement of SHIP in TLR2-induced neutrophil activation and acute lung injury. J. Immunol. 174:8064-8071.

35. Hazeki, K., K. Nigorikawa, and O. Hazeki. 2007. Role of phosphoinositide 3-kinase in innate immunity. Biol. Pharm. Bull. 30:1617-1623.

36. Williams, D. L., C. Li, T. Ha, T. Ozment-Skelton, J. H. Kalbfleisch, J. Preiszner, L. Brooks, K. Breuel, and J. B. Schweitzer. 2004. Modulation of the phosphoinositide 3-kinase pathway alters innate resistance to polymicrobial sepsis. J. Immunol. 172:449-456.

37. Schabbauer, G., M. Tencati, B. Pedersen, R. Pawlinski, and N. Mackman. 2004. PI3K-Akt pathway suppresses coagulation and inflammation in endotoxemic mice. Arterioscler. Thromb. Vasc. Biol. 24:1963-1969.

38. Cao, X., G. Wei, H. Fang, J. Guo, M. Weinstein, C. B. Marsh, M. C. Ostrowski, and S. Tridandapani. 2004. The inositol 3-phosphatase PTEN negatively regulates Fc gamma receptor signaling, but supports Toll-like receptor 4 signaling in murine peritoneal macrophages. J. Immunol. 172:4851-4857.

39. Doble, B. W. and J. R. Woodgett. 2003. GSK-3: tricks of the trade for a multi-tasking kinase. J. Cell Sci. 116:1175-1186.

40. Fillion, I., N. Ouellet, M. Simard, Y. Bergeron, S. Sato, and M. G. Bergeron. 2001. Role of chemokines and formyl peptides in pneumococcal pneumonia-induced monocyte/macrophage recruitment. J. Immunol. 166:7353-7361.

41. Frevert, C. W., S. Huang, H. Danaee, J. D. Paulauskis, and L. Kobzik. 1995. Functional characterization of the rat chemokine KC and its importance in neutrophil recruitment in a rat model of pulmonary inflammation. J. Immunol. 154:335-344.

42. Jones, M. R., B. T. Simms, M. M. Lupa, M. S. Kogan, and J. P. Mizgerd. 2005. Lung NF-kappaB activation and neutrophil recruitment require IL-1 and TNF receptor signaling during pneumococcal pneumonia. J. Immunol. 175:7530-7535.

43. Li, Y., Y. Jia, M. Pichavant, F. Loison, B. Sarraj, A. Kasorn, J. You, B. E. Robson, D. T. Umetsu, J. P. Mizgerd, K. Ye, and H. R. Luo. 2009. Targeted deletion of tumor suppressor PTEN augments neutrophil function and enhances host defense in neutropenia-associated pneumonia. Blood .

44. Marks, M., T. Burns, M. Abadi, B. Seyoum, J. Thornton, E. Tuomanen, and

L. A. Pirofski. 2007. Influence of neutropenia on the course of serotype 8 pneumococcal pneumonia in mice. Infect. Immun. 75:1586-1597.

45. Saura, M., C. Zaragoza, C. Bao, A. McMillan, and C. J. Lowenstein. 1999. Interaction of interferon regulatory factor-1 and nuclear factor kappaB during activation of inducible nitric oxide synthase transcription. J. Mol. Biol. 289:459-471.

46. Schabbauer, G., J. Luyendyk, K. Crozat, Z. Jiang, N. Mackman, S. Bahram, and P. Georgel. 2008. TLR4/CD14-mediated PI3K activation is an essential component of interferon-dependent VSV resistance in macrophages. Mol. Immunol. 45:2790-2796.

4.3.2. ANTI-INFLAMMATORY PROPERTIES OF THE PI3K PATHWAY ARE MEDIATED BY IL10/DUSP REGULATION

Philipp Günzl[1], Eva Hainzl[1], Ulrich Matt[2,3], Barbara Dillinger[1], Benedikt Mahr[1], Sylvia Knapp[2,3], Bernd R. Binder[1] and Gernot Schabbauer[1]

[1]Department of Vascular Biology and Thrombosis Research, Center for Biomolecular Medicine and Pharmacology; Medical University of Vienna, Vienna, Austria [2]Research Center for Molecular Medicine of the Austrian Academy of Sciences (CeMM), Vienna, Austria [3] Department of Medicine 1, Division of Infectious Diseases and Tropical medicine, Medical University Vienna, Vienna, Austria

Summary: Here we report how activation of the PI3K/PTEN signaling pathway downregulates pro-inflammatory gene expression by DUSP1 gene regulation.

Corresponding Author:

Gernot Schabbauer Ph.D.

Department of Vascular Biology and Thrombosis Research, Center for Biomolecular Medicine and Pharmacology, Medical University of Vienna

Schwarzspanierstrasse 17; 1090 Wien, Austria

Phone: 0043-1-4277-62508 FAX: 0043-1-4277-9625

E-mail: gernot.schabbauer@meduniwien.ac.at

Key words: PTEN, Inflammation, DUSP1, Macrophage

Abstract:

Resolution of inflammation is an important hallmark in the course of infectious diseases. Dysregulated inflammatory responses may have detrimental consequences for the affected organism. Therefore tight regulation of inflammation is indispensable.

Among numerous modulatory signaling pathways the PI-3 Kinase/PTEN signaling pathway has been recently proposed to be involved in the regulation of innate immune reactions.

Here we attempted to elucidate molecular mechanisms that contribute to the modulatory properties of the PI3K signaling pathway in inflammation. PTEN deficient macrophages, which harbor constitutively active PI3K, were analyzed in response to gram-negative bacteria and pathogen associated molecular patterns such as LPS. PTEN deficient cells showed reduced inflammatory cytokine production, which was accompanied by reduced MAPK signaling activation in early as well as late phase activation. Simultaneously we found increased levels of the MAPK phosphatase DUSP1 as well as the anti-inflammatory cytokine IL10.

Our data suggest that differential DUSP1 regulation coupled with enhanced IL10 production contribute to the anti-inflammatory properties of the PI3K pathway.

Introduction:

Tight regulation during onset as well as resolution of the innate immune response to pathogens or pathogen associated molecular patterns is of utmost importance for the affected host. In clinical settings, secondary bacterial infections with subsequent complications in patients are a major cause for morbidity and mortality. Gram-negative bacteria such as *Acinetobacter baumanii* or *Pseudomonas aeruginosa* account for severe nosocomial infections especially in immune compromised patients admitted to intensive care units. On the other hand overwhelming inflammatory responses to bacterial pathogens, which is often seen in cases of severe sepsis or acute lung injury, may lead to increased tissue damage, organ failure and ultimately death (19).

Several signaling molecules are implicated in down-modulation of inflammatory pathways, such as IRAK-M (Interleukin 1 Receptor-Associated Kinase M), SOCS (suppressors of cytokine signalling) family members and the Interleukin 10/Jak/Stat3 pathway (6,16,20). More recently the PI3K signaling pathway, which is activated by TLR agonists, and downstream signaling molecules, have been described by us and others to exert pronounced anti-inflammatory effects by way of effective limitation of pro-inflammatory gene expression (10,18,25,26,28,29).

The PI3K signaling pathway is immediately activated upon cell stimulation. The active enzyme, which consist of a catalytic p110 and a regulatory p85 subunit, generates $PI(3,4,5)P_3$, which leads to the recruitment of downstream kinases such as AKT. PI3K/AKT signaling serves pleiotropic functions, such as cell motility, phagocytosis and cell survival (3). Recent advances in the understanding of PI3K's role in innate immune regulation using genetic models suggest potent anti-inflammatory properties. Enhanced and sustained

PI3K activity effectively suppresses MAPK signaling (10,18). The molecular mechanism of PI3K's mode of inhibition of inflammatory pathways is still incompletely understood.

As a model to mimic constitutively active PI3K activity specifically in macrophages, we make use of a conditional deletion of the endogenous PI3K antagonist and tumor suppressor phosphatase and tensin homologue deleted on chromosome 10 (PTEN). Ablation of the pten gene by a cre-lox system driven by the LysM promoter leads to enhanced and sustained PI3K signaling activity in monocytes, macrophages and neutrophil granulocytes (5).

Here we show that activation of PTEN deficient macrophages by heat killed bacteria leads to suppressed MAP kinase activity in an early as well as in late phase activation. Transcription and release of pro-inflammatory cytokines such as TNFα and IL6 are reduced. In contrast anti-inflammatory IL10 is significantly upregulated in resting as well as stimulated PTEN deficient macrophages. Furthermore we found that among several investigated anti-inflammatory candidate genes, such as IRAK-M, a MAP kinase phosphatase (also known as DUSP or dual specificity phosphatase) is differentially regulated upon TLR stimulation. In fact DUSP1/MKP1 has been previously shown to exert potent innate immune-modulatory properties (11,24).

We propose that increased PI3K activity in PTEN deficient macrophages results in pronounced anti-inflammatory cellular properties through differential DUSP1 and IL10 regulation.

Materials & Methods:

Mice:

Floxed PTEN mice were kindly provided by T.W. Mak (27), LysM cre recombinase transgenic mice were a kind gift from R. Johnson (22). Intercrossed mice were backcrossed to a C57BL/6J background for at least 8 generations. Mice deficient for p85α were provided by S. Koyasu. This strain is backcrossed to a C57BL/6J backround for at least 13 generations. Littermate-controlled experiments were performed using 8-12 week old male mice. For genotyping, murine tissue was lysed in PCR-lysis buffer and direct PCR was performed using GoTaq DNA Polymerase (Promega, Madison, WI, USA). All animal studies were approved and comply with institutional guidelines (BMWF-66.009/0103-C/GT/2007).

Harvest of primary macrophages:

Thioglycollate-elicited peritoneal macrophages were isolated from $PTEN^{MC-KO}$ and $PTEN^{MC-WT}$ controls. In brief, 2ml of a 4% thioglycollate medium were injected intraperitoneally and macrophages were harvested three days later by peritoneal lavage with 5ml of Ringer's Solution. Macrophages were counted and seeded at a concentration of 10^6 cells per ml in RPMI-1640 medium (Invitrogen Corp., Carlsbad, CA, USA) supplemented with 10% fetal calf serum, 1% penicillin/streptomycin/fungizone (PSF) and 1% L-glutamine. After two hours, medium was exchanged to remove non-adherent cells; adherent cells were allowed to recover over night.

Stimulation of primary macrophages:

Thioglycollate-elicited peritoneal macrophages were stimulated *in vitro* with 100ng/ml ultra-pure LPS (Invitrogen Corp., Carlsbad, CA, USA) or 10^7 CFU/ml heat-killed *Acinetobacter baumannii* for the indicated time points. Recombinant murine IL-10 was obtained from ImmunoTools (Friesoythe, Germany).

Western Blotting and ELISA:

Macrophage cell lysates were separated by SDS-PAGE, blotted to Immobilon PVDF Transfer Membrane (Millipore, Bedford, MA, USA) and probed with primary antibodies against PTEN, IκB, phospho-IκB, p65, phospho-p65, phospho-ERK, p38, phospho-p38, phospho-JNK, phospho-DUSP1 (all Cell Signaling Technology, Beverly, MA), DUSP1 (M-19 clone, Santa Cruz Biotechnology, Santa Cruz, CA, USA) and β-Actin (Sigma, St. Louis, MO, USA). For detection, a secondary antibody conjugated with horseradish peroxidase (Amersham, Piscataway, NJ) was used. Membranes were developed using the chemiluminescence reagent assay SuperSignal West Femto and exposed in the FluorChem HD2 Chemiluminescence Imager (Alpha Innotech Corp., San Leandro, CA, USA). Bands were analyzed according to their molecular weight. Actin, non-phosphorylated p65 and non-phosphorylated p38 were used for normalization.

For ELISA measurements broncho-alveolar lavage and lung tissue samples were analyzed for TNFα, IL6 and IL10 using the Duoset ELISA kits (R&D Systems, Minneapolis).

Quantitative real-time RT-PCR:

Total RNA was isolated from naïve and stimulated macrophages using TRIzol Reagent (Invitrogen Corp., Carlsbad, CA, USA) according to manufacturer's protocol and reverse transcribed. Semi-quantitative real-time PCR was performed using Fast SYBR Green Mastermix (Applied Biosystems, Foster City, CA, USA) and StepOne Real-Time PCR System (Applied Biosystems, Foster City, CA, USA). Transcription levels of target genes were assayed in duplicates, normalized to GAPDH levels and depicted as fold induction of unstimulated macrophages. The following primer pairs have been used. (Table I)

Table I:

Gene	Forward primer (5'-3')	Reverse primer (5'-3')
A20	GACCATGGCACAACTCATCTCA	GTTAGCTTCATCCAACTTTGCGGCATTG
DUSP1	GGATATGAAGCGTTTTCGGCT	GGATTCTGCACTGTCAGGCA
DUSP2	TGGAGATCCTGTCCTTCCTG	CCTTCCGAGAAGCGTGATAG
DUSP4	CTACCTCGGCAGTGCCTATC	GACGGGGATGCACTTGTACT
DUSP5	TGGATGTGAAGCCCACCTCA	CGCACTTGGATGCGTGGTAG
DUSP10	CGCCTACTTGATGAAGCACA	AGGTTCGGGGAAATAATTGG
GAPDH	GGTCGTATTGGGCGCCTGGTCACC	CACACCCATGACGAACATGGGGGC
IL-6	TGCAAGTGCATCATCGTTGTTC	CCACGGCCTTCCCTACTTCA
IL-10	TGGCCCAGAAATCAAGGAGC	CAGCAGACTCAATACACACT
IRAK-M	TTTGAATGCAGCCAGTCTGA	GCATTGCTTATGGAGCCAAT
PTEN	ACACCGCCAAATTTAACTGC	TACACCAGTCCGTCCCTTTC
TLR2	TCAGCTCACCGATGAAGAAGC	TGTAACGCAACAGCTTCAGGAG
TLR4	TCTGGCATCATCTTCATTGTCC	GCGATACAATTCCACCTGCTG
TNF-α	GAACTGGCAGAAGAGGCACT	GGTCTGGCCCATAGAACTGA

Acinetobacter pneumonia and broncho-alveolar lavage:

A non-lethal *Acinetobacter* pneumonia was performed in mice as described previously (14,23). Briefly, *Acinetobacter baumannii* was obtained from American Type Culture Collection (ATCC 17961, Rockville, MD) and grown to log-phase. Mice were short-term anesthetized with isoflurane (Abbott, Wiesbaden, Germany) and 50µl of the bacterial suspension (approximately 10^7 CFUs) were inoculated intranasally. Mice were sacrificed 6h post infection, and bilateral bronchoalveolar-lavage (BAL) was performed by instilling 1ml of sterile saline as reported previously (15). Therefore, the trachea was exposed through a midline incision and canulated with a sterile 22-gauge Abbocath-T catheter (Abott, Wiesbaden, Germany). BAL fluids were subsequently spun down at 1250rpm for 5min, the supernatants frozen at -70°C for cytokine

analysis and the cell pellet lysed in sample buffer for Western blot analysis. Whole lungs were harvested and homogenized at 4°C in 4 volumes of sterile saline using a tissue homogenizer (Biospec Products, Bartlesville, OK, USA). CFUs were determined from serial dilutions of lung homogenates plated on blood agar plates and incubated at 37°C for 16h before colonies were counted. Cytokines were quantified in lung homogenates and BAL fluids using ELISA DuoSets (R&D Systems, Minneapolis, MN, USA) as described earlier (14).

Statistical Analysis:

Data were analyzed by GraphPad Prism 4 software using unpaired Student's t-test followed by post hoc tests, when appropriate. Values are expressed as mean ± standard deviation. Criteria for significance for all experiments were $p<0.05$.

Results:

Stimulation of PTEN deficient macrophages with heat killed *Acinetobacter baumannii* leads to reduced expression of pro-inflammatory cytokines

Expression and subsequent release of cytokines and chemokines is indispensable during the course of infectious diseases. Recognition of pathogens by immune competent cells will lead to the immediate release of cytokines in order to amplify the initial response to the potential threat.

First we measured the deletion efficiency in PTEN deficient macrophages at the level of mRNA transcription. We can show that thioglycollate elicited peritoneal macrophages derived from floxed PTEN LysM cre positive mice (fl/fl pten, lysM +) only marginally express PTEN mRNA as measured by quantitative real time RT-PCR (Fig. 1A). Furthermore we show by western blotting that PTEN protein expression in macrophages is down-regulated to undetectable levels. Though, PTEN protein levels are not changed in wildtype macrophages stimulated with heat-killed bacteria (Fig. 1B). Previously we could demonstrate that PTEN deficiency in macrophages leads to increased and sustained PI3K activity (18,25).

To analyze the effect of PTEN deficiency during the inflammatory response to clinically relevant pathogens in macrophages we used heat killed gram-negative *Acinetobacter baumannii in vitro*. We measured macrophage mRNA transcription of TNFα and IL6 by semi-quantitative PCR and quantitative real time RT-PCR. Bacteria-induced mRNA expression of both cytokines was significantly reduced in PTEN deficient macrophages (Fig. 1C+D) as compared to littermate control wildtype cells. Data was confirmed on protein level by ELISA analysis of supernatants (data not shown).

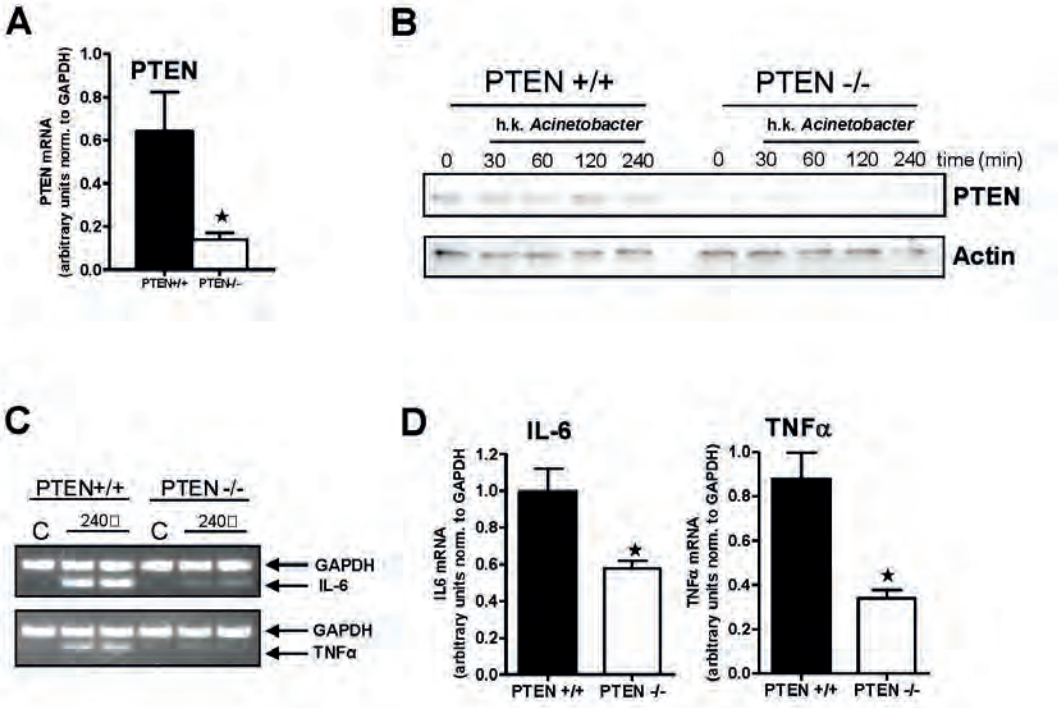

Figure 1: Loss of PTEN leads to a significantly decreased release of proinflammatory cytokines from macrophages upon stimulation with LPS.

(A) Quantitative real-time analysis of PTEN transcription in unstimulated PTEN+/+ and PTEN-/- macrophages (n=6 mice per group). (B) Western blot analysis of PTEN+/+ and PTEN-/- macrophages stimulated with heat-killed *Acinetobacter baumannii* for the indicated time points. Blots were probed with antibodies specific for PTEN. (C) IL-6 and TNF-α mRNA levels from PTEN+/+ and PTEN-/- macrophages 240min upon stimulation with heat-killed *Acinetobacter baumannii* is shown by semi-quantitative PCR analysis. GAPDH levels serve as loading control (n=2 mice per group). (D) Quantitative real-time analysis of IL-6 and TNF-α transcription in PTEN+/+ and PTEN-/- macrophages 240min upon stimulation with heat-killed *Acinetobacter baumannii* (n=3 mice per group). Target genes were normalized to GAPDH, results are not efficiency corrected. Data are presented as mean and standard deviation. Statistical significance is indicated by *($p<0.05$).

Downregulation of pro-inflammatory cytokines by PTEN deficiency is independent of changes in either Toll like receptor (TLR) expression, NFκB activation or expression of other anti-inflammatory molecules .

Initially it was unclear whether differential TLR expression accounted for the modulated pathogen responsiveness. Therefore we measured the steady state levels of the most important TLRs for the recognition of *Acinetobacter* in this respect. Gram-negative bacteria will be preferentially recognized by TLR4. Additionally TLR2 may also contribute in pathogen detection. Expression of both receptors was unaltered in unstimulated macrophages. Modulation of the PI3K/PTEN pathway does not influence mRNA levels of TLR2 and TLR4 (Fig. 2A).

Previously we have shown that PTEN is involved in the regulation of MAPK activation upon LPS/TLR4 stimulation (18). To analyze early (30 minutes and earlier) as well as late (60 minutes and later) effects of constitutively active PI3K on the TLR-activated NFκB pathway, PTEN deficient macrophages and wildtype littermate control cells were stimulated with heat killed *Acinetobacter baumannii* for the indicated time points. We determined expression and posttranslational modifications of the inhibitor of NFκB, IκB, and p65, which is one the major NFκB transcription factor subunits. As expected we detected phosphorylation of IkB and p65 within 30 minutes upon cell stimulation. IκB and p65 phosphorylation was only marginally different (Fig. 2B). Similarly we did not find any overt differences in degradation as well as resynthesis of IκB in PTEN deficient or wildtype macrophages stimulated with heat-killed bacteria (data not shown). These findings indicate that the TLR/NFκB pathway is nearly unaffected by PTEN deficiency upon treatment of macrophages with heat killed bacteria.

Moreover we analyzed the expression pattern of two inhibitory NFκB-dependent candidate genes upon stimulation with heat killed bacteria and LPS in PTEN -/- macrophages and littermate control wildtype cells. We chose IRAK-M and A20, since both interfere with the TLR4/NFκB signaling pathway (1,16). Interestingly mRNA levels of both genes were not changed in macrophages with or without PTEN in response to heat killed *Acinetobacter* 30' and 120' post stimulation, although mRNA transcription was markedly induced (Fig. 2C). We conclude from these data that these genes do not contribute to the anti-inflammatory properties we observed in cell with increased and sustained PI3K activity.

Figure 2: Differential transcription of pattern recognition receptors, activation of the NF-κB pathway or two potent anti-inflammatory mediators do not contribute to the anti-inflammatory effects of PTEN deficiency in macrophages.

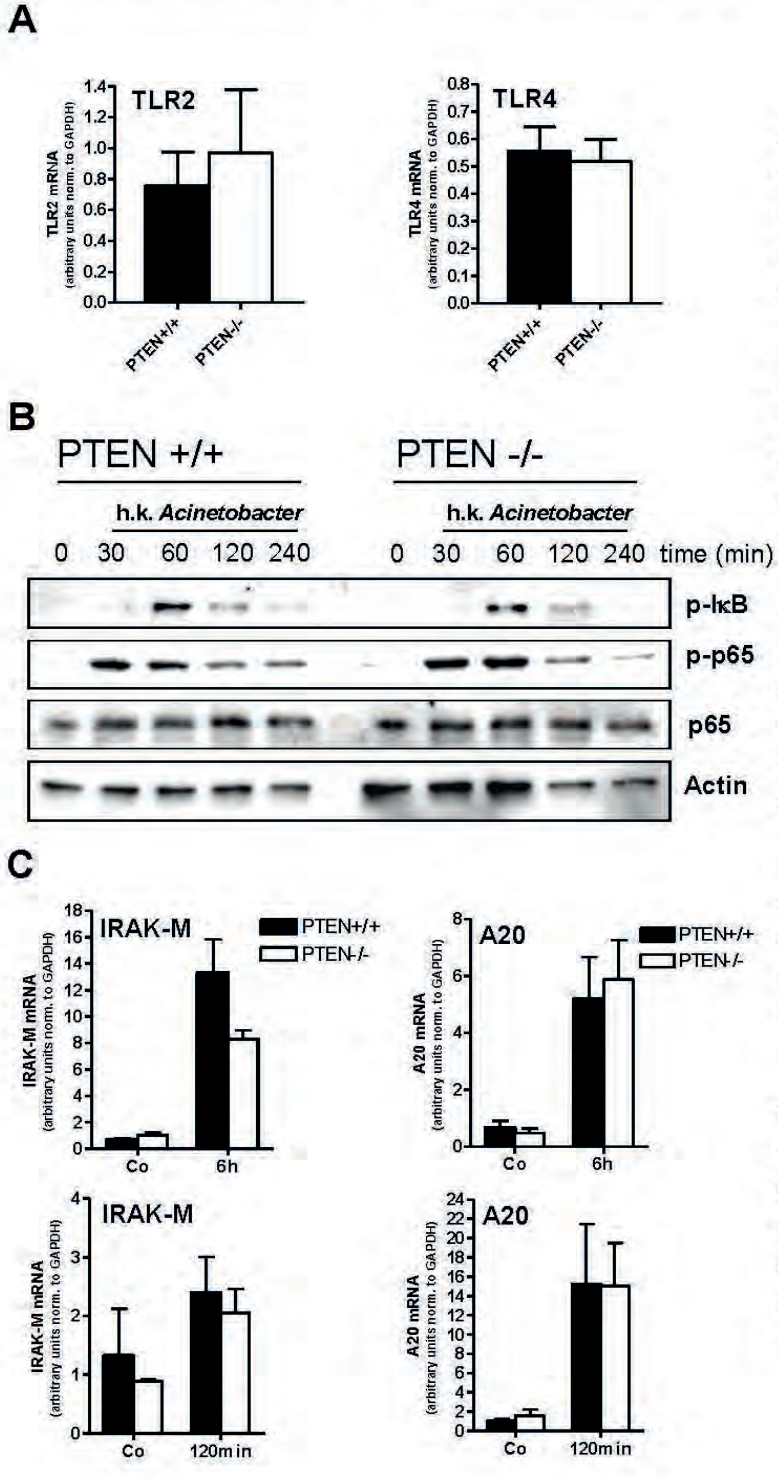

(A) Quantitative real-time analysis of TLR2 and TLR4 transcription in unstimulated PTEN+/+ and PTEN-/- macrophages (n=6 mice per group).

(B) Western blot analysis of PTEN+/+ and PTEN-/- macrophages stimulated with heat-killed *Acinetobacter baumannii* for the indicated time points. Blots were probed with antibodies specific for phospho-IκB, phospho-p65 and p65. Actin serves as a loading control. Representative Western blots of n=3 mice per group are shown.

(C) Quantitative real-time analysis of IRAK-M and A20 transcription in *Acinetobacter* stimulated PTEN+/+ and PTEN-/- macrophages (n=6 mice per group).

Target genes were normalized to GAPDH, results are not efficiency corrected. Data are presented as mean and standard deviation. Statistical significance is indicated by *($p<0.05$).

PTEN deletion in macrophages results in reduced early as well as late MAP kinase activity and increased MAPK phosphatase expression and stability in response to TLR agonists and IL10

The TLR signaling pathway utilizes the MAP kinase signaling complex, which consists of ERK, p38 and JNK, to activate transcription factors such as AP-1, ATF2 and ELK-1/EGR-1. Each of those factors importantly contributes to immediate inflammatory gene expression during the very early onset of the innate immune response (8,9,30).

We analyzed the effect of PTEN deficiency on early and late phase activation of the MAP kinases by heat-killed *Acinetobacter baumannii*. Previously we could show that either positive or negative modulation of the PI3K signaling pathway results in an immediate effect on MAPK activation (18). In this study we investigated effects on the regulation of late phase MAPK activation by PTEN as well as molecules that might be involved.

Macrophages with ablated PTEN gene and wildtype control cells were stimulated with heat killed *Acinetobacter*. We found that the initial as well as delayed activation of ERK1,2, p38 and JNK1,2 was limited in PTEN -/- macrophages. Interestingly bacteria-induced MAPK activation is sustained only in wildtype cells, as PTEN -/- macrophages showed reduced pMAPK levels at later time points, up to 240 minutes post induction (Fig. 3A).

In order to analyze the mechanisms by which PTEN deficiency alters MAPK activation, we sought to elucidate the PI3K-dependent regulation of enzymes that regulate the MAP kinase -activity and -phosphorylation. It is known that members of the MAPK phosphatase family or dual specificity phosphatases (DUSP) effectively limit the activity of ERK, p38 and JNK with varying specificity. DUSPs have been described as down-modulatory molecules in the innate

immune response to LPS in vitro and in vivo (4,12,24).

To determine the possibility that members of the DUSP family are intricately involved in the anti-inflammatory PTEN phenotype we described above, we sought to measure expression of potential DUSP candidates. *Acinetobacter*-stimulated macrophages were tested for their ability to express DUSP1, which is one of several MAPK phosphatases involved in innate immune mechanism (17). DUSP1 expression on mRNA and protein levels was immediately upregulated upon activation by heat-killed bacteria. Indeed PTEN deficiency led to a substantial increase in DUSP1 mRNA (Fig. 3A).

DUSP1 protein levels are very low in resting macrophages. However, we could detect slightly but still signifivantly elevated baseline protein levels of DUSP1 in PTEN deficient macrophages as compared to wildtype cells (Fig. 3B). Heat-killed *Acinetobacter* could stimulate DUSP protein synthesis within 60 minutes (Fig. 3C). Stimulating wildtype and PTEN deficient macrophages in a timecourse with 10^7 CFU heat-killed *Acinetobacter* led to the discovery that DUSP1 expression at early (15' and 30') as well as late time points (120') was substantially increased in PTEN deficient macrophages (Fig. 3C upper and lower panel).

In addition we found that concomitantly DUSP1 phosphorylation was enhanced in the PTEN deficient cells (Fig. 3C middle panel). As described by Brondello *et al.* phosphorylation of DUSP1 leads to reduced proteasomal degradation (2). These findings indicate that not only expression but also protein stability might be increased in macrophages with sustained PI3K activity.

Conversely we analyzed the effect of TLR-mediated DUSP1 expression in cells with greatly diminished PI3K activity to show that the effects we have observed in PTEN deficient cells is indeed due to the modulation of PI3K

activity. For that matter we made use of p85α deficient macrophages, which is the regulatory subunit of active class Ia PI3Ks. We can show that heat killed *Acinetobacter*-induced DUSP1 expression is reduced in cells with diminished PI3K activity (Fig. 3E), whereas simultaneously p38 activation as measured by phosphorylation was greatly enhanced in p85α deficient macrophages (Fig. 3F).

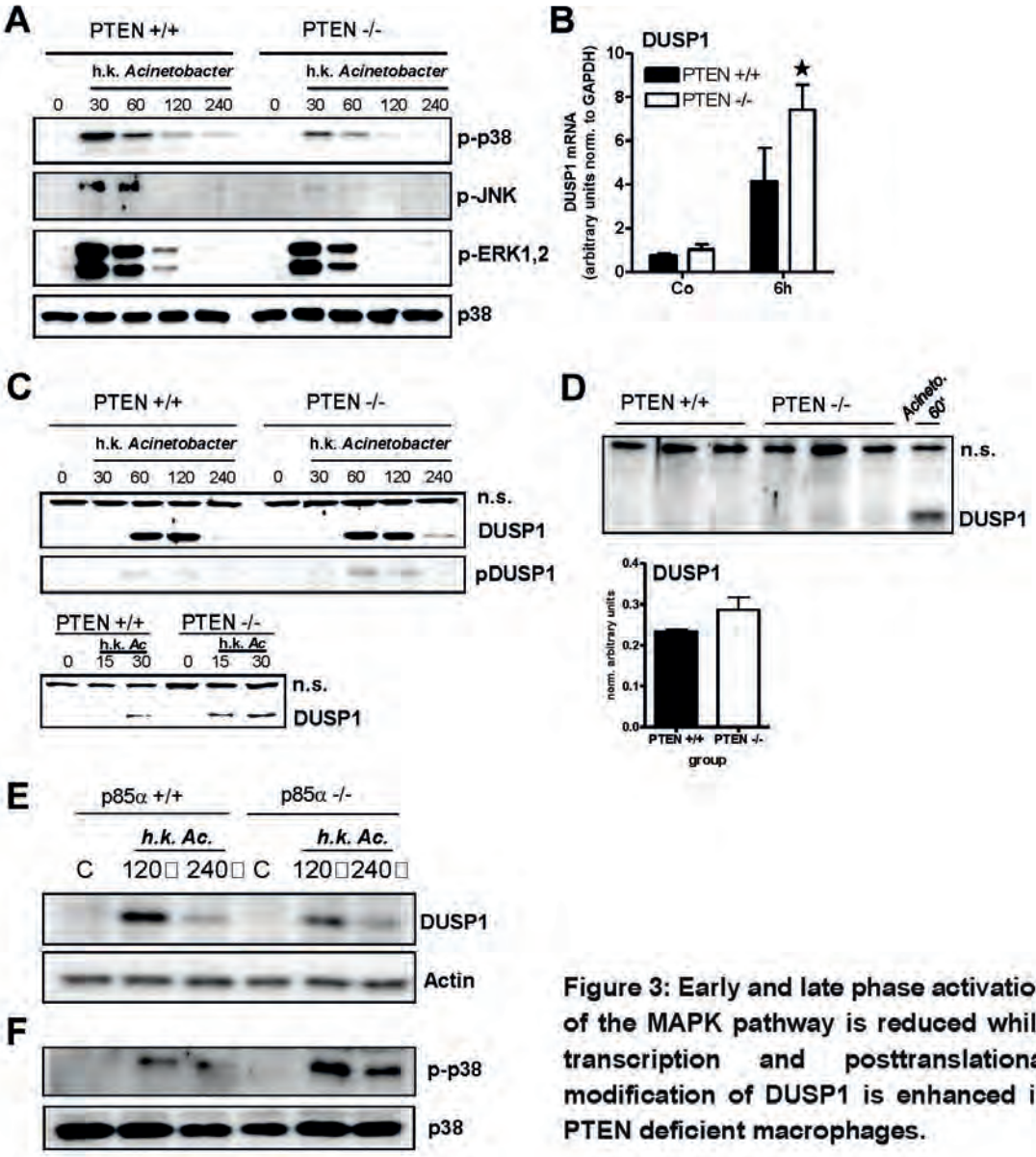

Figure 3: Early and late phase activation of the MAPK pathway is reduced while transcription and posttranslational modification of DUSP1 is enhanced in PTEN deficient macrophages.

(A) Western blot analysis of PTEN+/+ and PTEN-/- macrophages stimulated with heat-killed *Acinetobacter baumannii* for the indicated time points. Blots were probed with antibodies specific for phospho-ERK, phospho-p38 and phospho JNK. p38 serves as a loading control. Representative Western blots of n=3 mice per group are shown. (B) Quantitative real-time analysis of DUSP1 transcription in PTEN+/+ and PTEN-/- macrophages stimulated with heat-killed *Acinetobacter baumannii* for 240min (n=3 mice per group). (C) Western blot analysis of unstimulated PTEN+/+ and PTEN-/- macrophages with DUSP1 antibodies. Bacteria-induced DUSP1 is included as positive control. (D) Western blot analysis of PTEN+/+ and PTEN-/- macrophages stimulated with heat-killed *Acinetobacter baumannii* for the indicated time points. Blots were probed with antibodies specific for DUSP1 and phospho-DUSP1. Unspecific bands detected with DUSP1 antibody serve as loading control. (E) Western blot analysis of p85α +/+ and p85α -/- macrophages stimulated with *Acinetobacter baumannii* for the indicated time points. Blots were probed with antibodies specific for DUSP1 and p38. Actin serves as a loading control. Representative Western blots of n=3 mice per group are shown.

Increased IL10 expression in PTEN deficient macrophages

IL10 is among the most prominent anti-inflammatory cytokines released during inflammatory reactions. Analysis of stimulated macrophages revealed that IL10 is differentially regulated in PTEN deficient cells. We found that mRNA levels as well as IL10 cytokine levels released into the supernatant of cultured knock-out macrophages are substantially increased as compared to cells derived from littermate control mice (Fig. 4A+B).

To test the idea that IL10 or other important inflammatory stimuli may contribute to DUSP1 expression, we stimulated cells with IL10 and LPS. IL10 has already been described to regulate DUSP expression in a positive feedback loop (11). Interestingly we found that LPS as well as IL10 stimulated DUSP1 in macrophages. This effect was markedly enhanced in PTEN deficient cells (Fig. 4C). These data indicate that PTEN is involved in the regulation of TLR-dependent IL10 expression. Furthermore IL10 may contribute to the enhanced DUSP1 expression we observe in resting as well as stimulated PTEN deficient macrophages.

The role of PTEN in the elimination of pathogens in a murine model of *Acinetobacter*-induced pneumonia

To investigate the effect of PTEN deficiency in vivo we decided to apply a model of acute lung injury by intranasal infection with *Acinetobacter baumannii*. Infection in healthy wildtype mice is non-lethal, although a pronounced acute inflammatory response occurs. Usually the infection is contained within 24h and bacterial burden is significantly reduced in immune-competent mice.

In our *in vivo* model we decided to analyze two time points. We sacrificed infected mice at an early time point (6h post infection). Here we aimed to analyze the initial bacterial infection and increased lung inflammation, by cytokine measurements. Next we chose a late time point, 24h post infection. Here, we expected to detect containment of the infection by reduced bacterial burden in the lung.

Interestingly the bacterial burden in the PTEN deficient mice showed significantly enhanced pathogen persistence 24h post inoculation (Fig. 6A). One explanation for that might be a diminished inflammatory response, which is required to limit bacterial growth.

Indeed we found increased levels of TNFα and IL6 in the alveolar lavage in wildtype mice infected with *Acinetobacter baumannii*. Myeloid PTEN deficiency resulted in reduced levels of TNFα 6h post infection, similar to the *in vitro* data shown above (Fig. 5B). In contrast to our cell culture experiments, IL6 was unaffected undicating that cells other than macrophages are the main source for IL6 in this model (Fig. 5C). Interestingly IL10 was undetectable in the bronchial lavage (data not shown). Only when we measured IL10 in whole lung homogenates, we found that IL10 levels were significantly increased in PTEN deficient mice at all time points measured (Fig. 5D). Moreover 6h post infection

we analyzed the expression DUSP1 in the alveolar lavage cells, which are predominately macrophages. At this time, in addition to alveolar macrophages neutrophil granulocytes infiltrated the infected alveoli. In line with *in vitro* data obtained in macrophages, we found elevated levels of DUSP1 in these cells (Fig. 5E). In addition DUSP1 expression in *in vitro* stimulated macrophages as controls is shown (Fig. 5E, last lane). Analysis of the bacterial CFUs at 24h revealed that probably due to the diminished immune response, outgrowth of bacteria could not be prevented in PTEN deficient mice (Fig. 5A).

This indicates that probably due to hampering the inflammatory response in PTEN deficient mice by increased DUSP1 and IL10 expression, the bacterial infection cannot be properly contained.

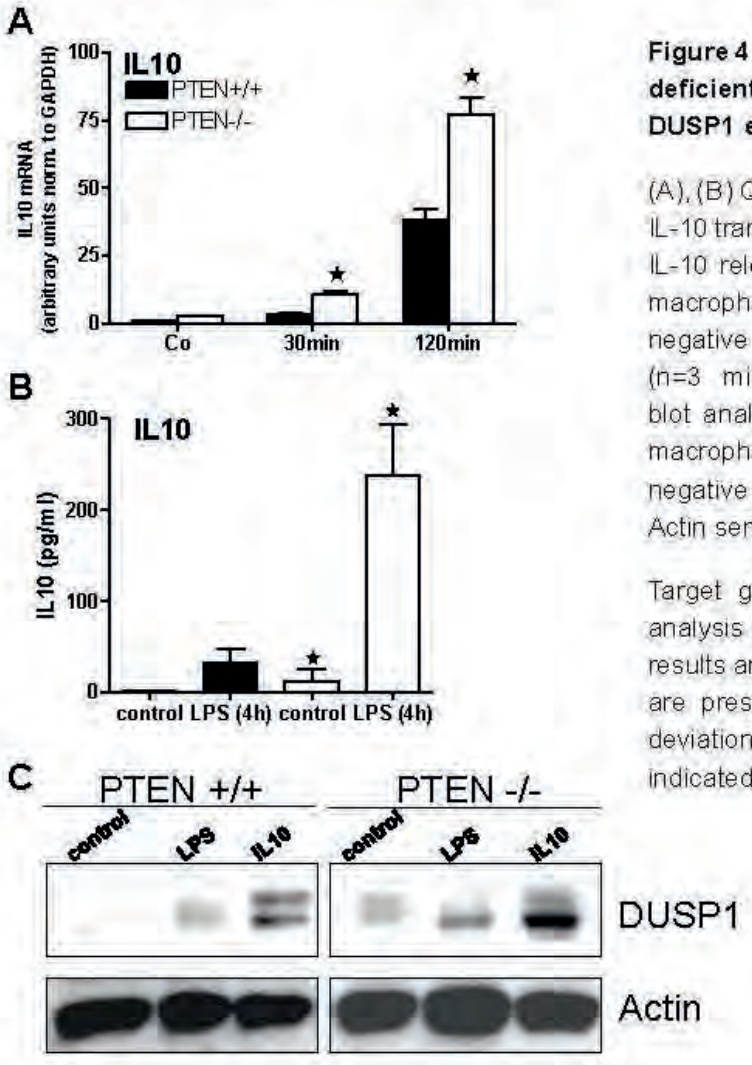

Figure 4: IL-10 is upregulated in PTEN deficient macrophages and induces DUSP1 expression.

(A), (B) Quantitative real-time analysis of IL-10 transcription and ELISA analysis of IL-10 release in PTEN+/+ and PTEN-/- macrophages stimulated with gram-negative LPS for the indicated timepoints (n=3 mice per group). (C) Western blot analysis of PTEN+/+ and PTEN-/- macrophages stimulated with gram-negative LPS or IL10 for 240 minutes. Actin serves as a loading control.

Target genes in quantitative real-time analysis were normalized to GAPDH, results are not efficiency corrected. Data are presented as mean and standard deviation. Statistical significance is indicated by *($p<0.05$).

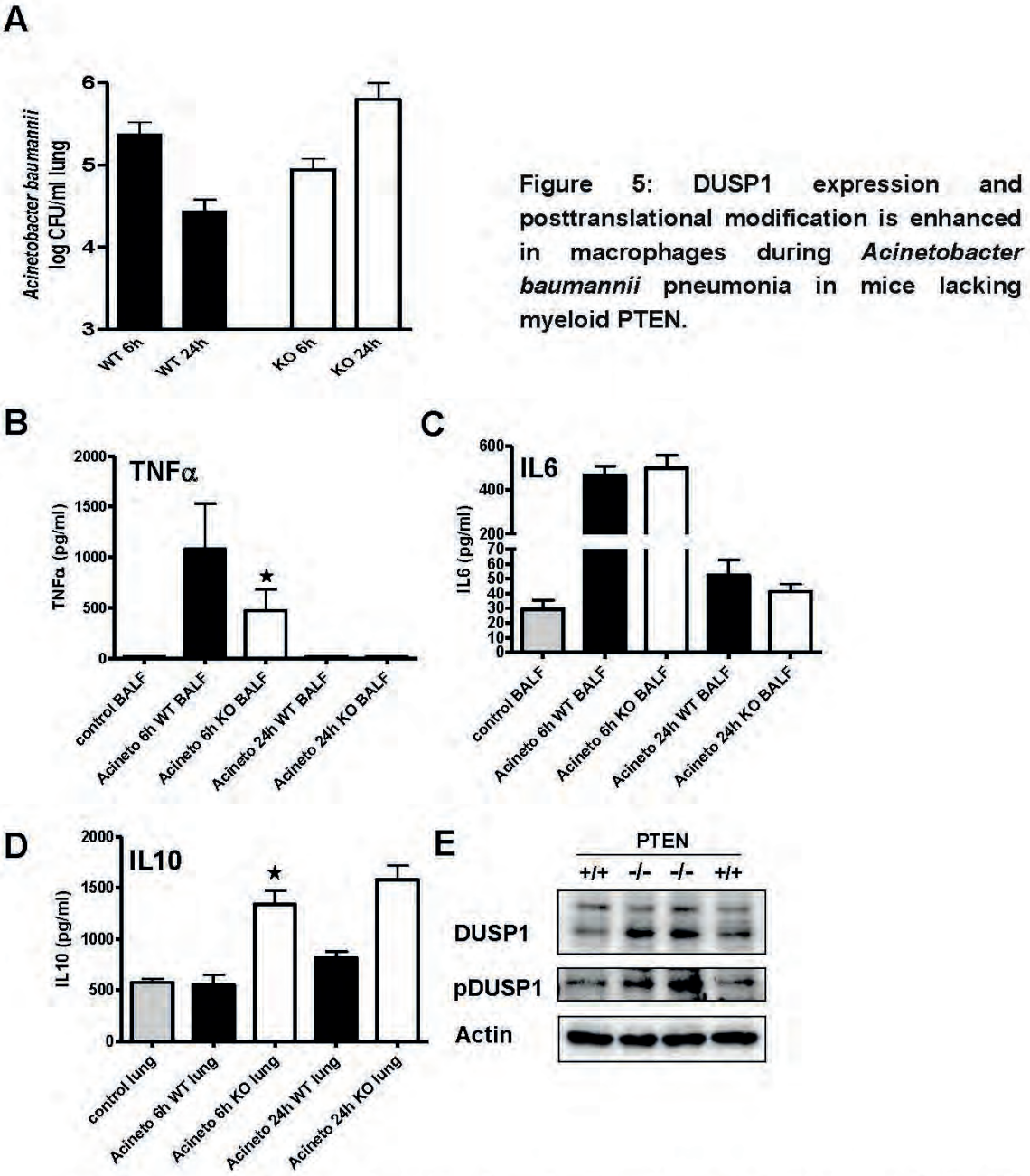

Figure 5: DUSP1 expression and posttranslational modification is enhanced in macrophages during *Acinetobacter baumannii* pneumonia in mice lacking myeloid PTEN.

(A) Quantification of CFUs in the lungs of PTEN$^{MC\text{-}WT}$ and PTEN$^{MC\text{-}KO}$ mice 6h and 24h after induction of *Acinetobacter baumannii* pneumonia (n=5-7 mice per group). (B), (C) Levels of TNF-α and IL-6 in the BAL fluids of PTEN$^{MC\text{-}WT}$ and PTEN$^{MC\text{-}KO}$ mice 6h and 24h after induction of *Acinetobacter baumannii* pneumonia quantified by ELISA (n=5-7 mice per group). (D) Levels of IL-10 in the lungs of PTEN$^{MC\text{-}WT}$ and PTEN$^{MC\text{-}KO}$ mice 6h and 24h after induction of *Acinetobacter baumannii* pneumonia quantified by ELISA (n=5-7 mice per group). (E) Western blot analysis of alveolar macrophages of PTEN$^{MC\text{-}WT}$ and PTEN$^{MC\text{-}KO}$ mice 24h after induction of *Acinetobacter baumannii* pneumonia. Blots were probed with antibodies specific for phospho-DUSP1 and DUSP1 (n=2 mice per group). Actin serves as a loading control. Representative Western blots of n=3 mice per group are shown.Data are presented as mean and standard deviation. Statistical significance is indicated by* ($p<0.05$).

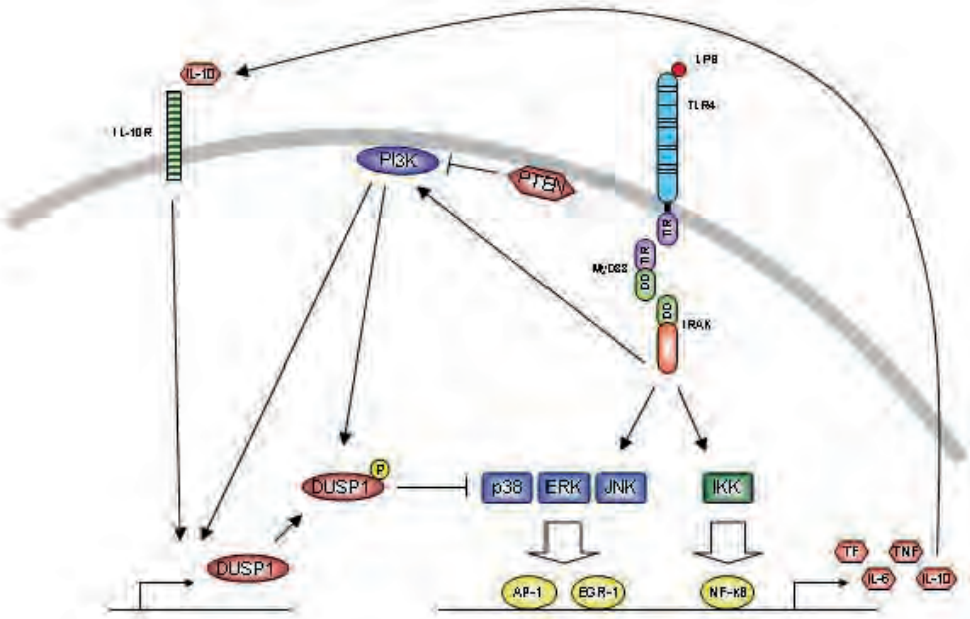

Figure 6: Model for the anti-inflammatory properties of PI3K mediated by DUSP1 and IL10.

Activation of the MAP kinases by bacterial products is limited by the PI3K signaling pathway via differential regulation of the MAPK phosphatase DUSP1. Activation of the PI3K pathway, which is efficiently regulated by the lipid phosphatase PTEN, leads to enhanced IL10 synthesis. IL10 in turn can influence DUSP1 expression, thereby limiting pro-inflammatory gene expression.

Discussion:

Despite the controversial data that have been published concerning the role of PI3K in innate immune regulation, we can show that constitutive activation of the PI3K signaling pathway by cell-type specific deletion of its antagonist PTEN results in reduced pro-inflammatory gene expression in murine macrophages and in an infectious in vivo model of acute lung injury. It is known that the PI3K pathway serves pleiotropic, rather pro-inflammatory functions in the immune response to invading pathogens, such as phagocytosis and chemotaxis. Nevertheless we speculate that PI3K and its counterpart PTEN are actively involved in the modulation of the magnitude of inflammatory responses essentially contributing to resolution of inflammation.

What molecules are responsible for the reduced pro-inflammatory gene expression by hyper-activation of the PI3K signaling pathway in macrophages?

DUSP1 gene regulation

Our findings support the notion that the PI3K pathway downregulates the TLR-induced MAPK activity by way of upregulation of DUSPs, which are specific MAPK phosphatases, whereas the TLR/NFκB pathway is nearly unaffected. Modulated DUSP gene expression at the early phase, 15' to 30' post stimulation, and late phase of activation, 60' to 120' as well as posttranscriptional modification are mediated by sustained PI3K activity in PTEN deficient cells, which we have shown earlier (18). Even baseline DUSP expression is increased in PTEN deficient macrophages. In addition we prove that the PTEN-mediated effects on DUSP1 as well as p38 are dependent on PI3K using cells deficient for the regulatory subunit of PI3K p85α.

Several DUSP family members are implicated in immune regulatory mechanisms. In particular DUSP1 is described as an essential factor in innate immunity modulating the activity MAPKs by dephosphorylation upon TLR stimulation (4,12,31). In this respect DUSP1 shows a substrate preference for p38 (p38>JNK>>ERK) (7). Intriguingly, in our hands all analyzed MAPKs, namely ERK, JNK as well as p38 are affected by PTEN deficiency. This may indicate that more than one DUSP protein is involved in the observed phenotype. Indeed we found DUSP2 differentially transcribed on mRNA level (data not shown). Since DUSP2 is implicated in the regulation of ERK as well as p38 (17), we believe that the differential DUSP2 expression in PTEN deficient macrophages may account for the general inhibition of MAPK activation.

DUSP1 protein modification

Moreover we found substantially increased phosphorylation of DUSP1 at Ser359 in macrophages with increased PI3K activity. It has been shown that phosphorylation of this site together with Ser364 confers stability of the enzyme by reduced proteasomal degradation (2). This indicates that in addition to the observed effects on the transcriptional level, posttranslational events on DUSP1 contribute to the reduced MAPK activity in PTEN deficient cells with markedly increased PI3K activity (Fig. 7).

IL10 regulation by PTEN

Furthermore we could provide evidence that the PI3K/PTEN pathway is involved in the regulation of steady-state levels as well as TLR-induced IL10 levels in macrophages. IL10 has been proven to directly affect the expression and synthesis of several pro-inflammatory markers via STAT3 activation (20,21). We found that non-induced as well as TLR ligand induced PTEN deficient macrophages produce significantly more IL10 than wildtype cells. This may indicate that IL10 autocrine action may contribute to the observed anti-inflammatory phenotype. However, so far we could not find a consistent effect of IL10 blocking antibodies on the PTEN-dependent immune-modulatory functions (data not shown), which may exclude an anti-inflammatory feedback loop by IL10 on the IL10-producing macrophages. Further analysis of PI3K/ PTEN-regulated IL10 release and downstream signal transduction are needed to draw any final conclusions. Nevertheless increased synthesis of IL10 by macrophages will have an impact on macrophages and the surrounding tissue in case of an acute inflammatory event, which is likely to occur in our *in vivo* model of *Acinetobacter*-induced pneumonia. Since IL10 has been shown to

influence DUSP1 (11), we think that IL10 should have some effect on the regulation of the MAP kinases as well (Fig. 7).

Negative effect on bacterial clearance in PTEN deficient mice

In previous studies as well as in the current work we could show *in vitro* that macrophage-specific deletion of PTEN results in reduced *Acinetobacter*- as well as LPS/TLR4-induced pro-inflammatory gene expression (18,25). In line with the observed *in vitro* data, analysis of lysM cre positive floxed PTEN mice and littermate controls infected with *Acinetobacter baumannii* in lungs revealed that TNFα release into the alveolar compartment was significantly reduced by PTEN deficiency. Although the reduced inflammatory response might be beneficial for the host tissue reducing cellular damage, the bacterial burden was markedly increased. Under normal circumstances wildtype mice mount an immediate immune response and hence can successfully eradicate the *Acinetobacter* infection within 24 hours (14,23). In contrast PTEN deficient mice show enhanced bacterial counts. Moreover PTEN is described to play an indispensable role in the recruitment of neutrophils to the site of infection (13). We can show in another model of acute lung injury that PTEN deficiency leads to reduced neutrophil alveolar influx (manuscript submitted). Our findings indicate that immune suppression and possible diminished neutrophil recruitment led to dysfunctional bacterial killing.

We conclude from our data that PI3K and its antagonist PTEN are part of important regulatory signaling complexes in the resolution of inflammatory responses and essentially contribute to orchestrate the innate immune defense to bacterial pathogens.

Abbreviations:

DUSP... dual specificity phosphatase

IRAK-M...interleukin 1 receptor-associated kinase M

MAPK...mitogen activated protein kinase

PI3-K...phosphatidylinositol-3 Kinase

PTEN... phosphatase and tensin homologue deleted on chromosome 10

SOCS...suppressors of cytokine signalling

TLR...toll like receptor

Acknowledgement:

This work was made possible by grant P19850-B12 from the Austrian Science Fund (FWF) (to G.S.).

We thank Thomas Nardelli for help with preparation of figures.

References:

1. Boone, D. L., E. E. Turer, E. G. Lee, R. C. Ahmad, M. T. Wheeler, C. Tsui, P. Hurley, M. Chien, S. Chai, O. Hitotsumatsu, E. McNally, C. Pickart, and A. Ma. 2004. The ubiquitin-modifying enzyme A20 is required for termination of Toll-like receptor responses. Nat. Immunol. 5:1052-1060.

2. Brondello, J. M., J. Pouyssegur, and F. R. McKenzie. 1999. Reduced MAP kinase phosphatase-1 degradation after p42/p44MAPK-dependent phosphorylation. Science 286:2514-2517.

3. Cantley, L. C. 2002. The phosphoinositide 3-kinase pathway. Science 296:1655-1657.

4. Chi, H., S. P. Barry, R. J. Roth, J. J. Wu, E. A. Jones, A. M. Bennett, and R. A. Flavell. 2006. Dynamic regulation of pro- and anti-inflammatory cytokines by MAPK phosphatase 1 (MKP-1) in innate immune responses. Proc. Natl. Acad.

Sci. U. S. A 103:2274-2279.

5. Clausen, B. E., C. Burkhardt, W. Reith, R. Renkawitz, and I. Forster. 1999. Conditional gene targeting in macrophages and granulocytes using LysMcre mice. Transgenic Res. 8:265-277.

6. Dalpke, A., K. Heeg, H. Bartz, and A. Baetz. 2008. Regulation of innate immunity by suppressor of cytokine signaling (SOCS) proteins. Immunobiology 213:225-235.

7. Franklin, C. C. and A. S. Kraft. 1997. Conditional expression of the mitogen-activated protein kinase (MAPK) phosphatase MKP-1 preferentially inhibits p38 MAPK and stress-activated protein kinase in U937 cells. J. Biol. Chem. 272:16917-16923.

8. Guha, M. and N. Mackman. 2001. LPS induction of gene expression in human monocytes. Cell Signal. 13:85-94.

9. Guha, M., M. A. O'Connell, R. Pawlinski, A. Hollis, P. McGovern, S. F. Yan, D. Stern, and N. Mackman. 2001. Lipopolysaccharide activation of the MEK-ERK1/2 pathway in human monocytic cells mediates tissue factor and tumor necrosis factor alpha expression by inducing Elk-1 phosphorylation and Egr-1 expression. Blood 98:1429-1439.

10. Gunzl, P. and G. Schabbauer. 2008. Recent advances in the genetic analysis of PTEN and PI3K innate immune properties. Immunobiology 213:759-765.

11. Hammer, M., J. Mages, H. Dietrich, F. Schmitz, F. Striebel, P. J. Murray, H. Wagner, and R. Lang. 2005. Control of dual-specificity phosphatase-1 expression in activated macrophages by IL-10. Eur. J. Immunol. 35:2991-3001.

12. Hammer, M., J. Mages, H. Dietrich, A. Servatius, N. Howells, A. C. Cato, and R. Lang. 2006. Dual specificity phosphatase 1 (DUSP1) regulates a subset of LPS-induced genes and protects mice from lethal endotoxin shock. J. Exp. Med. 203:15-20.

13. Heit, B., S. M. Robbins, C. M. Downey, Z. Guan, P. Colarusso, B. J. Miller, F. R. Jirik, and P. Kubes. 2008. PTEN functions to 'prioritize' chemotactic cues and prevent 'distraction' in migrating neutrophils. Nat. Immunol. 9:743-752.

14. Knapp, S., C. W. Wieland, S. Florquin, R. Pantophlet, L. Dijkshoorn, N. Tshimbalanga, S. Akira, and P. T. van der. 2006. Differential roles of CD14 and toll-like receptors 4 and 2 in murine Acinetobacter pneumonia. Am. J. Respir. Crit Care Med. 173:122-129.

15. Knapp, S., C. W. Wieland, '. van, V, O. Takeuchi, S. Akira, S. Florquin, and P. T. van der. 2004. Toll-like receptor 2 plays a role in the early inflammatory response to murine pneumococcal pneumonia but does not contribute to antibacterial defense. J. Immunol. 172:3132-3138.

16. Kobayashi, K., L. D. Hernandez, J. E. Galan, C. A. Janeway, Jr., R. Medzhitov, and R. A. Flavell. 2002. IRAK-M is a negative regulator of Toll-like receptor signaling. Cell 110:191-202.

17. Lang, R., M. Hammer, and J. Mages. 2006. DUSP meet immunology: dual

specificity MAPK phosphatases in control of the inflammatory response. J. Immunol. 177:7497-7504.

18. Luyendyk, J. P., G. A. Schabbauer, M. Tencati, T. Holscher, R. Pawlinski, and N. Mackman. 2008. Genetic analysis of the role of the PI3K-Akt pathway in lipopolysaccharide-induced cytokine and tissue factor gene expression in monocytes/macrophages. J. Immunol. 180:4218-4226.

19. Matthay, M. A. and G. A. Zimmerman. 2005. Acute lung injury and the acute respiratory distress syndrome: four decades of inquiry into pathogenesis and rational management. Am. J. Respir. Cell Mol. Biol. 33:319-327.

20. Moore, K. W., M. R. de Waal, R. L. Coffman, and A. O'Garra. 2001. Interleukin-10 and the interleukin-10 receptor. Annu. Rev. Immunol. 19:683-765.

21. O'Shea, J. J. and P. J. Murray. 2008. Cytokine signaling modules in inflammatory responses. Immunity. 28:477-487.

22. Peyssonnaux, C., V. Datta, T. Cramer, A. Doedens, E. A. Theodorakis, R. L. Gallo, N. Hurtado-Ziola, V. Nizet, and R. S. Johnson. 2005. HIF-1alpha expression regulates the bactericidal capacity of phagocytes. J. Clin. Invest 115:1806-1815.

23. Renckens, R., J. J. Roelofs, S. Knapp, A. F. de Vos, S. Florquin, and P. T. van der. 2006. The acute-phase response and serum amyloid A inhibit the inflammatory response to Acinetobacter baumannii Pneumonia. J. Infect. Dis. 193:187-195.

24. Salojin, K. V., I. B. Owusu, K. A. Millerchip, M. Potter, K. A. Platt, and T. Oravecz. 2006. Essential role of MAPK phosphatase-1 in the negative control of innate immune responses. J. Immunol. 176:1899-1907.

25. Schabbauer, G., J. Luyendyk, K. Crozat, Z. Jiang, N. Mackman, S. Bahram, and P. Georgel. 2008. TLR4/CD14-mediated PI3K activation is an essential component of interferon-dependent VSV resistance in macrophages. Mol. Immunol. 45:2790-2796.

26. Schabbauer, G., M. Tencati, B. Pedersen, R. Pawlinski, and N. Mackman. 2004. PI3K-Akt pathway suppresses coagulation and inflammation in endotoxemic mice. Arterioscler. Thromb. Vasc. Biol. 24:1963-1969.

27. Suzuki, A., M. T. Yamaguchi, T. Ohteki, T. Sasaki, T. Kaisho, Y. Kimura, R. Yoshida, A. Wakeham, T. Higuchi, M. Fukumoto, T. Tsubata, P. S. Ohashi, S. Koyasu, J. M. Penninger, T. Nakano, and T. W. Mak. 2001. T cell-specific loss of Pten leads to defects in central and peripheral tolerance. Immunity. 14:523-534.

28. Weichhart, T. and M. D. Saemann. 2008. The PI3K/Akt/mTOR pathway in innate immune cells: emerging therapeutic applications. Ann. Rheum. Dis. 67 Suppl 3:iii70-iii74.

29. Williams, D. L., C. Li, T. Ha, T. Ozment-Skelton, J. H. Kalbfleisch, J. Preiszner, L. Brooks, K. Breuel, and J. B. Schweitzer. 2004. Modulation of the phosphoinositide 3-kinase pathway alters innate resistance to polymicrobial sepsis. J. Immunol. 172:449-456.

30. Yao, J., N. Mackman, T. S. Edgington, and S. T. Fan. 1997. Lipopolysaccharide induction of the tumor necrosis factor-alpha promoter in human monocytic cells.

Regulation by Egr-1, c-Jun, and NF-kappaB transcription factors. J. Biol. Chem. 272:17795-17801.

31. Zhao, Q., X. Wang, L. D. Nelin, Y. Yao, R. Matta, M. E. Manson, R. S. Baliga, X. Meng, C. V. Smith, J. A. Bauer, C. H. Chang, and Y. Liu. 2006. MAP kinase phosphatase 1 controls innate immune responses and suppresses endotoxic shock. J. Exp. Med. 203:131-140.

5. Summary

This thesis comprises the work on three different endogenous modulators of inflammation and their implication in infectious diseases. In the first part we studied the role of oxidized phospholipids during *E. coli* peritonitis. Phospholipids get oxidized during inflammation, in this form they actively participate in the inflammatory process. Many experimental and clinical data on atherosclerosis exist, but studies on infectious diseases are very limited. LPS administration in the peritoneum together with OxPAPC resulted in improved survival due to impaired LPS recognition via the TLR4 complex [76]. This led us to investigate the role of OxPAPC during *E. coli* peritonitis using viable bacteria: in contrast to above described findings during endotoxemia, OxPAPC administration resulted in impaired survival during *E. coli* peritonitis *in vivo* (4.1.1). While cytokine production, neutrophil recruitment and bacterial killing remained unaffected, administration of OxPAPC at the onset of *E. coli* peritonitis inhibited phagocytosis of bacteria. In follow up studies we demonstrated the endogenous generation of oxidized phospholipids during *E. coli* peritonitis *in vivo*, and uncovered the mechanism by which they inhibit phagocytosis (4.1.2): OxPAPC diminished uptake of *E. coli* via an undirected "global" actin spread in macrophages. This event required specific, localized PKA activation at the AKAP WAVE-1, as deletion of WAVE-1 and pharmacological inhibition of PKA-AKAP interaction completely reversed OxPAPC's anti-phagocytic effects *in vitro* and *in vivo*. Thus, we have found how endogenously generated oxidized phospholipids negatively impact the outcome during *E. coli* peritonitis *in vivo*, and were the first to delineate the function of WAVE-1 in macrophages. These findings might represent an attractive option for therapeutic intervention in *E. coli* peritonitis, and opens the door for more studies on OxPAPC and WAVE-1 in other disease models.

The second part of the thesis studied the immunmodulatory properties of the fibrin derived peptide $B\beta_{15-42}$. This peptide has previously been shown to exert beneficial effects in a model of myocardial reperfusion injury by inhibiting vascular leak and leukocyte migration. These promising results prompted new studies in various disease models in which vascular leak plays an important pathophysiological role. We could demonstrate barrier protective effects of $B\beta_{15-42}$ *in vitro* and in three different disease models *in vivo* (Dengue shock syndrome, LPS shock-model, ALI). In endothelial cells thrombin-triggered stress fiber formation is mediated by the Src-kinase Fyn. Treatment with $B\beta_{15-42}$ led to dissociation of Fyn from VE-cadherin and association with p190RhoGAP, a known antagonist of RhoA activation. Thus, thrombin triggered stress fiber formation via RhoA was reduced. We could confirm these findings in Fyn knockout mice in ALI caused by LPS inhalation (4.2.2.).

ALI is a feared syndrome in intensive care units, which can either result from direct (i.e. pneumonia, acid aspiration), or indirect lung injury (i.e. trauma or shock). Acid aspiration mimics the main pathophysiological features of ALI, like edema formation and neutrophil influx. We could demonstrate that the fibrin-derived peptide $B\beta_{15-42}$ potently inhibited edema formation and neutrophil influx in two different models of ALI: acid aspiration and LPS inhalation (4.2.1 and 4.2.2). This attenuation of the inflammatory response moreover protected mice from a second hit with *Pseudomonas aeruginosa* (4.2.1). While acid aspiration resulted in tremendously enhanced inflammation and bacterial outgrowth upon a second hit with bacteria, treatment with $B\beta_{15-42}$, if given within two hours after the insult, led to reduced inflammation, and diminished bacterial load. *Ex vivo* studies with macrophages disclosed a potential mechanism for impaired bacterial clearance despite increased cytokine secretion after acid aspiration: phagocytosis in mice that underwent acid aspiration alone was severely impaired, whereas bacterial clearance in sham-treated and $B\beta_{15-}$

$_{42}$ treated animals remained intact. Concomitantly levels of IRAK-M, which is an important negative regulator of inflammation, were highly increased at the time of infection in mice that aspired acid, but back to base-line in animals treated with $B\beta_{15-42}$. Thus, $B\beta_{15-42}$ abates the initial insult, which restored antibacterial properties of alveolar macrophages, and ultimately improved survival during secondary *Pseudomonas aeruginosa* pneumonia. $B\beta_{15-42}$ might therefore represent a therapy during acute lung injury.

The third part of the thesis focused on the role of PTEN during clinically relevant pneumonia. While the precise role of PI3K during inflammation and infection is debated, the importance of this kinase in phagocytosis, leukocyte transmigration and bacterial killing is widely accepted. Data on the PI3K antagonist PTEN during infectious diseases is very limited. Considering that drugs targeting the PI3K pathway are in clinical testing, information on the role of PI3K and its antagonist PTEN during clinically relevant infections is of utmost importance. To gain more knowledge on PTEN's role during bacterial pneumonia, we made use of a conditional PTEN knockout mouse, in which PTEN is deleted in myeloid cells. While pro-inflammatory cytokines were consistently reduced in PTEN deficient mice *in vivo* and macrophages *in vitro* upon *S. pneumoniae* and *Acinetobacter baumannii* challenge (4.3.1 and 4.3.2), phagocytosis and iNOS production was increased (4.3.1). In sharp contrast to previous reports using *in vitro* migration assays, neutrophil influx in myeloid PTEN deficient mice was significantly reduced during *S. pneumoniae* pneumonia. Altogether myeloid PTEN deficiency resulted in reduced lung injury, and improved survival of myeloid PTEN deficient mice during *S. pneumoniae* pneumonia.

Acinetobacter baumannii and LPS stimulation in myeloid PTEN deficient cells bearing increased PI3K activity, identically to what we observed with *S. pneumonia*, led to reduced secretion of pro-inflammatory cytokines, but increased production of IL-10 (4.3.2). IL-10 activates the phosphatase DUSP-1 which inactivates MAPkinases. Thus, reduction of MAPkinase phosphorylation was most likely caused by levels of IL-10. These results suggest a new mechanism for the anti-inflammatory role of PI3K, und provide further insight into PTEN's role during bacterial pneumonia.

6. DISCUSSION AND CONCLUSION

Increasing resistance to antibiotics, the lack of efficient virostatic agents and the clinical enigma of sepsis urge for novel strategies to combat infectious diseases. The host's immune response is clearly needed to fend off pathogens, but a sustained and strong inflammation can be harmful at the same time. Therefore, therapeutic interference with the immune response during infections is undoubtedly a double-edged sword. In this respect, infections differ from other inflammations like autoimmune diseases, in which anti-inflammatory intervention is helpful to suppress unwanted inflammation. In order to intervene during an infectious process, a better understanding of the complex interactions between a specific pathogen and the immune system in clinically relevant disease model is required. The apparent differences between cell types, organs and pathogens tested urge the need for more well designed studies with careful interpretations drawn. This will give rise to an even more complex picture, but will allow drawing better conclusions about the *in vivo* relevance in a specific context.

Examples: the use of PAMPs like lipoteichoic acid (LTA) or LPS might be helpful for basic observations, but needs to be extended to living bacteria in a clinically relevant model. LTA, or any other PAMP is no living organism, therefore it does not multiply, but is cleared after a certain amount of time. The whole bacterium has many other PAMPs, and interacts with the immune system in a highly complex manner. Moreover LTA from i.e. *Staphyloccus aureus* is different to that of any other gram-positive bacterium. Thus, administration of single PAMPs only represents a sterile inflammation, and does not represent an infectious process. Therefore, referring to "gram-negative" bacteria by using LPS or "gram-positive" bacteria by using LTA is not admissible. Another important point is the site of infection: the same bacteria administered intraperito-

neally might cause a completely different pathophysiology than administered intravenously. For example referring to "*S. pyogenes* infection" if administered intranasally, although *S. pyogenes* usually does not cause pneumonia, has to be interpreted very cautiously. Why certain bacteria only affect certain organs is for most of the cases not understood at all, but at least has to be taken into account in experimental design. This might sound obvious, but overstatement and oversimplification of results very often tell another story, and should be interpreted differently. Animal models can only constitute an approximation to reality. They have to be standardized and reproducible, and the closer they mimic the actual disease the better they are.

Endogenous modulators of inflammation might constitute an attractive target for therapeutic intervention. Endogenous modulators often constitute a negative or positive feedback during sterile inflammations or infectious processes. Interference with a too strong activation or suppression might yield promising results. Again the molecular mechanisms in a precise context have to be known. For example, oxidized phospholipids: they are a by-product of oxygen radicals aimed to kill pathogens, and they show potent anti-inflammatory activity. This might constitute a negative feedback with the purpose of down regulating the inflammatory process after excessive production of oxygen radicals. We uncovered the potential of oxidized phospholipids to inhibit phagocytosis and delineated WAVE-1 as the key protein in this process. By blocking WAVE-1 in *E. coli* peritonitis proper phagocytosis might be restored without impairing other innate immune functions. Future work will have to delineate single compounds of oxidized phospholipid mixtures, as they certainly exert different effects on different cell types.

A naturally occurring plasmin digest product of fibrin, $B\beta_{15-42}$, might prove beneficial by its virtue to preserve endothelial barriers. $B\beta_{15-42}$ short half-live, and

the peptide's anergy towards leukocytes are interesting features in an infectious process. We could show a clear therapeutic benefit by administering $B\beta_{15-42}$ in a mouse model of acid aspiration, resulting in improved outcome during secondary *Pseudomonas aeruginosa* pneumonia. These promising results will hopefully find its way to clinical trials, where the precise role of pre-existing ALI and the therapeutic benefit of substances such as $B\beta_{15-42}$ might be worth investigating.

The capacity of PTEN to drive inflammation and suppress clearance of bacteria might render PTEN´s suppression beneficial in a defined context. More studies on the PI3K/PTEN pathway will probably reveal even higher complexity in terms of organs and pathogens tested. It will be also interesting to see some of the drugs targeting this pathway in clinical use. Will there be any side-effects like higher incidence of infections? And if so, will it concern specific infections? In this case, basic research findings like ours will have to be considered if a patient who is taking such a drug suffers from bacterial pneumonia.

The last century brought tremendous advances in medical science and clinical practice. Today, the amount of new data generated in basic medical research every year is shear breathtaking. But as the knowledge gets more and more detailed and complex, its translation into clinics will be more and more difficult. So what could be important things to focus on? In infectious diseases, therapeutic interference with positive and negative effects of resolution of inflammation might be an attractive option. Patients usually seek medical advice at later stages of infections, and diagnosis takes some time, also for patients who already are in the hospital in the case of nosocomial infections. In this context endogenous modulators as delineated above could be an attractive target.

However, new therapeutic interventions also require improved diagnostic tools in order to know the appropriate time point for intervention. We are only at the very beginning to fully understand the host's response to a specific infection, and therapies targeting the immune system might be found tomorrow or lie decades ahead.

7. ACKNOWLEGEMENT

In PhD studies a good supervisor is as vital as good collaboration is in research. I was lucky enough to have both. I am most grateful and indebted to my supervisor Sylvia Knapp. Not only did you provide me with a unique opportunity to work in a highly exciting field, but also you introduced me to a team of competent and lovely people. It was a privilege to work with them. I could barely tell left from right when I started, but supervise is what you did! You were always interested, always hungry for new input, always demanding. No matter how big or small a presentation, congress or paper, your focus was on producing the best possible quality of work. I consistently felt that we were moving forward and really enjoyed our discussions. More often than not, a problem seemed half a problem, because I could rely on your understanding and support. I once heard that a good boss helps you exceed your own expectations. Dear Sylvia, this is what you did. Thank you ever so much.

I am also indebted to our postdoc Omar Sharif. Without you, this thesis would not have been possible in the same way. You taught me basic molecular biology techniques; you were always ready to help, showed interest in my work and ready to give input. Our discussions during coffee breaks or over a beer (or two) were real high points amid some stressful times. You are most enjoyable company and became a really good friend. Thank you.

Our excellent technicians in the lab were of uttermost importance for this thesis. First of all I owe gratitude to Tanja Furtner, who was key for my PhD, especially with reagards to phagocytosis and supported me a hard period. I want to thank Karin Stich and Bianca Doninger, the other excellent technicians I was lucky enough to work with. Not only could I rely on your help whenever I went to Lab 1 or 3, but also on a welcoming smile. Essential for all my in vivo

work was Isabella Haslinger, our speed and mouse technician, big thanks to you too! The daily grind was so much easier to deal with sharing a desk with Ana Zivkovic. Your spirit is a pleasure and I miss our disscussions! Immanuel Elbau, thank you for your help with animal assays, I really enjoyed your company and your positive attitude is a delight! Thanks to Joana Warzawska for support in the acid aspiration project and all the other people working at 3P for help in many different ways. Gernot Schabbauer for teaching me all the mouse techniques and many other things I learned from you. It was a pleasure to work with you.

A big thanks to the Peter Petzelbauer team for the excellent collaboration and fruitful discussions; for all the confocal microscope support to Marion Gröger; to Ildiko Mesteri for all the histopathological scoring (and patience); to Olga Oskolkova for constant supply of excellent lipid preparations; to Wolfgang Dietl and Michael Bauer for helping with the acid aspiration; to all the hands at the Biomedizinische Versuchsanstalt, in particular Rita Böhs for her patience with us; to Harald Höger for excellent support with our WAVE-1 knockout mice!

It was great to get to know everyone at CeMM. The collaboration was excellent and went way beyond sharing knowledge at the Friday seminars. The retreats were great, so were the parties and congresses. Adriana Goncalves, Lisboa rocked! The enthusiasm Guilio Superti-Furga infused the institute with was remarkable and I felt privileged to be a part of it right from the start.

Work aside I want to acknowledge my family, Mutti first of all for being so strong and wonderful and always there for me; my brothers Flori and Wolfi, whom I am so proud of; so many friends who were always supportive, especially Josef, the best friend anyone can wish for. My final thanks go to Julia, not only for helping me with this thesis, but also for being my dear and beloved companion through the good times and the bad.

8. REFERENCES

1. Medzhitov, R., Preston-Hurlburt, P. & Janeway, C.A., Jr. A human homologue of the Drosophila Toll protein signals activation of adaptive immunity. *Nature* **388**, 394-397 (1997).
2. Iwasaki, A. & Medzhitov, R. Toll-like receptor control of the adaptive immune responses. *Nature immunology* **5**, 987-995 (2004).
3. O'Neill, L.A. How Toll-like receptors signal: what we know and what we don't know. *Current opinion in immunology* **18**, 3-9 (2006).
4. Kumar, H., Kawai, T. & Akira, S. Toll-like receptors and innate immunity. *Biochemical and biophysical research communications* **388**, 621-625 (2009).
5. Werts, C., Girardin, S.E. & Philpott, D.J. TIR, CARD and PYRIN: three domains for an antimicrobial triad. *Cell death and differentiation* **13**, 798-815 (2006).
6. Medzhitov, R. & Janeway, C., Jr. Innate immunity. *The New England journal of medicine* **343**, 338-344 (2000).
7. Dale, D.C., Boxer, L. & Liles, W.C. The phagocytes: neutrophils and monocytes. *Blood* **112**, 935-945 (2008).
8. de Groot, C.J., Huppes, W., Sminia, T., Kraal, G. & Dijkstra, C.D. Determination of the origin and nature of brain macrophages and microglial cells in mouse central nervous system, using non-radioactive in situ hybridization and immunoperoxidase techniques. *Glia* **6**, 301-309 (1992).
9. Landsman, L. & Jung, S. Lung macrophages serve as obligatory intermediate between blood monocytes and alveolar macrophages. *J Immunol* **179**, 3488-3494 (2007).
10. Gordon, S. & Taylor, P.R. Monocyte and macrophage heterogeneity. *Nat Rev Immunol* **5**, 953-964 (2005).
11. Smythies, L.E., *et al.* Human intestinal macrophages display profound inflammatory anergy despite avid phagocytic and bacteriocidal activity. *The Journal of clinical investigation* **115**, 66-75 (2005).
12. Loke, P., *et al.* Alternative activation is an innate response to injury that requires CD4+ T cells to be sustained during chronic infection. *J Immunol* **179**, 3926-3936 (2007).
13. Mosser, D.M. & Edwards, J.P. Exploring the full spectrum of macrophage activation. *Nat Rev Immunol* **8**, 958-969 (2008).
14. Martinez, F.O., Helming, L. & Gordon, S. Alternative activation of macrophages: an immunologic functional perspective. *Annual review of immunology* **27**, 451-483 (2009).
15. Gordon, S. The macrophage: past, present and future. *European journal of immunology* **37 Suppl 1**, S9-17 (2007).
16. Harth, G. & Horwitz, M.A. An inhibitor of exported Mycobacterium tuberculosis glutamine synthetase selectively blocks the growth of pathogenic mycobacteria in axenic culture and in human monocytes: extracellular proteins as potential novel drug targets. *The Journal of experimental medicine* **189**, 1425-1436 (1999).
17. Lawrence, T., Willoughby, D.A. & Gilroy, D.W. Anti-inflammatory lipid mediators and insights into the resolution of inflammation. *Nat Rev Immunol* **2**, 787-795 (2002).
18. Serhan, C.N., *et al.* Resolution of inflammation: state of the art, definitions and

terms. *Faseb J* **21**, 325-332 (2007).
19. Kubicka, U., *et al.* Normal human immune peritoneal cells: subpopulations and functional characteristics. *Scandinavian journal of immunology* **44**, 157-163 (1996).
20. Broche, F. & Tellado, J.M. Defense mechanisms of the peritoneal cavity. *Current opinion in critical care* **7**, 105-116 (2001).
21. Brook, I. Microbiology and management of abdominal infections. *Digestive diseases and sciences* **53**, 2585-2591 (2008).
22. Evans, H.L., *et al.* Diagnosis of intra-abdominal infection in the critically ill patient. *Current opinion in critical care* **7**, 117-121 (2001).
23. Wickel, D.J., Cheadle, W.G., Mercer-Jones, M.A. & Garrison, R.N. Poor outcome from peritonitis is caused by disease acuity and organ failure, not recurrent peritoneal infection. *Annals of surgery* **225**, 744-753; discussion 753-746 (1997).
24. Wheeler, A.P. & Bernard, G.R. Treating patients with severe sepsis. *The New England journal of medicine* **340**, 207-214 (1999).
25. Marshall, J.C. & Innes, M. Intensive care unit management of intra-abdominal infection. *Critical care medicine* **31**, 2228-2237 (2003).
26. Rubenfeld, G.D., *et al.* Incidence and outcomes of acute lung injury. *The New England journal of medicine* **353**, 1685-1693 (2005).
27. Bernard, G.R., *et al.* The American-European Consensus Conference on ARDS. Definitions, mechanisms, relevant outcomes, and clinical trial coordination. *American journal of respiratory and critical care medicine* **149**, 818-824 (1994).
28. Ware, L.B. & Matthay, M.A. The acute respiratory distress syndrome. *The New England journal of medicine* **342**, 1334-1349 (2000).
29. Holter, J.F., Weiland, J.E., Pacht, E.R., Gadek, J.E. & Davis, W.B. Protein permeability in the adult respiratory distress syndrome. Loss of size selectivity of the alveolar epithelium. *The Journal of clinical investigation* **78**, 1513-1522 (1986).
30. Strieter, R.M., Kunkel, S.L., Keane, M.P. & Standiford, T.J. Chemokines in lung injury: Thomas A. Neff Lecture. *Chest* **116**, 103S-110S (1999).
31. Matthay, M.A. & Zimmerman, G.A. Acute lung injury and the acute respiratory distress syndrome: four decades of inquiry into pathogenesis and rational management. *American journal of respiratory cell and molecular biology* **33**, 319-327 (2005).
32. McIntyre, R.C., Jr., Pulido, E.J., Bensard, D.D., Shames, B.D. & Abraham, E. Thirty years of clinical trials in acute respiratory distress syndrome. *Critical care medicine* **28**, 3314-3331 (2000).
33. Tsushima, K., *et al.* Acute lung injury review. *Internal medicine (Tokyo, Japan)* **48**, 621-630 (2009).
34. Matute-Bello, G., Frevert, C.W. & Martin, T.R. Animal models of acute lung injury. *Am J Physiol Lung Cell Mol Physiol* **295**, L379-399 (2008).
35. Petzelbauer, P., *et al.* The fibrin-derived peptide Bbeta15-42 protects the myocardium against ischemia-reperfusion injury. *Nature medicine* **11**, 298-304 (2005).
36. Atar, D., *et al.* Effect of intravenous FX06 as an adjunct to primary percutaneous coronary intervention for acute ST-segment elevation myocardial infarction results of the F.I.R.E. (Efficacy of FX06 in the Prevention of Myocardial Reperfusion Injury) trial. *Journal of the American College of Cardiology* **53**, 720-729 (2009).
37. Mizgerd, J.P. Lung infection--a public health priority. *PLoS medicine* **3**, e76

(2006).
38. Gold, H.S. & Moellering, R.C., Jr. Antimicrobial-drug resistance. *The New England journal of medicine* **335**, 1445-1453 (1996).
39. Flaherty, J.P. & Weinstein, R.A. Nosocomial infection caused by antibiotic-resistant organisms in the intensive-care unit. *Infect Control Hosp Epidemiol* **17**, 236-248 (1996).
40. Bartlett, J.G. & Mundy, L.M. Community-acquired pneumonia. *The New England journal of medicine* **333**, 1618-1624 (1995).
41. Lynch, J.P., 3rd. Hospital-acquired pneumonia: risk factors, microbiology, and treatment. *Chest* **119**, 373S-384S (2001).
42. Ikeda, M., Kihara, A. & Igarashi, Y. Lipid asymmetry of the eukaryotic plasma membrane: functions and related enzymes. *Biological & pharmaceutical bulletin* **29**, 1542-1546 (2006).
43. Hampton, M.B., Kettle, A.J. & Winterbourn, C.C. Inside the neutrophil phagosome: oxidants, myeloperoxidase, and bacterial killing. *Blood* **92**, 3007-3017 (1998).
44. Babior, B.M. Phagocytes and oxidative stress. *The American journal of medicine* **109**, 33-44 (2000).
45. Bochkov, V.N. Inflammatory profile of oxidized phospholipids. *Thromb Haemost* **97**, 348-354 (2007).
46. Watson, A.D., *et al.* Structural identification by mass spectrometry of oxidized phospholipids in minimally oxidized low density lipoprotein that induce monocyte/endothelial interactions and evidence for their presence in vivo. *The Journal of biological chemistry* **272**, 13597-13607 (1997).
47. Subbanagounder, G., *et al.* Determinants of bioactivity of oxidized phospholipids. Specific oxidized fatty acyl groups at the sn-2 position. *Arteriosclerosis, thrombosis, and vascular biology* **20**, 2248-2254 (2000).
48. Podrez, E.A., *et al.* A novel family of atherogenic oxidized phospholipids promotes macrophage foam cell formation via the scavenger receptor CD36 and is enriched in atherosclerotic lesions. *The Journal of biological chemistry* **277**, 38517-38523 (2002).
49. Chou, M.Y., *et al.* Oxidation-specific epitopes are dominant targets of innate natural antibodies in mice and humans. *The Journal of clinical investigation* **119**, 1335-1349 (2009).
50. Tsimikas, S., *et al.* Oxidized phospholipids, Lp(a) lipoprotein, and coronary artery disease. *The New England journal of medicine* **353**, 46-57 (2005).
51. Yoshimi, N., *et al.* Oxidized phosphatidylcholine in alveolar macrophages in idiopathic interstitial pneumonias. *Lung* **183**, 109-121 (2005).
52. Nakamura, T., Henson, P.M. & Murphy, R.C. Occurrence of oxidized metabolites of arachidonic acid esterified to phospholipids in murine lung tissue. *Analytical biochemistry* **262**, 23-32 (1998).
53. Imai, Y., *et al.* Identification of oxidative stress and Toll-like receptor 4 signaling as a key pathway of acute lung injury. *Cell* **133**, 235-249 (2008).
54. Horie, K., *et al.* Immunohistochemical colocalization of glycoxidation products and lipid peroxidation products in diabetic renal glomerular lesions. Implication for glycoxidative stress in the pathogenesis of diabetic nephropathy. *The Journal of clinical investigation* **100**, 2995-3004 (1997).
55. Houglum, K., *et al.* Excess iron induces hepatic oxidative stress and transforming growth factor beta1 in genetic hemochromatosis. *Hepatology (Baltimore, Md* **26**, 605-610 (1997).
56. Huber, J., *et al.* Oxidized membrane vesicles and blebs from apoptotic cells

contain biologically active oxidized phospholipids that induce monocyte-endothelial interactions. *Arteriosclerosis, thrombosis, and vascular biology* **22**, 101-107 (2002).
57. Chang, M.K., *et al.* Apoptotic cells with oxidation-specific epitopes are immunogenic and proinflammatory. *The Journal of experimental medicine* **200**, 1359-1370 (2004).
58. Subbanagounder, G., *et al.* Epoxyisoprostane and epoxycyclopentenone phospholipids regulate monocyte chemotactic protein-1 and interleukin-8 synthesis. Formation of these oxidized phospholipids in response to interleukin-1beta. *The Journal of biological chemistry* **277**, 7271-7281 (2002).
59. Newcombe, J., Li, H. & Cuzner, M.L. Low density lipoprotein uptake by macrophages in multiple sclerosis plaques: implications for pathogenesis. *Neuropathology and applied neurobiology* **20**, 152-162 (1994).
60. Dei, R., *et al.* Lipid peroxidation and advanced glycation end products in the brain in normal aging and in Alzheimer's disease. *Acta neuropathologica* **104**, 113-122 (2002).
61. Li, A.C. & Glass, C.K. The macrophage foam cell as a target for therapeutic intervention. *Nature medicine* **8**, 1235-1242 (2002).
62. Binder, C.J., *et al.* Innate and acquired immunity in atherogenesis. *Nature medicine* **8**, 1218-1226 (2002).
63. Hansson, G.K. & Libby, P. The immune response in atherosclerosis: a double-edged sword. *Nat Rev Immunol* **6**, 508-519 (2006).
64. Paoletti, R., Gotto, A.M., Jr. & Hajjar, D.P. Inflammation in atherosclerosis and implications for therapy. *Circulation* **109**, III20-26 (2004).
65. Leitinger, N. Oxidized phospholipids as modulators of inflammation in atherosclerosis. *Current opinion in lipidology* **14**, 421-430 (2003).
66. Kiechl, S., *et al.* Oxidized phospholipids, lipoprotein(a), lipoprotein-associated phospholipase A2 activity, and 10-year cardiovascular outcomes: prospective results from the Bruneck study. *Arteriosclerosis, thrombosis, and vascular biology* **27**, 1788-1795 (2007).
67. Pluddemann, A., Neyen, C. & Gordon, S. Macrophage scavenger receptors and host-derived ligands. *Methods (San Diego, Calif* **43**, 207-217 (2007).
68. Suzuki, H., *et al.* A role for macrophage scavenger receptors in atherosclerosis and susceptibility to infection. *Nature* **386**, 292-296 (1997).
69. Febbraio, M., *et al.* Targeted disruption of the class B scavenger receptor CD36 protects against atherosclerotic lesion development in mice. *The Journal of clinical investigation* **105**, 1049-1056 (2000).
70. Manning-Tobin, J.J., *et al.* Loss of SR-A and CD36 activity reduces atherosclerotic lesion complexity without abrogating foam cell formation in hyperlipidemic mice. *Arteriosclerosis, thrombosis, and vascular biology* **29**, 19-26 (2009).
71. Hazen, S.L. Oxidized phospholipids as endogenous pattern recognition ligands in innate immunity. *The Journal of biological chemistry* **283**, 15527-15531 (2008).
72. Podrez, E.A., *et al.* Identification of a novel family of oxidized phospholipids that serve as ligands for the macrophage scavenger receptor CD36. *The Journal of biological chemistry* **277**, 38503-38516 (2002).
73. Walton, K.A., *et al.* Receptors involved in the oxidized 1-palmitoyl-2-arachidonoyl-sn-glycero-3-phosphorylcholine-mediated synthesis of interleukin-8. A role for Toll-like receptor 4 and a glycosylphosphatidylinositol-anchored protein. *The Journal of biological chemistry* **278**, 29661-29666 (2003).
74. Binder, C.J., *et al.* Pneumococcal vaccination decreases atherosclerotic lesion

formation: molecular mimicry between Streptococcus pneumoniae and oxidized LDL. *Nature medicine* **9**, 736-743 (2003).
75. Caligiuri, G., *et al.* Phosphorylcholine-targeting immunization reduces atherosclerosis. *Journal of the American College of Cardiology* **50**, 540-546 (2007).
76. Bochkov, V.N., *et al.* Protective role of phospholipid oxidation products in endotoxin-induced tissue damage. *Nature* **419**, 77-81 (2002).
77. Riedemann, N.C. & Ward, P.A. Oxidized lipid protects against sepsis. *Nature medicine* **8**, 1084-1085 (2002).
78. von Schlieffen, E., *et al.* Multi-hit inhibition of circulating and cell-associated components of the toll-like receptor 4 pathway by oxidized phospholipids. *Arteriosclerosis, thrombosis, and vascular biology* **29**, 356-362 (2009).
79. Erridge, C., Kennedy, S., Spickett, C.M. & Webb, D.J. Oxidized phospholipid inhibition of toll-like receptor (TLR) signaling is restricted to TLR2 and TLR4: roles for CD14, LPS-binding protein, and MD2 as targets for specificity of inhibition. *The Journal of biological chemistry* **283**, 24748-24759 (2008).
80. Bluml, S., *et al.* Oxidized phospholipids negatively regulate dendritic cell maturation induced by TLRs and CD40. *J Immunol* **175**, 501-508 (2005).
81. Bluml, S., *et al.* The oxidation state of phospholipids controls the oxidative burst in neutrophil granulocytes. *J Immunol* **181**, 4347-4353 (2008).
82. Rouhanizadeh, M., *et al.* Oxidized-1-palmitoyl-2-arachidonoyl-sn-glycero-3-phosphorylcholine induces vascular endothelial superoxide production: implication of NADPH oxidase. *Free radical biology & medicine* **39**, 1512-1522 (2005).
83. Kronke, G., *et al.* Oxidized phospholipids induce expression of human heme oxygenase-1 involving activation of cAMP-responsive element-binding protein. *The Journal of biological chemistry* **278**, 51006-51014 (2003).
84. Nonas, S., *et al.* Oxidized phospholipids reduce vascular leak and inflammation in rat model of acute lung injury. *American journal of respiratory and critical care medicine* **173**, 1130-1138 (2006).
85. Birukov, K.G., *et al.* Epoxycyclopentenone-containing oxidized phospholipids restore endothelial barrier function via Cdc42 and Rac. *Circulation research* **95**, 892-901 (2004).
86. Miller, Y.I., *et al.* Toll-like receptor 4-dependent and -independent cytokine secretion induced by minimally oxidized low-density lipoprotein in macrophages. *Arteriosclerosis, thrombosis, and vascular biology* **25**, 1213-1219 (2005).
87. Martin, T.R. & Wurfel, M.M. A TRIFfic perspective on acute lung injury. *Cell* **133**, 208-210 (2008).
88. Mosesson, M.W. Fibrinogen and fibrin structure and functions. *J Thromb Haemost* **3**, 1894-1904 (2005).
89. Tanaka, K.A., Key, N.S. & Levy, J.H. Blood coagulation: hemostasis and thrombin regulation. *Anesthesia and analgesia* **108**, 1433-1446 (2009).
90. Ribes, J.A., Francis, C.W. & Wagner, D.D. Fibrin induces release of von Willebrand factor from endothelial cells. *The Journal of clinical investigation* **79**, 117-123 (1987).
91. Montesano, R., Pepper, M.S., Vassalli, J.D. & Orci, L. Phorbol ester induces cultured endothelial cells to invade a fibrin matrix in the presence of fibrinolytic inhibitors. *Journal of cellular physiology* **132**, 509-516 (1987).
92. Nicosia, R.F. & Ottinetti, A. Modulation of microvascular growth and morphogenesis by reconstituted basement membrane gel in three-dimensional cultures of rat aorta: a comparative study of angiogenesis in matrigel, collagen, fibrin, and plasma clot. *In Vitro Cell Dev Biol* **26**, 119-128 (1990).
93. Kudryk, B., *et al.* Measurement in human blood of fibrinogen/fibrin fragments

containing the B beta 15-42 sequence. *Thrombosis research* **25**, 277-291 (1982).
94. Chalupowicz, D.G., Chowdhury, Z.A., Bach, T.L., Barsigian, C. & Martinez, J. Fibrin II induces endothelial cell capillary tube formation. *The Journal of cell biology* **130**, 207-215 (1995).
95. Bach, T.L., Barsigian, C., Yaen, C.H. & Martinez, J. Endothelial cell VE-cadherin functions as a receptor for the beta15-42 sequence of fibrin. *The Journal of biological chemistry* **273**, 30719-30728 (1998).
96. Loike, J.D., *et al.* CD11c/CD18 on neutrophils recognizes a domain at the N terminus of the A alpha chain of fibrinogen. *Proceedings of the National Academy of Sciences of the United States of America* **88**, 1044-1048 (1991).
97. Drew, A.F., Liu, H., Davidson, J.M., Daugherty, C.C. & Degen, J.L. Wound-healing defects in mice lacking fibrinogen. *Blood* **97**, 3691-3698 (2001).
98. Drew, A.F., *et al.* Crescentic glomerulonephritis is diminished in fibrinogen-deficient mice. *American journal of physiology* **281**, F1157-1163 (2001).
99. Wilberding, J.A., *et al.* Development of pulmonary fibrosis in fibrinogen-deficient mice. *Annals of the New York Academy of Sciences* **936**, 542-548 (2001).
100. Yellon, D.M. & Hausenloy, D.J. Myocardial reperfusion injury. *The New England journal of medicine* **357**, 1121-1135 (2007).
101. Zacharowski, K., Zacharowski, P., Reingruber, S. & Petzelbauer, P. Fibrin(ogen) and its fragments in the pathophysiology and treatment of myocardial infarction. *Journal of molecular medicine (Berlin, Germany)* **84**, 469-477 (2006).
102. Zacharowski, K., *et al.* The effects of the fibrin-derived peptide Bbeta(15-42) in acute and chronic rodent models of myocardial ischemia-reperfusion. *Shock (Augusta, Ga* **27**, 631-637 (2007).
103. Roesner, J.P., *et al.* The fibrin-derived peptide Bbeta15-42 is cardioprotective in a pig model of myocardial ischemia-reperfusion injury. *Critical care medicine* **35**, 1730-1735 (2007).
104. Roesner, J.P., *et al.* A double blind, single centre, sub-chronic reperfusion trial evaluating FX06 following haemorrhagic shock in pigs. *Resuscitation* **80**, 264-271 (2009).
105. Roesner, J.P., *et al.* Bbeta15-42 (FX06) reduces pulmonary, myocardial, liver, and small intestine damage in a pig model of hemorrhagic shock and reperfusion. *Critical care medicine* **37**, 598-605 (2009).
106. Weiland, J.E., *et al.* Lung neutrophils in the adult respiratory distress syndrome. Clinical and pathophysiologic significance. *Am Rev Respir Dis* **133**, 218-225 (1986).
107. Abraham, E. Neutrophils and acute lung injury. *Critical care medicine* **31**, S195-199 (2003).
108. Modig, J. & Hallgren, R. Pathophysiologic significance of lung granulocytes in human adult respiratory distress syndrome induced by septic or traumatic shock. *Acta Chir Scand* **153**, 267-271 (1987).
109. Chalhoub, N. & Baker, S.J. PTEN and the PI3-kinase pathway in cancer. *Annual review of pathology* **4**, 127-150 (2009).
110. Engelman, J.A., Luo, J. & Cantley, L.C. The evolution of phosphatidylinositol 3-kinases as regulators of growth and metabolism. *Nat Rev Genet* **7**, 606-619 (2006).
111. Rommel, C., Camps, M. & Ji, H. PI3K delta and PI3K gamma: partners in crime in inflammation in rheumatoid arthritis and beyond? *Nature reviews* **7**, 191-201 (2007).
112. Cantley, L.C. The phosphoinositide 3-kinase pathway. *Science (New York, N.Y*

296, 1655-1657 (2002).
113. Suzuki, A., Nakano, T., Mak, T.W. & Sasaki, T. Portrait of PTEN: messages from mutant mice. *Cancer science* **99**, 209-213 (2008).
114. Okkenhaug, K. & Vanhaesebroeck, B. PI3K in lymphocyte development, differentiation and activation. *Nature reviews* **3**, 317-330 (2003).
115. Günzl, P. & Schabbauer, G. Recent advances in the genetic analysis of PTEN and PI3K innate immune properties. *Immunobiology* **213**, 759-765 (2008).
116. Suzuki, A., *et al.* High cancer susceptibility and embryonic lethality associated with mutation of the PTEN tumor suppressor gene in mice. *Curr Biol* **8**, 1169-1178 (1998).
117. Arbibe, L., *et al.* Toll-like receptor 2-mediated NF-kappa B activation requires a Rac1-dependent pathway. *Nature immunology* **1**, 533-540 (2000).
118. Marja Ojaniemi, V.G.K.H.M.L.K.V.M.H. Phosphatidylinositol 3-kinase is involved in Toll-like receptor 4-mediated cytokine expression in mouse macrophages. Vol. 33 597-605 (2003).
119. Rhee, S.H., Kim, H., Moyer, M.P. & Pothoulakis, C. Role of MyD88 in phosphatidylinositol 3-kinase activation by flagellin/toll-like receptor 5 engagement in colonic epithelial cells. *The Journal of biological chemistry* **281**, 18560-18568 (2006).
120. Guha, M. & Mackman, N. The phosphatidylinositol 3-kinase-Akt pathway limits lipopolysaccharide activation of signaling pathways and expression of inflammatory mediators in human monocytic cells. *The Journal of biological chemistry* **277**, 32124-32132 (2002).
121. Aksoy, E., *et al.* Inhibition of phosphoinositide 3-kinase enhances TRIF-dependent NF-kappa B activation and IFN-beta synthesis downstream of Toll-like receptor 3 and 4. *European journal of immunology* **35**, 2200-2209 (2005).
122. Schabbauer, G., Tencati, M., Pedersen, B., Pawlinski, R. & Mackman, N. PI3K-Akt pathway suppresses coagulation and inflammation in endotoxemic mice. *Arteriosclerosis, thrombosis, and vascular biology* **24**, 1963-1969 (2004).
123. Wrann, C.D., *et al.* The phosphatidylinositol 3-kinase signaling pathway exerts protective effects during sepsis by controlling C5a-mediated activation of innate immune functions. *J Immunol* **178**, 5940-5948 (2007).
124. Zhang, W.J., Wei, H., Hagen, T. & Frei, B. Alpha-lipoic acid attenuates LPS-induced inflammatory responses by activating the phosphoinositide 3-kinase/Akt signaling pathway. *Proceedings of the National Academy of Sciences of the United States of America* **104**, 4077-4082 (2007).
125. Yu, Y., *et al.* TLR5-mediated phosphoinositide 3-kinase activation negatively regulates flagellin-induced proinflammatory gene expression. *J Immunol* **176**, 6194-6201 (2006).
126. Luyendyk, J.P., *et al.* Genetic analysis of the role of the PI3K-Akt pathway in lipopolysaccharide-induced cytokine and tissue factor gene expression in monocytes/macrophages. *J Immunol* **180**, 4218-4226 (2008).
127. Fukao, T., *et al.* Selective loss of gastrointestinal mast cells and impaired immunity in PI3K-deficient mice. *Nature immunology* **3**, 295-304 (2002).
128. Fukao, T., *et al.* PI3K-mediated negative feedback regulation of IL-12 production in DCs. *Nature immunology* **3**, 875-881 (2002).
129. Martin, M., Rehani, K., Jope, R.S. & Michalek, S.M. Toll-like receptor-mediated cytokine production is differentially regulated by glycogen synthase kinase 3. *Nature immunology* **6**, 777-784 (2005).
130. Underhill, D.M. & Ozinsky, A. Phagocytosis of microbes: complexity in action. *Annual review of immunology* **20**, 825-852 (2002).

131. Stephens, L., Ellson, C. & Hawkins, P. Roles of PI3Ks in leukocyte chemotaxis and phagocytosis. *Current opinion in cell biology* **14**, 203-213 (2002).
132. Chen, L., *et al.* Two phases of actin polymerization display different dependencies on PI(3,4,5)P3 accumulation and have unique roles during chemotaxis. *Molecular biology of the cell* **14**, 5028-5037 (2003).
133. Vieira, O.V., *et al.* Distinct roles of class I and class III phosphatidylinositol 3-kinases in phagosome formation and maturation. *The Journal of cell biology* **155**, 19-25 (2001).
134. Ellson, C.D., *et al.* Phosphatidylinositol 3-phosphate is generated in phagosomal membranes. *Current Biology* **11**, 1631-1635 (2001).
135. Fratti, R.A., Backer, J.M., Gruenberg, J., Corvera, S. & Deretic, V. Role of phosphatidylinositol 3-kinase and Rab5 effectors in phagosomal biogenesis and mycobacterial phagosome maturation arrest. *The Journal of cell biology* **154**, 631-644 (2001).
136. Sasaki, T., *et al.* Function of PI3Kgamma in thymocyte development, T cell activation, and neutrophil migration. *Science (New York, N.Y* **287**, 1040-1046 (2000).
137. Hirsch, E., *et al.* Central role for G protein-coupled phosphoinositide 3-kinase gamma in inflammation. *Science (New York, N.Y* **287**, 1049-1053 (2000).
138. Del Prete, A., *et al.* Defective dendritic cell migration and activation of adaptive immunity in PI3Kgamma-deficient mice. *The EMBO journal* **23**, 3505-3515 (2004).
139. Li, Z., *et al.* Roles of PLC-beta2 and -beta3 and PI3Kgamma in chemoattractant-mediated signal transduction. *Science (New York, N.Y* **287**, 1046-1049 (2000).
140. Curnock, A.P., Logan, M.K. & Ward, S.G. Chemokine signalling: pivoting around multiple phosphoinositide 3-kinases. *Immunology* **105**, 125-136 (2002).
141. Maus, U.A., *et al.* Importance of phosphoinositide 3-kinase gamma in the host defense against pneumococcal infection. *American journal of respiratory and critical care medicine* **175**, 958-966 (2007).
142. Subramanian, K.K., *et al.* Tumor suppressor PTEN is a physiologic suppressor of chemoattractant-mediated neutrophil functions. *Blood* **109**, 4028-4037 (2007).
143. Heit, B., Tavener, S., Raharjo, E. & Kubes, P. An intracellular signaling hierarchy determines direction of migration in opposing chemotactic gradients. *The Journal of cell biology* **159**, 91-102 (2002).
144. Heit, B., *et al.* PTEN functions to 'prioritize' chemotactic cues and prevent 'distraction' in migrating neutrophils. *Nature immunology* **9**, 743-752 (2008).
145. Li, Y., *et al.* Targeted deletion of tumor suppressor PTEN augments neutrophil function and enhances host defense in neutropenia-associated pneumonia. *Blood* **113**, 4930-4941 (2009).
146. Zhu, D., *et al.* Deactivation of phosphatidylinositol 3,4,5-trisphosphate/Akt signaling mediates neutrophil spontaneous death. *Proceedings of the National Academy of Sciences of the United States of America* **103**, 14836-14841 (2006).
147. Cao, X., *et al.* The inositol 3-phosphatase PTEN negatively regulates Fc gamma receptor signaling, but supports Toll-like receptor 4 signaling in murine peritoneal macrophages. *J Immunol* **172**, 4851-4857 (2004).
148. Canetti, C., *et al.* Activation of phosphatase and tensin homolog on chromosome 10 mediates the inhibition of FcgammaR phagocytosis by prostaglandin E2 in alveolar macrophages. *J Immunol* **179**, 8350-8356 (2007).

149. Raftopoulou, M., Etienne-Manneville, S., Self, A., Nicholls, S. & Hall, A. Regulation of cell migration by the C2 domain of the tumor suppressor PTEN. *Science (New York, N.Y* **303**, 1179-1181 (2004).
150. Marone, R., Cmiljanovic, V., Giese, B. & Wymann, M.P. Targeting phosphoinositide 3-kinase: moving towards therapy. *Biochimica et biophysica acta* **1784**, 159-185 (2008).

9. CURRICULUM VITAE Dr.med.univ. ULRICH MATT

***24.03.1980 in Hall in Tirol**

nationality: Austrian

Formation

since 10/2009	Residency in internal medicine at the Kantonsspital Schaffhausen / Switzerland
2006 – 2009	PhD Student at the Center for Molecular Medicine of the Austrian Academy of Sciences and at the Department of Internal Medicine 1, Division of Infectious Diseases & Tropical Medicine, Medical University of Vienna
01/2006	Conferral of doctorate in medicine, Medical University of Vienna
2004 - 2005	Erasmus international study exchange program, Faculté de Medicine, Rennes I, France
2002 – 2004	Student at Vienna Medical University
1999 - 2002	Student at Leopold Franzens Universität Innsbruck (Faculty of Medicine), Austria
01 – 08/1999	Military service as a paramedic
06/1998	"Matura" at the Franziskanergymnasium Hall in Tirol

Publications

- **Matt U**, Sharif O, Furtner T, Fang Zhang, Elbau I, Zivkovic A, Stich K, Oskolkova O, Doninger B, Perkmann T, Schabbauer G, Binder CJ, Bochkov VN, Scott JD and Knapp S; WAVE-1 anchors PKA to facilitate the detrimental effects of oxidized phospholipids during Gram negative sepsis; submitted

- Schabbauer G, **Matt U (shared first author)**, Günzl P, Furtner T, Hainzl E, Mesteri I, Doninger B, Binder BR and Knapp S; Myeloid PTEN promotes inflammation but impairs bactericidal activities during murine pneumococcal pneumonia; Journal of Immunology; in press

- Günzl P, Hainzl E, **Matt U**, Dillinger B, Mahr B, Knapp S, Binder BR and Schabbauer G; Anti-inflammatory properties of the PI3K pathway are mediated by IL10/DUSP regulation; submitted

- **Matt U**, Warszawska JM, Bauer M, Dietl W, Mesteri I, Doninger B, Haslinger I, Schabbauer G, Perkmann T, Binder CJ, Reingruber S, Petzelbauer P and Knapp S; $B\beta_{15-42}$ protects against acid-induced acute lung injury and secondary Pseudomonas pneumonia in vivo, American Journal of Respiratory and Critical Care Medicine; 2009; 180(12):1208-17

- Lagler H, Sharif O, Haslinger I, **Matt U**, Stich K, Furtner T, Doninger B, Schmid K, de Vos AF, and Knapp S; TREM-1 activation alters the dynamics of pulmonary IRAK-M expression in vivo and improves host defense against pneumococcal pneumonia; Journal of Immunology; 2009; 183(3)2027-36
- Fürnkranz U, Nagl M, Gottardi W, **Matt U**, Aspöck H; N-chlorotaurine shows cytotoxic activities against promastigotes and amastigotes of Leishmania spp; Journal of Medical Microbiology; 2009; 58(Pt 10):1298-302
- Gröger M, Pasteiner W, Ignatyev G, **Matt U**, Knapp S, Atrasheuskaya A, Bukin E, Friedl P, Zinkl D, Hofer R, Zacharowski K, Petzelbauer P and Reingruber S; Peptide Bbeta15-42 preserves endothelial barrier function in shock in a Fyn-dependent manner; PLOS one; 2009; 4(4):e5391
- Knapp S, **Matt U**, Leitinger N, van der Poll T.; Oxidized phospholipids inhibit phagocytosis and impair outcome in gram-negative sepsis in vivo; Journal of Immunology; 2007; 178(2):993-1001
- Lagler H, **Matt U**, Sillaber C, Winkler S, Graninger W.; Successful treatment of visceral leishmaniasis with liposomal amphotericin B; Acta Biomed. 2006; Suppl 2:22-5

Conferences

07 / 2009 — 5th PhD-symposium of the Medical University of Vienna, poster: $B\beta_{15-42}$ protects against acid-induced acute lung injury and secondary Pseudomonas pneumonia in vivo

04 / 2009 — 3rd Austrian Infectious Disease congress, Saalfelden, Austria; poster award, 1st prize: Oxidized phospholipids inhibit phagocytosis via a PKA-/ AKAP dependent mechanism

09 / 2008 — TOLL-congress, Lisbon, Portugal – Poster: Oxidized phospholipids inhibit phagocytosis via a PKA-dependent mechanism

09 / 2008 — Joint Annual Meeting of Immunology of the Austrian and German Societies, Vienna – selected oral presentation: PTEN importantly contributes to PMN influx during pneumococcal pneumonia in vivo

03 / 2008 — 4th PhD-symposium of the Medical University of Vienna, selected oral presentation: PhD Symposium, selected oral presentation: Unexpected role for PTEN in the inflammatory response to Streptococcus pneumonia induce pneumonia in mice

08 / 2007 — EMDS, European Macrophage and Dendritic Cell Society, 21st annual meeting, Innsbruck – selected oral presentation: PTEN importantly contributes to PMN influx during pneumococcal pneumonia in vivo

08 / 2007 — 1st CeMM conference, Drug Action and Chemical Biology in the Post-Genomic Era, Vienna

03 / 2007 — 7th World Congress on Trauma, Shock, Inflammation and Sepsis, Munich, Germany, poster: Oxidized phospholipids inhibit phagocytosis and impair outcome in gram-negative sepsis in vivo

06 / 2007 3rd PhD-symposium of the Medical University of Vienna, selected oral presentation: Oxidized phospholipids inhibit the phagocytic capacity of professional phagocytes thereby impairing outcome in gram-negative sepsis in vivo

10 / 2006 6th International Cytokine Conference, Vienna, Poster: Oxidized phospholipids inhibit phagocytosis and impair outcome in gram-negative sepsis in vivo

Others

- Research award "Intensivmedizin" of the "Deutsche Gesellschaft für Internistische Intensivmedizin und Notfallmedizin" 2010

  Patent filed on "WAVE1 Inhibition in the medical intervention of inflammatory diseases and systemic infammatory response syndroms" shared with Sylvia Knapp and Omar Sharif (10/09)
- Co-supervision (together with Prof. Dr. Sylvia Knapp, PhD) of the diploma thesis: "PTEN and phagocytosis: impact of macrophage subset and pathogen" by Immanuel Elbau
- 07 / 2004 Tropical and Travel Medicine, Rostock - Brown Universities Summer School in Infectious Diseases, Rostock, Germany
- 08 / 2003 Medical Health Project Mongolia, Fabula (Verein für Kulturtransfer), Ulaan Baatar, Mongolia; project organization and participation

Languages

German	Mother Tongue
English	fluent – written and spoken
French	fluent – written and spoken
Spanish	basic